NEW TRENDS IN EARLY-STAGE LUNG CANCER PRESENTING AS GROUND-GLASS OPACITIES: CLINICAL, PATHOLOGICAL AND MOLECULAR ASPECTS

EDITED BY: Chen Chen, Kezhong Chen and Kai He
PUBLISHED IN: Frontiers in Oncology

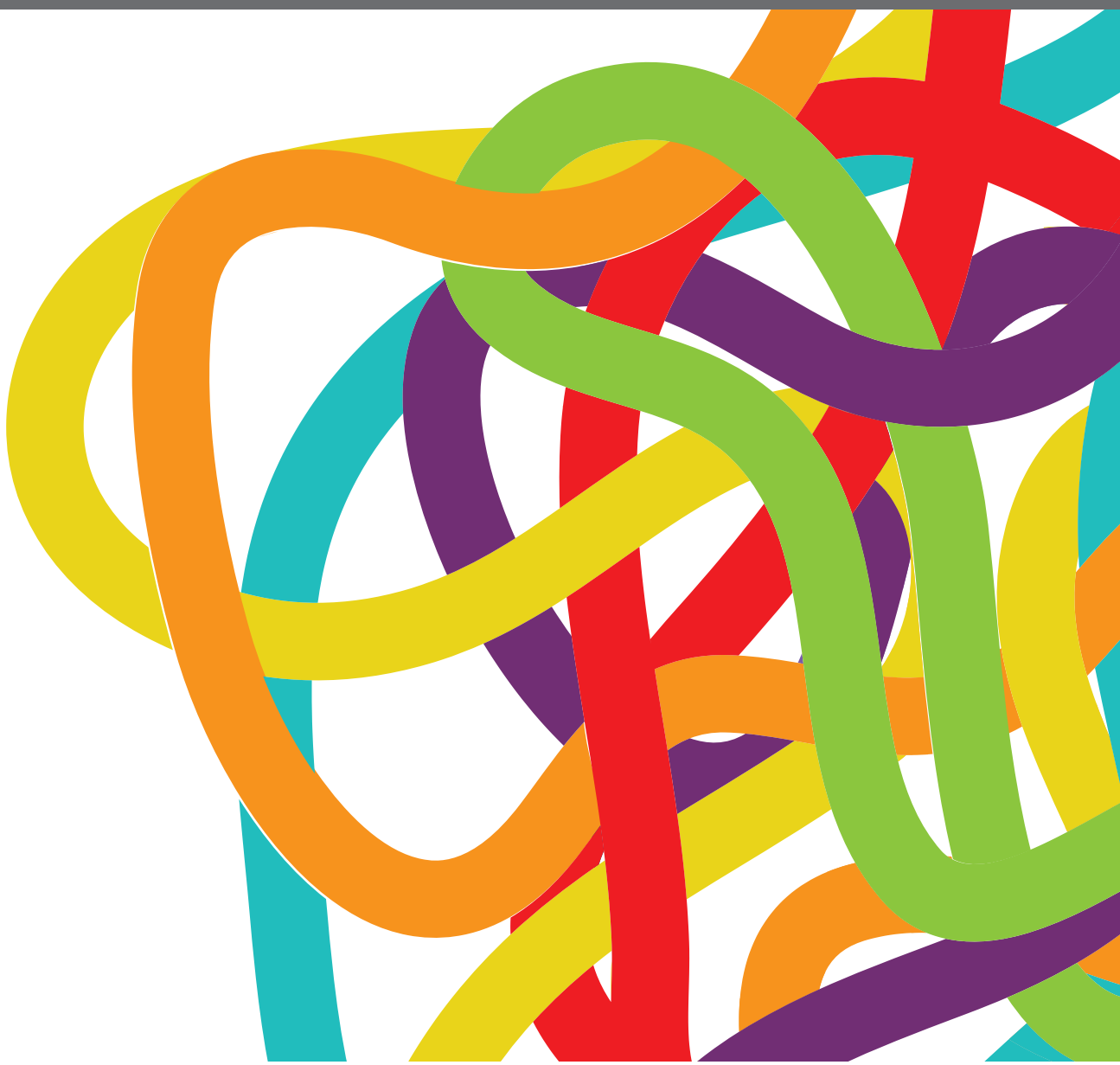

frontiers Research Topics

ISSN 1664-8714
ISBN 978-2-88974-043-7
DOI 10.3389/978-2-88974-043-7

About Frontiers

Frontiers is more than just an open-access publisher of scholarly articles: it is a pioneering approach to the world of academia, radically improving the way scholarly research is managed. The grand vision of Frontiers is a world where all people have an equal opportunity to seek, share and generate knowledge. Frontiers provides immediate and permanent online open access to all its publications, but this alone is not enough to realize our grand goals.

Frontiers Journal Series

The Frontiers Journal Series is a multi-tier and interdisciplinary set of open-access, online journals, promising a paradigm shift from the current review, selection and dissemination processes in academic publishing. All Frontiers journals are driven by researchers for researchers; therefore, they constitute a service to the scholarly community. At the same time, the Frontiers Journal Series operates on a revolutionary invention, the tiered publishing system, initially addressing specific communities of scholars, and gradually climbing up to broader public understanding, thus serving the interests of the lay society, too.

Dedication to Quality

Each Frontiers article is a landmark of the highest quality, thanks to genuinely collaborative interactions between authors and review editors, who include some of the world's best academicians. Research must be certified by peers before entering a stream of knowledge that may eventually reach the public - and shape society; therefore, Frontiers only applies the most rigorous and unbiased reviews.
Frontiers revolutionizes research publishing by freely delivering the most outstanding research, evaluated with no bias from both the academic and social point of view. By applying the most advanced information technologies, Frontiers is catapulting scholarly publishing into a new generation.

What are Frontiers Research Topics?

Frontiers Research Topics are very popular trademarks of the Frontiers Journals Series: they are collections of at least ten articles, all centered on a particular subject. With their unique mix of varied contributions from Original Research to Review Articles, Frontiers Research Topics unify the most influential researchers, the latest key findings and historical advances in a hot research area! Find out more on how to host your own Frontiers Research Topic or contribute to one as an author by contacting the Frontiers Editorial Office: frontiersin.org/about/contact

NEW TRENDS IN EARLY-STAGE LUNG CANCER PRESENTING AS GROUND-GLASS OPACITIES: CLINICAL, PATHOLOGICAL AND MOLECULAR ASPECTS

Topic Editors:
Chen Chen, Central South University, China
Kezhong Chen, Peking University People's Hospital, China
Kai He, The Ohio State University, United States

Citation: Chen, C., Chen, K., He, K., eds. (2022). New Trends in Early-Stage Lung Cancer Presenting as Ground-Glass Opacities: Clinical, Pathological and Molecular Aspects. Lausanne: Frontiers Media SA. doi: 10.3389/978-2-88974-043-7

Table of Contents

frontiers in Oncology

EDITORIAL
published: 23 November 2021
doi: 10.3389/fonc.2021.792252

Editorial: New Trends in Early-Stage Lung Cancer Presenting as Ground-Glass Opacities: Clinical, Pathological and Molecular Aspects

Kezhong Chen[1] *and Chen Chen*[2]*

[1] Department of Thoracic Surgery, Peking University People's Hospital, Beijing, China, [2] Department of Thoracic Surgery, The Second Xiangya Hospital of Central South University, Changsha, China

Keywords: lung cancer, ground-glass opacities, treatment, diagnosis, early-stage, multiple lesions, molecular change

Editorial on the Research Topic

New Trends in Early-Stage Lung Cancer Presenting as Ground-Glass Opacities: Clinical, Pathological and Molecular Aspects

Ground-Glass Opacity (GGO)-associated lung cancers are radiologically distinct clinical entities. Consensus or guidelines suggest that the clinical management decision on ground-glass nodules (GGN) should be based on the initial size, percentage of solid portion, and growth rate of GGNs, but are inconsistent in terms of the GGN cutoff size for surgical intervention and low-dose CT scan (LDCT) follow-up frequency (1–3). In addition, the unpredictable aggressive potential and highly heterogeneous characteristics of GGNs add another layer of complexity for GGN management. Thus, effectively treating GGNs remains challenging for clinicians who may have to rely on their individual experiences. To address this knowledge gap, we initiated this Research Topic to further explore the clinical manifestations, pathological features, and genetic changes that will assist in the diagnosis and decision-making of treatment of early-stage lung cancer presenting as GGOs. A number of interesting studies closely related to this field were included.

Previous studies have shown that most resected GGNs are histologically atypical adenomatous hyperplasia (AAH), adenocarcinoma *in situ* (AIS), minimally invasive adenocarcinoma (MIA), and lepidic predominant adenocarcinoma, which are considered to have a low risk for regional lymph node metastasis, vascular invasion, or pleural invasion. In the WHO 5th lung cancer TNM clinical classification, AIS has been removed from preinvasive to precursor lesions, companied with AAH (4). Wang et al. reported that using a radiomics prediction model in patients with subcentimeter GGOs to distinguish AAH from early lung adenocarcinomas. The model turns to have the potentiality to improve preoperative prediction accuracy for AAH nodules and may help to avoid unnecessarily aggressive operations for patients with AAH.

Prospective multicenter validation with higher accuracy is needed for routine clinical application as surgeons are unwilling to defer surgery based on false-negative predictions that will delay the treatment of invasive lesions. GGNs with a solid component are more likely related to invasive adenocarcinoma with poor prognosis. Xi et al. and Tsutani et al. studies confirmed the solid size of GGNs has a decisive effect on prognosis and provided an accurate solid tumor size cutoff for high-risk patients. Qi et al. reported that in small-sized lung adenocarcinoma, consolidation tumor ratio (CTR) is the best sign for predicting lung cancer spread through air spaces (STAS).

OPEN ACCESS

Edited and reviewed by:
Lizza E. L. Hendriks, Maastricht University Medical Centre, Netherlands

***Correspondence:**
Chen Chen
chenchen1981412@csu.edu.cn

Specialty section:
This article was submitted to Thoracic Oncology, a section of the journal Frontiers in Oncology

Received: *10 October 2021*
Accepted: *02 November 2021*
Published: *23 November 2021*

Citation:
Chen K and Chen C (2021) Editorial: New Trends in Early-Stage Lung Cancer Presenting as Ground-Glass Opacities: Clinical, Pathological and Molecular Aspects. Front. Oncol. 11:792252. doi: 10.3389/fonc.2021.792252

While ensuring the treatment effect, reducing the extent of resection and improving the quality of life are both important issues in surgical research for early-stage lung cancer in recent years (5). Handa et al. reviewed the transition of treatment strategies for NSCLC with GGNs according to a series of clinical trials. The primary endpoint of clinical trial JCOG 0802 is the overall survival between segmentectomy and lobectomy for NSCLC patients with tumors less than 2cm. After a long time of patients' enrollment, this trial finally presented results this year and showed a longer OS of segmentectomy for patients with GGN lesions, indicating further prompted limited resection may be an optimal choice (6). Wu et al. compared perioperative outcomes between precise and routine segmentectomy for GGNs and showed their advantages, respectively. Precise segmentectomy is a technique improvement, but whether it could bring oncological improvement is still unclear. In addition, the learning curve and technical barriers of precise segmentectomy may delay its widespread application in low-volume centers and for inexperienced thoracic surgeons.

Due to the widespread use of low-dose computed tomography and computer-aided detection/diagnosis systems (CADe/x), multiple pulmonary nodules have become an increasingly recognized phenomenon, especially GGNs frequently appearing as extremely multiple nodules (≥3), which presents a challenge for diagnosis and treatment. Two studies identified the phenomenon of different GGNs originating from the same clone in the same patient (7, 8). Those GGNs were all in close proximity which might result in dissemination along the airway. Whether these multiple GGNs sharing the same mutation affect the prognosis needs to be explored with longer follow-up. Wang et al. collected a large cohort of patients with large numbers of GGNs to investigate the clinical and pathologic features, surgical methods, and prognosis of these patients and found the proportion of malignant nodules did not increase significantly with the increasing number of nodules and no lymph node invasion was observed, which suggested that the number of nodules may not affect surgical strategy or prognosis, providing insights for the treatment strategy of such patients.

The indolent clinical course and superior survival of GGNs imply a unique underlying biology. However, the molecular characteristics of GGNs have not been systemically studied. Wei et al. systematically reviewed the molecular alterations in lung adenocarcinoma (LUAD) with GGNs and revealed the correlation between driver mutations and the radiological progression. Ouyang et al. reported that the occurrence of GGOs may be related to hereditary or genetic factors. A whole-exome sequencing of lung cancer performed as GGN revealed the key genetic mutational events that potentially maintain the relatively inert nature of GGN and its progression from GGN to aggressively advanced lung adenocarcinoma (8).

In addition to accumulating molecular alterations, cancer evolution is constantly shaped by the dynamic interaction between cancer cells and host factors, particularly immune surveillance. Zhang et al. found IL-6 expression status and NK cell levels of early lung adenocarcinoma as GGN is significantly reduced. Stimulation of IL-6 could activate NK cells, suggesting that the immune response in the tumor microenvironment might play a critical role in the development of GGOs. Wu et al. reported based on two cases, that synchronous GGNs may not be sensitive to anti-PD-1/PD-L1 based therapy. In this study, the proportion of CD8+T cells was lower in synchronous GGNs than in primary lung cancers, while tumor-associated macrophages showed significant enrichment in the tumor microenvironment of GGNs (9). A recently published study further performed multiomics analysis of a consecutive clinical cohort prospective observational cohort study to characterize pulmonary nodules with or without GGO component and found GGO-associated lung cancers with lower mutational burden, less active immune environment, and less ctDNA shedding, revealing that the intrinsic biological features may have contributed to the indolent clinical course of GGO-associated lung cancers. This supports the hypothesis that GGO may represent early carcinogenesis of a subset of LUADs when cancer cells and anti-tumor immune response are at equilibrium and provides mechanistic insights into the diagnosis and treatment of these radiologically distinct clinical entities (10).

Because of the unique biological, psychological, and environmental characteristics of each patient, clinical management of GGNs should be customized to meet individual patients' needs. As minimally invasive surgical technology improves, surgical resection of GGNs is becoming increasingly safe and less invasive, and the lung function and quality of life can also be maximally preserved. Surgical resection of GGNs removes the potential risk of malignant progression of the GGNs and relieves patients' anxiety. Nevertheless, surgery is also associated with risks of postoperative complications. Thoracic surgeons should weigh the benefits and risks of surgical resection carefully before making a therapeutic decision. Careful consideration of the indication for surgery is crucial for the effective management of GGNs and to avoid overtreatment.

With several updates and novel findings, this Research Topic will provide new insight for a better understanding of the clinicopathological and molecular characteristics of GGOs. Surgeons and oncologists will broaden their knowledge and find new clues for the treatment of early-stage lung cancer presenting as single or multiple GGOs. Further investigations on the natural course of GGNs will undoubtedly improve our understanding of the unique biological characteristics of GGNs and thus provide clinical evidence for determining the optimal timing of surgical resection. In addition, studies on molecular and genetic mechanisms underlying the adverse progression of GGNs could reveal potential therapeutic targets to prevent or delay GGN progression.

AUTHOR CONTRIBUTIONS

KC and CC contributed to the conceptualization and writing the manuscript. All authors contributed to the article and approved the submitted version.

FUNDING

KC is supported by the National Natural Science Foundation of China (No. 82072566) and Peking University People's Hospital Research and Development Funds (RS2019-01). CC is supported

by the Hunan Provincial Natural Science Foundation (No. 2020SK53419, No. 2019JJ50953 and No. 2021JJ30926), Hunan Provincial Key Area R&D Program NO. 2019SK2253, CSCO Cancer Research Foundation (CSCO-Y-young2019-034 and CSCO-2019Roche-073), and the Changsha Municipal Natural Science Foundation NO. kq2014246.

REFERENCES

1. Bai C, Choi CM, Chu CM, Anantham D, Chung-Man Ho J, Khan AZ, et al. Evaluation of Pulmonary Nodules: Clinical Practice Consensus Guidelines for Asia. *Chest* (2016) 150(4):877–93. doi: 10.1016/j.chest.2016.02.650
2. Pedersen JH, Rzyman W, Veronesi G, D'Amico TA, Van Schil P, Molins L, et al. Recommendations From the European Society of Thoracic Surgeons (ESTS) Regarding Computed Tomography Screening for Lung Cancer in Europe. *Eur J Cardiothorac Surg* (2017) 51(3):411–20. doi: 10.1093/ejcts/ezw418
3. MacMahon H, Naidich DP, Goo JM, Lee KS, Leung ANC, Mayo JR, et al. Guidelines for Management of Incidental Pulmonary Nodules Detected on CT Images: From the Fleischner Society 2017. *Radiology* (2017) 284(1):228–43. doi: 10.1148/radiol.2017161659
4. Cooper WA, Bubendorf L, Kadota K, Landanyi M, MacMahon H, Matsubara D, et al. *WHO Classification of Tumours Thoracic Tumours. 5th Ed*. Lyon, France: IARC (2021) p. 64–74.
5. Altorki NK, Wang X, Wigle D, Gu L, Darling G, Ashrafi AS, et al. Perioperative Mortality and Morbidity After Sublobar *Versus* Lobar Resection for Early-Stage Non-Small-Cell Lung Cancer: *Post-Hoc* Analysis of an International, Randomised, Phase 3 Trial (CALGB/Alliance 140503). *Lancet Respir Med* (2018) 6(12):915–24. doi: 10.1016/S2213-2600(18)30411-9
6. Asamura H, Okada M, Saji H, Tsuboi M, Nakajima R. Randomized Trial of Segmentectomy Compared to Lobectomy in Small-Sized Peripheral Non–Small Cell Lung Cancer. In: *Presented at: 101st Annual Meeting of the American Association for Thoracic Surgery: A Virtual Learning Experience* (2021). pp. 311–2.
7. Li R, Li X, Xue R, Yang F, Wang S, Li Y, et al. Early Metastasis Detected in Patients With Multifocal Pulmonary Ground-Glass Opacities (GGOs). *Thorax* (2018) 73(3):290–2. doi: 10.1136/thoraxjnl-2017-210169
8. Li Y, Li X, Li H, Zhao Y, Liu Z, Sun K, et al. Genomic Characterisation of Pulmonary Subsolid Nodules: Mutational Landscape and Radiological Features. *Eur Respir J* (2020) 55(2):1901409. doi: 10.1183/13993003.01409-2019
9. Wu F, Li W, Zhao W, Zhou F, Xie H, Shi J, et al. Synchronous Ground-Glass Nodules Showed Limited Response to Anti-PD-1/PD-L1 Therapy in Patients With Advanced Lung Adenocarcinoma. *Clin Transl Med* (2020) 10(3):e149. doi: 10.1002/ctm2.149
10. Chen K, Bai J, Reuben A, Zhao H, Kang G, Zhang C, et al. Multiomics Analysis Reveals Distinct Immunogenomic Features of Lung Cancer With Ground-Glass Opacity. *Am J Respir Crit Care Med* (2021) 204(10):1180–92. doi: 10.1164/rccm.202101-0119OC

ACKNOWLEDGMENTS

We would like to acknowledge all the authors, editors, and reviewers for their dedication to this Research Topic. Despite the pandemic, their enthusiasm and dedication greatly contribute to the successful completion of this Research Topic.

Conflict of Interest: The authors declare that the research was conducted in the absence of any commercial or financial relationships that could be construed as a potential conflict of interest.

frontiers in Oncology

ORIGINAL RESEARCH
published: 11 January 2021
doi: 10.3389/fonc.2020.548430

Predictors of CT Morphologic Features to Identify Spread Through Air Spaces Preoperatively in Small-Sized Lung Adenocarcinoma

Lin Qi[1†], Ke Xue[2†], Yongjun Cai[3], Jinjuan Lu[1], Xiaohu Li[4] and Ming Li[1*]*

[1] Department of Radiology, Huadong Hospital, Fudan University, Shanghai, China, [2] Department of Plastic and Reconstructive Surgery, Shanghai Ninth People's Hospital, School of Medicine, Shanghai Jiao Tong University, Shanghai, China, [3] Department of Pathology, Huadong Hospital affiliated to Fudan University, Shanghai, China, [4] Department of Radiology, First Affiliated Hospital of Anhui Medical University, Hefei, China

OPEN ACCESS

Edited by:
Chen Chen,
Central South University, China

Reviewed by:
Noriyoshi Sawabata,
Nara Medical University, Japan
Di Lu,
Southern Medical University, China
Xiao Long Liu,
Jingling Hospital, China

***Correspondence:**
Ming Li
ming_li@fudan.edu.cn
Xiaohu Li
lixiaohu@ahmu.edu.cn

[†]These authors have contributed equally to this work

Specialty section:
This article was submitted to Thoracic Oncology, a section of the journal Frontiers in Oncology

Received: *20 August 2020*
Accepted: *29 October 2020*
Published: *11 January 2021*

Citation:
Qi L, Xue K, Cai Y, Lu J, Li X and Li M (2021) Predictors of CT Morphologic Features to Identify Spread Through Air Spaces Preoperatively in Small-Sized Lung Adenocarcinoma. Front. Oncol. 10:548430. doi: 10.3389/fonc.2020.548430

Objectives: This study aimed to explore the predictive CT features of spread through air spaces (STAS) in patients with small-sized lung adenocarcinoma.

Methods: From January 2017 to May 2019, patients with confirmed pathology of small-sized lung adenocarcinoma (less than or equal to 2 cm) and who underwent surgery were retrospectively analyzed. The clinical, pathological, and surgical information and CT features were analyzed.

Results: A total of 47 patients with STAS (males, 61.7%; mean age, 56 ± 8years) and 143 patients without STAS (males, 58%; mean age, 53 ± 11 years) were included. Pathologically, papillary, micropapillary, solid predominant subtypes, and vascular and pleural invasion were most commonly observed features in the STAS group. Radiologically, higher consolidation tumor ratio (CTR), presence of spiculation, satellites, ground glass ribbon sign, pleural attachment, and unclear tumor–lung interface were more commonly observed features in the STAS group. CTR, presence of ground glass ribbons and pleural connection, and absence of cystic airspaces were considered as stable predictors of STAS in multivariate logistic models. The receiver operating characteristic curve (ROC) analysis for predicting STAS demonstrated higher area under the curve (AUC) in the model that used CTR (0.760, 95% confidence interval, 0.69–0.83) for predicting STAS than in the model that used long diameter of entire lesion (0.640).

Conclusions: CTR is the best CT sign for predicting STAS in small-sized lung adenocarcinoma. The ground glass ribbon is a newly found indicator and has the potential for predicting STAS.

Keywords: bronchial neoplasms, x-ray computed, tomography, adenocarcinoma of lung, spread through air spaces

HIGHLIGHTS

1. Higher consolidation tumor ratio, presence of ground glass ribbons, satellites, pleural connection, and unclear tumor–lung interface are predictive CT features of STAS in small-sized adenocarcinoma.
2. During the follow-up of lung nodules, the ground glass ribbon sign is regarded as a new feature, although there is no increase in the entire size or solid component, arising suspicion for cancer with STAS.
3. In small-sized STAS-positive adenocarcinomas that are present near the interlobular fissure, the disseminated foci can spread along the congenital defect of the interlobar fissure towards the adjacent lung lobe.

INTRODUCTION

The concept of spread through air spaces (STAS) is regarded as an additional pattern of invasion of lung cancer proposed by the World Health Organization classification of lung tumors in 2015. It consists of micropapillary clusters, solid nests, or single cells beyond the edge of the tumor invading into the air spaces surrounding the lung parenchyma (1). Validation studies on STAS considered it as a significant prognostic factor for distant and locoregional recurrence in patients undergoing limited resection, which decreased the overall survival in patients with lung cancers (2–5). STAS is an insidious invasive pattern that is not visible to pathologists on gross examination and to surgeons on external examination of tumor specimen at the time of surgery. So far, it remained unknown as to which imaging methods can be used for preoperative detection of it. For small-sized lung adenocarcinoma (less than or equal to 2 cm), limited resection can be usually performed, and its precise preoperative prediction of STAS on computed tomography (CT) before surgery remains crucial and challenging. This enables chest surgeons to change the treatment strategy from wedge resection to lobectomy, thereby reducing the recurrence rate. We hypothesize that some CT morphological predictors can predict STAS of small-sized lung adenocarcinoma before surgery, so as to avoid inappropriate sublobectomy of those patients. We performed comprehensive imaging and pathological statistical analysis to determine the imaging predictors predicting STAS in small-sized lung adenocarcinoma.

MATERIALS AND METHODS

This study has been approved by the institutional review board of Huadong Hospital, and patients' informed consent was waived off due to retrospective nature of the study design.

Abbreviations: CT, Computed tomography; STAS, Spread through air spaces; CTR, Consolidation tumor ratio; AUC, Area under the curve; ROC Receiver operating characteristic; mGGNs, Mixed ground-glass nodules; EGFR, Epidermal growth factor receptor; pGGNs, Pure ground-glass nodules.

Study Population

From January 2017 to May 2019, all consecutive patients at our institution were recruited, who underwent curative surgical resection and pathologically diagnosed with small-sized primary lung adenocarcinoma, which were staged T1–2 compliant with the eighth edition of the tumor, node, and metastasis (TNM) classification (6). A total of 257 patients with pathologically confirmed small-sized adenocarcinoma (equal or less than 2 cm in diameter) were included. The exclusion criteria were as follows: (1) patients who underwent preoperative neoadjuvant chemotherapy (n = 15); (2) with a time interval more than 3 months between the last CT examination and surgical resection, or who did not undergo CT examination in our hospital (n = 45); and (3) with serious breathing artifacts on CT image (n = 7). The flowchart of patients' selection was shown in **Figure 1**.

The information regarding the following parameters were collected from the database: (1) patient characteristics (such as age, gender, smoking status, tumor markers); (2) surgical methods (pneumonectomy, lobectomy, segmentectomy, or wedge resection); (3) pathological findings (composition, lymph node metastasis, pleural/vessel invasion, STAS); (4) epidermal growth factor receptor (EGFR) mutations; and (5) CT characteristics.

Pathological Analysis

Pathological diagnosis and categorization of adenocarcinoma were done based on the 2011 edition of pulmonary adenocarcinoma classification (7). Surgically resected specimens were fixed in 10% formalin, placed in paraffin to block, sectioned into thin sections, and then stained with hematoxylin and eosin. Pathological analysis was performed by a pathologist with 32 years of experience (Li Xiao). STAS was considered to exist when the micropapillary clusters, solid nests, or single cells spread within the air spaces beyond the edge of the main tumor according to the 2015 WHO classification (8). Tumor cells that spread through the mucus were distinguished from STAS, and the edge of the adenocarcinoma with mucinous characteristics was defined as alveolar space filled with mucin. EGFR mutation was evaluated in all participants.

CT Acquisition and Analysis

Chest CT scans were obtained with 64-slice Discovery CT750 HD (GE Healthcare) and 64-slice GE Light speed VCT using similar protocols, which were as follows: 1.25-mm slice thickness with a 1.25-mm reconstruction interval; pitch of 0.984; tube voltage, 120 kVp; tube current, 250 mAs; and bone reconstruction kernel. All images were reviewed and measured with a standard lung window (window width, 1,500 HU; window level, −500 HU) and a mediastinal window (window width, 350 HU; window level, 50 HU). All lesions were measured on the maximum plane of axial images.

The size of the entire lesion was defined as the average of long and short axial diameters, and all the measurements were rounded to the nearest millimeter according to the 2017 guidelines for management of incidental pulmonary nodules

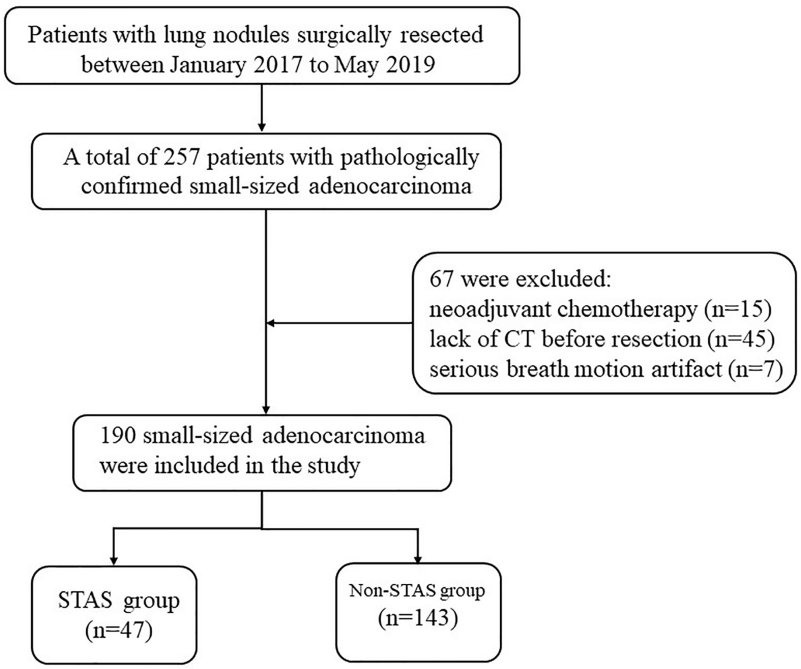

FIGURE 1 | Flowchart of patient selection procedure. STAS, spread through air spaces; CT, computed tomography.

from the Fleischner Society (9). All lesions with long axial diameters were measured on the maximum transverse reconstructed images. For mixed ground-glass nodules (mGGNs), the size of the solid components was measured using the same method as that of a mediastinal window. The maximum long diameter was used to define the TNM stage. The consolidation tumor ratio (CTR) was defined as the proportion of maximum consolidation diameter divided by the maximum tumor diameter.

The morphological characteristics of the nodules such as nodule density (solid, part solid, or pure ground glass), location, shape (round or oval, irregular), vascular change (normal, convergent or dilated), and cystic air spaces were included. Air spaces were defined as containing congenital cysts, emphysematous bullae, and bronchiectasis airways, which in turn were comprised of bubble-like lucencies and air bronchogram simultaneously.

The edge features of the lesions were as follows: (1) ground glass ribbon sign is a CT finding with a band-shaped ground glass opacity and blurred edge, which was emitted from the edge of the nodule and extended to the adjacent lung. If the lesion was present close to the visceral pleura, then it reaches the adjacent visceral pleura, without pleura thickening, pulling, or indentation; (2) tumor–lung interface: clear or unclear; (3) lobulation: is defined as a wavy or scalloped configuration of the edge of the nodule; and (4) spiculation sign: is defined as the presence of strands with soft tissue density that extends from the margin of the nodule into the lung.

Nodule-pleural types: (1) no connection, (2) attachment, with or without indentation, and (3) closeness through ground glass ribbon or spiculation, with or without traction. Morphological analysis was performed by two radiologists with nine and 15 years of experience in chest radiologic diagnosis (Lin Qi and Ming Li), and were blinded to the results of the pathological results. Any disagreements between them were resolved by reaching a consensus.

Statistical Analysis

Statistical analysis was carried out by SPSS 22.0 software and GraphPad Prism. The values were described as means ± standard deviation (SD) or sample rate. The normality of variables was tested using Shapiro–Wilk test. For categorical variables, the data between the two groups were compared by Pearson's chi-squared test and Fisher's exact test. For continuous variables, the data were compared by unpaired t test or Mann–Whitney U test. Binary logistic analysis for multivariate regression analysis was performed to identify independent predictors of adenocarcinoma with STAS. Variables with p values less than 0.1 by pairwise comparison were included in multivariate analysis. ROC analysis and Youden index were used to determine the cutoff value of CTR for predicting adenocarcinomas with STAS. For binary logistic analysis and ROC analysis, the nodular density of the lesions was divided into two types: solid nodules and subsolid nodules; the satellite lesions into present and absent types; and nodule-pleural relationships were divided into connection and non-connection types. The AUCs of the predictive CT features were compared by

DeLong test. A p value of less than 0.05 was considered to be significant.

RESULTS

Demographics, Surgical, and Pathological Data

Demographics, surgical strategies, and pathological data were presented in **Table 1**. One hundred and ninety patients with small-sized lung adenocarcinoma were finally enrolled in our study, which included 47 patients with STAS and 143 patients without STAS. The mean age of the patients was 55 ± 14 years and included 112 males and 78 females. Fifty-six participants were heavy smokers (>30 packs/year and quit smoking within the past 15 years). Seventy-one (37.4%) participants underwent sublobar resection, and 119 (62.6%) accepted lobectomy or pneumonectomy. There were no significant differences between STAS and non-STAS groups with regard to age, sex, heavy smokers, and surgery strategy. Significant differences between the two groups were observed in predominant histologic subtypes, where acinar and lepidic are the most common predominant subtypes in the non-STAS group, while papillary, micropapillary, and solid subtypes were more commonly observed in the STAS group. There was no significant difference observed in cribriform subtype between the two groups. Vascular (p = 0.001) and pleural invasion (p < 0.0001) were the most commonly observed in adenocarcinomas with STAS patients. No significant difference was present in EGFR mutations.

CT Characteristics of Two Groups

CT characteristics of all lesions in STAS and non-STAS groups were shown in **Table 2**. No significant differences were shown in the long axial diameter of entire tumor and solid component, but a statistically significant difference was observed in CTR between the STAS and non-STAS groups (0.9 ± 0.2 *vs.* 0.6 ± 0.4, p = 0.0001). Only one case (1/47, 2.1%) in the STAS group showed pure ground glass density (**Figure 2**), while 32 cases (32/143, 22.4%) in the non-STAS had pure ground glass nodules (pGGNs, p = 0.0007). The number of SNs in the STAS group was more than that in non-STAS group (61.7 *vs.* 28.7%, p < 0.0001). The number of mGGNs showed no significant differences between the two groups.

There were no significant differences regarding lobe location, shape, lobulation, and vascular changes. Spiculation was more frequently observed in the STAS groups (72.3 *vs.* 40.6%, p = 0.0001). The ground glass ribbon sign and the unclear tumor–lung interface were more commonly observed in the STAS group than that in non-STAS group (68 *vs.* 5.6%, p < 0.0001; 31.9 *vs.* 16.1%, p = 0.019). In the STAS group, there were more GGNs and solid satellites around the tumor than those in the non-STAS group (19.4 *vs.* 0, p < 0.0001; 14.9 *vs.* 2.1%, p = 0.003). More STAS lesions had attachment to the visceral pleura than non-STAS lesions (31.9 *vs.* 9.1%, p = 0.0001) (**Figure 3**).

CT Characteristics for Predicting STAS

The imaging features of STAS were evaluated by conducting multivariate logistic analysis (**Table 3**) and receiver operating characteristic curve analysis. Variables with p values of less than 0.10 in univariate analysis were included in multivariate logistic analysis, which included CTR, shape, spiculation, cystic airspaces, ground glass ribbons, tumor–lung interface, nodule density, satellite lesions, and pleural connection (**Figure 4**). CTR and nodule density showed significant correlation, so CTR was separately listed by establishing two regression models. In model 1, the presence of cystic airspaces, ground glass ribbon sign, unclear tumor–lung interface, pleural connection, and CTR were considered as predictive factors in STAS patients (p < 0.05). In model 2 that included CTR and nodule density simultaneously, the predictive factors were similar to the results of model 1.

The ROC analysis for predicting STAS demonstrated higher area under the curve (AUC) in the model that used CTR (0.760,

TABLE 1 | Demographics, pathological analysis, and types of surgery of participants with pathologically T1a and T1b lung adenocarcinoma.

	Total (n = 190)	STAS (n = 47)	Non-STAS (n = 143)	t or z value	p
Age (years)	55 ± 14	56 ± 8	53 ± 11	1.778	0.100
Male, n [%]	112 [58.9]	29 [61.7]	83 [58]	0.443	0.658
Heavy smoke, n [%]	56 [29.5]	16 [34.0]	37 [25.9]	1.083	0.279
Surgery				1.933	0.05
Sublobar resection, n [%]	71 [37.4]	12 [25.6]	59 [41.3]		
Lobectomy or pneumonectomy, n [%]	119 [62.6]	35 [74.5]	84 [58.7]		
Pathology					
Predominant histologic subtypes					
Lepidic, n [%]	30 [15.8]	0	30 [21.0]	–	0.0001***
Acinar, n [%]	87 [45.8]	5 [10.6]	82 [57.3]	–	<0.0001****
Papillary or micropapillary, n [%]	38 [25.9]	27 [57.4]	11 [7.7]	7.398	<0.0001****
Solid, n [%]	26 [13.7]	12 [25.5]	14 [9.8]	2.724	0.006**
Cribriform, n [%]	9 [4.7]	3 [6.4]	6 [4.2]	–	0.692
Vascular invasion (+), n [%]	26 [13.7]	12 [25.6]	11 [7.7]	3.253	0.001**
Pleural invasion (+), n [%]	31 [16.3]	19 [40.4]	17 [11.9]	4.331	<0.0001****
EGFR mutation (+), n [%]	78 [41.1]	12 [25.5]	66 [46.2]	0.493	0.013*

*STAS, spread through air spaces; EGFR, epidermal growth factor receptor. Significant level marks: p < 0.05 *, p < 0.01 **, p < 0.001 ***, p < 0.0001 ****.*

TABLE 2 | CT characteristics of small-sized adenocarcinoma in STAS+ and STAS- groups.

	Total (n=190)	STAS (n=47)	Non-STAS (n=143)	t, F, or z value	p value
Measurements					
LD $_{entire}$ (mm)	15 ± 4	16 ± 4	14 ± 3	4.025	0.055
LD $_{solid}$ (mm)	10 ± 6	15 ± 5	9 ± 6	2.408	0.122
CTR	0.7 ± 0.4	0.9 ± 0.2	0.6 ± 0.4	23.868	0.0001***
Nodule density					
pGGNs	33 [17.4]	1 [2.1]	32 [22.4]	–	0.0007***
mGGNs	87 [45.8]	17 [36.2]	70 [49.0]	1.526	0.127
SNs	70 [36.8]	29 [61.7]	41 [28.7]	4.073	<0.0001****
Location (lobe)				0.588	0.557
Upper lobes	94 [49.5]	25 [53.2]	69 [48.3]		
Non-upper lobes	76 [40]	22 [46.8]	74 [51.7]		
Location (field)				0.326	0.745
Central	69 [36.3]	18 [38.3]	51 [35.7]		
Peripheral	121 63.7]	29 [61.7]	92 [64.3]		
Shape				1.849	0.064
Round or oval	95 [50]	29 [61.7]	66 [46.2]		
Irregular	95 [50]	18 [38.3]	77 [53.8]		
Vascular change				0.602	0.547
normal	106 [55.8]	28 [59.6]	78 [54.5]		
convergent	84 [44.2]	19 [40.4]	65 [45.5]		
Cystic airspaces, n [%]	73 [38.4]	11 [23.4]	62 [43.4]	2.440	0.015*
Edge features					
Ground glass ribbon sign	34 [17.9]	22 [46.8]	12 [8.4]	5.961	<0.0001****
Unclear tumor-lung interface	38 [20]	15 [31.9]	23 [16.1]	2.354	0.019*
Lobulation	70 [36.8]	16 [34.0]	54 [37.8]	0.459	0.647
Spiculation	92 [48.4]	34 [72.3]	58 [40.6]	3.782	0.0002***
Satellite lesions					
Absent	171 [90]	31 [66.0]	140 [97.9]	–	<0.0001****
Ground glass satellites	9 [4.7]	9 [19.4]	0	–	<0.0001****
Solid satellites	10 [5.3]	7 [14.9]	3 [2.1]	–	0.003**
Nodule-pleural types					
No connection	93 [48.9]	11 [23.4]	82 [57.3]	4.038	<0.0001****
Closeness	69 [36.3]	21 [44.7]	48 [33.6]	1.369	0.169
Attachment	28 [14.7]	15 [31.9]	13 [9.1]	3.83	0.0001***

*LD $_{entire}$, long diameter of entire tumor; LD $_{solid}$, long diameter of solid component; CTR, consolidation tumor ratio; STAS, spread through air spaces; pGGNs, pure ground glass nodules; mGGNs, mixted ground glass nodules; SNs, solid nodules. Significant level marks: p < 0.05 *, p < 0.01 **, p < 0.001 ***, p < 0.0001 ****.*

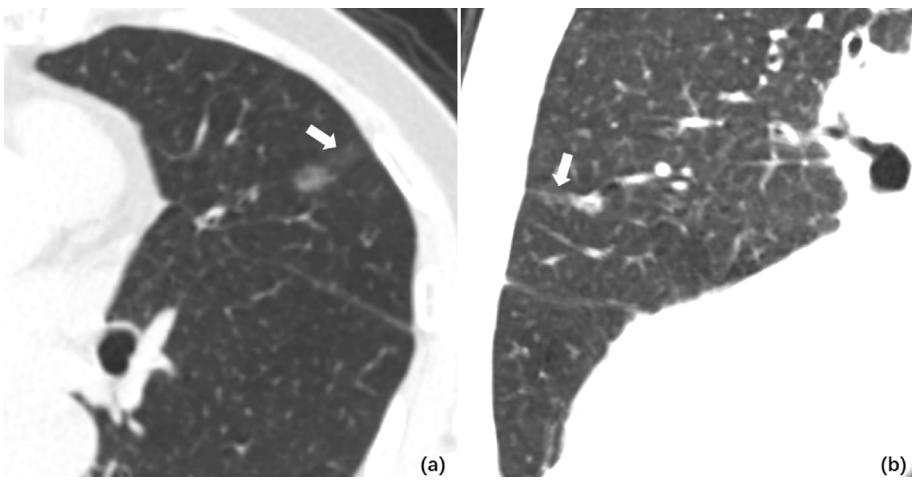

FIGURE 2 | **(A)** Axial CT image of pGGO performed STAS pathologically. A ground glass ribbon sign was observed on the margin of the lesion and extended to the adjacent costal parietal pleura (white arrow), which was defined as a CT finding of a band-shaped ground glass opacity with blurred edge that emits from the edge of the nodule and extends into the adjacent lung **(B)**. Multi-plane reconstruction with ground glass ribbon sign as the long axis. The shape of ribbon sign was displayed more clearly after adjusting the window width and level.

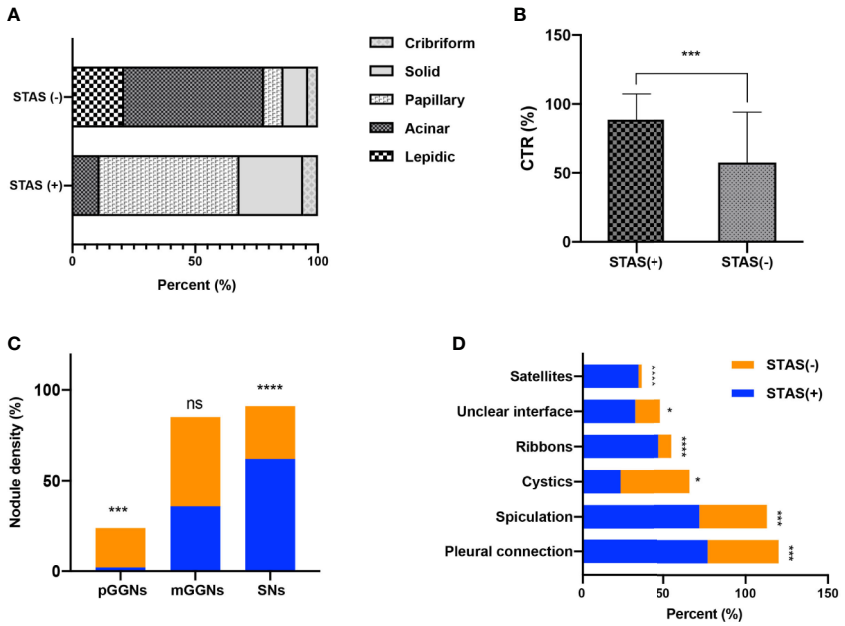

FIGURE 3 | Bar graph shows the comparison of predominant subtypes between STAS-positive and STAS-negative groups **(A)**; there is statistically significant difference in CTR between the two groups **(B)**; the number of SNs in STAS group is more than that in non-STAS group **(C)**; presence of spiculation, satellites, and ground glass ribbon sign, pleural attachment, and unclear tumor–lung interface was more common in STAS group **(D)**. *P<0.05; **P<0.01; ***P<0.001; ****P<0.0001.

TABLE 3 | Multivariable Logistic Analysis of radiologic predictors of adenocarcinoma with STAS.

	Model 1			Model 2		
	OR	**95% CI**	***p*-value**	**OR**	**95% CI**	***p*-value**
Nodule shapes	2.155	0.768–6.048	0.145	0.509	1.18–1.45	0.206
Spiculation	0.977	0.242–3.947	0.974	0.509	2.19–3.45	0.206
Cystic airspaces	13.781	3.751–50.63	0.001	0.062	0.02–0.25	0.001
Ground glass ribbon sign	0.114	0.029–0.454	0.002	8.468	2.03–35.32	0.003
Boundary	0.243	0.07–0.842	0.026	4.871	1.31–18.12	0.018
Satellite lesions	0.585	0.176–1.947	0.382	3.263	0.45–23.48	0.24
Pleural connection	0.183	0.059–0.563	0.003	5.829	1.80–18.93	0.003
Nodule density	–	–	–	0.146	0.00–2.34	0.086
CTR	0.01	0.001–0.173	0.001	0.003	0.00–0.10	0.001

CTR, consolidation tumor ratio; CI, confidence interval; OR, odds ratio.

95% confidence interval, 0.69–0.83) for predicting STAS than in the model that used long diameter of entire lesion (0.640). (**Figure 5**). There was no statistical significance in the differences between AUCs of CTR and diameter of entire lesion ($p < 0.05$).

DISCUSSION

STAS is recently recognized as an additional pattern of tumor invasion in lung adenocarcinoma and is considered as a major risk factor of recurrence in early stage lung adenocarcinoma patients when treated with limited resection (2, 3, 10–13). Kadota K et al. (2) have reported that the risk of recurrence, which included the 5-year cumulative incidence of recurrence, distant and locoregional recurrence, was significantly higher in patients with STAS-positive small-sized lung adenocarcinoma when compared to those with STAS-negative tumors. Therefore, retrospective analysis was conducted to those pathologically proved small-sized lung adenocarcinoma with and without STAS, exploring whether CT features could assist in predicting STAS before undergoing surgical procedures to decide tumor margin in conditions of limited resection and guide the choice of postoperative treatment strategies (8, 14, 15).

Our study confirmed that STAS-positive small-sized lung adenocarcinomas had distinct morphologic, pathologic, and genetic characteristics, and CTR was an important imaging

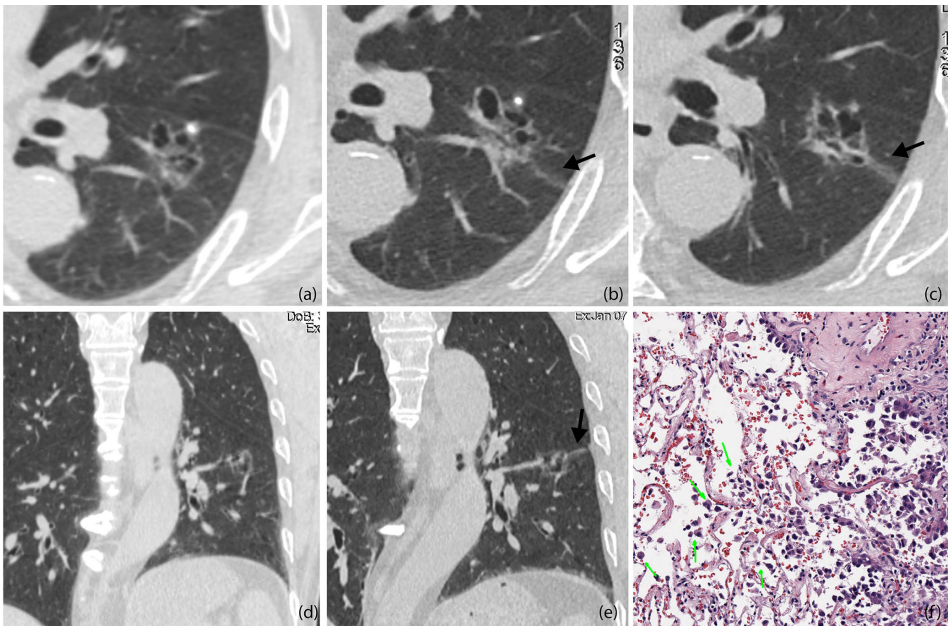

FIGURE 4 | **(A, D)** Baseline axial **(A)** and coronal **(D)** CT images of STAS-positive adenocarcinoma in a 51-year-old man. An irregular ground glass nodule with multiple cystic cavities was detected with clear edges, so he was recommended 6–12 months follow-up **(B, C, E)**. Axial CT images on the 8-month follow-up **(B, C)**. The entire size of the lesion did not change, but some cysts were larger than before, and a ground glass ribbon sign was newly found on the edge of the lesion (black arrow), which was defined as a CT finding of a band-shaped ground glass opacity with blurred edge that emits from the edge of the nodule and extends into the adjacent lung **(E)**. Coronal reconstructed image clearly shows the ribbon sign, stretching to the adjacent visceral pleural (black arrow) **(F)**. The patient was recommended lung lobe resection and was confirmed invasive adenocarcinoma with STAS pathologically. Photomicrograph shows single cell pattern STAS consisting of scattered discohesive single cells (green arrow).

predictor of STAS, which was similar to the results of previous studies (4, 10, 11, 16, 17). Pathologically, the predominant subtypes of STAS positive adenocarcinoma included papillary, micropapillary and solid, while that of STAS negative tumors included lepidic and acinar. The vascular and pleural invasion and EGFR mutation were regarded as the more common features in STAS positive adenocarcinoma.

Recent studies confirmed that direct signs of STAS are far beyond the spatial resolution of state-of-art CT scanner, even on high-resolution CT images, which demonstrating that the prediction of STAS on CT images should be performed by indirect signs rather than direct visualization (18). Kim et al. reported a larger series of STAS+ adenocarcinomas (n = 94) containing different tumor sizes and pathological stages and suggested that the percentage of solid component was an independent predictor of STAS and a cut-off value of 90% with a sensitivity of 89.2% and a specificity of 60.3%. Our study focuses on the morphological features of small-sized lung adenocarcinoma positive for STAS. Therefore, there are some similarities as well as differences in conclusions due to the different research groups. Similar to Kim et al., we found that CTR (equivalent to percentage of solid component in Kim's study) was the best predictive CT feature with a cut-off value of 83% and with a sensitivity of 91.5%, a specificity of 62.9%. The diagnostic efficacy of CTR in the two studies is similar, indicating that even if the study populations are different, CTR shows stable prediction performance in predicting STAS. In our study, no differences were found in maximum diameters of the entire lesion and solid component between tumors positive for STAS and that negative for STAS, while Kim et al. reported that the maximum diameter of solid component was greater in STAS-positive adenocarcinoma. The reason might be that our study limited the maximum diameter of the included lesions (less than 2 cm in diameter), while Kim's study did not. In our cohort, 61.7% of STAS-positive tumors were solid nodules (CTR = 1), while 71.3% of STAS-negative lesions were non-solid lesions, indicating that solid small-sized tumors were more likely accompanied with STAS. This suggested the requirement of partial resection with enlarged margin or lobe resection.

Several studies (19–21) showed that satellite centrilobular nodules, branching opacities, typically with ill-defined margins and ground glass attenuation, are discriminatory CT characteristics that are suggestive of macroscopic tumor spread through airways. Similar to those studies, our study confirmed that several signs on CT images could predict STAS in small-sized primary lung adenocarcinoma, including presence of spiculation, satellites, ground glass ribbon sign, pleural attachment, and unclear tumor–lung interface. Among these features, some edge characteristics, such as ground glass ribbon sign, spiculation, and ground glass satellites demonstrated strong

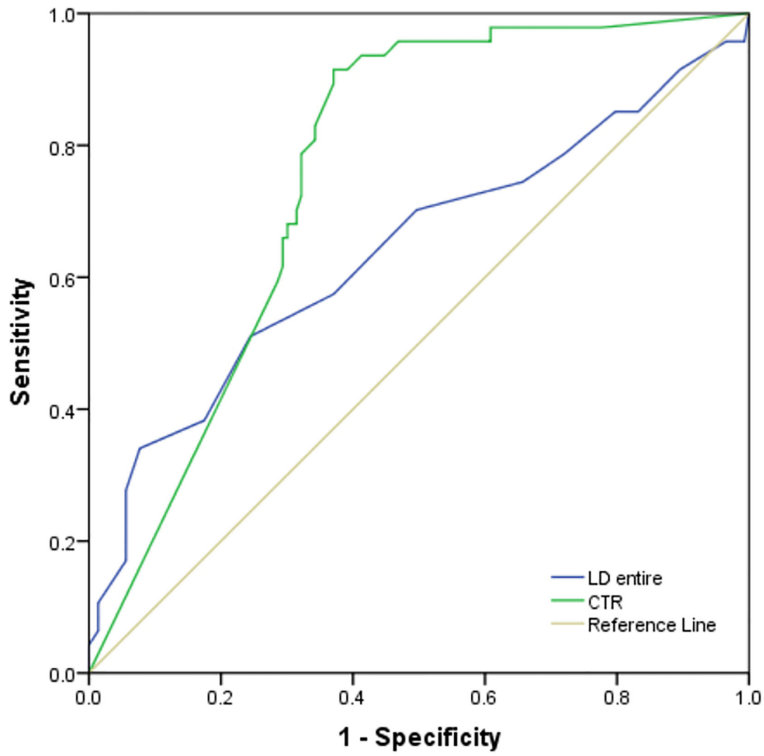

FIGURE 5 | The ROC analysis for predicting STAS demonstrated higher area under the curve (AUC) in the model that used CTR (0.760, 95% confidence interval, 0.69–0.83) for predicting STAS than in the model that used long diameter of entire lesion (0.640).

discriminative power than the remaining ones. Ground glass ribbon sign is the newly proposed CT feature in our study for indicating STAS and was defined as a CT finding of a band-shaped ground glass opacity with blurred edge that emits from the edge of the nodule and extends into the adjacent lung. Pathologically, this sign may be related to decreased air spaces in the distal part of the alveoli that is caused by the obstruction of the surrounding lung parenchyma beyond the tumor, or the obstruction of terminal bronchiolar. The predominant composition of STAS-negative small-sized adenocarcinoma was usually considered to be the lepidic subtype, and it was usually well-defined, without terminal bronchiolar obstruction and corresponding ground glass ribbon sign. While in STAS-positive adenocarcinoma, micropapillary clusters and solid nests surrounding the air spaces could block the marginal alveolar cavities, leading to a decrease in the air content of the distal alveolar cavities. Several studies reported that STAS does not occur in pGGNs (10, 18–21).

In our study, only one patient with pGGO was pathologically confirmed to have STAS, and a ground glass ribbon sign was observed on the margin of the lesion, which was extended to the adjacent costal parietal pleura. The reason for this might be that resection was more likely performed for partly solid or solid nodules, and most of the pGGOs were recommended to follow-up until they become partially solid nodules before undergoing resection. We alluded that in the setting of GGO adenocarcinoma the Ribbon sign might be an early marker of STAS before a solid component develops. This might be potentially used as an indication for early resection of slowly growing GGOs. However, future multicenter validation studies are needed to consolidate our findings. Masai et al. (3) demonstrated that STAS and tumor margins smaller than 1 cm are significant risk factors for local recurrence in early stage lung cancer after limited resection. In our study, we observed on pathological sections that tumor cells of STAS-positive small-sized adenocarcinoma can spread to the adjacent lung lobe through the congenital pores of the interlobular fissure (**Figure 6**). It can be shown that pathological STAS is one of the risk factors for metastasis of early adenocarcinoma after local pneumonectomy.

Our study has several limitations. Firstly, this was a retrospective single-center study, and the sample size included was small. So, comparative studies with a large number of pathological and CT images are needed to confirm these assumptions. Secondly, we only included adenocarcinomas in our study. Different histologic types of lung cancer and some inflammatory granulomas that are easily confused with lung cancer should also be included in the future studies. Thirdly, due to a shorter postoperative follow-up time, our study did not

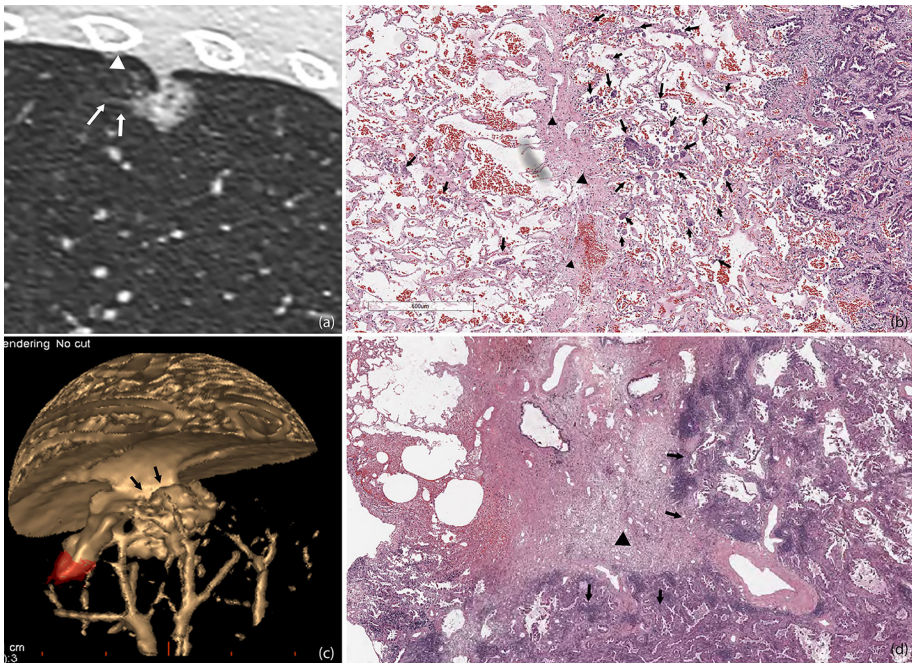

FIGURE 6 | STAS in a 45-year-old man with micropapillary predominant subtype of invasive adenocarcinoma **(A)**. Multiplanar reconstructed CT image (width, 1,500 HU; level, –600 HU) shows a ground glass-density spiculation extending into the adjacent lungs (arrow), and several ground glass-density satellite foci with a diameter of 1–2 mm were observed at the edge of the lesion (white triangle) **(B)**. Photomicrograph shows multiple solid nests clusters alveolar disseminations at the edge of one side of the lesion (arrow), spreading through the interlobular fissure (black triangle) to the alveolar cavities of the adjacent pulmonary lobe **(C)**. Volume render reconstructed image shows visceral pleural indentation **(D)**. Photomicrograph shows visceral pleural invasion, indentation, and thickening.

report the prognostic information of the two groups. Future research will assess the prognostic impact of STAS and local recurrence in stage I lung adenocarcinoma.

In conclusion, CTR is the most robust CT sign for predicting STAS in small-sized lung adenocarcinoma. Other CT features also have good diagnostic efficacy factors including spiculation, the ground glass ribbon sign, pleural connection, and satellites. Among them, the ground glass ribbon is a newly found indicator and has the potential for predicting STAS.

DATA AVAILABILITY STATEMENT

The original contributions presented in the study are included in the article/supplementary materials. Further inquiries can be directed to the corresponding author.

ETHICS STATEMENT

The studies involving human participants were reviewed and approved by the institutional review board of Huadong Hospital, and patients' informed consent was waived off due to retrospective nature of the study design. Written informed consent for participation was not required for this study in accordance with the national legislation and the institutional requirements.

AUTHOR CONTRIBUTIONS

LQ and KX: manuscript writing and data analysis. YC: pathology diagnosis. JL: data organizing and analysis. XL: manuscript revision. ML: research decision. All authors contributed to the article and approved the submitted version.

FUNDING

This study was supported by the National Natural Science Foundation of China (61976238); National Natural Science Foundation of China (82071897); Research Fund of Huadong Hospital (2019lc008); Shanghai Municipal Health Commission (20204Y0299); Medical Imaging Key Program of Wise Information Technology of 120, Health Commission of Shanghai 2018ZHYL0103 (ML), "Future Star" of famous doctors' training plan of Fudan University.

REFERENCES

1. Travis WD, Brambilla E, Nicholson AG, Yatabe Y, Austin JHM, Beasley MB, et al. The 2015 World Health Organization Classification of Lung Tumors: Impact of Genetic, Clinical and Radiologic Advances Since the 2004 Classification. *J Thorac Oncol* (2015) 10:1243–60. doi: 10.1097/JTO.0000000000000630
2. Kadota K, Nitadori J-I, Sima CS, Ujiie H, Rizk NP, Jones DR, et al. Tumor Spread through Air Spaces is an Important Pattern of Invasion and Impacts the Frequency and Location of Recurrences after Limited Resection for Small Stage I Lung Adenocarcinomas. *J Thorac Oncol* (2015) 10:806–14. doi: 10.1097/JTO.0000000000000486
3. Masai K, Sakurai H, Sukeda A, Suzuki S, Asakura K, Nakagawa K, et al. Prognostic Impact of Margin Distance and Tumor Spread Through Air Spaces in Limited Resection for Primary Lung Cancer. *J Thorac Oncol* (2017) 12:1788–97. doi: 10.1016/j.jtho.2017.08.015
4. Blaauwgeers H, Flieder D, Warth A, Harms A, Monkhorst K, Witte B, et al. A Prospective Study of Loose Tissue Fragments in Non-Small Cell Lung Cancer Resection Specimens: An Alternative View to "Spread Through Air Spaces". *Am J Surg Pathol* (2017) 41:1226. doi: 10.1097/PAS.0000000000000889
5. Dai C, Xie H, Su H, She Y, Zhu E, Fan Z, et al. Tumor Spread through Air Spaces Affects the Recurrence and Overall Survival in Patients with Lung Adenocarcinoma >2 to 3 cm. *J Thorac Oncol* (2017) 12:1052–60. doi: 10.1016/j.jtho.2017.03.020
6. Detterbeck FC, Chansky K, Groome P, Bolejack V, Crowley J, Shemanski L, et al. The IASLC Lung Cancer Staging Project: Methodology and Validation Used in the Development of Proposals for Revision of the Stage Classification of NSCLC in the Forthcoming (Eighth) Edition of the TNM Classification of Lung Cancer. *J Thorac Oncol* (2016) 11:1433–46. doi: 10.1016/j.jtho.2016.06.028
7. Travis WD, Brambilla E, Noguchi M, Nicholson AG, Geisinger K, Yatabe Y, et al. International Association for the Study of Lung Cancer/American Thoracic Society/European Respiratory Society: international multidisciplinary classification of lung adenocarcinoma: executive summary. *Proc Am Thorac Soc* (2011) 8:381–5. doi: 10.1513/pats.201107-042ST
8. Warth A, Beasley MB, Mino-Kenudson M. Breaking New Ground: The Evolving Concept of Spread through Air Spaces (STAS). *J Thorac Oncol* (2017) 12:176–8. doi: 10.1016/j.jtho.2016.10.020
9. Macmahon H, Naidich DP, Goo JM, Lee KS, Leung ANC, Mayo JR, et al. Guidelines for Management of Incidental Pulmonary Nodules Detected on CT Images: From the Fleischner Society 2017. *Radiology* (2017) 284:228–43. doi: 10.1148/radiol.2017161659
10. Kim SK, Kim TJ, Chung MJ, Kim TS, Lee KS, Zo JI, et al. Lung Adenocarcinoma: CT Features Associated with Spread through Air Spaces. *Radiology* (2018) 289:831–40. doi: 10.1148/radiol.2018180431
11. Shiono S, Yanagawa N. Spread through air spaces is a predictive factor of recurrence and a prognostic factor in stage I lung adenocarcinoma. *Interact Cardiovasc Thorac Surg* (2016) 23:567–72. doi: 10.1093/icvts/ivw211
12. Warth A. Spread through air spaces (STAS): a comprehensive update. *Transl Lung Cancer Res* (2017) 6:501–7. doi: 10.21037/tlcr.2017.06.08
13. Morimoto J, Nakajima T, Suzuki H, Nagato K, Iwata T, Yoshida S, et al. Impact of free tumor clusters on prognosis after resection of pulmonary adenocarcinoma. *J Thorac Cardiovasc Surg* (2016) 152:64–72. doi: 10.1016/j.jtcvs.2016.03.088
14. Ma K, Zhan C, Wang S, Shi Y, Jiang W, Wang Q, et al. Spread Through Air Spaces (STAS): A New Pathologic Morphology in Lung Cancer. *Clin Lung Cancer* (2019) 20:e158–62. doi: 10.1016/j.cllc.2018.10.007
15. Kalemkerian GP, Loo BW, Akerley W, Attia A, Bassetti M, Boumber Y, et al. NCCN Guidelines Insights: Small Cell Lung Cancer, Version 2.2018. *J Natl Compr Canc Netw* (2018) 16:1171–82. doi: 10.6004/jnccn.2018.0079
16. Morales-Oyarvide V, Mino-Kenudson MJPI. Tumor islands and spread through air spaces: Distinct patterns of invasion in lung adenocarcinoma. *Pathol Int* (2016) 66:1–7. doi: 10.1111/pin.12368
17. Naidich DP. Is Spread of Tumor through Air Spaces a Concern for Interpreting Lung Nodules on CT Images? *Radiology* (2018) 289:841–2. doi: 10.1148/radiol.2018181764
18. Ledda RE, Milanese G, Gnetti L, Borghesi A, Sverzellati N, Silva M, et al. Spread through air spaces in lung adenocarcinoma: is radiology reliable yet? *J Thorac Dis* (2019) 11:S256–61. doi: 10.21037/jtd.2019.01.96
19. de Margerie-Mellon C, Onken A, Heidinger BH, VanderLaan PA, Bankier AA. CT Manifestations of Tumor Spread Through Airspaces in Pulmonary Adenocarcinomas Presenting as Subsolid Nodules. *J Thorac Imaging* (2018) 33:402–8. doi: 10.1097/RTI.0000000000000344
20. Toyokawa G, Yamada Y, Tagawa T, Kamitani T, Yamasaki Y, Shimokawa M, et al. Computed tomography features of resected lung adenocarcinomas with spread through air spaces. *J Thorac Cardiovasc Surg* (2018) 156:1670–6. doi: 10.1016/j.jtcvs.2018.04.126
21. Akira M, Atagi S, Kawahara M, Iuchi K, Johkoh T. High-resolution CT findings of diffuse bronchioloalveolar carcinoma in 38 patients. *Am J Roentgenol* (1999) 173:1623–9. doi: 10.2214/ajr.173.6.10584811

Conflict of Interest: The authors declare that the research was conducted in the absence of any commercial or financial relationships that could be construed as a potential conflict of interest.

frontiers in Oncology

ORIGINAL RESEARCH
published: 04 March 2021
doi: 10.3389/fonc.2021.608353

Morphological Subtypes of Tumor Spread Through Air Spaces in Non-Small Cell Lung Cancer: Prognostic Heterogeneity and Its Underlying Mechanism

Huikang Xie[1†], Hang Su[2†], Erjia Zhu[2†], Chang Gu[2], Shengnan Zhao[1], Yunlang She[2], Yijiu Ren[2], Dong Xie[2], Hui Zheng[2], Chunyan Wu[1], Chenyang Dai[2] and Chang Chen[2*]*

[1] Department of Pathology, Shanghai Pulmonary Hospital, Tongji University School of Medicine, Shanghai, China,
[2] Department of Thoracic Surgery, Shanghai Pulmonary Hospital, Tongji University School of Medicine, Shanghai, China

OPEN ACCESS

Edited by:
Chen Chen,
Central South University, China

Reviewed by:
Noriyoshi Sawabata,
Nara Medical University, Japan
Mari Mino-Kenudson,
Massachusetts General Hospital and Harvard Medical School, United States

***Correspondence:**
Chang Chen
chenthoracic@163.com
Chenyang Dai
daichenyang@tongji.edu.cn

[†]These authors have equally contributed to this work

Specialty section:
This article was submitted to Thoracic Oncology, a section of the journal Frontiers in Oncology

Received: 20 September 2020
Accepted: 15 January 2021
Published: 04 March 2021

Citation:
Xie H, Su H, Zhu E, Gu C, Zhao S, She Y, Ren Y, Xie D, Zheng H, Wu C, Dai C and Chen C (2021) Morphological Subtypes of Tumor Spread Through Air Spaces in Non-Small Cell Lung Cancer: Prognostic Heterogeneity and Its Underlying Mechanism. Front. Oncol. 11:608353. doi: 10.3389/fonc.2021.608353

Background: Tumor spread through air spaces (STAS) has three morphologic subtypes: single cells, micropapillary clusters, and solid nests. However, whether their respective clinical significance is similar remains unclear.

Methods: We retrospectively reviewed 803 patients with resected non-small cell lung cancer (NSCLC) from January to December 2009. Recurrence-free survival (RFS) and overall survival (OS) were compared among patients stratified by STAS subtypes. We also performed a prospective study of NSCLC resection specimens to evaluate the influence of a prosecting knife on the presence of STAS subtypes during specimen handling (83 cases).

Results: STAS was found in 370 NSCLCs (46%), including 47 single cell STAS (13%), 187 micropapillary cluster STAS (50%), and 136 solid nest STAS (37%). STAS-negative patients had significantly better survival than patients with micropapillary cluster STAS (RFS: $P < 0.001$; OS: $P < 0.001$) and solid nest STAS (RFS: $P < 0.001$; OS: $P < 0.001$), but similar survival compared with those with single cell STAS (RFS: $P = 0.995$; OS: $P = 0.71$). Multivariate analysis revealed micropapillary cluster (RFS: $P < 0.001$; OS: $P < 0.001$) and solid nest STAS (RFS: $P = 0.001$; OS: $P = 0.003$) to be an independent prognostic indicator, but not for single cell STAS (RFS: $P = 0.989$; OS: $P = 0.68$). Similar results were obtained in subgroup analysis of patients with adenocarcinoma. The prospective study of NSCLC specimens suggested that 18 cases were considered as STAS false-positive, and most were singe cell pattern (13/18, 72%).

Conclusions: Single cell STAS was the common morphologic type of artifacts produced by a prosecting knife. A precise protocol of surgical specimen handling is required to minimize artifacts as much as possible.

Keywords: spread through air spaces, spread through a knife surface, non-small cell lung cancer, prognosis, artifact

INTRODUCTION

Tumor spread through air spaces (STAS) was added as a novel invasive pattern of lung adenocarcinoma (ADC) in the 2015 World Health Organization (WHO) classification (1). Subsequently, numerous studies consistently demonstrated STAS to be a prognostic risk factor for patients with ADC (2–12). This adverse impact extended to cases of squamous cell carcinoma (SQCC) and pleomorphic carcinoma, among others (13–16). Thus, STAS was recognized as a unique invasive type of non-small cell lung cancer (NSCLC) and attracted tremendous interests.

According to the 2015 WHO classification, STAS has three morphologic subtypes: single cells, micropapillary clusters, and solid nests. Our previous study showed that micropapillary cluster STAS was the most common type in ADC (6), and other studies found SQCC only featured solid nest STAS (13–15), which suggested the potential heterogeneity among STAS subtypes. Three STAS patterns were considered as one group in all published studies concerning clinicopathologic features and prognostic effect. Thus, it was unclear whether each subtype had distinct clinical behaviors.

In this study, we used a large retrospective cohort of patients with resected NSCLC to investigate the clinical characteristics of three STAS subtypes, with a focus on the survival outcomes. If differences among subtypes were observed, the potential mechanism was also explored.

MATERIALS AND METHODS

Study Cohort

The institutional review board of Shanghai Pulmonary Hospital approved this study (No. K17-159). We reviewed 1,123 patients with lung cancer who underwent surgical resection at our hospital between January 1, 2009, and December 31, 2009. Patients with neoadjuvant therapy, multiple primary lung cancers, small cell lung cancer, metastatic tumor, minimally invasive adenocarcinoma, and adenocarcinoma *in situ* were excluded. After applying these criteria, a total of 803 patients with NSCLC were identified (**Figure 1A**). The tumors were classified according to the 2015 WHO classification and staged on the basis of the eighth edition of the TNM classification (1, 17). Patients' clinical data were retrospectively extracted from electronic medical records. We also prospectively included 83 cases of NSCLC resection specimens from August 1, 2017 to August 15, 2017, according to the same inclusion and exclusion criteria to evaluate the influence of a prosecting knife on the presence of STAS subtypes during specimen handling (**Figure 1B**).

Histopathologic Evaluation of STAS Subtypes

Tumor specimen slides were microscopically evaluated by two pathologists (H.X. and S.Z.) who were not aware of the clinical data. STAS was defined as tumor cells observed within air spaces in the surrounding lung parenchyma beyond the edge of the main tumor (1). The methods to distinguish STAS from artifacts and alveolar macrophages reported by Kadota et al. were adopted in this study (2). If diagnosis was still uncertain, immunohistochemistry for tumor cell marker (cytokeratin [AE1/AE3]) and macrophage marker (CD68) was performed.

STAS has three morphologic patterns: (1) single cell pattern (**Figures 2A, B**), defined as discohesive single tumor cells within air spaces; (2) micropapillary cluster pattern (**Figures 2C, D**), defined as papillary structures without central fibrovascular cores filling as an alveolus; and (3) solid nest pattern (**Figures 2E, F**), defined as solid collections of tumor cells within an alveolus. Two pathologists (H.X. and S.Z.) categorized STAS into single cell, micropapillary cluster, or solid nest subtype independently. If any disagreement occurred, consensus was achieved after discussion.

Survival Analyses for STAS Subtypes

The outcomes of interest were recurrence-free survival (RFS) and overall survival (OS), which were calculated using the Kaplan-Meier method and compared using the log-rank test among STAS subtype groups. Survival information was collected from outpatient clinic re-visit records (clinical, radiologic, and pathologic evaluation) and telephone follow-up through December 31, 2016. Multivariate survival analyses were conducted by using the Cox proportional hazards model to identify independent prognostic factors for RFS and OS. The

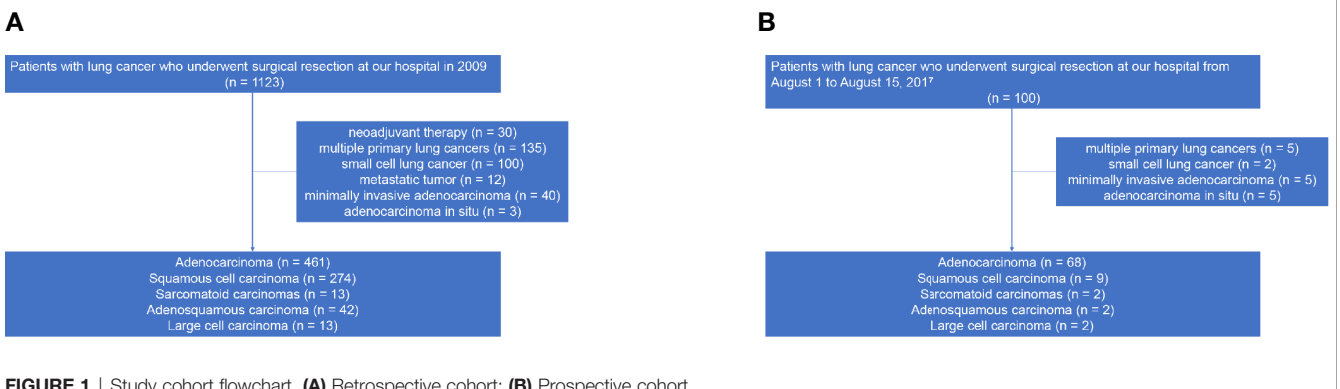

FIGURE 1 | Study cohort flowchart. **(A)** Retrospective cohort; **(B)** Prospective cohort.

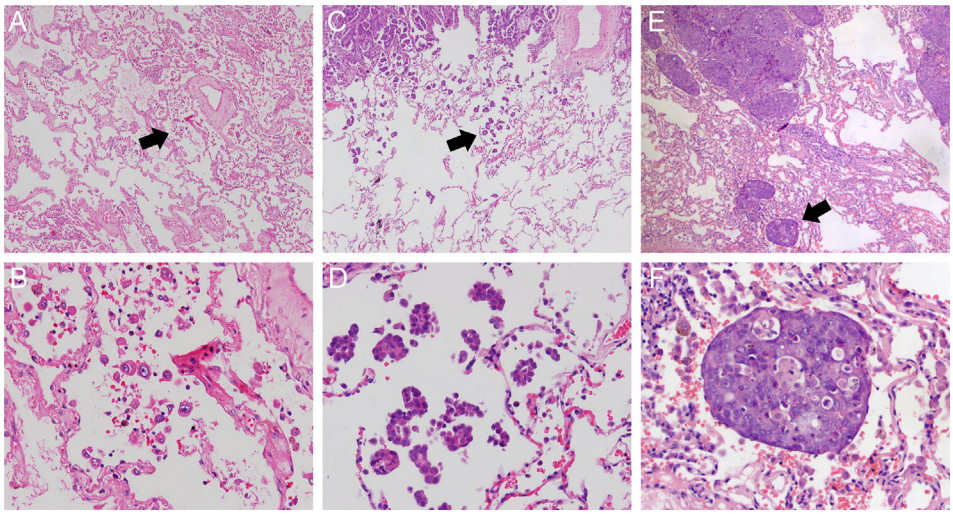

FIGURE 2 | Morphologic features of *STAS* including single cell pattern (original magnification: ×40 in **(A)** and ×200 in **(B)** micropapillary cluster pattern (original magnification: ×40 in **(C)** and ×200 in **(D)** and solid nest pattern (original magnification: ×40 in **(E)** and ×200 in **(F)**. STAS, spread through air spaces.

variables were examined first using univariate analysis, and those with P value < 0.1 were incorporated into a multivariate model. We also assessed the prognostic significance of STAS subtypes in patients with ADC.

Prospective Assessment of the Influence of a Prosecting Knife on STAS Subtypes

Two published studies suggested that STAS may partly be attributed to artifacts caused by a prosecting knife during specimen handling (18, 19). Our study also evaluated the influence of a prosecting knife on the presence of STAS subtypes. The same inclusion criteria used in the retrospective cohort were adopted to prospectively recruit patients with NSCLC who underwent surgery at our hospital between August 1, 2017, and August 15, 2017.

The lung cancer specimens were prosected and sampled according to the following protocol (**Figure 3A**): (1) the lung cancer specimen was cut at its largest diameter using a clean, long prosecting knife, thus dividing the sample into two; (2) one tissue piece was randomly selected and divided into two sections along the vertical direction of the first cut by using a second clean knife; and (3) all specimens were cut in a single continuous direction to avoid excessive tumor tissue contamination caused by drawing the knife back and forth. Eventually, two tissue blocks were obtained. The upper block contained normal lung tissue and then tumor tissue, and the lower block contained tumor tissue and then normal lung tissue.

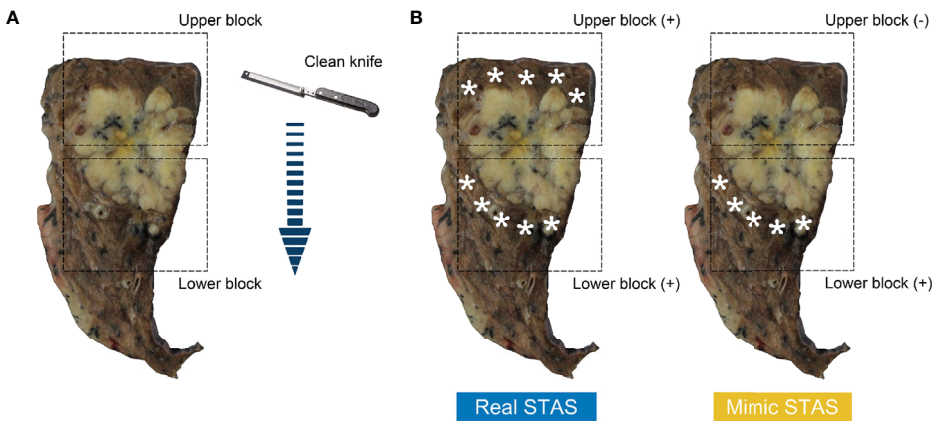

FIGURE 3 | Surface of cross-section from resected lung specimen after the first cut **(A)**; arrow indicates cutting path. Tissue blocks in the rectangular box contains normal lung tissue above tumor (upper block) and below tumor (lower block). The diagrams of the definition of real STAS and mimic STAS **(B)**; pentagram indicates displaced tumor cells in normal lung tissue. STAS, spread through air spaces.

According to the cutting path, the normal lung tissue of the upper block was in contact with a clean blade, whereas that of the lower block was exposed to the blade after it made contact with tumor tissues. Hence, displaced tumor cells observed in the normal tissue of the lower block have the potential to theoretically be artifacts caused by contaminated blades. Morimoto and his colleagues found that free tumor clusters that had similar definitions of STAS were present in all directions of the main tumor (20). Therefore, cases could be considered as having real STAS when displaced tumor cells were identified in both upper and lower blocks, whereas cases were defined as having mimic STAS when displaced tumor cells were observed in the lower block but absent in the upper block (**Figure 3B**).

Histopathologic Evaluation and Quantitative Comparison of STAS in Tissue Blocks

The surgically resected specimens were fixed with formalin, cut serially into 5-mm-thick slices, and macroscopically examined. Additional consecutive 4-μm-thick sections were cut from a selected tissue block and stained with hematoxylin and eosin. For each case, 5 to 10 tumor slides were reviewed. These slides were evaluated by two pathologists (H.X. and S.Z.) who were blinded to the information on sections and tissue blocks. The pattern and quantity of STAS were evaluated in each tissue block. The methodology was introduced in detail in a previous study (19). Briefly, all STAS in one visual field under a 10× objective were recorded as one occurrence, regardless of the absolute quantity of STAS in that field. The total number of STAS in the corresponding tissue block was estimated as the sum of all positive 10× objective fields in the H&E section. STAS with the largest number was considered the predominant subtype. If any disagreement occurred between the two reviewers, a third observer (C.W.) reviewed these slides.

Statistical Analysis

All clinicopathologic data were presented as median (range), mean ± standard deviation, and number (percent). The Pearson χ^2 test for categorical variables and Student *t* test or one-way ANOVA for numerical variables were applied to compare the groups. A two-sided P value of less than 0.05 was considered statistically significant. All analyses were performed using SPSS 22.0 (IBM Corporation, Armonk, NY) and GraphPad Prism 7.0 (GraphPad Software, San Diego, CA).

RESULTS

Patient Characteristics

We identified 803 patients with NSCLC in the retrospective cohort. **Table 1** shows their detailed clinicopathological characteristics. Of these patients, 524 (65%) were men and 507 (63%) had no smoking history. The median age of this cohort was 60 years (range 29-91). ADC was the most common histological type (58%) (**Table 1**).

Incidence and Features of STAS

Tumor STAS was identified in 370 of 803 patients (46%). STAS was more likely to be observed in patients with no smoking history (P = 0.049), elevated carcinoembryonic antigen (CEA) level (P < 0.001), ADC (P < 0.001), lymph node metastasis (P < 0.001) and high pathologic TNM stage (P < 0.001) (**Table 1**).

TABLE 1 | Characteristics of patients with non-small cell lung cancer stratified by tumor spread through air spaces.

Variables	All patients	STAS (-)	STAS (+)	*P* value
	N = 803	N = 433	N = 370	
Age				
Median (range)	60 (29-91)	60 (29-91)	60 (33-82)	0.783
≤65	543 (68)	292 (67)	251 (68)	0.904
>65	260 (32)	141 (33)	119 (32)	
Gender				0.209
Male	524 (65)	291 (67)	233 (63)	
Female	279 (35)	142 (33)	137 (37)	
Smoking				0.049
Non-smoker	507 (63)	260 (60)	247 (67)	
Current or ex-smoker	296 (37)	173 (40)	123 (33)	
Carcinoembryonic antigen				<0.001
Normal	714 (89)	403 (93)	311 (84)	
High	89 (11)	30 (7)	59 (16)	
Tumor location				0.022
Upper & Middle	547 (68)	310 (72)	237 (64)	
Lower	256 (32)	123 (28)	133 (36)	
Surgical type				0.041
Limited resection	40 (5)	15 (4)	25 (7)	
Lobectomy	662 (82)	369 (85)	293 (79)	
Others	101 (13)	49 (11)	52 (14)	
Tumor histological type				<0.001
Adenocarcinoma	461 (58)	226 (52)	235 (64)	
Squamous cell carcinoma	274 (34)	178 (41)	96 (26)	
Others	68 (8)	29 (7)	39 (10)	
Tumor size				0.118
≤3 cm	465 (58)	265 (61)	200 (54)	
>3-5 cm	226 (28)	111 (26)	115 (31)	
≥5 cm	112 (14)	57 (13)	55 (15)	
Visceral pleural invasion				0.167
Absent	513 (64)	286 (66)	227 (61)	
Present	290 (36)	147 (34)	143 (39)	
Lymph node metastasis				<0.001
Negative	578 (72)	359 (83)	219 (59)	
N1 positive	47 (6)	17 (4)	30 (8)	
N2 positive	178 (22)	57 (13)	121 (33)	
Pathologic TNM stage				<0.001
Stage I	458 (57)	291 (67)	167 (45)	
Stage II	130 (16)	63 (15)	67 (18)	
Stage III/IV	215 (27)	79 (18)	136 (37)	
STAS Subtype				–
Single cell	47 (6)	–	47 (13)	
Micropapillary cluster	187 (23)	–	187 (50)	
Solid nest	136 (17)	–	136 (37)	
Postoperative chemotherapy				0.482
No	334 (42)	185 (43)	149 (40)	
Yes	469 (58)	248 (57)	221 (60)	

Values are presented as median (range) or n (%). STAS, spread through air spaces.

Correlation of Clinicopathologic Characteristics with Different Types of STAS

When STAS was stratified by three morphologic patterns, 47 cases had single cell STAS (13%), 187 cases had micropapillary cluster STAS (50%), and 136 cases had solid nest STAS (37%) (**Table 2**). Large tumor size, lymph node metastasis, and high

pathologic TNM stage were more frequently identified in tumors with micropapillary cluster STAS and solid nest STAS than those with single cell STAS (tumor size: $P < 0.001$; lymph node metastasis: $P < 0.001$; TNM stage: $P = 0.003$). In addition, female sex, no smoking history, and ADC were closely associated with the presence of single cell STAS and micropapillary cluster STAS, whereas male sex, a history of smoking, and SQCC were more common in tumors with solid nest STAS (gender: $P < 0.001$; smoking history: $P < 0.001$; histological type: $P < 0.001$) (**Table 2**).

Survival Analyses

Figures 4A, B shows that patients without STAS had better RFS ($P < 0.001$) and OS ($P < 0.001$) than those with STAS. When stratifying STAS-positive patients by morphologic subtypes, patients without STAS had significantly better survival than did patients with micropapillary cluster STAS (RFS: $P < 0.001$; OS: $P < 0.001$) and solid nest STAS (RFS: $P < 0.001$; OS: $P < 0.001$), but comparable survival to that of patients with single cell STAS (RFS: $P = 0.995$; OS: $P = 0.71$) (**Figures 4C, D**).

In addition, multivariate analyses confirmed that the presence of micropapillary cluster STAS (RFS: hazard ratio [HR] = 1.75, 95% confidence interval [CI]: 1.30-2.37, $P < 0.001$; OS: HR = 1.99, 95% CI: 1.44-2.76, $P < 0.001$) and solid nest STAS (RFS: HR = 1.60, 95% CI: 1.21-2.14, $P = 0.001$; OS: HR = 1.55, 95% CI: 1.16-2.07, $P = 0.003$) was indicated as an independent prognostic factor, but the presence of single cell STAS was not (RFS: HR = 1.00, 95% CI: 0.59-1.70, $P = 0.989$; OS: HR = 1.13, 95% CI: 0.63-2.03, $P = 0.68$) (**Table 3**).

Subgroup Analysis of Patients with ADC

We also assessed the clinical significance of STAS subtypes in patients with ADC. Similar results were acquired in this subgroup when compared with those in entire cohort.

Tumor STAS was identified in 235 patients with ADC (51%), including 43 cases with single cell STAS (18%), 179 cases with micropapillary cluster STAS (76%), and 13 cases with solid nest STAS (6%) (**Supplementary Table 1**). The proportions of lymph node metastasis and high pathologic TNM stage were greater in tumors with micropapillary cluster STAS and solid nest STAS than in those with single cell STAS (lymph node metastasis: $P = 0.003$; TNM stage: $P = 0.025$). (**Supplementary Table 2**) Single cell STAS was observed in lepidic (11/103, 11%), acinar (17/224, 8%), papillary (12/85, 14%) and solid (3/37, 8%) predominant ADC, except for micropapillary predominant ADC. Micropapillary cluster STAS was observed in lepidic (14/103, 14%), acinar (104/224, 46%), papillary (34/85, 40%) and solid (16/37, 43%) predominant ADC. Interestingly, micropapillary STAS had a significant association with micropapillary predominant ADC (11/12, 92%). Whereas solid nest STAS was more common in patients with solid predominant ADC (Lepidic: 2/103, 2%; Acinar: 4/224, 2%; Papillary: 1/85 1%; Micropapillary: 0/12, 0%; Solid: 6/37, 16%).

Supplementary Figures 1A, B shows that STAS significantly stratified the RFS ($P < 0.001$) and OS ($P < 0.001$) in patients with ADC. Further analyses indicated that, when compared to patients with ADC without STAS, similar survival outcomes were found in those with ADC with single cell STAS (RFS: $P = 0.639$; OS: $P = 0.708$), but worse survival outcomes in those with ADC with micropapillary cluster STAS (RFS: $P < 0.001$; OS: $P < 0.001$) or with solid nest STAS (RFS: $P < 0.001$; OS: $P = 0.002$) (**Supplementary Figures 1C, D**). Multivariate analyses revealed micropapillary cluster STAS (RFS: HR = 1.67, 95% CI: 1.18-2.37, $P = 0.004$; OS: HR = 1.73, 95% CI: 1.19-2.51, $P = 0.004$) and solid nest STAS (RFS: HR = 2.13, 95% CI: 1.02-4.45, $P = 0.043$; OS: HR = 2.09, 95% CI: 0.95-4.63, $P = 0.068$) to be a risk factor for survival, but single cell STAS was not (RFS: HR = 0.82, 95% CI:

TABLE 2 | Characteristics of patients with non-small cell lung cancer stratified by subtypes of tumor spread through air spaces.

	Single cell STAS	Micropapillary cluster STAS	Solid nest STAS	*P* value
	N = 47	N = 187	N = 136	
Age				
Median (range)	59 (35-78)	61 (33-82)	61 (36-79)	0.335
≤65	37 (79)	124 (66)	90 (66)	0.232
>65	10 (21)	63 (34)	46 (32)	
Gender				<0.001
Male	18 (38)	102 (55)	113 (83)	
Female	29 (62)	85 (45)	23 (17)	
Smoking				<0.001
Non-smoker	37 (79)	143 (77)	67 (49)	
Current or ex-smoker	10 (21)	44 (23)	69 (51)	
Carcinoembryonic antigen				0.031
Normal	41 (87)	148 (79)	122 (90)	
High	6 (13)	39 (21)	14 (10)	
Tumor location				0.339
Upper & Middle	32 (68)	113 (60)	92 (68)	
Lower	15 (32)	74 (40)	44 (32)	
Surgical type				0.001
Limited resection	4 (9)	14 (7)	7 (5)	
Lobectomy	40 (85)	157 (84)	96 (71)	
Others	3 (6)	16 (9)	33 (24)	
Tumor histological type				<0.001
Adenocarcinoma	43 (92)	179 (96)	13 (10)	
Squamous cell carcinoma	2 (4)	1 (1)	93 (68)	
Others	2 (4)	7 (4)	30 (22)	
Tumor size				<0.001
≤3 cm	35 (74)	114 (61)	51 (38)	
>3-5 cm	8 (17)	59 (32)	48 (35)	
≥5 cm	4 (9)	14 (7)	37 (27)	
Visceral pleural invasion				0.01
Absent	30 (64)	101 (54)	96 (71)	
Present	17 (36)	86 (46)	40 (29)	
Lymph node metastasis				<0.001
Negative	38 (81)	93 (50)	88 (65)	
N1 positive	2 (4)	24 (13)	4 (3)	
N2 positive	7 (15)	70 (37)	44 (32)	
Pathologic TNM stage				0.003
Stage I	32 (68)	83 (44)	52 (38)	
Stage II	6 (13)	28 (15)	33 (24)	
Stage III/IV	9 (19)	76 (41)	51 (38)	
Postoperative chemotherapy				0.732
No	21 (45)	76 (41)	52 (38)	
Yes	26 (55)	111 (59)	84 (62)	

Values are presented as median (range) or n (%). STAS, spread through air spaces.

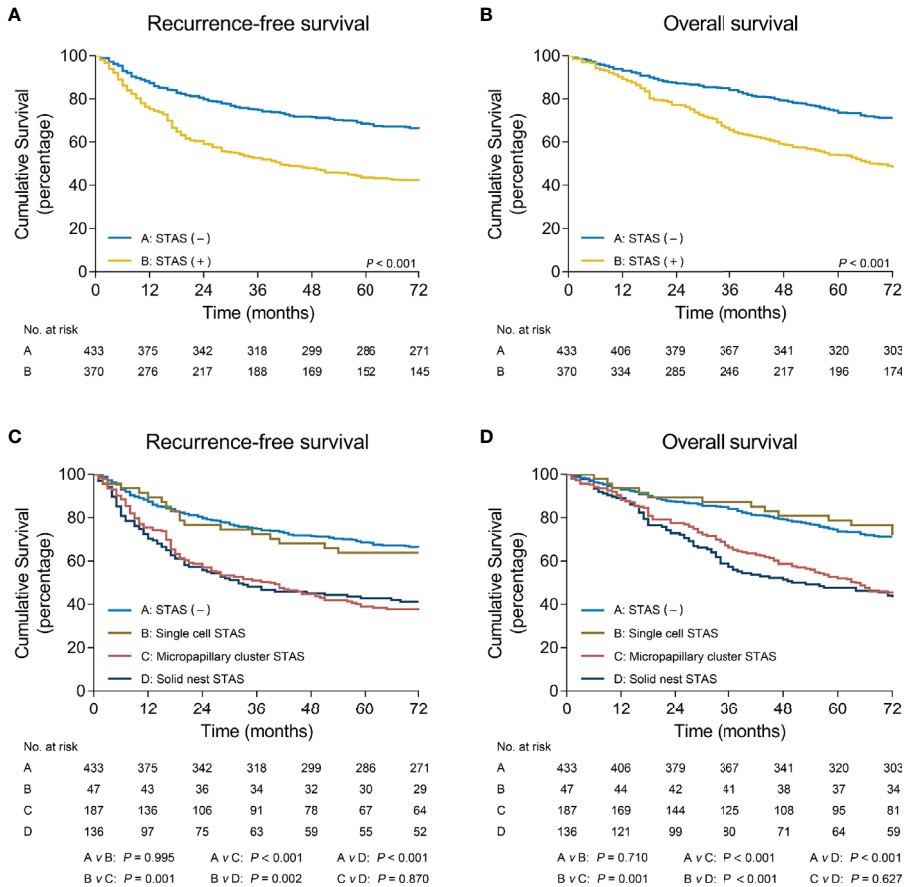

FIGURE 4 | Recurrence-free survival **(A)** and overall survival **(B)** in patients with non-small cell lung cancer stratified by STAS. Recurrence-free survival **(C)** and overall survival **(D)** in patients with non-small cell lung cancer stratified by STAS subtypes. STAS, spread through air spaces.

0.45-1.49, $P = 0.517$; OS: HR = 0.94, 95% CI: 0.48-1.83, $P = 0.843$) (**Supplementary Table 3**).

Influence of a Prosecting Knife on STAS Subtypes

Because single cell STAS was not a significant prognostic factor, we next verified the hypothesis that single cell STAS was the artifact caused by a prosecting knife during specimen handling. A total of 83 patients with NSCLC who underwent surgery at our department met the inclusion criteria. **Supplementary Table 4** shows baseline characteristics of patients and pathologic results of tumors. All lung cancer specimens were prosected and sampled according to the standard protocol.

Incidence and Features of STAS in Tissue Blocks

After histologic evaluation, 45 of 83 patients (54%) had displaced tumor cells in at least one tissue block (**Figure 5A**). The mean fields of displaced tumor cells were significantly greater in the lower part of the cuts than in the upper part ($P < 0.001$) (**Figure 5B**). Of these 45 patients, 27 (60%) were identified as having displaced tumor cells in both two blocks and diagnosed as having real STAS. The remaining 18 (40%) had displaced tumor cells in lower block but not in upper block; they were considered to have mimic STAS (**Figure 5A**). In patients with real STAS, upper blocks still had fewer fields of STAS compared to lower blocks ($P = 0.016$) (**Figure 5B**). In patients with mimic STAS, a great number of displaced tumor cells presented as single cell pattern (13/18, 72%) and in ADCs (16/18, 89%).

Distribution of STAS Stratified by Morphologic Subtype

When subclassifying cases according to the morphologic features of STAS, 17 cases had single cell pattern, 19 cases had micropapillary pattern, and 9 cases had solid nest pattern (**Supplementary Figure 2**).

Supplementary Figure 2A shows the distribution of single cell STAS in 17 cases; the lower blocks had significantly more displaced tumor cells than the corresponding upper blocks ($P < 0.001$) (**Supplementary Figure 2B**). Of these 17 cases, 4 cases (24%) with real STAS and 13 cases (76%) with mimic STAS. No statistical difference in the number of positive fields was observed between upper blocks and lower blocks in patients with real single cell STAS ($P = 0.495$) (**Supplementary Figure 2B**).

TABLE 3 | Cox proportional hazards regression model for recurrence-free survival and overall survival in patients with non-small cell lung cancer.

Variables	Recurrence-free survival			Overall survival		
	Univariate Analysis	Multivariate Analysis		Univariate Analysis	Multivariate Analysis	
	P value	HR (95% CI)	*P* value	*P* value	HR (95% CI)	*P* value
Age						
>65 vs. ≤65	0.036	1.19 (0.96-1.48)	0.113	<0.001	1.48 (1.19-1.84)	<0.001
Gender						
Female vs. Male	0.177			0.004	0.71 (0.55-0.92)	0.009
Smoking						
Current or ex-smoker vs. Non-smoker	0.372			0.159		
Carcinoembryonic antigen						
High vs. Normal	<0.001	1.75 (1.33-2.30)	<0.001	<0.001	1.83 (1.38-2.41)	<0.001
Tumor location						
Lower lobe vs. Upper & middle lobe	0.262			0.45		
Surgical type						
Lobectomy & others vs. Limited resection	0.331			0.066	0.45 (0.29-0.71)	0.001
Tumor histological type						
SQCC & others vs. Adenocarcinoma	0.013	1.30 (0.97-1.75)	0.085	<0.001	1.63 (1.18-2.24)	0.003
Tumor size	<0.001		<0.001	<0.001		0.007
3-5 cm vs. ≤3cm	0.002	1.14 (0.90-1.45)	0.281	<0.001	1.26 (0.98-1.62)	0.073
≥5 cm vs. ≤3cm	<0.001	1.86 (1.39-2.50)	<0.001	<0.001	1.62 (1.19-2.21)	0.002
Visceral pleural invasion						
Present vs. Absent	0.013	1.17 (0.94-1.47)	0.168	0.017	1.36 (1.07-1.72)	0.012
Lymph node metastasis						
Positive vs. Negative	<0.001	2.48 (1.99-3.11)	<0.001	<0.001	2.48 (1.96-3.14)	<0.001
STAS Subtype	<0.001			<0.001		<0.001
Single cell STAS vs. Negative	0.998	1.00 (0.59-1.70)	0.989	0.717	1.13 (0.63-2.03)	0.68
Micropapillary cluster STAS vs. Negative	<0.001	1.75 (1.30-2.37)	<0.001	<0.001	1.99 (1.44-2.76)	<0.001
Solid nest STAS vs. Negative	<0.001	1.60 (1.21-2.14)	0.001	<0.001	1.55 (1.16-2.07)	0.003
Postoperative chemotherapy						
Yes vs. No	0.45			0.485		

HR, hazard ratio; CI, confidence interval; STAS, spread through air spaces.

Among 19 patients with micropapillary cluster STAS, 14 patients were considered as having real STAS (79%), and the remaining 5 patients had mimic STAS (21%) (**Supplementary Figure 2C**). The number of micropapillary cluster STAS fields in lower blocks was significantly higher than that in upper blocks in all cases ($P < 0.001$) and in cases with real STAS ($P = 0.009$) (**Supplementary Figure 2D**).

A solid nest pattern was observed in 9 cases (**Supplementary Figure 2E**). All patients (100%) had STAS in upper blocks and thus were considered as having real STAS. The number of positive fields of solid nest STAS was similar between upper and lower blocks ($P = 0.998$) (**Supplementary Figure 2F**).

DISCUSSION

To the best of our knowledge, this is the first study to examine the clinical significance of three STAS patterns. Our results suggested that unlike micropapillary cluster STAS and solid nest STAS, single-cell STAS was not significantly associated with pathologic features of aggressive tumor behavior (larger tumor size, lymph node metastasis, and high TNM stage). More importantly, the presence of single-cell STAS failed to stratify the prognosis in the study cohort, whereas micropapillary cluster STAS and solid nest STAS were confirmed as independent prognostic factors for both RFS and OS. Similar results were found in the subgroup of patients with ADC. Evidence of heterogeneity among STAS subtypes raises the question of whether single-cell STAS occurs as a mechanical artifact caused by specimen processing. Our prospective study of resected specimens verified that a prosecting knife blade disseminated tumor cells into normal lung tissues, thus leading to mimic STAS, which mostly presented as a single-cell pattern (72%).

Kadota et al (2). first defined STAS and reported its clinical significance in lung ADCs in 2015. They also reported three morphological patterns of STAS: (1) micropapillary structures consisting of papillary structures without central fibrovascular cores that occasionally form ring-like structures within air spaces; (2) solid nests or tumor islands consisting of solid collections of tumor cells filling air spaces; and (3) single cells consisting of scattered discohesive single cells. In addition, our previous study reported that STAS was always identified simultaneously with high-grade histologic patterns. Specifically, STAS occurred less frequently in lepidic-predominant ADC and more frequently in micropapillary and solid-predominant subtypes. However, few studies have investigated whether the three patterns of STAS have different features and correlations

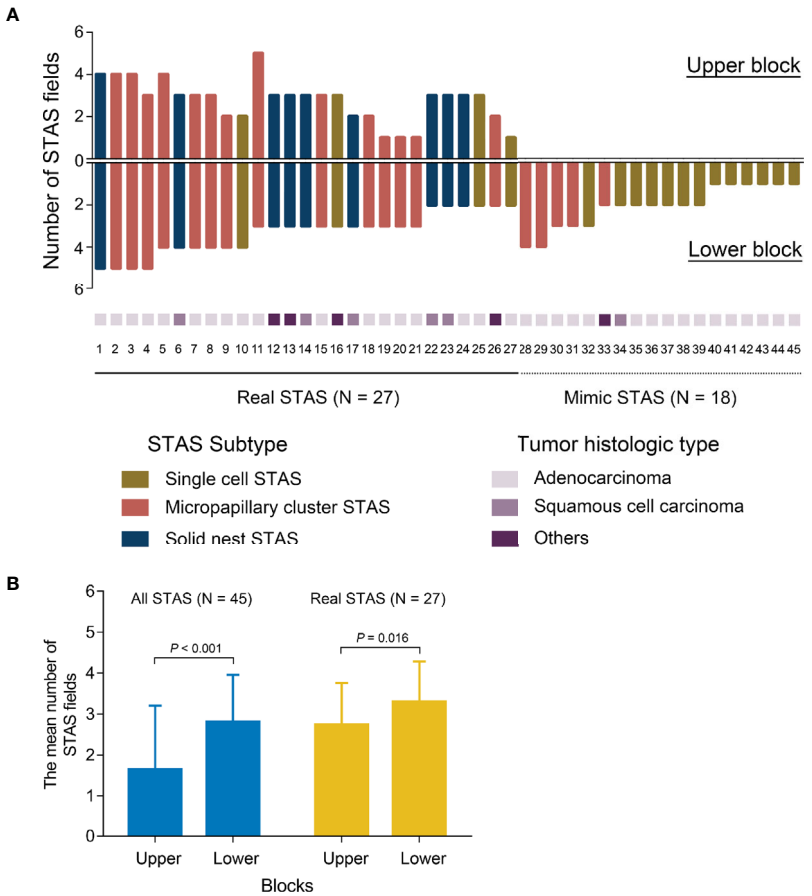

FIGURE 5 | The distribution and quantity of STAS in each tissue block **(A)**. The quantitative comparison of all STAS and real STAS between upper blocks and lower blocks **(B)**. STAS, spread through air spaces.

with pathologic subtypes of lung ADC. We found that micropapillary cluster STAS was more prevalent than single-cell STAS in every subtype of ADC. Furthermore, our results revealed that single-cell STAS failed to stratify the prognosis in the study cohort. Only micropapillary cluster STAS and solid nest STAS were independent prognostic factors for both RFS and OS. This is the first report about the prognostic impact of the three subtypes of STAS. This result indicated that single-cell STAS may occur as a mechanical artifact caused by specimen processing.

Since the introduction of STAS in 2015, many retrospective studies have unanimously shown its clinical and prognostic value in all major histologic types of NSCLC (2–16), proving that STAS is a biological phenomenon. Even with such sufficient published evidence, STAS is still controversial (18, 19, 21). Thunnissen and colleagues found that tumor fragments and individual cells could be spread into normal lung tissues through a knife surface (STAKS) and suggested that STAS might be an artifact (18). In the present study, we identified the possibility that most single-cell STAS could be artifacts because they lacked clinical and prognostic value. We then validated this speculation. These results have several important implications. First, single-cell STAS was the most common diagnostic pitfall and should be diagnosed very cautiously in retrospective studies. Generally, detailed records of specimen handling were unavailable in retrospective studies; thus, the potential effect of STAKS could not be eliminated. Second, a precise protocol of surgical specimen handling will be required to minimize artifacts as much as possible.

The key question that led to the speculation of STAS being an artifact rather than an invasive pattern was the survival of the tumor cells after detaching from the main tumor and floating freely in the air spaces without a vascular supply. Onozato and colleagues used an algorithm for 3-dimensional reconstruction of paraffin-embedded tissues and found that tumor islands (similar to the solid nest pattern) were connected to each other and to the main tumor at different levels, supporting the possibility that tumor islands gain access to energy supply from the main tumor (22). In a recent study, a high-quality 3-dimensional reconstruction and multiplex immunofluorescence study reported by Yagi and her colleagues revealed that micropapillary structures in normal air spaces that appeared to be free floating on 2-dimensional evaluation

were actually attached to alveolar walls and capillaries through vessel cooption on 3-dimensional evaluation, thus gaining access to an energy supply (23). The study strongly support the hypothesis that solid nest STAS and micropapillary cluster STAS represent intraparenchymal invasion rather than artifacts, which is consistent with our findings. However, how single tumor cells can survive within air spaces remains unclear. If tumor cells can obtain access to an energy supply by adhering to the alveolar wall, individually scattered tumor cells suspended in the alveolar spaces seem to lack an energy supply and thus would hypothetically have difficulty surviving, which supports our findings that most displaced single tumor cells were artifacts rather than invasive growth.

Our results indicated that knife blades caused a small number of false-positive STAS cases with a micropapillary cluster pattern (28%). Yagi and colleagues found that micropapillary structures within airspaces in the main tumor area were connected to alveolar walls (23). Our findings suggested that the adhesive force was weak and could be easily broken by a knife. A similar phenomenon was reported by Isaka and colleagues (24). They found that micropapillary clusters could be aspirated out within airway secretions from the bronchus in which the tumor was located. More importantly, our results also revealed that a knife blade increased the number of micropapillary clusters in tumors with real STAS. Recently, Uruga and colleagues reported a semiquantitative assessment of STAS based on a retrospective analysis of 208 cases (5). Patients with early-stage ADC could be classified into high-STAS (≥ 5 single cells or clusters), low-STAS (1-4 single cells or clusters) and no-STAS groups. The survival analyses indicated that the high-STAS group was associated with worse RFS than the low-STAS and no-STAS groups. Nevertheless, considering that STAKS was neglected in this retrospective study, the possibility that STAS was overestimated cannot be entirely ruled out. For this reason, this semiquantitative method should be better verified in prospective studies.

Our results showed that the knife blade only slightly changed the frequency and quantity of displaced tumor cells with a solid nest pattern; thus, STAKS probably had little influence on findings related to solid nest STAS. Three retrospective studies investigated the prognostic implications of STAS in 445, 216, and 220 patients with SQCC, and all STAS-positive cases showed a solid nest pattern and were significantly associated with worse survival outcomes (13–15). Consequently, the prognostic value of STAS in SQCCs is still trustworthy even when STAKS is not taken into consideration.

Some limitations of this study should be addressed. First, this was a single-center study with some potential biases, and the results should be externally validated. Second, we proved the mechanical influence of a knife blade on STAS, but one could reasonably speculate that there might be additional mechanical forces on a tumor during specimen handling; thus, further studies are needed to explore their roles in the spread of tumor cells. Finally, the retrospective cohort and prospective cohort were two individual cohorts from 2009 and 2017, respectively. For the retrospective cohort, STAKS could not be evaluated because tumor specimens were processed following routine clinical protocols in 2009. For the prospective cohort, the results of survival analysis are not reliable for patients because of the short follow-up time. Thus, the prognostic impact of STAKS cannot be directly validated. Despite this limitation, the results of our study could provide some important information. Our data showed that single-cell STAS was not a prognostic factor and that a large proportion of single-cell STAS could be artifacts. This result indicated that the nonsignificant prognostic result of single-cell STAS was caused by single-cell STAKS. A precise protocol to eliminate single-cell STAKS should be designed in the future. Micropapillary cluster STAS and STAKS were highly associated with the presence of micropapillary components. This result indicated that micropapillary STAS may be cell clusters from micropapillary components in lung adenocarcinoma. Although some micropapillary STAS could be caused by a prosecting knife, the result also indicated the presence of a micropapillary component in lung adenocarcinoma. The presence of micropapillary clusters in airspaces merely reflects the aggressive biology of the tumor and dictates patient outcomes, irrespective of whether the clusters are real or artifacts (25).

CONCLUSIONS

The presence of micropapillary cluster STAS and solid nest STAS were independent prognostic factors for shortened survival. However, single-cell STAS did not have prognostic significance, and most might be contaminants produced by a prosecting knife. Thus, single-cell STAS should be diagnosed very cautiously in retrospective studies because detailed records of specimen handling are generally unavailable to eliminate the potential effect of STAKS. In addition, a precise protocol of surgical specimen handling is required to minimize artifacts as much as possible.

DATA AVAILABILITY STATEMENT

The original contributions presented in the study are included in the article/**Supplementary Material**. Further inquiries can be directed to the corresponding authors.

ETHICS STATEMENT

This study was carried out in accordance with the principles of the Helsinki Declaration of the World Medical Association. The study protocol was approved by the Institutional Review Board of Shanghai Pulmonary Hospital (No. FK-17-159).

AUTHOR CONTRIBUTIONS

(I) Conception and design: HX, CD, CW, and CC. (II) Administrative support: CW and CC. (III) Provision of study materials or patients: HS, EZ, and CG. (IV) Collection and

assembly of data: SZ, YS, YR, DX, and HZ. (V) Data analysis and interpretation: HX, CD. (VI) Manuscript writing: All authors. All authors contributed to the article and approved the submitted version.

FUNDING

Supported by the grants from National Natural Science Foundation of China (NSFC 9195910169 and NSFC 81770091 and NSFC 81902335 and NSFC 81802256) and the "Chen Guang" project supported by Shanghai Municipal Education Commission and Shanghai Education Development Foundation (18CG19) and the "Outstanding young talent" project supported by Shanghai Pulmonary Hospital (FKYQ1907), Shanghai Rising Star Program (20QA1408300) and Clinical Research Plan of SHDC (SHDC2020CR4028 and SHDC2020CR1021B) and National Key Research and Development Project (2019YFE0101200), Shanghai Science and Technology Committee (20YF1441100 and 20XD1403000 and 18DZ2293400), Shanghai Municipal Health Commission (2019SY072 and 2018ZHYL0102), Shanghai Pulmonary Hospital Innovation group project (Shanghai pulmonary hospital Innovation group project–"Chang Chen") the Clinical Research Project of Shanghai Pulmonary Hospital (FK18001 and FK1904 and FKGG1805 and FK1936 and FK1943 and FKLY20007 and FKCX1906), Clinical Research Foundation of Shanghai Pulmonary Hospital (FK1944).

SUPPLEMENTARY MATERIAL

The Supplementary Material for this article can be found online at: https://www.frontiersin.org/articles/10.3389/fonc.2021.608353/full#supplementary-material

Supplementary Figure 1 | Recurrence-free survival (A) and overall survival (B) in patients with adenocarcinoma stratified by STAS. Recurrence-free survival (C) and overall survival (D) in patients with adenocarcinoma stratified by STAS subtypes. STAS, *spread through air spaces*.

Supplementary Figure 2 | The distribution and quantity of STAS subtypes in each tissue block (A, single cell; C, micropapillary cluster; E, solid nest). The quantitative comparison of all STAS subtypes and real STAS subtypes between upper blocks and lower blocks (B, single cell; D, micropapillary cluster; F, solid nest). STAS, *spread through air spaces*.

REFERENCES

1. Travis WD, Brambilla E, Burke A, Marx A, Nicholson AG. *WHO classification of tumours of the lung, pleura, thymus and heart. 4th edition*. Lyon, France: International Agency for Research on Cancer (2015).
2. Kadota K, Nitadori J, Sima CS, Ujiie H, Rizk NP, Jones DR, et al. Tumor spread through air spaces is an important pattern of invasion and impacts the frequency and location of recurrences after limited resection for small stage I lung adenocarcinomas. *J Thorac Oncol* (2015) 10:806–14. doi: 10.1097/JTO.0000000000000486
3. Warth A, Muley T, Kossakowski CA, Goeppert B, Schirmacher P, Dienemann H, et al. Prognostic impact of intra-alveolar tumor spread in pulmonary adenocarcinoma. *Am J Surg Pathol* (2015) 39:793–801. doi: 10.1097/PAS.0000000000000409
4. Shiono S, Yanagawa N. Spread through air spaces is a predictive factor of recurrence and a prognostic factor in stage I lung adenocarcinoma. *Interact Cardiovasc Thorac Surg* (2016) 23:567–72. doi: 10.1093/icvts/ivw211
5. Uruga H, Fujii T, Fujimori S, Kohno T, Kishi K. Semiquantitative assessment of tumor spread through air spaces (stas) in early-stage lung adenocarcinomas. *J Thorac Oncol* (2017) 12:1046–51. doi: 10.1016/j.jtho.2017.03.019
6. Dai C, Xie H, Su H, She Y, Zhu E, Fan Z, et al. Tumor spread through air spaces affects the recurrence and overall survival in patients with lung adenocarcinoma >2 to 3 cm. *J Thorac Oncol* (2017) 12:1052–60. doi: 10.1016/j.jtho.2017.03.020
7. Masai K, Sakurai H, Sukeda A, Suzuki S, Asakura K, Nakagawa K, et al. Prognostic impact of margin distance and tumor spread through air spaces in limited resection for primary lung cancer. *J Thorac Oncol* (2017) 12:1788–97. doi: 10.1016/j.jtho.2017.08.015
8. Toyokawa G, Yamada Y, Tagawa T, Kozuma Y, Matsubara T, Haratake N, et al. Significance of spread through air spaces in resected pathological stage I lung adenocarcinoma. *Ann Thorac Surg* (2018) 105:1655–63. doi: 10.1016/j.athoracsur.2018.01.037
9. Toyokawa G, Yamada Y, Tagawa T, Kinoshita F, Kozuma Y, Matsubara T, et al. Significance of spread through air spaces in resected lung adenocarcinomas with lymph node metastasis. *Clin Lung Cancer* (2018) 19:395–400 e391. doi: 10.1016/j.cllc.2018.04.002
10. Toyokawa G, Yamada Y, Tagawa T, Oda Y. Significance of spread through air spaces in early-stage lung adenocarcinomas undergoing limited resection. *Thorac Cancer* (2018) 9:1255–61. doi: 10.1111/1759-7714.12828
11. Eguchi T, Kameda K, Lu S, Bott MJ, Tan KS, Montecalvo J, et al. Lobectomy is associated with better outcomes than sublobar resection in spread through air spaces (STAS)-positive T1 lung adenocarcinoma: a propensity score-matched analysis. *J Thorac Oncol* (2018) 14(1):87–98. doi: 10.1016/j.jtho.2018.09.005
12. Liu Y, Chen D, Qiu X, Duan S, Zhang Y, Li F, et al. Relationship between MTA1 and spread through air space and their joint influence on prognosis of patients with stage I-III lung adenocarcinoma. *Lung Cancer* (2018) 124:211–8. doi: 10.1016/j.lungcan.2018.07.040
13. Lu S, Tan KS, Kadota K, Eguchi T, Bains S, Rekhtman N, et al. Spread through air spaces (STAS) is an independent predictor of recurrence and lung cancer-specific death in squamous cell carcinoma. *J Thorac Oncol* (2017) 12:223–34. doi: 10.1016/j.jtho.2016.09.129
14. Kadota K, Kushida Y, Katsuki N, Ishikawa R, Ibuki E, Motoyama M, et al. Tumor spread through air spaces is an independent predictor of recurrence-free survival in patients with resected lung squamous cell carcinoma. *Am J Surg Pathol* (2017) 41:1077–86. doi: 10.1097/PAS.0000000000000872
15. Yanagawa N, Shiono S, Endo M, Ogata S. Tumor spread through air spaces is a useful predictor of recurrence and prognosis in stage I lung squamous cell carcinoma, but not in stage II and III. *Lung Cancer* (2018) 120:14–21. doi: 10.1016/j.lungcan.2018.03.018
16. Yokoyama S, Murakami T, Tao H, Onoda H, Hara A, Miyazaki Y, et al. Tumor spread through air spaces identifies a distinct subgroup with poor prognosis in surgically resected lung pleomorphic carcinoma. *Chest* (2018) 154:838–47. doi: 10.1016/j.chest.2018.06.007
17. Detterbeck FC, Boffa DJ, Kim AW, Tanoue LT. The eighth edition lung cancer stage classification. *Chest* (2017) 151:193–203. doi: 10.1016/j.chest.2016.10.010
18. Thunnissen E, Blaauwgeers HJ, de Cuba EM, et al. Ex vivo artifacts and histopathologic pitfalls in the lung. *Arch Pathol Lab Med* (2016) 140:212–20. doi: 10.5858/arpa.2015-0292-OA
19. Blaauwgeers H, Flieder D, Warth A, Yick CY, Flieder DB. A prospective study of loose tissue fragments in non-small cell lung cancer resection specimens: an alternative view to "Spread Through Air Spaces". *Am J Surg Pathol* (2017) 41:1226–30. doi: 10.1097/PAS.0000000000000889
20. Morimoto J, Nakajima T, Suzuki H, Nagato K, Iwata T, Yoshida S, et al. Impact of free tumor clusters on prognosis after resection of pulmonary Impact of free tumor clusters on prognosis after resection of pulmonary adenocarcinoma. *J Thorac Cardiovasc Surg* (2016) 152:64–72. doi: 10.1016/j.jtcvs.2016.03.088
21. Blaauwgeers H, Russell PA, Jones KD, Radonic T, Thunnissen E. Pulmonary loose tumor tissue fragments and spread through air spaces (STAS): Invasive pattern or artifact? A critical review. *Lung Cancer* (2018) 123:107–11. doi: 10.1016/j.lungcan.2018.07.017
22. Onozato ML, Kovach AE, Yeap BY, Morales-Oyarvide V, Klepeis VE, Tammireddy S, et al. Tumor islands in resected early-stage lung adenocarcinomas are associated with unique clinicopathologic and

molecular characteristics and worse prognosis. *Am J Surg Pathol* (2013) 37:287–94. doi: 10.1097/PAS.0b013e31826885fb
23. Yagi Y, Aly RG, Tabata K, Barlas A, Rekhtman N, Eguchi T, et al. Three-Dimensional Histologic, Immunohistochemical, and Multiplex Immunofluorescence Analyses of Dynamic Vessel Co-Option of Spread Through Air Spaces in Lung Adenocarcinoma. *J Thorac Oncol* (2020) 15(4):589–600. doi: 10.1016/j.jtho.2019.12.112
24. Isaka T, Yokose T, Miyagi Y, Washimi K, Nishii T, Ito H, et al. Detection of tumor spread through airspaces by airway secretion cytology from resected lung cancer specimens. *Pathol Int* (2017) 67:487–94. doi: 10.1111/pin.12570
25. Shih AR, Mino-Kenudson M. Updates on spread through air spaces (STAS) in lung cancer. *Histopathology* (2020) 77(2):173–80. doi: 10.1111/his.14062

Conflict of Interest: The authors declare that the research was conducted in the absence of any commercial or financial relationships that could be construed as a potential conflict of interest.

frontiers in Oncology

ORIGINAL RESEARCH
published: 12 April 2021
doi: 10.3389/fonc.2021.616149

Prognostic Impact of Radiological Consolidation Tumor Ratio in Clinical Stage IA Pulmonary Ground Glass Opacities

*Junjie Xi†, Jiacheng Yin†, Jiaqi Liang, Cheng Zhan, Wei Jiang, Zongwu Lin, Songtao Xu and Qun Wang**

Department of Thoracic Surgery, Zhongshan Hospital, Fudan University, Shanghai, China

OPEN ACCESS

Edited by:
Kezhong Chen,
Peking University People's Hospital, China

Reviewed by:
Arnold Manfred Herskovic,
Rush University, United States
Yong Yang,
Nanjing Medical University, China
Jian Cui,
Beijing Chuiyangliu Hospital, China

***Correspondence:**
Qun Wang
WangQun_zshospital@163.com

†These authors have contributed equally to this work

Specialty section:
This article was submitted to Thoracic Oncology, a section of the journal Frontiers in Oncology

Received: *11 October 2020*
Accepted: *16 March 2021*
Published: *12 April 2021*

Citation:
Xi J, Yin J, Liang J, Zhan C, Jiang W, Lin Z, Xu S and Wang Q (2021) Prognostic Impact of Radiological Consolidation Tumor Ratio in Clinical Stage IA Pulmonary Ground Glass Opacities. Front. Oncol. 11:616149. doi: 10.3389/fonc.2021.616149

Objectives: Our study aimed to validate pathologic findings of ground-glass nodules (GGOs) of different consolidation tumor ratios (CTRs), and to explore whether GGOs could be stratified according to CTR with an increment of 0.25 based on its prognostic role.

Methods: We retrospectively evaluated patients with clinical stage IA GGOs who underwent curative resection between 2011 and 2016. The patients were divided into 4 groups according to CTR step by 0.25. Cumulative survival rates were calculated by the Kaplan-Meier method. Univariate and multivariate Cox regression analyses were conducted to obtain the risk factors on relapse-free survival (RFS). The surv_function of the R package survminer was used to determine the optimal cutoff value. Receiver operating characteristic (ROC) analysis was generated to validate optimal cutoff points of factors.

Results: A total of 862 patients (608 women; median age, 59y) were included, with 442 patients in group A (CTR ≤ 0.25), 210 patients in group B (0.25<CTR ≤ 0.5), 173 patients in group C (0.5<CTR ≤ 0.75), and 37 patients in group D (0.75<CTR<1). The rate of adenocarcinoma *in situ* (AIS) or minimally invasive adenocarcinoma (MIA) in group A (70.6%) was much higher than other three groups (p<0.001). Multivariable Cox regression revealed that CTR (HR, 1.865; 95%CI, 1.312-2.650; p = 0.001) and lymph node metastasis (HR, 10.407; 95%CI, 1.957-55.343; p = 0.006) were independent prognostic factors for recurrence free survival. In addition, CTR was the only risk factor for the presence of micropapillary or solid pattern (OR=133.9, 95%CI:32.2-556.2, P<0.001) and lymph node metastasis (OR=292498.8, 95%CI:1.2-7.4×10^{10}, P=0.047). Paired comparison showed that rate of presence of micropapillary or solid pattern was highest in group D, followed by group C and group A/B (p<0.001). Lymph node metastasis occurred in group D only (p=0.002).

Conclusions: CTR is an independent prognostic factor for clinical stage IA lung adenocarcinoma manifesting as GGO in CT scan. Radiologic cutoffs of CTR 0.50 and 0.75 were able to subdivide patients with different prognosis.

Keywords: lung cancer, early-stage, computed tomography, ground-glass opacities, consolidation

INTRODUCTION

Ground glass opacity (GGO) is a radiological finding in computed tomography (CT) with a hazy opacity that does not obscure the underlying bronchial structures or pulmonary vessels (1–3). Lung adenocarcinoma with GGO component is correlated with excellent prognosis (4). Both consolidation size and consolidation tumor ratio (CTR) were reported to be prognostic factors for GGOs (5–7).

Previous studies revealed that GGO dominant (CTR ≤ 0.5) part-solid nodules were less invasive than solid dominant (CTR>0.5) part-solid nodules (8–14). In the 2015 World Health Organization classification of lung tumors (15), micropapillary and solid components in adenocarcinoma represent poor differentiation and worse biology behavior. It has been reported that these two poor differentiated components correlate with poor prognosis (16–19), and it has been verified in clinical stage I non-small-cell lung cancer as well (20–22). Pathologic components of lung adenocarcinoma might transform into prognostic information in the long term to some extent. Few studies have investigated the pathologic subtypes of GGOs of different CTRs, with an increment of 0.25. Our study is to investigate prognostic factors of GGOs, and then to explore whether GGOs should be studied according to CTR with an increment of 0.25, considering both survival and pathology.

PATIENTS AND METHODS

This study was conducted in accordance with the amended Declaration of Helsinki. Ethics committee on human research of Zhongshan Hospital approved the protocol (approval number: B2019-232R), and written informed consent was obtained from all patients before surgery for the use of surgical samples and clinical information for medical research.

Patient Selection

We retrospectively reviewed the records of patients with GGOs who underwent curative resection at our institute between January 2011 and December 2016. All patients received thin-section CT scan (collimation ≤1.5mm) before surgery. For patients with solid component ≥6mm in the lung window, PET/CT was regularly recommended. Most patients underwent standard lobectomy, while sublobar resection (segmentectomy and wedge resection) was performed for a section of patients with tumors ≤ 2cm. A minimum of three N2 stations sampled or complete lymph node dissection was a routine schedule for all patients. Inclusion criteria were as follows: (1) GGO with maximum consolidation diameter ≤ 3cm in the lung window, (2) clinically no lymph node metastasis (shortest diameter of hilar or mediastinal lymph nodes less than 1.0cm on CT scan or no positive fluorodeoxyglucose uptake of hilar or mediastinal lymph nodes on PET/CT), (3) pathologically confirmed primary lung adenocarcinoma, and (4) R0 (complete) resection. Cases with no pathologic subtype data were excluded. Finally, 862 stage IA patients were included.

The patients were divided into 4 groups according to CTR: group A (CTR ≤ 0.25), group B (0.25<CTR ≤ 0.5), group C (0.5<CTR ≤ 0.75), and group D (0.75<CTR<1).

CT Measurement

The lung windows were set at a window width of 1500 Hounsfield units (HU) and a window level -500 HU. GGO is defined as a hazy opacity in lung without obscuring the underlying bronchial structures or pulmonary vessels. Pathologically, GGO mainly turns out to be lepidic but also non-lepidic growth patterns in lung adenocarcinomas. The consolidation component is defined as an area of increased opacity that completely obscures the underlying bronchial structures and pulmonary vessels. The longest diameters of the solid portion and total tumor size in the lung window were measured, respectively. The CTR was defined as the ratio of the maximum size of consolidation to the maximum tumor size in the lung window (**Figure 1**). For multiple GGOs, the dominant lesions were investigated. In circumstances that multiple solid components existed in one pulmonary nodule, the largest consolidation was measured. Two independent radiologists with at least 5-year experience reviewed the CT scans and determined tumor sizes. 102 of 862 nodules (11.8% disagreement) were discordant in the solid component size. The nodules with discrepancy were adjudicated by the third radiologist (with 15-year experience in chest radiology) and final results were settled by consensus.

Pathologic Examination

All resection specimens were formalin-fixed and stained with hematoxylin and eosin. Pleural invasion was established using elastin stains in case that it was difficult to diagnose pleural invasion. Pathologic diagnosis was made according to the 2011 International Association for the Study of Lung Cancer/American Thoracic Society/European Respiratory Society (IASCL/ATS/ERS) classification. Each histological component (lepidic, acinar, papillary, micropapillary, and solid) was recorded. The predominant pattern was defined as the pattern with the largest percentage.

Follow-Up Protocol

The initial postoperative surveillance schedule includes a chest CT scan and a history and physical examination (H&P) examination every 3-6 months for first 2 years, followed by an annual chest CT and an H&P for subsequent years. Brain contrast-enhanced magnetic resonance imaging (MRI) and emission computed tomography (ECT) bone scan were performed every 6 months and 12 months respectively for all patients in the first 3 years and upon occurrence of the corresponding symptoms.

Statistical Analysis

Differences in categorical variables were compared using chi-square test or Fisher's exact test. Continuous variables were compared using paired t test. Bonferroni adjustments were included for multiple comparisons. Estimation of survival

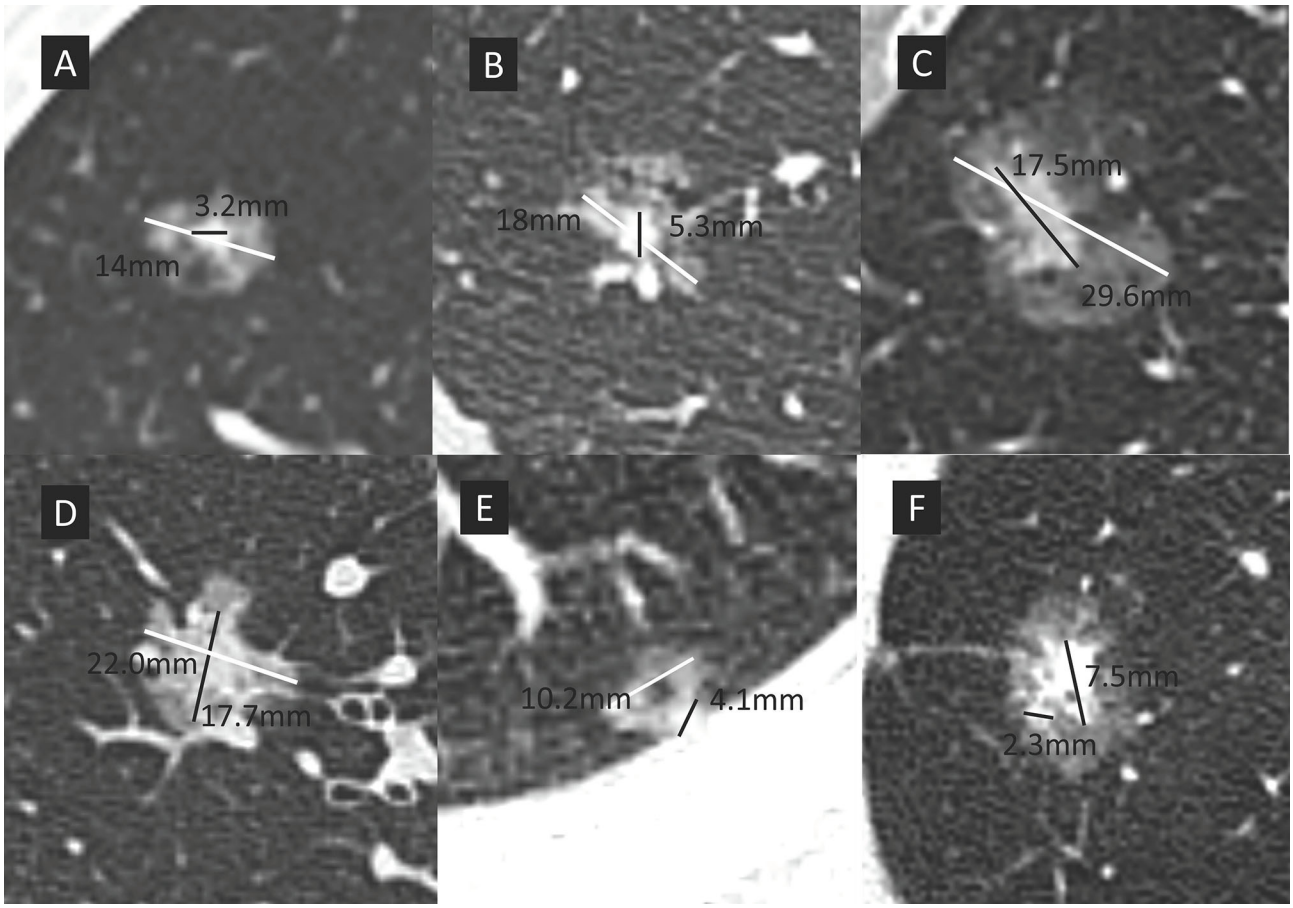

FIGURE 1 | The maximum size of consolidation is divided by the maximum tumor size in the lung window to give the consolidation tumor ratio (CTR). White line represents the maximum overall nodule dimension, black line represents the long axis of the solid component. Patients were divided into 4 groups according to CTR. **(A)** group A, CTR ≤ 0.25; **(B)** group B, 0.25<CTR ≤ 0.5; **(C)** group C, 0.5<CTR ≤ 0.75; **(D)** group D, 0.75<CTR<1; **(E)** a sub-solid nodule with cystic component, the solid components abuts the chest wall and cystic components, makes the accurate measurement challenging. The largest solid dimension was selected for measurement; **(F)** two separate solid components existed in the same nodule (maximum diameter, 7.5mm). Only the largest component needs to be measured in nodules with multiple solid components.

curves of recurrence free survival (RFS) was generated by the Kaplan-Meier method, and survival curves were compared using the log-rank test. Logistic regression was used for dichotomous outcomes. Univariate and multivariate analyses using Cox's proportional hazard model were conducted to obtain the risk factors for relapse-free survival (RFS). Factors with P- value <0.10 were included in multivariate analysis. The surv_cutpoint function in R package "survminer" was applied to determine the optimal cutoff of CTR for RFS. ROC analyses were generated to validate the cutoff value of CTR for RFS and calculate the optimal cutoff values of CTR for micropapillary/solid pathologic subtypes and lymph node metastasis. All statistical tests were 2-sided and statistical significance was defined as $P < 0.05$. Statistical analysis was conducted using Statistical Package for Social Sciences (SPSS) 20.0 software (SPSS Inc., Chicago, IL, USA), GraphPrism 5.0 software (GraphPad Software, Inc., La Jolla, CA, USA) and R version 4.0.3 (http://www.r-project.org/). The R package included survival, survminer and ggplot2.

RESULTS

Clinicopathological Characteristics

The clinicopathological characteristics of the patients are demonstrated in **Table 1**. The majority of the patients were female, with no significant difference achieved among four groups (P=0.06). With higher CTR, lobectomy was chosen more frequently than sublobar resection (P<0.001). Both whole tumor size and consolidation size were higher in group C and group D. There was no significant difference in the rate of smoking history between the four groups (P=0.333). As to pathologic subtype, the rate of adenocarcinoma *in situ* (AIS) or minimally invasive adenocarcinoma (MIA) was 70.6% in group A, which was much higher than the other three groups (P<0.001).

Cox Regression

Univariate and multivariate analyses results were summarized in **Table 2**. Age, gender, surgical mode, surgical approach, whole

TABLE 1 | Clinicopathological Characteristics of Patients.

	Group A	Group B	Group C	Group D	Overall	*P Value*
Gender						0.060
female	328 (74.2%)	135 (64.3%)	121 (69.9%)	24 (64.9%)	608(70.5%)	
male	114 (25.8%)	75 (35.7%)	52 (30.1%)	13 (35.1%)	254 (29.5%)	
Age						<0.001
Mean (SD)	53.7 (11.5)	58.6 (10.6)	60.3 (9.4)	61.3 (9.8)	56.6 (11.1)	
Median	56.0	59.5	61.0	60.0	59.0	
Surgical mode						<0.001
lobectomy	163 (36.9%)	116 (55.2%)	115 (66.7%)	26 (70.3%)	420 (48.7%)	
sublobar resection	279(63.1%)	94 (44.8%)	58 (33.3%)	11 (29.7%)	442 (51.3%)	
Surgical approach						0.005
VATS	440 (99.5%)	208 (99.0%)	167 (96.5%)	35 (94.6%)	850 (98.6%)	
thoracotomy	2 (0.5%)	2 (1.0%)	6 (3.5%)	2 (5.4%)	12 (1.4%)	
Whole tumor size						<0.001
Mean (SD)	10.5 (4.6)	15.9 (6.3)	18.7 (7.5)	18.2 (6.9)	13.7 (6.8)	
Median	9.0	15.0	17.0	17.0	12.0	
Consolidation size						<0.001
Mean (SD)	0.4 (1.1)	6.3 (2.8)	11.5 (4.8)	14.9 (5.5)	4.7 (5.7)	
Median	0.0	6.0	10.0	13.0	3.0	
CTR						<0.001
Mean (SD)	0.03 (0.07)	0.39 (0.07)	0.62 (0.07)	0.83 (0.05)	0.27 (0.28)	
Median	0.00	0.39	0.60	0.82	0.25	
Smoking history						0.333
no smoking history	413 (93.4%)	194 (92.4%)	154 (89.0%)	34 (91.9%)	795 (92.2%)	
current smoker or have smoking history	29 (6.6%)	16 (7.6%)	19 (11.0%)	3 (8.1%)	67 (7.8%)	
Pathologic subtype						<0.001
AIS	101 (22.9%)	7 (3.3%)	2 (1.2%)	0 (0%)	110 (12.8%)	
MIA	221 (47.7%)	36 (17.1%)	19 (11.0%)	2 (5.4%)	268 (31.1%)	
Lepidic dominant	28 (6.3%)	27 (12.9%)	22 (12.7%)	2 (5.4%)	79 (9.2%)	
Acinar dominant	99 (22.4%)	135 (64.3%)	125 (72.3%)	29 (78.4%)	388 (45.0%)	
Papillary dominant	3 (0.7%)	5 (2.4%)	5 (2.9%)	4 (10.8%)	17 (2.0%)	
Differentiation						<0.001
well/moderate	436 (98.6%)	202 (96.2%)	156 (90.2%)	23 (62.2%)	817 (94.8%)	
poorly	6 (1.4%)	8 (3.8%)	17 (9.8%)	14 (37.8%)	45 (5.2%)	
Pleural invasion						<0.001
no pleural invasion	638 (99.1%)	189 (90.0%)	142 (82.1%)	27 (73.0%)	796 (92.3%)	
pleural invasion	4 (0.9%)	21 (10.0%)	31 (17.9%)	10 (27.0%)	66 (7.7%)	
Lymph node metastasis						<0.001
negative	442 (100%)	210 (100%)	173 (100%)	35 (94.6%)	860 (99.8%)	
positive	0 (0%)	0 (0%)	0 (0%)	2 (5.4%)	2 (0.2%)	

SD, stand deviation; VATS, video-assisted thoracic surgery; CTR, consolidation/tumor ratio; AIS, adenocarcinoma in situ; MIA, minimally invasive adenocarcinoma.

tumor size, consolidation size, CTR, smoking history, differentiation, pleural invasion, and lymph node metastasis were included in the analysis. For RFS, surgical approach, whole tumor size, consolidation size, CTR, differentiation, pleural invasion, and lymph node metastasis were included in the multivariate analysis. CTR (HR, 1.865; 95%CI, 1.312-2.650; $p = 0.001$) and lymph node metastasis (HR, 10.407; 95%CI, 1.957-55.343; $p = 0.006$) were identified as independent prognostic factors.

Survival Analysis

The follow-up duration ranged from 2 to 108 months (mean: 47 months). The RFS survival curves of 4 groups were demonstrated in **Figure 2**. There was no relapse in group A and group B. The log-rank test between group A/B and group C/D revealed a significant difference in RFS (p<0.001). The difference turned out to be insignificant between group C and group D (P=0.096). Surv_function was used to determine the optimal cutoff value of CTR for RFS, which is 0.53 (**Figure 3A**). ROC analysis also indicated that the optimal cutoff point of CTR for RFS was 0.53, with the area under the ROC curve (AUC) of 0.902 (**Figure 3B**). There was significant difference in 5-year RFS rate between groups CTR ≤ 0.53 and 0.53<CTR<1 (P<0.0001) (**Figure 3C**).

Logistic Regression Analysis

To investigate risk factors for the presence of micropapillary or solid pattern and lymph node metastasis, logistic regression analyses were performed. Preoperative parameters were included, such as age, gender, whole tumor size, consolidation size, CTR, and smoking history. CTR was the only risk factor for the presence of micropapillary or solid pattern (OR=133.9, 95% CI:32.2-556.2, $P<0.001$) and lymph node metastasis (OR=292498.8, 95%CI:1.2-7.4×10^{10}, P=0.047).

Differences in Presence of Micropapillary/ Solid Component and Lymph Node Metastasis

The presence of micropapillary/solid component of the 4 groups was showed in **Table 3**. The difference between group A/B and

TABLE 2 | Univariate and Multivariate Survival Analysis for Relapse-free Survival.

Variables	Univariate			Multivariate		
	HR	95%CI	*P* Value	HR	95%CI	*P* Value
Age	1.051	0.987-1.119	0.118			
Gender						
female	1					
male	0.881	0.234-3.322	0.851			
Surgical mode						
lobectomy	1					
sublobar resection	0.595	0.173-2.042	0.409			
Surgical approach						
VATS	1					
thoracotomy	5.839	0.733-46.530	0.096			
Whole tumor size	1.064	0.997-1.136	0.061			
Consolidation size	1.147	1.073-1.227	<0.001			
CTR	2.011	1.420-2.848	<0.001	1.865	1.312-2.650	0.001
Smoking history						
no smoking history	1					
current smoker or have smoking history	0.044	0.000-915.826	0.539			
Differentiation						
AIS/MIA/IAD without micropapillary or solid component	1					
IAD with micropapillary and/or solid component	8.326	2.172-31.916	0.002			
Pleural invasion						
no pleural invasion	1					
pleural invasion	9.287	2.823-30.551	<0.001			
Lymph node metastasis						
negative	1			1		
positive	75.776	15.608-367.889	<0.001	10.407	1.957-55.343	0.006

HR, hazard ratio; CI, confidence interval; VATS, video-assisted thoracic surgery; CTR, consolidation/tumor ratio; Well/moderate differentiation. AIS, adenocarcinoma in situ; MIA, minimally invasive adenocarcinoma; IAD, invasive adenocarcinoma.

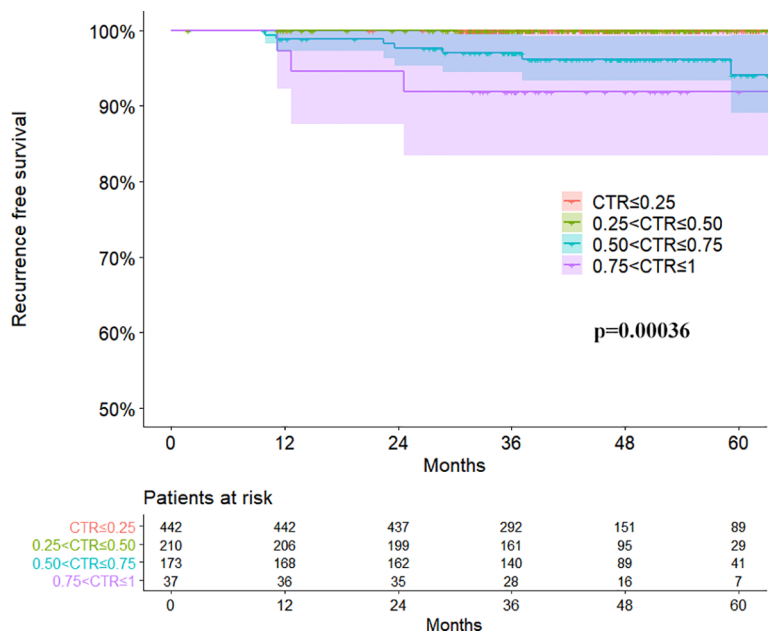

FIGURE 2 | Recurrence free survival curves of four groups divided by consolidation tumor ratio in clinical stage IA lung adenocarcinomas.

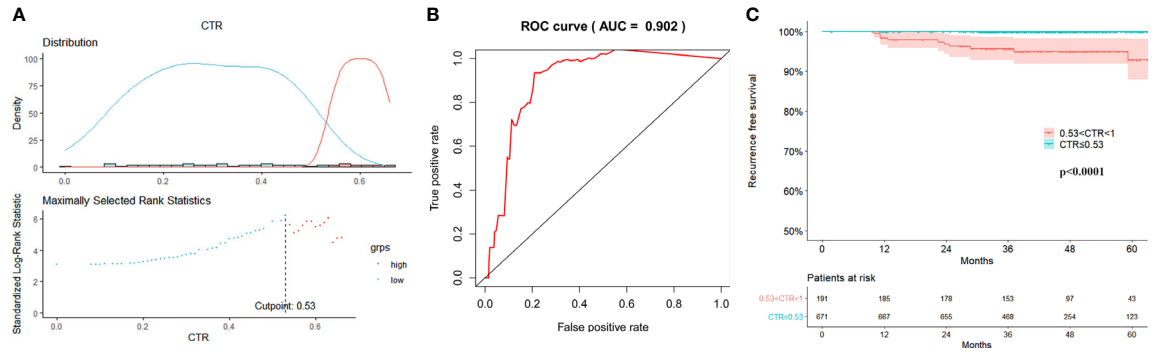

FIGURE 3 | Optimal cutoff value of consolidation tumor ratio for recurrence free survival (RFS). **(A)** Surv_function provided a cutoff value of consolidation tumor ratio (CTR) 0.53 that corresponded to the most significant relation with RFS; **(B)** In receiver operating characteristics analysis, the optimum cutoff value of CTR for RFS was 0.53, area under the ROC curve (AUC) was 0.902; **(C)** The 5-year RFS was significantly different between groups CTR ≤ 0.53 and 0.53<CTR<1 (P < 0.001).

group C/D was significant (*P*<0.001). Paired comparison showed that the presence rate of micropapillary/solid component in group D was significantly higher than other 3 groups (P<0.001), the presence rate of micropapillary/solid component in group C was significantly higher than group B (P=0.030) and group A (P<0.001), while there was no significant difference between group A and group B (P=0.084). ROC curve revealed the optimal cutoff value of CTR for poor differentiation was 0.47 (**Figure 4A**).

Lymph node metastasis occurred in group D only (**Table 4**), and the difference was significant (*P*=0.002). Paired comparison showed that lymph node metastasis rate in group D was significantly higher than the other 3 groups, while there was no significant difference between group A, group B, and group C. ROC curve revealed the optimal cutoff value of CTR for lymph node metastasis was 0.76 (**Figure 4B**).

Comment

The incidence of GGOs has been rising in recent years with the widespread use of CT scan, especially thin-section CT scan. A majority of resected GGOs were confirmed to be early-stage lung adenocarcinoma or atypical adenomatous hyperplasia. In both retrospective and prospective studies, patients with GGO lesions have a better survival rate than patients with pure solid lung cancer after surgical resection (2, 3, 23–26). For pure GGO lesion patients, the lung cancer specific survival rate was reported to be 100% (24, 25, 27).

Even though the prognosis for GGO is good, there remains recurrence and lung cancer specific death. It is important to know the prognostic factors for GGOs, which may help determine the treatment regimen and resection extension. CTR has been considered to be associated with outcomes in pulmonary GGOs. In some retrospective studies, CTR of 0.5 is suggested as a cutoff value for pathological noninvasiveness in GGO lesions (8–13). Japan Clinical Oncology Group (JCOG) 0201 (28), a prospective radiological study, suggested that noninvasive adenocarcinoma could be defined as an adenocarcinoma ≤2cm with CTR ≤ 0.25. The survival outcomes of JCOG 0201 revealed that the criteria of nodules ≤3cm with CTR ≤0.5 also identify a group of patients with excellent prognosis (29). Thus, the eligibility criteria for JCOG 0802, a prospective clinical trial to compare lobectomy and sublobar resection, were changed to be tumor ≤2cm with CTR>0.5, instead of CTR>0.25 (30). In some retrospective studies, consolidation tumor size was recognized as a prognostic factor as well (5, 31). In the eighth TNM staging system (7), the clinical T stage of part-solid GGO is suggested to be determined by the solid component. Whereas, Hattori and his colleagues (14) found that neither consolidation tumor size nor CTR was associated with overall survival in part-solid lung cancer. In our study, CTR was found to be an independent prognostic factor for RFS in the multivariate COX regression analysis.

As CTR is an independent prognostic factor for GGO, it is then reasonable to study how to divide GGOs with CTR. CTR cutoff value of 0.5 is commonly used to divide GGOs into GGO-predominant nodules and solid-predominant nodules. In our study, the RFS survival rate of GGO-predominant nodules (group A and B, no relapse) was significantly higher than that of solid-predominant nodules (group C and D). The survival of group D was worse than group C, but the difference was not significant (P=0.096). Hattori and his colleagues (26) retrospectively analyzed 497 clinical stage IA radiologic invasive adenocarcinomas, in which 177 nodules were solid-predominant part-solid GGOs. When the solid-predominant part-solid GGOs were divided into two groups with 0.75 of CTR as cutoff, the 5-year overall survival was equivalent in the two groups (95.3% versus 96.8%, $p = 0.703$). These results may indicate that 0.5 is a good cutoff for CTR, and neither GGO-

TABLE 3 | Presence of micropapillary/solid component in 4 groups.

		Group			
		A	B	C	D
Micropapillary/ Solid component	not present	436(98.6%)	202(96.2%)	156(90.2%)	23(62.2%)
	present	6(1.4%)	8(3.8%)	17(9.8%)	14(37.8%)

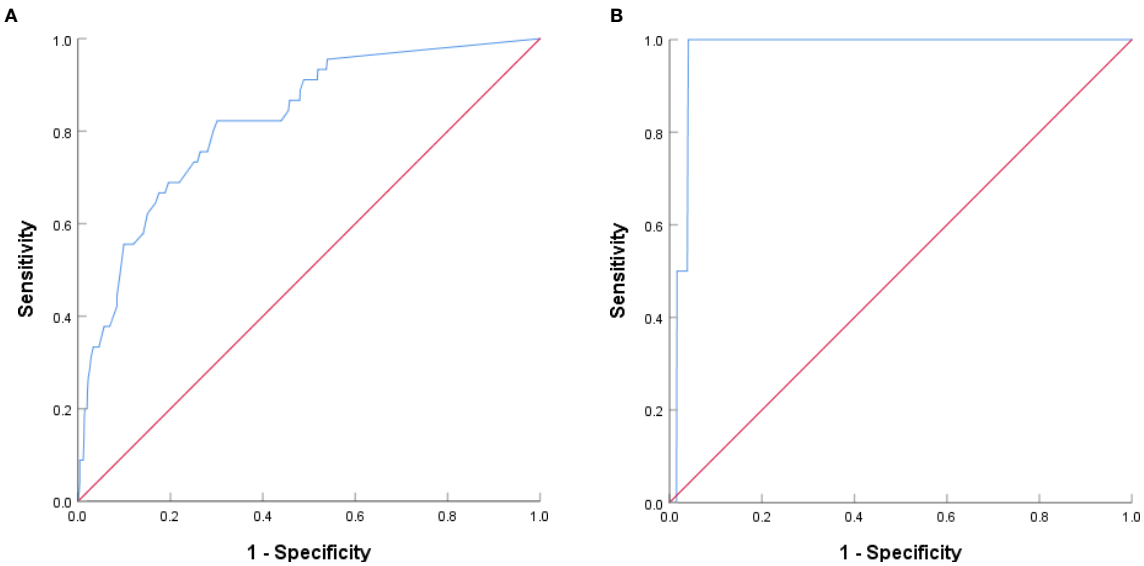

FIGURE 4 | ROC curve analysis based on CTR for poor differentiation and lymph node metastasis. **(A)** The AUC indicated the diagnostic power of CTR for poor differentiation, AUC was 0.822 (95% confidence interval (CI): 0.760-0.883), with a sensitivity of 82.2% and specificity of 69.9% by the Youden's index. **(B)** The AUC indicated the diagnostic power of CTR for lymph node metastasis, AUC was 0.972 (95% confidence interval (CI): 0.953-0.992), with a sensitivity of 100.0% and specificity of 95.9% by the Youden's index.

TABLE 4 | Lymph node metastasis in 4 groups.

		Group			
		A	B	C	D
Lymph node metastasis	No	442 (100.0%)	210 (100.0%)	173 (100.0%)	35 (94.6%)
	Yes	0(0.0%)	0(0.0%)	0(0.0%)	2(5.4%)

predominant GGOs nor solid-predominant GGOs should be divided further. However, as tumors with GGO component have excellent prognosis, studies for GGO lesions demand longer follow-up duration and larger sample size compared with studies for solid tumors, if overall survival or relapse-free survival is chosen to be the exclusive endpoints. Besides, as average life expectancy has been increased in China for years, patients cannot accept a similar 5-year survival rate but a worse 10-year survival rate.

In 1995, Noguchi and his colleagues reviewed 236 surgically resected small peripheral adenocarcinomas ≤2 cm and proposed a pathologic classification of 6 types based on tumor growth patterns (32). In Noguchi's classification, type D is poorly differentiated adenocarcinoma with lower survival rate than type A, B or C. In 2011, IASLC/ATS/ERS proposed a new histological classification of pulmonary adenocarcinoma (19). Micropapillary subtype was introduced to the new classification since micropapillary component was a poor prognostic factor (20, 33). Even in early-stage lung cancer, the presence of micropapillary and solid pattern still correlated with poor survival in several studies (21, 22, 34, 35). The poorly-differentiated patterns represent worse biological behavior of the tumors to some extent. Unlike survival data, pathological information can be collected in short term without concerning insufficient follow-up duration.

To determine whether CTR is associated with the presence of micropapillary or solid pattern and lymph node metastasis, we performed logistic regression analyses, and confirmed that CTR was the only risk factor for the presence of micropapillary or solid pattern (OR=133.9, 95%CI:32.2-556.2, $P<0.001$) and lymph node metastasis (OR=292498.8, 95%CI:1.2-7.4×10^{10}, $P=0.047$). Further analysis showed that the rate of presence of micropapillary or solid pattern was highest in group D, followed by group C and group A/B; the rate of lymph node metastasis was significantly higher in group D than other 3 groups. The biological behavior was different between group A/B, group C and group D. To better study solid-predominant GGOs, the subdivision seems necessary. Considering the good prognosis, sublobar resection could be enough for GGOs. Recent studies have reported similar survival outcomes of part-solid adenocarcinoma treated with sublobar resection and lobectomy (2, 26). However, heterogeneity exists among solid dominant GGOs. As a visual and accessible variable in the clinical work, CTR might provide prognostic implications for appropriate candidates of sublobar resection. Prospective clinical trials are warranted to validate this.

There are several limitations to this study. Firstly, this is a retrospective study that may inevitably lead to bias. Secondly, the sample size for group D is small. Thirdly, longer follow-up is needed to investigate postoperative outcomes of patients with GGO lesions. As mentioned above, a larger sample size or longer follow-up may have led to significant survival difference between group C and group D. Fourthly, volumetric measurement is a

potential approach in measuring the consolidation as it could provide the profile of total solid components within a nodule. However, volumetric measurement is too early to be applied into clinical practice considering the inconveniency and its dependency on nodule density and segmentation algorithms, etc. Currently, the cutoffs of CTR are still being explored and appropriate grouping could distinguish the prognosis well. Further studies are needed to elaborate the role of volumetric measurement in pulmonary GGOs.

In conclusion, consolidation tumor ratio is an independent prognostic factor for clinical stage IA lung adenocarcinoma manifesting as GGO in CT scan. Radiologic cutoffs of CTR 0.50 and 0.75 were able to subdivide patients with different prognosis. Prospective cohort study is warranted to validate our observations.

DATA AVAILABILITY STATEMENT

The raw data supporting the conclusions of this article will be made available by the authors, without undue reservation.

ETHICS STATEMENT

This study was approved by the ethics committee on human research of Zhongshan Hospital (approval number: B2019-232R), and written informed consent was obtained from all patients before surgery for the use of surgical samples and clinical information for medical research.

AUTHOR CONTRIBUTIONS

JX, JY and JL collected data, conducted the data analysis, interpreted the results, and wrote the main manuscript. CZ, ZL, WJ, SX, and QW designed the research, supervised the data analysis, interpreted the data, and critically revised the article. All authors contributed to the article and approved the submitted version.

FUNDING

This study was supported by the National Natural Science Foundation of China (Nos: 81572295). The funding agency played no part in study design, data analysis, interpretation of data, or manuscript preparation.

ACKNOWLEDGMENTS

No potential conflicts of interest exist with any companies/organizations whose products or services may be discussed in this article. No sponsor was related with the development of the research and manuscript.

REFERENCES

1. Hansell DM, Bankier AA, MacMahon H, McLoud TC, Müller NL, Remy J. Fleischner Society: Glossary of terms for thoracic imaging. *Radiology* (2008) 246:697–722. doi: 10.1148/radiol.2462070712
2. Ye T, Deng L, Wang S, Xiang J, Zhang Y, Hu H, et al. Lung Adenocarcinomas Manifesting as Radiological Part-Solid Nodules Define a Special Clinical Subtype. *J Thorac Oncol* (2019) 14:617–27. doi: 10.1016/j.jtho.2018.12.030
3. Miyoshi T, Aokage K, Katsumata S, Tane K, Ishii G, Tsuboi M. Ground-Glass Opacity Is a Strong Prognosticator for Pathologic Stage IA Lung Adenocarcinoma. *Ann Thorac Surg* (2019) 108:249–55. doi: 10.1016/j.athoracsur.2019.01.079
4. Sone S, Nakayama T, Honda T, Tsushima K, Li F, Haniuda M, et al. Long-term follow-up study of a population-based 1996-1998 mass screening programme for lung cancer using mobile low-dose spiral computed tomography. *Lung Cancer* (2007) 58:329–41. doi: 10.1016/j.lungcan.2007.06.022
5. Maeyashiki T, Suzuki K, Hattori A, Matsunaga T, Takamochi K, Oh S. The size of consolidation on thin-section computed tomography is a better predictor of survival than the maximum tumour dimension in resectable lung cancer. *Eur J Cardio-Thoracic Surg* (2013) 43:915–8. doi: 10.1093/ejcts/ezs516
6. Huang TW, Lin KH, Huang HK, Chen YI, Ko KH, Chang CK, et al. The role of the ground-glass opacity ratio in resected lung adenocarcinoma. *Eur J Cardio-Thoracic Surg* (2018) 54:229–34. doi: 10.1093/ejcts/ezy040
7. Travis WD, Asamura H, Bankier AA, Beasley MB, Detterbeck F, Flieder DB, et al. The IASLC Lung Cancer Staging Project : Proposals for Coding T Categories for Subsolid Nodules and Assessment of Tumor Size in Part-Solid Tumors in the Forthcoming Eighth Edition of the TNM Classification of Lung Cancer. *J Thorac Oncol* (2016) 11:1204–23. doi: 10.1016/j.jtho.2016.03.025
8. Asamura H, Suzuki K, Watanabe S. A Clinicopathological Study of Resected Subcentimeter Lung Cancers: A Favorable Prognosis for Ground Glass Opacity Lesions. *Ann Thorac Surg* (2003) 76:1016–22. doi: 10.1016/S0003-4975(03)00835-X
9. Ikeda N, Maeda J, Yashima K, Tsuboi M, Kato H, Akada S, et al. A clinicopathological study of resected adenocarcinoma 2 cm or less in diameter. *Ann Thorac Surg* (2004) 78:1011–6. doi: 10.1016/j.athoracsur.2004.03.048
10. Suzuki K, Kusumoto M, Watanabe SI, Tsuchiya R, Asamura H. Radiologic classification of small adenocarcinoma of the lung: Radiologic-pathologic correlation and its prognostic impact. *Ann Thorac Surg* (2006) 81:413–9. doi: 10.1016/j.athoracsur.2005.07.058
11. Aoki T, Tomoda Y, Watanabe H, Nakata H, Kasai T, Hashimoto H, et al. Peripheral lung adenocarcinoma: Correlation of thin-section CT findings with histologic prognostic factors and survival. *Radiology* (2001) 220:803–9. doi: 10.1148/radiol.2203001701
12. Matsuguma H, Yokoi K, Anraku M, Kondo T, Kamiyama Y, Mori K, et al. Proportion of ground-glass opacity on high-resolution computed tomography in clinical T1 N0 M0 adenocarcinoma of the lung: A predictor of lymph node metastasis. *J Thorac Cardiovasc Surg* (2002) 124:278–84. doi: 10.1067/mtc.2002.122298
13. Nakata M, Sawada S, Yamashita M, Saeki H, Kurita A, Takashima S, et al. Objective radiologic analysis of ground-glass opacity aimed at curative limited resection for small peripheral non-small cell lung cancer. *J Thorac Cardiovasc Surg* (2005) 129:1226–31. doi: 10.1016/j.jtcvs.2004.10.032
14. Hattori A, Matsunaga T, Takamochi K, Oh S, Suzuki K. Neither Maximum Tumor Size nor Solid Component Size Is Prognostic in Part-Solid Lung Cancer: Impact of Tumor Size Should Be Applied Exclusively to Solid Lung Cancer. *Ann Thorac Surg* (2016) 102:407–15. doi: 10.1016/j.athoracsur.2016.02.074
15. Travis WD, Brambilla E, Nicholson AG, Yatabe Y, Austin JHM, Beasley MB, et al. The 2015 World Health Organization Classification of Lung Tumors:

Impact of Genetic, Clinical and Radiologic Advances since the 2004 Classification. *J Thorac Oncol* (2015) 10:1243–60. doi: 10.1097/JTO.0000000000000630
16. Sumiyoshi S, Yoshizawa A, Sonobe M, Kobayashi M, Fujimoto M, Tsuruyama T, et al. Pulmonary adenocarcinomas with micropapillary component significantly correlate with recurrence, but can be well controlled with EGFR tyrosine kinase inhibitors in the early stages. *Lung Cancer* (2013) 81:53–9. doi: 10.1016/j.lungcan.2013.04.003
17. Cakir E, Yilmaz A, Demirag F, Oguztuzun S, Sahin S, Yazici UE, et al. Prognostic significance of micropapillary pattern in lung adenocarcinoma and expression of apoptosis-related markers: Caspase-3, bcl-2, and p53. *Apmis* (2011) 119:574–80. doi: 10.1111/j.1600-0463.2011.02778.x
18. Yoshizawa A, Sumiyoshi S, Sonobe M, Kobayashi M, Fujimoto M, Kawakami F, et al. Validation of the IASLC/ATS/ERS lung adenocarcinoma classification for prognosis and association with EGFR and KRAS gene mutations: Analysis of 440 Japanese patients. *J Thorac Oncol* (2013) 8:52–61. doi: 10.1097/JTO.0b013e3182769aa8
19. Travis WD, Brambilla E, Noguchi M, Nicholson AG, Geisinger KR, Yatabe Y, et al. International association for the study of lung cancer/American Thoracic Society/European Respiratory Society international multidisciplinary classification of lung adenocarcinoma. *J Thorac Oncol* (2011) 6:244–85. doi: 10.1097/JTO.0b013e318206a221
20. Satoh Y, Hoshi R, Horai T, Okumura S, Nakagawa K, Ishikawa Y, et al. Association of cytologic micropapillary clusters in cytology samples with lymphatic spread in clinical stage I lung adenocarcinomas. *Lung Cancer* (2009) 64:277–81. doi: 10.1016/j.lungcan.2008.09.017
21. Xu S, Xi J, Jiang W, Lu S, Wang Q. Solid component and tumor size correlate with prognosis of stage IB lung adenocarcinoma. *Ann Thorac Surg* (2015) 99:961–7. doi: 10.1016/j.athoracsur.2014.10.079
22. Qian F, Yang W, Wang R, Xu J, Wang S, Zhang Y, et al. Prognostic significance and adjuvant chemotherapy survival benefits of a solid or micropapillary pattern in patients with resected stage IB lung adenocarcinoma. *J Thorac Cardiovasc Surg* (2018) 155:1227–35.e2. doi: 10.1016/j.jtcvs.2017.09.143
23. Hattori A, Matsunaga T, Takamochi K, Oh S. Prognostic impact of a ground glass opacity component in the clinical T classification of non – small cell lung cancer. *J Thorac Cardiovasc Surg* (2017) 154:2102–10.e1. doi: 10.1016/j.jtcvs.2017.08.037
24. Chang B, Hwang JH, Choi YH, Chung MP, Kim H, Kwon OJ, et al. Natural history of pure ground-glass opacity lung nodules detected by low-dose CT scan. *Chest* (2013) 143:172–8. doi: 10.1378/chest.11-2501
25. Kakinuma R, Noguchi M, Ashizawa K, Kuriyama K, Maeshima AM, Koizumi N, et al. Natural history of pulmonary subsolid nodules: A prospective multicenter study. *J Thorac Oncol* (2016) 11:1012–28. doi: 10.1016/j.jtho.2016.04.006
26. Hattori A, Matsunaga T, Takamochi K, Oh S, Suzuki K. Importance of Ground Glass Opacity Component in Clinical Stage IA Radiologic Invasive Lung Cancer. *Ann Thorac Surg* (2017) 104:313–20. doi: 10.1016/j.athoracsur.2017.01.076
27. Mao R, She Y, Zhu E, Chen D, Dai C, Wu C, et al. A Proposal for Restaging of Invasive Lung Adenocarcinoma Manifesting as Pure Ground Glass Opacity. *Ann Thorac Surg* (2019) 107:1523–31. doi: 10.1016/j.athoracsur.2018.11.039
28. Suzuki K, Koike T, Asakawa T, Kusumoto M, Asamura H, Nagai K, et al. A prospective radiological study of thin-section computed tomography to predict pathological noninvasiveness in peripheral clinical ia lung cancer (Japan Clinical Oncology Group 0201). *J Thorac Oncol* (2011) 6:751–6. doi: 10.1097/JTO.0b013e31821038ab
29. Asamura H, Hishida T, Suzuki K, Koike T. Radiographically determined noninvasive adenocarcinoma of the lung : Survival outcomes of Japan Clinical Oncology Group 0201. *J Thorac Cardiovasc Surg* (2013) 146:24–30. doi: 10.1016/j.jtcvs.2012.12.047
30. Nakagawa K, Watanabe SI, Kunitoh H, Asamura H. The Lung Cancer Surgical Study Group of the Japan Clinical Oncology Group: Past activities, current status and future direction. *Jpn J Clin Oncol* (2017) 47:194–9. doi: 10.1093/jjco/hyw169
31. Tsutani Y, Miyata Y, Nakayama H, Okumura S, Adachi S, Yoshimura M, et al. Prognostic significance of using solid versus whole tumor size on high-resolution computed tomography for predicting pathologic malignant grade of tumors in clinical stage IA lung adenocarcinoma: A multicenter study. *J Thorac Cardiovasc Surg* (2012) 143:607–12. doi: 10.1016/j.jtcvs.2011.10.037
32. Nouguchi M, Morikawa A, Kawasaki M, Matsno Y, Yamada T, Hirohashi S, et al. Small Adenocarcinoma of the Lung. Histologic Characteristics and Prognosis. *Cancer* (1995) 75:2844–52. doi: 10.1002/1097-0142(19950615)75:12<2844::AID-CNCR2820751209>3.0.CO;2-#
33. Sánchez-mora N, Cebollero M, Monroy V, Moreno N, Lara-martínez JM, Herranz M, et al. Micropapillary lung adenocarcinoma : a distinctive histologic subtype with prognostic significance . Case series. *Hum Pathol* (2008) 39:324–30. doi: 10.1016/j.humpath.2007.05.029
34. Nakagawa K, Shirakusa T, Ph D, Tsuchiya E, Ph D, Ishikawa Y, et al. Early-Stage Lung Adenocarcinomas With a Micropapillary Pattern, a Distinct Pathologic Marker for a Significantly Poor Prognosis. *Am J Surg Pathol* (2003) 27:101–9. doi: 10.1097/00000478-200301000-00011
35. Yoshida Y, Aya N, Ushiku S, Sato J. Micropapillary histological subtype in lung adenocarcinoma of 2 cm or less : impact on recurrence and clinical predictors. *Gen Thorac Cardiovasc Surg* (2017) 0:. doi: 10.1007/s11748-017-0747-3

Conflict of Interest: The authors declare that the research was conducted in the absence of any commercial or financial relationships that could be construed as a potential conflict of interest.

frontiers in Oncology

SYSTEMATIC REVIEW
published: 12 April 2021
doi: 10.3389/fonc.2021.629394

Adjuvant EGFR-TKIs for Patients With Resected EGFR-Mutant Non-Small Cell Lung Cancer: A Meta-Analysis of 1,283 Patients

Rui-Lian Chen[1], Ling-Ling Sun[1], Yang Cao[1], Han-Rui Chen[1], Jing-Xu Zhou[1], Chu-Ying Gu[1], Ying Zhang[2,3], Si-Yu Wang[4], Wei Hou[2,3] and Li-Zhu Lin[1]**

[1] Integrative Cancer Centre, The First Affiliated Hospital of Guangzhou University of Chinese Medicine, Guangzhou, China, [2] Department of Oncology, Guang'anmen Hospital, China Academy of Chinese Medical Sciences, Beijing, China, [3] Cancer Project Team of China Center for Evidence Based Traditional Chinese Medicine, Beijing, China, [4] Department of Thoracic Surgery, Sun Yat-sen University Cancer, Guangzhou, China

OPEN ACCESS

Edited by:
Kai He,
The Ohio State University,
United States

Reviewed by:
Zhongxing Liao,
University of Texas MD Anderson Cancer Center, United States
Greg Durm,
Indiana University, United States

***Correspondence:**
Wei Hou
houwei1964@163.com
Li-Zhu Lin
lizhulin26@yahoo.com

Specialty section:
This article was submitted to Thoracic Oncology, a section of the journal Frontiers in Oncology

Received: 14 November 2020
Accepted: 12 March 2021
Published: 12 April 2021

Citation:
Chen R-L, Sun L-L, Cao Y, Chen H-R, Zhou J-X, Gu C-Y, Zhang Y, Wang S-Y, Hou W and Lin L-Z (2021) Adjuvant EGFR-TKIs for Patients With Resected EGFR-Mutant Non-Small Cell Lung Cancer: A Meta-Analysis of 1,283 Patients. Front. Oncol. 11:629394. doi: 10.3389/fonc.2021.629394

Background: Cisplatin-based chemotherapy was previously considered as the standard adjuvant therapy for improved overall survival (OS) in patients with non-small cell lung cancer (NSCLC) after surgery. However, the benefit was limited due to high risks of recurrence and adverse events. In the present study, the efficacy of adjuvant epidermal growth factor receptor tyrosine kinase inhibitors (EGFR-TKIs) for EGFR-mutant patients after surgery was investigated using the latest updated data.

Methods: This meta-analysis included a comprehensive range of relevant studies identified from database searches. Disease-free survival (DFS) and OS with hazard ratios (HRs) were calculated using random-effect or fixed-effect models. Subgroup analysis was also performed.

Results: A total of seven randomized clinical trials were included in the meta-analysis and involved 1,283 NSCLC patients harboring EGFR mutations. In resected EGFR-mutant NSCLC patients, adjuvant EGFR-TKIs were significantly better than chemotherapy in terms of DFS (HR: 0.41; 95%CI: 0.24–0.70, P = 0.001), without showing any benefit in OS (HR: 0.72; 95%CI: 0.37–1.41, P = 0.336). No significant difference in DFS was observed between patients with EGFR exon 19 deletion and those with L858R mutation. Resected EGFR-mutant NSCLC patients treated with osimertinib experienced improved DFS and a lower risk of brain recurrence than those treated with gefitinib or erlotinib. Adjuvant EGFR-TKIs reduced the risk of bone and lung relapse, without decreasing the risk of local recurrence and liver relapse.

Conclusion: This meta-analysis shows that adjuvant EGFR-TKI therapy could significantly prolong DFS in patients with resected EGFR-mutant NSCLC. Treatment with osimertinib showed improved DFS with a lower risk of brain recurrence than treatment with gefitinib or erlotinib for resected disease.

Keywords: adjuvant EGFR-TKIs, non-small-cell lung cancer, EGFR mutation, resected, meta-analysis, brain recurrence

INTRODUCTION

Lung cancer remains the leading cause of cancer-related mortality worldwide (1). Among the patients diagnosed each year with non-small cell lung cancer (NSCLC), 20–25% of cases with early-stage (I–IIIA) disease are suitable for surgical resection with curative intent (2). Postoperative cisplatin-based chemotherapy has been recommended as adjuvant treatment in resected NSCLC patients, except for subjects with stage IA and part of stage IB (3, 4). However, the therapy only resulted in a 16% decrease in the risk of disease recurrence and a 5% increase in 5-year overall survival (OS) (5).

Molecular-targeted drugs have been successfully used as adjuvant therapy for several types of cancers, for example, imatinib for gastrointestinal stromal tumors (6, 7). Epidermal growth factor receptor (EGFR) mutations are common oncogenic driver mutations in NSCLC patients, such as EGFR exon 19 deletion and L858R mutation. EGFR tyrosine kinase inhibitors (EGFR-TKIs) are considered as standard first-line treatment for advanced NSCLC harboring EGFR mutations, with improved progression-free survival (PFS) and quality of life (8, 9). This has promoted the investigation of their use as adjuvant therapy in resected patients.

The ADAURA trial showed that the disease-free survival (DFS) of patients treated with osimertinib was significantly longer than that with a placebo in resected EGFR-mutant NSCLC patients with stage IB to IIIA disease, consistent with the results of the CTONG 1104 and EVAN trials. However, in several previous trials, conflicting results regarding the efficacy of adjuvant EGFR-TKIs in resected NSCLC patients were reported (10–13). Furthermore, advanced NSCLC patients harboring EGFR exon 19 deletion experienced a better prognosis, compared with those harboring L858R mutation when treated with EGFR-TKIs (14, 15). In early-stage NSCLC disease, the difference in the efficacy of EGFR-TKI based on EGFR mutation status was not previously reported. In addition, the recurrence rate of resected NSCLC is approximately 30–75%, with poor postoperative morbidity (16, 17). Understanding the recurrence patterns after treatment with adjuvant EGFR-TKIs can help immediately identify the sites prone to recurrence, and the prognosis can be improved with appropriate surveillance strategies in clinical practice. However, evidence regarding the long-term tumor recurrence patterns after EGFR-TKIs as adjuvant therapy is scare. In advanced EGFR-mutant NSCLC disease, first-line treatment with osimertinib showed improved clinical benefit and reduced the risk of the central nervous system recurrence compared with gefitinib or erlotinib treatment (18). In resected disease, the difference in clinical outcome and brain relapse between treatment with osimertinib *versus* gefitinib or erlotinib has not been investigated. Thus, a meta-analysis to investigate the effects of adjuvant EGFR-TKIs is urgently needed. In the present study, the difference in clinical outcome based on the generation of EGFR-TKI or mutation status was investigated, and tumor recurrence patterns were explored with the subgroup analyses. The results of this study may provide more information and guidance for researchers and clinicians in the management of adjuvant therapy in resected EGFR-mutant NSCLC patients.

METHODS

Study Eligibility and Selection

The PubMed, Embase, and the Cochrane Library databases were used in a systematic search for studies published up to September 20, 2020 with no start date limit applied. The search terms used were "lung cancer", "adjuvant or resected or operable", "erlotinib or gefitinib or icotinib or afatinib or dacomitinib or osimertinib" and "randomized control trial". We also searched meeting abstracts from the American Society of Clinical Oncology, European Society for Medical Oncology, World Conference on Lung Cancer and American Association for Cancer Research for Medical Oncology websites.

Eligible studies that met the following criteria were included: Phase II or III randomized control trials (RCTs); and comparisons of survival in stage I–IIIA NSCLC patients treated with adjuvant EGFR-TKIs *versus* adjuvant chemotherapy or placebo; and studies with reported hazard ratios (HRs) for survival analysis (DFS or OS) or the number of events for disease relapse patterns and adverse events (AEs) in EGFR-mutant lung cancer from the overall patient population or subgroups analyses. The exclusion criteria were as follows: studies with irretrievable or insufficient data for statistical analysis; single-arm trials, observational studies, editorials, reviews, and commentaries; duplicate studies; and abstracts and studies written in languages other than English. Two authors (L-LS and H-RC) independently searched the databases and screened articles using the titles and abstracts to find potentially relevant studies.

Data Extraction

All candidate articles were independently evaluated and extracted by two investigators (R-LC and J-XZ), and all discrepancies were resolved by the consensus among all authors. From each study, the first author name, clinical trial name, trial phase, EGFR mutation status, generation of adjuvant EGFR-TKIs, other baseline clinicopathologic characteristics, planned and received treatment and toxicity, survival outcomes, and relapse patterns were extracted. The quality of the included studies was independently assessed by two authors (YC and YZ), according to the five-point Jadad scoring system (19).

Statistical Analysis

The HRs and 95% confidence intervals (CIs) for the DFS and OS of resected EGFR-mutant NSCLC patients were derived from the overall patient population and subgroups within each individual study. For dichotomous outcomes, the number of patients was used to calculate odds ratio (OR) estimates of trials with the Mantel–Haenszel method, such as disease relapse patterns and AEs.

There are two common statistical models for meta-analysis, the fixed-effect model and the random-effect model. The fixed-effect model depends on the hypothesis that all studies in the meta-analysis share a true effect size. In contrast, in the random-effect model, the true effect size may differ from study to study. The random-effect model is often considered

as the appropriate model (20). Heterogeneity among the trials was assessed using the Q-test and was quantified with I^2 values (21). An I^2 statistic >50% or P value <0.05 was defined as significant heterogeneity among trials. If significant heterogeneity was observed, the random-effect model was used for analysis. If significant heterogeneity was not found, the fixed-effect model was applied (22). In addition, the funnel plot and the Begg's and Egger's tests were performed. All reported P-values were two sided, and the statistically significant level was set at 0.05. The meta-analysis was performed in accordance with recommendations from the Cochrane Collaboration and the Preferred Reporting Items for Systematic Reviews and Meta-Analyses guidelines, using Stata/SE version 16.0 software (Stata Corporation, College Station, TX, USA).

Subgroup Analysis

A series of subgroup analyses were conducted to explore the effects of variables on the efficacy of EGFR inhibitors for resected EGFR-mutant NSCLC. The subgroup included EGFR mutation status (exon 19 deletion *vs.* L858R mutation), age (age ≥65 years *vs.* <65 years), sex (male *vs.* female), smoking status (smokers *vs.* non-smokers), histology (adenocarcinoma *vs.* non-adenocarcinoma), generation of EGFR-TKIs (gefitinib or erlotinib *vs.* osimertinib), and the relapse patterns.

RESULTS

Characteristics of the Included Studies

A total of 3,058 relevant records were identified from databases and conferences using our search strategy. After screening the titles and abstracts of the articles, the full texts of 31 articles were reviewed for eligibility (**Figure 1**). Among these, seven RCTs were finally considered eligible for our meta-analysis based on the inclusion and exclusion criteria. Detailed data on disease relapse in the CTONG 1104 trial was reported in another article by Xu et al. (23). A total of 1,283 EGFR-mutant patients were identified in seven studies (10–13, 24–26). All cases in five studies were diagnosed NSCLC with an activating EGFR mutation (12, 13, 24–26). The proportion of resected EGFR-mutant NSCLC patients was 16.5 and 3.0% in the RADIANT and NCIC CTG BR19 (CTSUBR19) studies, respectively (10, 11). The clinical characteristics and the quality assessment of the included studies are presented in **Table 1**.

Effects of EGFR-TKIs on DFS and OS in Patients With Resected EGFR-Mutant NSCLC

EGFR-mutant NSCLC patients showed improved DFS after treatment with adjuvant EGFR-TKIs compared with the control group. Pooled HRs based on the seven RCTs indicated

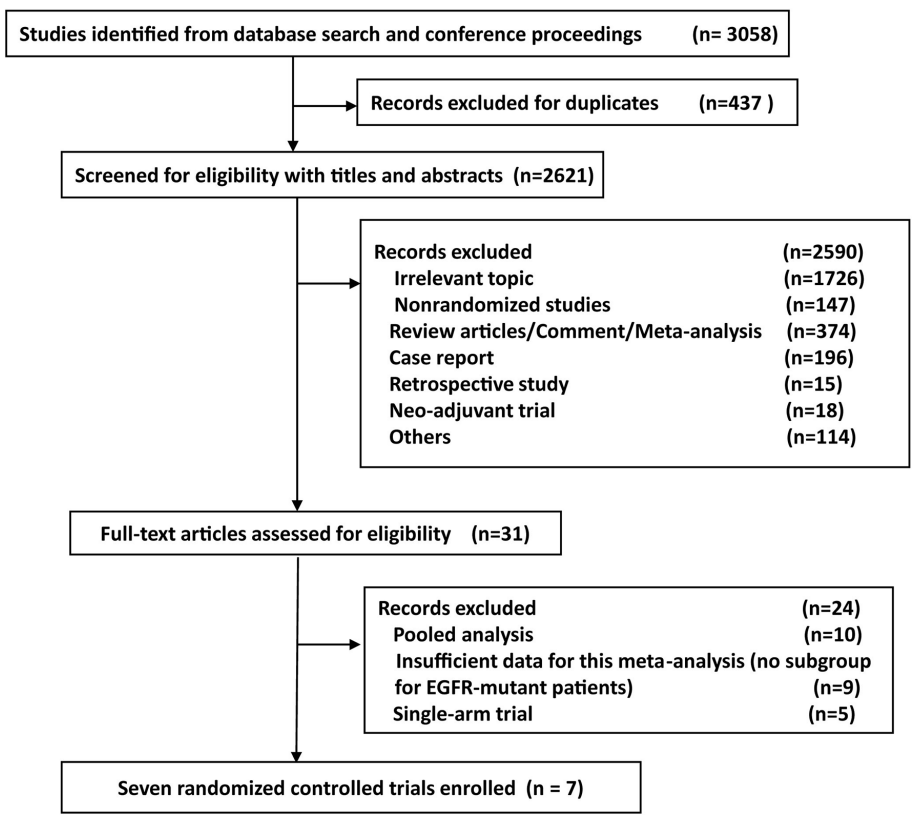

FIGURE 1 | The flowchart of study selection process for the meta-analysis.

TABLE 1 | Characteristics of the included trials in the meta-analysis.

Clinical trials	Authors	Phase	Age (median)	Stage	Treatment groups	EGFR-mutant Patients	Disease-free survival	Overall survival	Quality assessment
							HR (95%CI)	HR (95%CI)	
RADIANT (11)	Kelly et al. (2015)	3	61	IB–IIIA	Erlotinib *vs* Placebo	161	0.61 (0.38–0.98)	1.09 (0.55–2.16)	6
CTSUBR19 (10)	Goss et al. (2013)	3	NA	IB–IIIA	Gefitinib *vs* Placebo	15	1.84 (0.44–7.73)	0.83 (0.54–1.26)	5
Li et al. (24)	Li et al. (2014)	2	59.5	IIIA	Chemotherapy + gefitinib *vs* chemotherapy	60	0.37 (0.16–0.85)	0.61 (0.42–0.87)	3
Feng et al. (25)	Feng et al. (2015)	2	57	IB–IIIA	Chemotherapy + icotinib *vs* chemotherapy	41	0·22 (0·04–1.15)	0·86 (0·62–1·20)	3
CTONG 1104 (13)	Zhong et al. (2018)	3	58	II–IIIA	Gefitinib *vs* VP	222	0.60 (0.42–0.87)	0.92 (0.62–1.36)	5
EVAN (12)	Yue et al. (2018)	2	59	IIIA	Erlotinib *vs* VP	102	0.27(0.14–0.53)	0.17(0.05–0.58)	5
ADAURA (26)	Wu et al. (2020)	3	NA	IB–IIIA	Osimertinib *vs* Placebo	682	0.20(0.15–0.27)	NA	6

VP, Vinorelbine plus cisplatin; NA, not available.

a lower risk of disease progression with EGFR-TKIs when compared with the control group (HR: 0.41; 95%CI: 0.24–0.70, P = 0.001, **Figure 2A**). Significant heterogeneity in DFS was observed among the trials (I^2 = 82.2%, P < 0.001).

OS data were not available in the study by Feng et al. and not immature in the ADAURA trial. Thus, the analysis of OS was from five RCTs with available data. No significant improvement was observed between adjuvant EGFR-TKI therapy and the control group in resected EGFR-mutant NSCLC (HR: 0.72; 95%CI: 0.37–1.41, P = 0.336, **Figure 2B**). Significant heterogeneity in OS was found (I^2 = 66.0%, P = 0.019).

Effects of EGFR Mutation Status on DFS

To further explore the effects of EGFR mutation status on DFS, subgroup analyses of DFS in patients with exon 19 deletion *versus* L858R mutation were performed. The pooled survival estimates were based on 660 NSCLC patients harboring exon 19 deletion from seven RCTs and showed that EGFR-TKI treatment had a favorable effect on DFS (HR: 0.30; 95%CI: 0.12–0.72; P = 0.007, **Figure 2C**) There was significant heterogeneity in the analysis (I^2 = 83.8%, P < 0.001). A total of 565 patients harboring L858R mutation experienced improved DFS with EGFR-TKI therapy compared with the control group (HR: 0.44; 95%CI: 0.33–0.60; P < 0.001, **Figure 2C**), with no significant heterogeneity (I^2 = 0.9%, P = 0.401). No significant difference in DFS was observed between EGFR exon 19 deletion and L858R mutation subgroups ($P_{\text{for heterogeneity}}$ = 0.290).

Subgroup Analysis Based on Clinical Characteristics

The results of our subgroup analyses are shown in **Figure 3**. For most of the subgroups (sex, age, smoking history, and generation of EGFR-TKIs), the DFS benefit of EGFR-TKIs was greater than the control group. For the histology subgroup, a significant DFS advantage of EGFR-TKIs was observed in EGFR-mutant NSCLC patients with adenocarcinoma, but not in those with non-adenocarcinoma. Furthermore, in patients with resected EGFR-mutant NSCLC, the DFS for osimertinib was longer than that for first-generation EGFR-TKIs, with a statistically significant difference (osimertinib *vs.* gefitinib or erlotinib, HR: 0.20; 95% CI: 0.15–0.27 *vs.* 0.53; 0.41–0.67; $P_{\text{for heterogeneity}}$ < 0.001).

Effects of EGFR-TKIs on Disease Relapse

Data on disease relapse were not reported in the EVAN and RADIANT trials, or in Feng's study. Based on the available data reported from four trials (the ADAURA trial only reported brain recurrence), the effects of EGFR-TKIs on disease relapse were analyzed. EGFR-TKI therapy reduced the risk of bone relapse (OR: 0.40; 95%CI: 0.19–0.85; **Figure 4C**) and lung relapse (OR: 0.51; 95%CI: 0.30–0.86; **Figure 4D**), without decreasing the risk of local recurrence (OR: 0.73; 95%CI: 0.27–1.98, **Figure 4B**) and liver relapse (OR: 0.43; 95%CI: 0.12–1.52, **Figure 4E**). The addition of EGFR-TKIs decreased the distant metastasis risk (OR: 0.59; 95%CI: 0.35–1.00; **Figure 4A**), although the difference was not statistically significant (P = 0.052).

No significant difference was observed in the brain recurrence with EGFR-TKIs compared with the control group (**Figure 4F**).

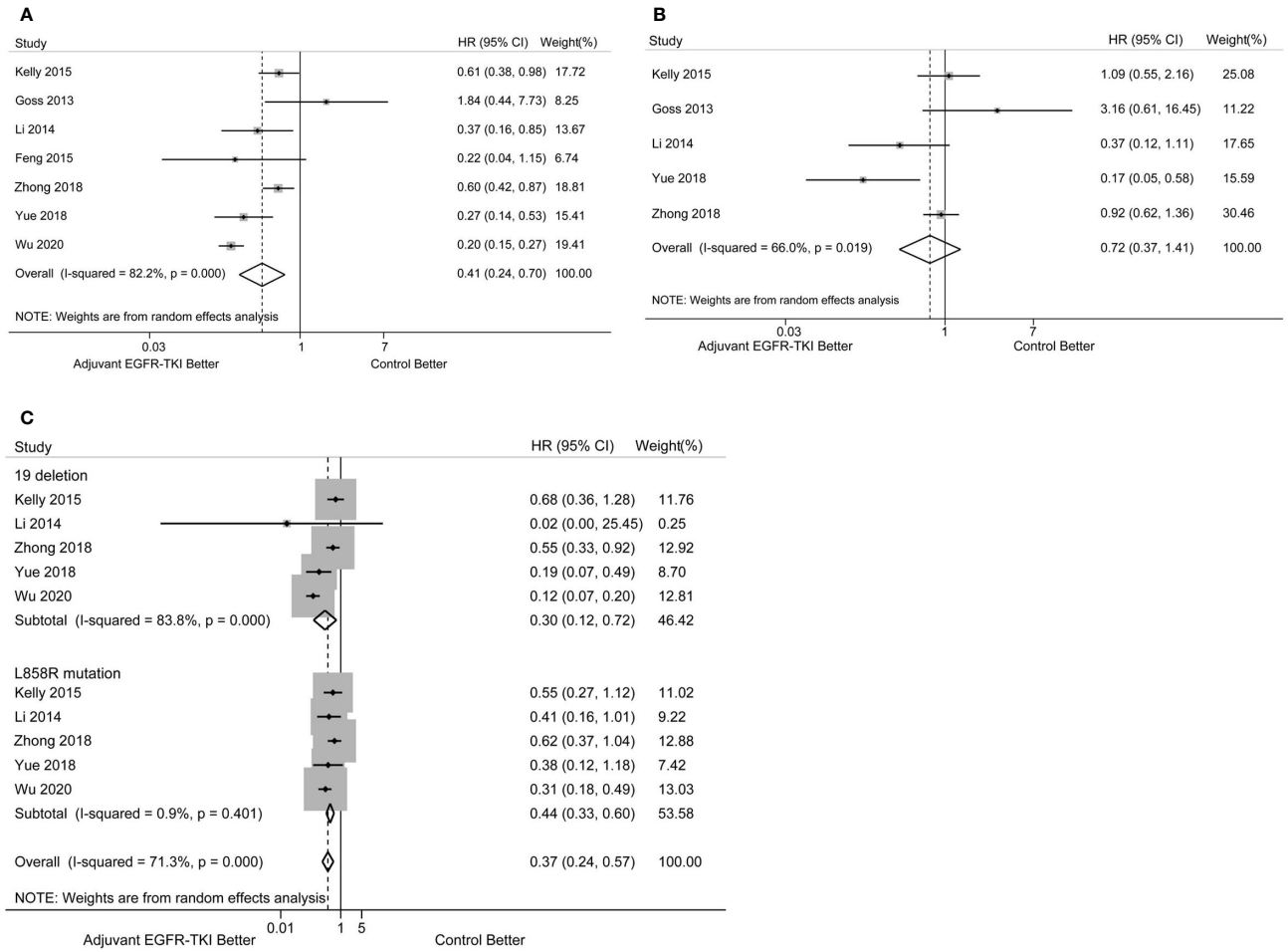

FIGURE 2 | **(A)** Forest plot of hazard ratio (HR) for disease-free survival (DFS) with adjuvant EGFR-TKI *versus* the control group in EGFR-mutant resected NSCLC patients. **(B)** Forest plot of HR for overall survival (OS) with adjuvant EGFR-TKI *versus* control arms in EGFR-mutant resected NSCLC patients. **(C)** Forest plot of HR for DFS with adjuvant EGFR-TKI *versus* the control group in NSCLC patients with EGFR exon 19 deletion and L858R mutation.

Subgroup analysis was performed to evaluate the effects of different generations of EGFR-TKIs. The risk of brain relapse with osimertinib treatment was significantly lower than with gefitinib or erlotinib treatment (osimertinib, OR: 0.11; 95%CI: 0.04–0.32; gefitinib or erlotinib, OR: 0.95; 95%CI: 0.36–2.49; $P_{\text{for heterogeneity}} < 0.001$; **Figure 4F**). The incidence of brain recurrence was 1% (95%CI: 0–3%) in the osimertinib group and 17% (95% CI: 10–28%) in the gefitinib or erlotinib group, with a significant difference as shown in **Figure S1**.

AEs

The AEs of EGFR-TKIs are shown in **Table 2**. Among the 623 EGFR-mutant patients treated with EGFR-TKIs, the rate of AEs of any grade was 86.92% (95%CI: 65.83–95.82%), and the rate of AEs of overall grade 3 or higher was 14.09% (95%CI: 8.23–23.07%). The most common severe AEs included rash (5.09%, 95%CI: 1.51–15.81%), diarrhea (2.57%, 95%CI: 1.58–4.15%), nausea or vomiting (1.93%, 95%CI: 1.10–3.36%), pneumonia (0.78%, 95%CI: 0.20–3.07%), and fatigue (0.35%, 95%CI: 0.05–2.44%).

Study Quality and Publication Bias

Randomized treatment allocation sequences were generated in all trials. Four trials were open-label, and three were double-blind. The Jadad score ranged from 3 to 6, indicating a high quality (**Table 1**). The funnel plot, as well as Egger's and Begg's tests, showed no publication bias in the overall or subgroup populations (all $P > 0.05$).

DISCUSSION

Our large meta-analysis of 1,283 patients with resected EGFR-mutant NSCLC from seven RCTs showed that patients treated with adjuvant EGFR-TKIs experienced improved DFS, with tolerated AEs, compared with chemotherapy or a placebo. No

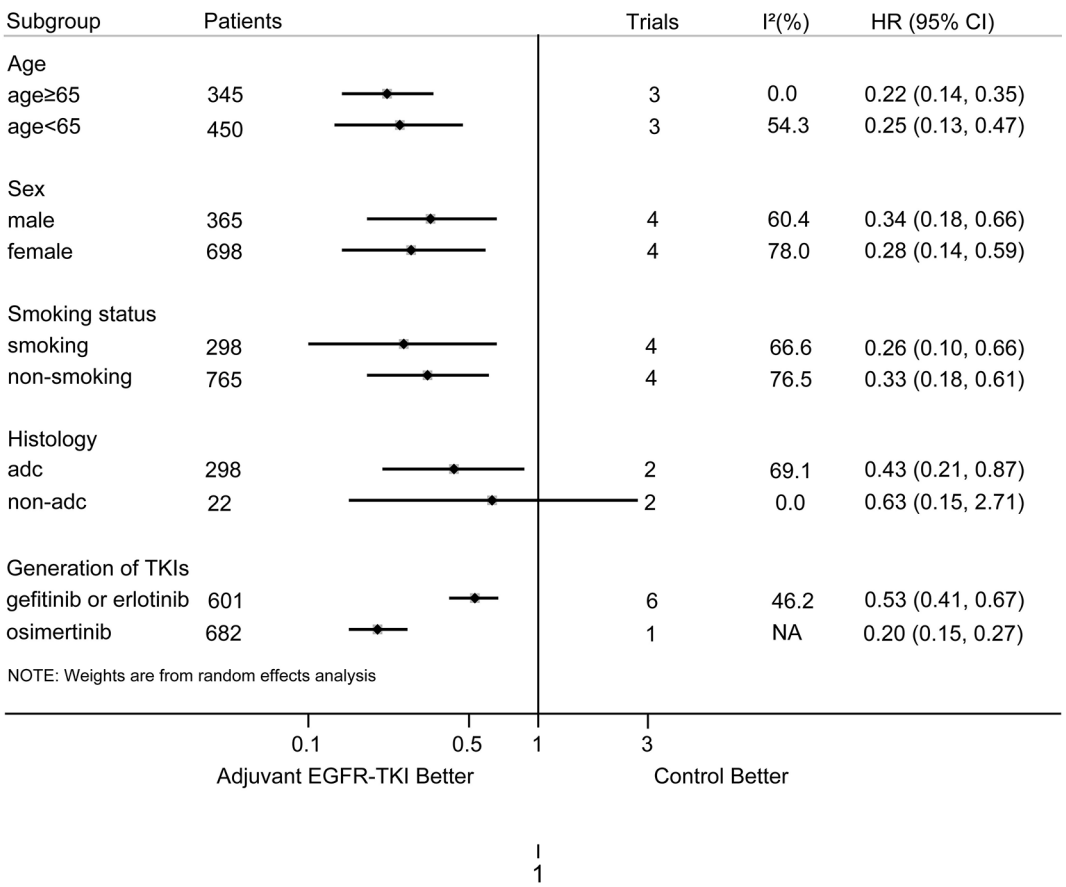

FIGURE 3 | Subgroup analysis on DFS according to age, sex, smoking status, histology, and generation of EGFR-TKIs. NA, not available; adc, adenocarcinoma; non-adc, non-adenocarcinoma.

significant difference in OS was observed in the adjuvant EGFR-TKI group.

Conflicting results regarding the clinical benefit of adjuvant EGFR-TKIs in resected NSCLC patients were reported in previous trials. The CTSUBR19 (10) and RADIANT (11) and trials indicated that resected EGFR-mutant NSCLC patients did not obtain significantly improved clinical benefit of EGFR-TKI treatment; however, significant improved DFS with EGFR-TKIs was observed in the EVAN, CTONG 1104, and ADAURA trials (12, 13, 26). These conflicting results may be due to the different populations investigated in these studies. The EVAN trial and the study by Li et al. enrolled only patients with stage IIIA. All patients in the CTONG 1104 trial and 60% of patients in the ADAURA trial were stages II–IIIA (12, 13, 26). However, most patients in the CTSUBR19 and RADIANT trials were stages I–II (10, 11).

In some meta-analyses, NSCLC patients with EGFR mutation reportedly obtained clinical benefit from adjuvant EGFR-TKI therapy (27–30). However, those meta-analyses included retrospective studies, which are lower in quality than RCTs. Our study is the largest meta-analysis of resected EGFR-mutant NSCLC patients from RCTs to date. Compared with previous meta-analyses, the high quality of data strengthens the evidence on the efficacy of adjuvant EGFR-TKI therapy. In addition, the differences in clinical effects of EGFR-TKIs based on EGFR mutation status (exon 19 deletion *vs.* L858R mutation) were investigated in our meta-analysis. Furthermore, the effects of different generations of EGFR-TKIs and the long-term tumor recurrence patterns were analyzed. The heterogeneity of DFS and OS across studies was substantial in our meta-analysis, which may be due to sex, age, smoking history, histology, stage, and generation of EGFR-TKIs. In advanced NSCLC disease, patients harboring EGFR exon 19 deletion experienced improved PFS with EGFR-TKIs compared with those harboring L858R mutation (15, 31). However, in resected NSCLC, the difference in outcome between patients with these EGFR mutation types treated with adjuvant EGFR-TKIs was not investigated in any study. Our meta-analysis shows that the clinical benefit of adjuvant EGFR-TKIs was observed in early-stage patients harboring EGFR exon 19 deletion or L858R mutation; the difference between the two mutation types was non-significant. There are several possible complicated reasons why our result differs from those of advanced-stage patients reported in previous studies. First,

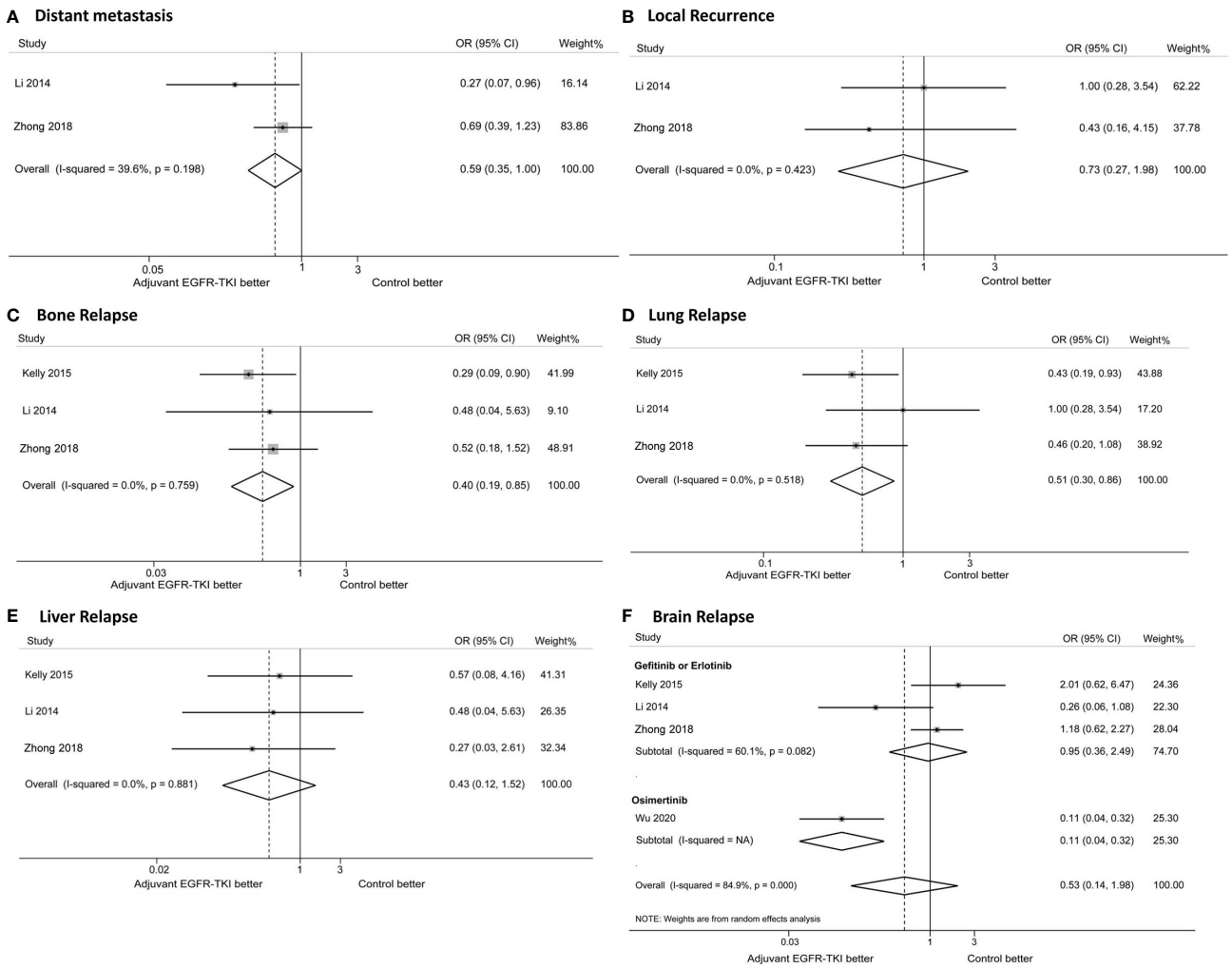

FIGURE 4 | Forest plots of odd ratios (ORs) for distant metastasis **(A)**, local recurrence **(B)**, bone relapse **(C)**, lung relapse **(D)**, brain relapse **(D)**, liver relapse **(E)** and brain relapse **(F)**. * Due to no event was reported, the study by Li was excluded in the analysis of liver relapse, and the study by Kelly was excluded in the analysis of distant metastasis and local recurrence.

TABLE 2 | Severe Adverse events in EGFR-TKIs treatment arm.

Severe adverse events	Li et al. (24)	Kelly et al. (11)	Zhong et al. (13)	Yue et al. (12)	Wu et al. (26)	Incidence (95%CI),%
rash	2	19	1	2	NA	5.09 (1.51–15.81)
diarrhea	1	5	1	1	8	2.57(1.58–4.15)
nausea/vomiting	0	0	3	3	6	1.93(1.10–3.36)
Pneumonia	NA	0	1	1	NA	0.78 (0.20-3.07)
fatigue	0	1	0	0	NA	0.35 (0.05–2.44)
All ≥grade 3 AE	6	30	13	6	22	14.09 (8.23–23.07)
Any grade	28	93	61	29	327	86.92 (65.83–95.82)

AE, adverse event.

the tumor burden in advanced NSCLC patients was higher than that in early-stage NSCLC cases after surgery. Therefore, the abundance of EGFR mutations may be high in patients with metastatic NSCLC. The clinical benefit of EGFR-TKIs was reportedly closely associated with the abundance of EGFR mutations (32). Second, the sample size of patients in the analysis of EGFR mutation status was not large in our meta-analysis; thus, additional studies with a larger cohort are necessary. The biological behavior of early-stage NSCLC may differ from that of advanced-stage NSCLC.

Our meta-analysis shows that resected EGFR-mutant NSCLC patients treated with osimertinib experienced significantly longer DFS and a reduced risk of brain recurrence, compared with those who received gefitinib or erlotinib. In preclinical studies, osimertinib could induce apoptosis and exert better effects against EGFR-mutant tumor compared with first-generation EGFR-TKIs, with significant results observed in xenograft and transgenic models (33, 34). In previous studies, osimertinib had better exposure in the brain than other EGFR-TKIs due to the greater penetration of the blood–brain barrier (35, 36). In addition, first-line treatment with osimertinib showed significant clinical benefit in terms of PFS and OS in advanced EGFR-mutant NSCLC patients with a decreased the risk of brain progression compared with gefitinib or erlotinib (18, 37, 38). Similar to EGFR-mutant patients with metastatic disease, the superior efficacy of osimertinib was also observed in those with resected NSCLC in our meta-analysis.

Currently, concerns regarding EGFR-TKIs as adjuvant treatment in resected NSCLC remain. First, the early use of EGFR-TKIs could change the biological behaviors in NSCLC patients and lead to more complicated resistance mechanisms, compared with those just waiting until disease recurrence. Treatment duration is another concern. EGFR-mutant patients enrolled in the CTONG 1104 and EVAN trials were treated with adjuvant gefitinib or erlotinib for two years or until disease recurrence; however, patients in the ADAURA trial were treated with adjuvant osimertinib for three years. Re-biopsy is widely used to evaluate the resistance mechanisms after disease relapse and to modify the treatment strategy accordingly. The biological behaviors of relapse disease after treatment with adjuvant EGFR-TKIs requires further investigation. Circulating tumor DNA (ctDNA) has been considered as an excellent predictor of disease recurrence and used to identify the molecular residual disease. In a study of patients with localized lung cancer treated with curative intent, ctDNA was detected in 94% of patients with disease relapse before radiographic recurrence at a median of 5.2 months post-treatment (39). Additional research is needed on using ctDNA to identify molecular residual disease to determine the EGFR-TKI treatment duration and provide personalized adjuvant treatment.

The present study has several limitations. First, data for the analysis of NSCLC patients was derived from published clinical trials rather than from each individual patient. Therefore, analyzing the influence of disease stage accurately is difficult. Second, part of the data in our meta-analysis were derived from subgroup analyses of published RCTs. Thus, some important information was not collected from subgroup results, such as smoking history, stage, sex, and EGFR mutation status. Due to the lack of information on the stage of each patient, specific subgroup analyses of stage I, stage II, and stage III patients could not be performed.

CONCLUSION

Despite the above limitations, the results of the current study have significant implications. This meta-analysis indicates that adjuvant EGFR-TKI therapy brought significant clinical benefit in terms of DFS in resected EGFR-mutant NSCLC patients. Osimertinib had longer DFS with lower risk of brain recurrence than gefitinib or erlotinib for resected NSCLC; however, additional studies are warranted.

DATA AVAILABILITY STATEMENT

The original contributions presented in the study are included in the article/**Supplementary Material**. Further inquiries can be directed to the corresponding author.

AUTHOR CONTRIBUTIONS

Conception and design: L-ZL, WH, and R-LC. Data collection or management: R-LC, L-LS, H-RC and J-XZ. Data evaluation: YC and ZY. Statistical analysis: R-LC, L-LS and C-YG. Manuscript writing and revising: R-LC, S-YW and L-ZL. All authors contributed to the article and approved the submitted version.

FUNDING

This study was supported by grant from Traditional Chinese medicine evidence-based capacity building project (grant number 2019XZZX–ZL001), Pilot project of Integrated traditional Chinese and western medicine clinical collaboration for major and difficult diseases (lung cancer).

ACKNOWLEDGMENTS

We thank the China Academy of Chinese Medical Sciences, China Center for Evidence Based Traditional Chinese Medicine.

SUPPLEMENTARY MATERIAL

The Supplementary Material for this article can be found online at: https://www.frontiersin.org/articles/10.3389/fonc.2021.629394/full#supplementary-material.

Supplementary Figure 1 | Forest plots ot the incidence of brain recurrence.

REFERENCES

1. Siegel RL, Miller KD, Jemal A. Cancer statistics, 2020. *CA Cancer J Clin* (2020) 70:7–30. doi: 10.3322/caac.21590
2. Burdett S, Pignon JP, Tierney J, Tribodet H, Stewart L, Le Pechoux C, et al. Adjuvant chemotherapy for resected early-stage non-small cell lung cancer. *Cochrane Database Syst Rev* (2015) 3:CD011430. doi: 10.1002/14651858.CD011430
3. Bradbury P, Sivajohanathan D, Chan A, Kulkarni S, Ung Y, Ellis PM. Postoperative Adjuvant Systemic Therapy in Completely Resected Non-Small-Cell Lung Cancer: A Systematic Review. *Clin Lung Cancer* (2017) 18:259–73.e8. doi: 10.1016/j.cllc.2016.07.002

4. Pignon JP, Tribodet H, Scagliotti GV, Douillard JY, Shepherd FA, Stephens RJ, et al. Lung adjuvant cisplatin evaluation: a pooled analysis by the LACE Collaborative Group. *J Clin Oncol* (2008) 26:3552–9. doi: 10.1200/JCO.2007.13.9030
5. Remon J, Lianes P, Martinez S, Velasco M, Querol R, Zanui M. Adjuvant treatment in resected non-small cell lung cancer: current and future issues. *Crit Rev Oncol Hematol* (2013) 88:375–86. doi: 10.1016/j.critrevonc.2013.05.017
6. Corless CL, Ballman KV, Antonescu CR, Kolesnikova V, Maki RG, Pisters PW, et al. Pathologic and molecular features correlate with long-term outcome after adjuvant therapy of resected primary GI stromal tumor: the ACOSOG Z9001 trial. *J Clin Oncol* (2014) 32:1563–70. doi: 10.1200/jco.2013.51.2046
7. Dematteo RP, Ballman KV, Antonescu CR, Maki RG, Pisters PW, Demetri GD, et al. Adjuvant imatinib mesylate after resection of localised, primary gastrointestinal stromal tumour: a randomised, double-blind, placebo-controlled trial. *Lancet* (2009) 373:1097–104. doi: 10.1016/s0140-6736(09)60500-6
8. Maemondo M, Inoue A, Kobayashi K, Sugawara S, Oizumi S, Isobe H, et al. Gefitinib or chemotherapy for non-small-cell lung cancer with mutated EGFR. *N Engl J Med* (2010) 362:2380–8. doi: 10.1056/NEJMoa0909530
9. Wu YL, Zhou C, Liam CK, Wu G, Liu X, Zhong Z, et al. First-line erlotinib versus gemcitabine/cisplatin in patients with advanced EGFR mutation-positive non-small-cell lung cancer: analyses from the phase III, randomized, open-label, ENSURE study. *Ann Oncol* (2015) 26:1883–9. doi: 10.1093/annonc/mdv270
10. Goss GD, O'Callaghan C, Lorimer I, Tsao MS, Masters GA, Jett J, et al. Gefitinib versus placebo in completely resected non-small-cell lung cancer: results of the NCIC CTG BR19 study. *J Clin Oncol* (2013) 31:3320–6. doi: 10.1200/JCO.2013.51.1816
11. Kelly K, Altorki NK, Eberhardt WE, O'Brien ME, Spigel DR, Crino L, et al. Adjuvant Erlotinib Versus Placebo in Patients With Stage IB-IIIA Non-Small-Cell Lung Cancer (RADIANT): A Randomized, Double-Blind, Phase III Trial. *J Clin Oncol* (2015) 33:4007–14. doi: 10.1200/JCO.2015.61.8918
12. Yue D, Xu S, Wang Q, Li X, Shen Y, Zhao H, et al. Erlotinib versus vinorelbine plus cisplatin as adjuvant therapy in Chinese patients with stage IIIA EGFR mutation-positive non-small-cell lung cancer (EVAN): a randomised, open-label, phase 2 trial. *Lancet Respir Med* (2018) 6:863–73. doi: 10.1016/S2213-2600(18)30277-7
13. Zhong WZ, Wang Q, Mao WM, Xu ST, Wu L, Shen Y, et al. Gefitinib versus vinorelbine plus cisplatin as adjuvant treatment for stage II-IIIA (N1-N2) EGFR-mutant NSCLC (ADJUVANT/CTONG1104): a randomised, open-label, phase 3 study. *Lancet Oncol* (2018) 19:139–48. doi: 10.1016/S1470-2045(17)30729-5
14. Riely GJ, Pao W, Pham D, Li AR, Rizvi N, Venkatraman ES, et al. Clinical course of patients with non-small cell lung cancer and epidermal growth factor receptor exon 19 and exon 21 mutations treated with gefitinib or erlotinib. *Clin Cancer Res* (2006) 12:839–44. doi: 10.1158/1078-0432.CCR-05-1846
15. Lee CK, Wu YL, Ding PN, Lord SJ, Inoue A, Zhou C, et al. Impact of Specific Epidermal Growth Factor Receptor (EGFR) Mutations and Clinical Characteristics on Outcomes After Treatment With EGFR Tyrosine Kinase Inhibitors Versus Chemotherapy in EGFR-Mutant Lung Cancer: A Meta-Analysis. *J Clin Oncol* (2015) 33:1958–65. doi: 10.1200/JCO.2014.58.1736
16. Wong ML, McMurry TL, Stukenborg GJ, Francescatti AB, Amato-Martz C, Schumacher JR, et al. Impact of age and comorbidity on treatment of non-small cell lung cancer recurrence following complete resection: A nationally representative cohort study. *Lung Cancer* (2016) 102:108–17. doi: 10.1016/j.lungcan.2016.11.002
17. Sugimura H, Nichols FC, Yang P, Allen MS, Cassivi SD, Deschamps C, et al. Survival after recurrent nonsmall-cell lung cancer after complete pulmonary resection. *Ann Thorac Surg* (2007) 83:409–17. doi: 10.1016/j.athoracsur.2006.08.046. discussioin 17-8.
18. Soria JC, Ohe Y, Vansteenkiste J, Reungwetwattana T, Chewaskulyong B, Lee KH, et al. Osimertinib in Untreated EGFR-Mutated Advanced Non-Small-Cell Lung Cancer. *N Engl J Med* (2018) 378:113–25. doi: 10.1056/NEJMoa1713137
19. Jadad AR, Moore RA, Carroll D, Jenkinson C, Reynolds DJ, Gavaghan DJ, et al. Assessing the quality of reports of randomized clinical trials: is blinding necessary? *Control Clin Trials* (1996) 17:1–12. doi: 10.1016/0197-2456(95)00134-4
20. Borenstein M, Hedges LV, Higgins JP, Rothstein HR. A basic introduction to fixed-effect and random-effects models for meta-analysis. *Res Synth Methods* (2010) 1:97–111. doi: 10.1002/jrsm.12
21. Higgins JP, Thompson SG, Deeks JJ, Altman DG. Measuring inconsistency in meta-analyses. *BMJ* (2003) 327:557–60. doi: 10.1136/bmj.327.7414.557
22. DerSimonian R, Laird N. Meta-analysis in clinical trials. *Control Clin Trials* (1986) 7:177–88. doi: 10.1016/0197-2456(86)90046-2
23. Xu ST, Xi JJ, Zhong WZ, Mao WM, Wu L, Shen Y, et al. The Unique Spatial-Temporal Treatment Failure Patterns of Adjuvant Gefitinib Therapy: A Post Hoc Analysis of the ADJUVANT Trial (CTONG 1104). *J Thorac Oncol* (2019) 14:503–12. doi: 10.1016/j.jtho.2018.11.020
24. Li N, Ou W, Ye X, Sun H-B, Zhang L, Fang Q, et al. Pemetrexed-Carboplatin Adjuvant Chemotherapy With or Without Gefitinib in Resected Stage IIIA-N2 Non-Small Cell Lung Cancer Harbouring EGFR Mutations: A Randomized, Phase II Study. *Ann Surg Oncol* (2014) 21:2091–96. doi: 10.1245/s10434-014-3586-9
25. Feng S, Wang Y, Cai K, Wu H, Xiong G, Wang H, et al. Randomized Adjuvant Chemotherapy of EGFR-Mutated Non-Small Cell Lung Cancer Patients with or without Icotinib Consolidation Therapy. *PLoS One* (2015) 10:e0140794. doi: 10.1371/journal.pone.0140794
26. Wu YL, Tsuboi M, He J, John T, Grohe C, Majem M, et al. Osimertinib in Resected EGFR-Mutated Non-Small-Cell Lung Cancer. *N Engl J Med* (2020) 383:1711–23. doi: 10.1056/NEJMoa2027071
27. Huang Q, Li J, Sun Y, Wang R, Cheng X, Chen H. Efficacy of EGFR Tyrosine Kinase Inhibitors in the Adjuvant Treatment for Operable Non-small Cell Lung Cancer by a Meta-Analysis. *Chest* (2016) 149:1384–92. doi: 10.1016/j.chest.2015.12.017
28. Raphael J, Vincent M, Boldt G, Shah PS, Rodrigues G, Blanchette P. Adjuvant Epidermal Growth Factor Receptor Tyrosine Kinase Inhibitors (TKIs) in Resected Non-Small Cell Lung Cancer (NSCLC): A Systematic Review and Meta-analysis. *Am J Clin Oncol* (2019) 42:440–45. doi: 10.1097/coc.0000000000000533
29. Lu D, Wang Z, Liu X, Feng S, Dong X, Shi X, et al. Differential effects of adjuvant EGFR tyrosine kinase inhibitors in patients with different stages of non-small-cell lung cancer after radical resection: an updated meta-analysis. *Cancer Manage Res* (2019) 11:2677–90. doi: 10.2147/cmar.s187940
30. Yuan Y, Huang Q, Gu C, Chen H. Disease-free survival improved by use of adjuvant EGFR tyrosine kinase inhibitors in resectable non-small cell lung cancer: an updated meta-analysis. *J Thorac Dis* (2017) 9:5314–21. doi: 10.21037/jtd.2017.12.58
31. Zhang Y, Sheng J, Kang S, Fang W, Yan Y, Hu Z, et al. Patients with exon 19 deletion were associated with longer progression-free survival compared to those with L858R mutation after first-line EGFR-TKIs for advanced non-small cell lung cancer: a meta-analysis. *PLoS One* (2014) 9:e107161. doi: 10.1371/journal.pone.0107161
32. Zhou Q, Zhang XC, Chen ZH, Yin XL, Yang JJ, Xu CR, et al. Relative abundance of EGFR mutations predicts benefit from gefitinib treatment for advanced non-small-cell lung cancer. *J Clin Oncol* (2011) 29:3316–21. doi: 10.1200/jco.2010.33.3757
33. Cross DA, Ashton SE, Ghiorghiu S, Eberlein C, Nebhan CA, Spitzler PJ, et al. AZD9291, an irreversible EGFR TKI, overcomes T790M-mediated resistance to EGFR inhibitors in lung cancer. *Cancer Discov* (2014) 4:1046–61. doi: 10.1158/2159-8290.cd-14-0337
34. Shi P, Zhang S, Zhu L, Qian G, Ren H, Ramalingam SS, et al. The Third-Generation EGFR Inhibitor, Osimertinib, Promotes c-FLIP Degradation, Enhancing Apoptosis Including TRAIL-Induced Apoptosis in NSCLC Cells with Activating EGFR Mutations. *Transl Oncol* (2019) 12:705–13. doi: 10.1016/j.tranon.2019.02.006
35. Ballard P, Yates JW, Yang Z, Kim DW, Yang JC, Cantarini M, et al. Preclinical Comparison of Osimertinib with Other EGFR-TKIs in EGFR-Mutant NSCLC Brain Metastases Models, and Early Evidence of Clinical Brain Metastases Activity. *Clin Cancer Res* (2016) 22:5130–40. doi: 10.1158/1078-0432.ccr-16-0399

36. Colclough N, Chen K, Johnström P, Strittmatter N, Yan Y, Wrigley GL, et al. Preclinical Comparison of the Blood-brain barrier Permeability of Osimertinib with Other EGFR TKIs. *Clin Cancer Res* (2021) 27:189–201. doi: 10.1158/1078-0432.ccr-19-1871
37. Ramalingam SS, Vansteenkiste J, Planchard D, Cho BC, Gray JE, Ohe Y, et al. Overall Survival with Osimertinib in Untreated, EGFR-Mutated Advanced NSCLC. *N Engl J Med* (2020) 382:41–50. doi: 10.1056/NEJMoa1913662
38. Reungwetwattana T, Nakagawa K, Cho BC, Cobo M, Cho EK, Bertolini A, et al. CNS Response to Osimertinib Versus Standard Epidermal Growth Factor Receptor Tyrosine Kinase Inhibitors in Patients With Untreated EGFR-Mutated Advanced Non-Small-Cell Lung Cancer. *J Clin Oncol* (2018) 36:3290–7. doi: 10.1200/jco.2018.78.3118. Jco2018783118
39. Chaudhuri AA, Chabon JJ, Lovejoy AF, Newman AM, Stehr H, Azad TD, et al. Early Detection of Molecular Residual Disease in Localized Lung Cancer by Circulating Tumor DNA Profiling. *Cancer Discov* (2017) 7:1394–403. doi: 10.1158/2159-8290.cd-17-0716

Conflict of Interest: The authors declare that the research was conducted in the absence of any commercial or financial relationships that could be construed as a potential conflict of interest.

frontiers in Oncology

REVIEW
published: 15 April 2021
doi: 10.3389/fonc.2021.655651

Transition of Treatment for Ground Glass Opacity–Dominant Non-Small Cell Lung Cancer

Yoshinori Handa, Yasuhiro Tsutani and Morihito Okada*

Department of Surgical Oncology, Hiroshima University, Hiroshima, Japan

Lobectomy has been the standard surgical treatment for non-small cell lung cancer (NSCLC). Over the decades, with the dramatic development of radiographic tools, such as high-resolution computed tomography (HRCT), and the widespread practice of low-dose helical CT for screening, the number of cases diagnosed with small-cell lung cancers with ground glass opacity (GGO) at early stages has been increasing. Accordingly, mainly after 2000, many retrospective studies and prospective trials have shown that patients with lung adenocarcinoma with GGO have a good prognosis and may be candidates for sublobar resection. Previous studies indicated that HRCT findings including the maximum diameter of the tumor, GGO ratio, and a consolidation/tumor ratio (CTR) are simple and useful tools to predict tumor invasiveness and prognosis in patients with NSCLC with GGO. Thus, sublobar resection may be considered a "standard therapy" for peripheral GGO-dominant small-cell lung adenocarcinomas. Ultimately, some of such tumors might not require surgical resection. A multicenter, prospective study has just begun in Japan to evaluate the validity of follow-up for small-sized GGO-dominant small-cell lung cancer. Lung cancers that do not require surgery should be identified. This study reviewed retrospective and prospective studies on GGO tumors and discussed the treatment strategies for such tumors.

Keywords: non-small cell lung cancer, ground glass opacity (GGO), lobectomy, sublobar resection (SLR), prognosis

OPEN ACCESS

Edited by:
Kezhong Chen,
Peking University People's Hospital, China

Reviewed by:
Satoshi Shiono,
Yamagata Prefectural Central Hospital, Japan
Terumoto Koike,
Niigata University, Japan
Shinkichi Takamori,
National Hospital Organization Kyushu Cancer Center, Japan

****Correspondence:***
Yasuhiro Tsutani
yatsutani@msn.com

Specialty section:
This article was submitted to Thoracic Oncology, a section of the journal Frontiers in Oncology

Received: *19 January 2021*
Accepted: *29 March 2021*
Published: *15 April 2021*

Citation:
Handa Y, Tsutani Y and Okada M (2021) Transition of Treatment for Ground Glass Opacity–Dominant Non-Small Cell Lung Cancer. Front. Oncol. 11:655651. doi: 10.3389/fonc.2021.655651

INTRODUCTION

Lobectomy has been the standard surgical treatment for non-small cell lung cancer (NSCLC), even when it is in its early stage. In 1973, Jensik et al. (1) suggested that segmental resection is equivalent to lobectomy and represent an adequate operation for small stage I NSCLC. This article started a debate regarding the optimal surgical approach for early-stage NSCLC. In 1995, however, a randomized trial reported that sublobar resection for stage IA NSCLC did not result in improved morbidity, mortality, or postoperative pulmonary function and was associated with higher rates of locoregional recurrence and death relative to lobectomy (2). In this trial, in patients who underwent sublobar resection, recurrence showed a 75% increase ($p = 0.02$) attributable to a tripling of the local recurrence rate ($p = 0.008$), 30% increase in overall death rate ($p = 0.08$), and 50% increase in death due to cancer ($p = 0.09$) compared to patients undergoing lobectomy. Two years later, another multicenter study showed a similar trend in increased local recurrence in patients who underwent

sublobar resection (wedge resection) (3). Eventually, sublobar resection has been performed only for patients unable to tolerate lobectomy as a "somewhat poor quality" alternative.

Over the decades, with the dramatic development of radiographic tools, such as high-resolution computed tomography (HRCT) and the widespread practice of low-dose helical CT for screening, lung cancers, especially many small lung cancers with ground glass opacity (GGO), are increasingly diagnosed. Recently, approximately 40% patients who underwent operations were reported to be diagnosed with stage IA NSCLC (4). Therefore, treatment of patients with very early-stage lung cancer *via* lobectomy, which is a more aggressive procedure than sublobar resection, has become controversial. In the 2000s, many retrospective studies have demonstrated that patients with lung adenocarcinoma with GGO have good prognoses and the potential to be candidates for sublobar resection. Now, appropriate treatment for NSCLC with GGO needs to be fully discussed.

We reviewed the literature and summarized the "new trend in early-stage lung cancer presenting as GGO," mainly in terms of surgical treatment. Thus, we evaluated appropriate treatment strategy for NSCLC with GGO.

PROGNOSIS OF NSCLC WITH GGO COMPONENT AND SUBLOBAR RESECTION

Mainly after 2000, several clinical studies have demonstrated that patients with lung adenocarcinoma with GGO have good prognoses (5–8). We examined 436 of 502 consecutive patients with stage IA adenocarcinoma and had undergone preoperative HRCT; 66 patients with tumors with pure GGO were excluded. Tumor type (without GGO, n = 137; with GGO, n = 299) and surgical results were analyzed. Tumors without GGO showed a significantly greater association ($P < 0.001$) with lymphatic, vascular, and pleural invasion and lymph node metastasis compared with tumors with GGO. Namely, most tumors with GGO are diagnosed as pathological non- or less-invasive lung adenocarcinomas, such as adenocarcinoma *in situ* (AIS), minimally invasive adenocarcinoma (MIA), former bronchioloalveolar carcinoma, and Noguchi type A-B adenocarcinomas, which presented similar results to those of a previous report (5). Additionally, Asamura et al. previously analyzed the correlation between radiologic findings of GGO-dominant tumors and pathological characteristics and reported that GGO lesions constitute true early lung cancers, namely, minimal or noninvasive tumors (9). The disease-free survival also worsened in patients with pure solid tumors ($P = 0.0006$) (4). Similarly, Hattori et al. retrospectively evaluated 1029 surgically resected early-stage NSCLCs. All tumors were classified into two groups: with GGO group or pure solid group. They revealed that on multivariable analysis, the presence of a GGO was an independent significant prognostic factor of overall survival (OS) (hazard ratio [HR], 0.314; 95% confidence interval [CI], 0.181–0.529: $P < 0.001$) (6). In particular, GGO-dominant lung cancer was reported to have excellent prognosis. Asamura et al. (5) reported that in the Japan Clinical Oncology Group [JCOG] 0201 study, patients diagnosed with GGO-dominant lung adenocarcinoma have a good prognosis (**Table 1**). This prospective, multi-institutional study was performed with 233 male and 312 female patients (median age, 62 years) to define early (noninvasive) adenocarcinomas of the lung on image diagnosis,; the median follow-up period of all patients was 7.1 years (range, 0–8.5 years). The JCOG 0201 study showed that the 5-year OS was 96.7% for patients with a consolidation/tumor ratio (CTR) ≤ 0.5 and a ≤30 mm tumor, and 97.1% for those with CTR ≤ 0.25 and a ≤20 mm tumor. In addition, the incidence of pathological invasiveness (pathological N+ or ly+ or v+) was 1.1% in patients with a CTR ≤ 0.5 and a ≤30 mm tumor, and 0.3% in those with CTR ≤ 0.25 and a ≤20 mm tumor. This study concluded that the radiologic criteria of a CTR ≤ 0.25 and ≤20 mm, and CTR ≤ 0.50 in ≤30 mm were both able to define a homogeneous group of patients with an excellent prognosis before surgery. In addition, we demonstrated that patients with GGO-dominant (CTR ≤ 0.5) lung adenocarcinomas rarely had pathologically invasive tumors and had an excellent prognosis (8) (**Table 1**). We evaluated 610 consecutive patients with clinical stage IA lung adenocarcinoma who underwent complete

TABLE 1 | Summary of previous large cohort studies evaluating GGO dominant NSCLC.

	n	Follow up	Size	CTR	Performed Surgical Procedure WR/Sg/Lob	Pathologically invasiveness (pN+ or ly+ or v+)	Prognosis
JCOG 0201 (7)	35	7.1y	≤20mm	≤0.25	0(0%)/0(0%)/35(100.0%)	1 patient (2.9%)	**5-year OS**; 97.1% **5-year RFS**; 97.1%
	54	7.1y	21–30 mm	≤0.5	0(0%)/0(0%)/54(100.0%)	N.S	**5-year OS**; 96.3% **5-year RFS**; 94.4%
	121	7.1y	≤30mm	≤0.5	0(0%)/0(0%)/121(100.0%)	6 patients (5.0%) (breakdown N.S)	**5-year OS**; 96.7% **5-year RFS**; 95.9%
JCOG 0804 (10)	314	5.5y	≤20mm	≤0.25	258(77.5%)/56(22.5%)/0(0%)	N.S	**5-year RFS**; 99·7%
Tsutani et al. (8)	239	3.5y	≤30mm	≤0.5	93(38.9%)/56(23.4%)/90(37.7%)	3 patients with ly+ (1.3%) 2 patients with v+ (0.8%) 1 patient with pl+ (0.4%) 2 patients with pN+ (0.8%)	**3-year OS** 98.7%(WR)/98.2%(Seg)/97.6%(Lob) **3-year RFS** 98.7%(WR)/96.1%(Seg)/96.4%(Lob)

CTR, consolidation/tumor ratio; Lob, lobectomy; N.S, not stated; OS, overall survival; RFS, recurrence free survival; Seg, segmentectomy; WR, wedge resection.

resection after preoperative HRCT and revealed 239 (39.2%) patients were CTR ≤ 0.5. Based on the results, no significant difference in 3-year recurrence-free survival (RFS) was observed among patients who underwent lobectomy (96.4%), segmentectomy (96.1%), and wedge resection (98.7%) of GGO-dominant tumors (P = 0.44). Multivariate Cox analysis showed that surgical procedure did not affect RFS in GGO-dominant tumors. We revealed that GGO-dominant clinical stage IA lung adenocarcinomas are a uniform group of tumors that exhibit low-grade malignancy and have an extremely favorable prognosis and thus can be successfully treated with sublobar resection. In particular, in a ≤20 mm tumor, surgeons can successfully treat lung cancer patients *via* wedge resection that does not include lymph node dissection. The prognosis of patients with lung adenocarcinoma is better when tumors include GGO, compared with those with pure solid tumors. However, whether the prognosis of patients with tumors with GGO tumors is favorable regardless of the solid component size remains unknown. We retrospectively analyzed the clinicopathological findings and prognoses of 856 patients with tumors with GGO based on the size of the solid component during a median follow-up of 45 months; among the 1215 patients with lung adenocarcinoma, it was revealed that the prognostic impact of a solid component size less than or equal to 2 cm and >2 cm significantly differed after complete resection (10).

Preoperative HRCT findings (GGO ratio, CTR) showed that GGO is a simple and useful tool for predicting the prognosis of NSCLC candidates for sublobar resection. The nonrandomized confirmatory phase III study (JCOG 0804/WJOG 4507L) conducted by the JCOG and West Japan Oncology Group (WJOG) evaluated the efficacy and safety of sublobar resection for GGO-dominant lung cancer defined with HRCT only by prospective, multicenter, and large cohort analysis (314 registered patients) (**Figure 1**). The selection criteria were maximum tumor diameter ≤ 20 mm, CTR ≤ 0.25, no recurrence of the original lung cancer, and a 5-year RFS rate of 99.7% after sublober resection, primarily wedge resection (**Table 1**). Their results were clearer and showed that HRCT was very useful in selecting patients suitable for sublobar resection (11).

Another prognostic factor used as a surrogate of tumor aggressiveness is the high tumor maximum standard uptake value (SUVmax) on 18F-fluorodeoxyglucose-positron emission tomography/CT (FDG-PET) (12–16). High SUV max NSCLC demonstrate invasive pathologic characteristics, and poorer postoperative outcomes were suggested when compared with tumors with lower SUV max. Previous study reported that a higher ratio of tumor SUVmax to tumor size was associated with worse DFS (12). Additionally, hypermetabolic tumors were reported to be associated with substantially higher invasiveness (13). Other studies also have reported that a higher tumor SUVmax was associated with higher grade tumors and aggressive histopathologic subtypes (i.e., micropapillary and solid subtypes of adenocarcinoma), and in many cases, NSCLC with GGO have lower SUV max tumor on FDG-PET (14). We have also observed that SUVmax on FDG-PET was an important preoperative factor for predicting the pathologic malignant grade and prognosis in lung adenocarcinoma (15, 16). As stated in our paper (8), GGO-dominant tumors have a low median SUVmax of 0.9 and are generally low in malignancy, but some of the highest tumors have a SUVmax of 9.8. Furthermore, GGO-dominant tumors showing a high SUVmax may be pathologically malignant and have lymph node metastasis. We previously identified the predictors of pathologic lymph node involvement in clinical stage IA lung adenocarcinoma (17). In this study, we revealed the pathologic node-negative status criteria of solid tumor size <0.8 cm on HRCT or a

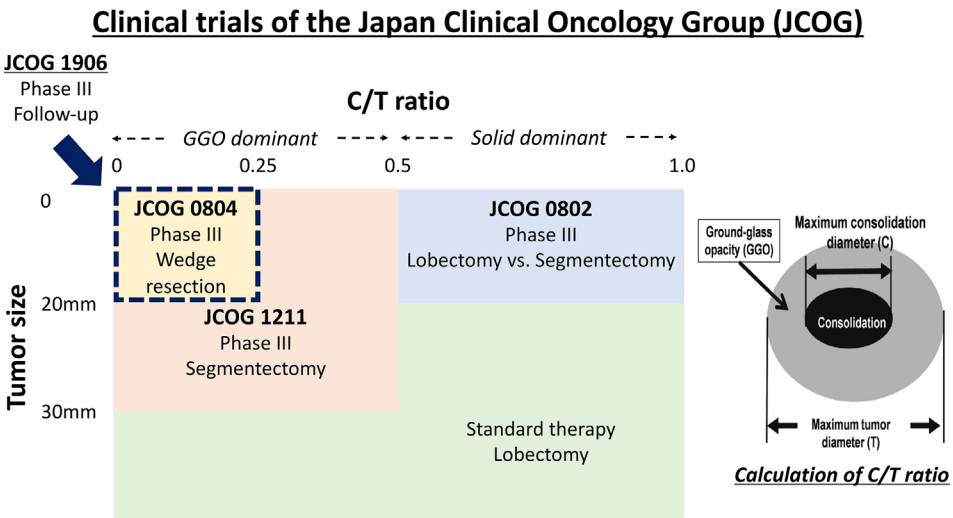

FIGURE 1 | Schema of clinical trials of the Japan Clinical Oncology Group (JCOG) Study.

SUVmax<1.5 on FDG-PET/CT. Therefore, conversely, in other cases, lymph node metastasis cannot be denied. In combination with other pieces of literature (12–16), tumors showing a high SUVmax need to be resected by more than segmentectomy, even when it is constituted by the GGO component. We think that the treatment strategy is clearly different depending on SUVmax; namely, for small GGO-dominant tumors with low standard uptake value (SUV), it may be reasonable to be resected by wedge resection, but for those with high SUV, more than segmentectomy should be considered. The role of PET/CT might be limited in the evaluation of very small lung nodules, however, the good prognosis of NSCLC with GGO can be confirmed from the viewpoint of FDG-PET.

Sublobar resection has several advantages than lobectomy. It reportedly improves postoperative quality of life by preserving the pulmonary function (18, 19). Harada et al. reported that a positive and significant correlation was found between the number of resected segments versus loss of forced vital capacity ($r = 0.518$, $p < 0.0001$ at 2 months; $r = 0.604$, $p < 0.0001$ at 6 months) and loss of forced expiratory volume in 1 second ($r = 0.492$, $p < 0.0001$ at 2 months; $r = 0.512$, $p < 0.0001$ at 6 months). The postoperative reduction of forced vital capacity ($p = 0.0006$) and forced expiratory volume in 1 second ($p = 0.0007$) was significantly less in the segmentectomy group. They concluded that the extent of removed lung parenchyma directly affected that of postoperative functional loss even at 6 months after surgery, and segmentectomy offered significantly better functional preservation compared with lobectomy (18). We emphasized that preserving as much healthy lung tissue as possible reduces the prevalence of surgery and improves postoperative quality of life. In addition, patients with GGO-dominant lung cancer survive long enough to be at risk for the next lung cancer, increasing the likelihood of further resection (19). The smaller the initial amount of excision, the more unlimited treatment options for subsequent lung cancer. Perhaps, some surgeons may be concerned that sublobar resection may increase local recurrence, however, in combination with these circumstances, it may be reasonable to perform sublobar resection as the "standard treatment" for lung adenocarcinoma with a maximum tumor diameter of 20 mm or less and a CTR of 0.25 or less.

EXPANSION OF INDICATIONS FOR SEGMENTECTOMY IN 21–30 MM NSCLC WITH GGO COMPONENT

Sublobular resection is generally considered lung cancer smaller than 20 mm. However, the excellent prognosis of GGO-dominant lung cancer allowed us to consider expanding its indications for sublobar resection. JCOG 0201 shows that patients with a CTR of 0.5 or less and tumors of 21-30 mm have a 5-year OS of 96.3% and a 5-year RFS of 94.4% (5). In addition, GGO-dominated tumors of 21-30 mm rarely showed pathological invasiveness, and there was no difference in survival analysis, specifically, for tumors of 21-30 mm, where GGO predominates, 3-year RFS was similar in patients who underwent lobectomy (93.7%) and segmentectomy (92.9%). Therefore, we have shown that GGO-dominant and 21-30 mm tumors may also be candidates for sublobar resection (8). It was necessary to distinguish between wedge resection and segmentectomy to clarify which procedure was used. We recommended segmentectomy and not wedge resection for sublobar resection of 21–30 mm tumors because these tumors could metastasize to lymph node, and taking a sufficient surgical margin often is difficult in a 21–30 mm tumor. In our study, 2 (2.4%) of 84 patients with a GGO-dominant 21-30 mm tumor metastasized to the lymph nodes, but in patients with a GGO-dominant tumor of 20 mm or less, no lymph node metastasis was seen. Among sublobar resections, segmentectomy involves anatomical resection in the hilar region, thereby allowing more lymph nodes to be dissected. The prognostic impact of lymph node dissection on lung cancer treatment has remained unclear. The main role of lymph node dissection has been to prevent understaging. A higher number of lymph nodes sampled during surgery improve the accuracy of pathologic staging, thereby preventing the misclassification of patients with lymph node involvement as having stage I disease (20). Moreover, in several reports, it has been shown that lymph node dissection has an important prognostic impact. In previous studies using SEER data, it has been shown that the number of lymph nodes evaluated during surgery was a strong predictor of survival for stage I NSCLC (21). As previously mentioned, we revealed the pathologic node-negative status criteria of solid tumor size of <0.8 cm on HRCT or a SUVmax of <1.5 on FDG-PET/CT (17). Therefore, conversely, lymph node metastasis cannot be denied, and lymphadenectomy should be performed in other cases. The optimal extent of resection margin and lymph node dissection in segmentectomy has not been elucidated, and future study is warranted; however, we believe that segmentectomy is superior to wedge resection when the hilar lymph nodes are dissected and have sufficient surgical margin.

Currently, a nonrandomized confirmatory trial of segmentectomy (JCOG 1211) is underway since September 2013 with the aim of confirming the effectiveness of segmentectomy for clinical T1N0 GGO-dominant lung cancer based on HRCT (**Figure 1**) (22). A total of 390 patients from 42 Japanese institutions are recruited within 4 years. The primary endpoint of this study is a 5-year relapse-free survival in all of the patients who undergo a segmentectomy for a lung nodule. The secondary endpoints are OS, annual relapse-free survival, disease-free survival, proportion of local relapse, postoperative pulmonary function, proportion of segmentectomy completion, proportion of R0 resection completion by segmentectomy, adverse events, and serious adverse events. Patient accrual have already ended in November 2015 and a primary analysis will be conducted in 2021. This study is a crucial trial of lung segmentectomy for early stage lung cancer.

GENE EXPRESSION OF NSCLC WITH GGO COMPONENT

Suda K conducted a retrospective analysis of the Japanese Joint Committee of Lung Cancer Registry database (a nationwide database for patients with surgically resected lung cancer; n = 18,973). They evaluated 5780 patients had been tested for an EGFR mutation, and revealed the presence of an EGFR mutation was significantly correlated with the presence of GGO ($P < 0.001$) and better prognosis (23). GGO component of NSCLC is often pathologically reflect adenocarcinoma *in situ* (AIS), minimally invasive adenocarcinoma (MIA), and lepidic component. We previously evaluated gene expression of NSCLC comprehensively. Ito M et al. evaluated typical driver mutation for lung cancer, EGFR mutation, in 394 resected pN0M0 lung adenocarcinomas (24). In this study, we revealed that the frequency of EGFR mutation is higher in adenocarcinoma with a concomitant lepidic component, such as AIS and MIA. On the contrary, EGFR wild type tumors are likely to be invasive adenocarcinoma cases without a lepidic component. These results revealed that NSCLC with GGO component might have room for therapeutic intervention in terms of gene expression, considering the effectiveness of treatment by epidermal growth factor receptor-tyrosine kinase inhibitors. Further investigations on gene expression in NSCLC with GGO component will be needed.

POTENTIAL OF FOLLOW-UP FOR GGO-DOMINANT NSCLC

Some small lung cancers with GGO have been reported to have no pathological invasiveness and significantly longer doubling times than normal lung adenocarcinomas (25, 26). Aoki et al. reported that all type A and B tumors by Noguchi criteria had a tumor doubling time of more than 1 year, on the other hand, the tumor doubling time was less than 1 year in almost (87%) of the types D, E, and F tumors. In addition, Kakinuma et al. evaluate the natural course of the progression of pulmonary subsolid nodules (SSNs) (27). A total of 795 patients with 1229 SSNs were included from eight Japanese facilities. SSNs were classified into three categories: pure ground glass nodules (PGGNs), heterogeneous GGNs (HGGNs) (solid component detected only in lung windows), and part-solid nodules. Among the 1046 PGGNs, 13 (1.2%) developed into HGGNs and 56 (5.4%) developed into part-solid nodules. Among the 81 HGGNs, 16 (19.8%) developed into part-solid nodules. For the PGGNs, the mean period until their development into part-solid nodules was 3.8 ± 2.0 years, whereas the mean period for the HGGNs was 2.1 ± 2.3 years ($p = 0.0004$). In patients who underwent surgical resection, invasive adenocarcinomas were diagnosed only among the part-solid nodules, corresponding to 1% (12 patients) of all 1229 SSNs.

Some GGO-dominant NSCLC might not require surgical resection itself. In several pieces of literature, it has been indicated that the outcomes of stereotactic body radiotherapy and radiofrequency ablation for operable early-stage NSCLC were as good as those in previous surgery studies (28–31). In the future, surgeons may need clinical trials that compare sublobar resection and radiotherapy. In addition, now, multicenter, prospective study has just begun in Japan to evaluate the validity of follow-up for GGO-dominant small lung cancer (maximum tumor diameter ≤2 cm and CTR ≤ 0.25) without pulmonary resection. (JCOG 1906, UMIN000040818) (**Figure 1**). A total of 680 patients from 42 Japanese institutions are planned to be recruited within 5 years. The primary endpoint of this study is a 10-year OS in all of the patients who undergo follow-up. Sublobar resection, even a wedge resection, is a surgical procedure that requires general anesthesia and carries a considerable risk of adverse events. If the surgery itself can be avoided, it is the least invasive treatment for the patient. Ultimately, lung cancer that does not require surgery needs to be identified in the future.

DISCUSSION

From many retrospective studies and JCOG 0804 trial previously mentioned, we believe that it is rational to perform sublobar resection as the "standard treatment" for lung adenocarcinoma with a maximum tumor diameter of ≤20 mm and CTR ≤ 0.25 (**Figure 1**), and in selecting either segmentectomy or wedge resection, segmentectomy is superior to wedge resection in dissecting the hilar lymph nodes. For lung adenocarcinoma with a maximum tumor diameter of ≤20 mm and 0.25 ≤ CTR ≤ 0.5, the standard is a lobectomy, but sublobar resection is also possible based on past data. If you can get a sufficient surgical margin, wedge resection might be enough. For the treatment of GGO-dominant lung adenocarcinoma with a maximum tumor diameter of 20–30 mm, the standard is a lobectomy, but sublobar resection is also possible based on data as previously described. To secure a surgical margin, surgeons should choose segmentectomy in principle. If surgeons can get sufficient surgical margin, wedge resection can be chosen. Finally, the results of JCOG 1211 must be awaited. Ultimately, lung cancer that does not require lung resection may be identified. Thus, further investigations into the treatment of GGO-dominant lung cancer are needed.

AUTHOR CONTRIBUTIONS

YH and YT designed this study. MO supervised the study. YH and YT collected clinical information, and interpreted all of the data. All authors contributed to the article and approved the submitted version.

ACKNOWLEDGMENTS

The authors would like to thank Enago (www.enago.jp) for the English language revision.

REFERENCES

1. Jensik RJ, Faber LP, Milloy FJ, Monson DO. Segmental resection for lung cancer. A fifteen-year experience. *J Thorac Cardiovasc Surg* (1973) 66:563–72. doi: 10.1016/S0022-5223(19)40590-4
2. Ginsberg RJ, Rubinstein LV. Randomized trial of lobectomy versus. limited resection for T1 N0 non-small cell lung cancer. Lung Cancer Study Group. *Ann Thorac Surg* (1995) 60:615–22. doi: 10.1016/0003-4975(95)00537-U
3. Landreneau RJ, Sugarbaker DJ, Mack MJ, Hazelrigg SR, Luketich JD, Fetterman L, et al. Wedge resection versus lobectomy for stage 1 (T1N0M0) non-small cell lung cancer. *J Thorac Cardiovasc Surg* (1997) 113:691–700. doi: 10.1016/S0022-5223(97)70226-5
4. Goya T, Asamura H, Yoshimura H, Kato H, Shimokata K, Tsuchiya R, et al. Prognosis of 6644 resected non-small cell lung cancers in Japan: a Japanese lung cancer registry study. *Lung Cancer* (2005) 50:227–34. doi: 10.1016/j.lungcan.2005.05.021
5. Asamura H, Hishida T, Suzuki K, Koike T, Nakamura K, Kusumoto M, et al. Japan Clinical Oncology Group Lung Cancer Surgical Study Group radiographically determined noninvasive adenocarcinoma of the lung: survival outcomes of Japan Clinical Oncology Group 0201. *Thorac Cardiovasc Surg* (2013) 146:24–30. doi: 10.1016/j.jtcvs.2012.12.047
6. Hattori A, Matsunaga T, Takamochi K, Oh S, Suzuki K. Prognostic impact of a ground glass opacity component in the clinical T classification of non-small cell lung cancer. *J Thorac Cardiovasc Surg* (2017) 154:2102–10. doi: 10.1016/j.jtcvs.2017.08.037
7. Tsutani Y, Miyata Y, Yamanaka T, Nakayama H, Okumura S, Adachi S, et al. Solid tumors versus mixed tumors with a ground-glass opacity component in patients with clinical stage IA lung adenocarcinoma: prognostic comparison using high-resolution computed tomography findings. *J Thorac Cardiovasc Surg* (2013) 146:17–23. doi: 10.1016/j.jtcvs.2012.11.019
8. Tsutani Y, Miyata Y, Nakayama H, Okumura S, Adachi S, Yoshimura M, et al. Appropriate sublobar resection choice for ground glass opacity-dominant clinical stage IA lung adenocarcinoma: wedge resection or segmentectomy. *Chest* (2014) 145:66–71. doi: 10.1378/chest.13-1094
9. Asamura H, Suzuki K, Watanabe S, Matsuno Y, Maeshima A, Tsuchiya R. A clinicopathological study of resected subcentimeter lung cancers: a favorable prognosis for ground glass opacity lesions. *Ann Thorac Surg* (2003) 76 (4):1016–22. doi: 10.1016/S0003-4975(03)00835-X
10. Mimae T, Tsutani Y, Miyata Y, Imai K, Ito H, Nakayama H, et al. Solid tumor size of 2 cm divides outcomes of patients with mixed ground glass opacity lung tumors. *Ann Thorac Surg* (2020) 109:1530–6. doi: 10.1016/j.athoracsur.2019.12.008
11. Suzuki K, Watanabe SI, Wakabayashi M, Saji H, Aokage K, Moriya Y, et al. A single-arm study of sublobar resection for ground glass opacity dominant peripheral lung cancer. *J Thorac Cardiovasc Surg* (2020) S0022-5223 (20):33043-9. doi: 10.1016/j.jtcvs.2020.09.146
12. Stiles BM, Nasar A, Mirza F, Paul S, Lee PC, Port JL, et al. Ratio of positron emission tomography uptake to tumor size in surgically resected nonsmall cell lung cancer. *Ann Thorac Surg* (2013) 95:397–403; discussion 404. doi: 10.1016/j.athoracsur.2012.07.038
13. Ghaly G, Rahouma M, Kamel MK, Nasar A, Harrison S, Nguyen AB, et al. Clinical predictors of nodal metastases in peripherally clinical T1a N0 non-small cell lung cancer. *Ann Thorac Surg* (2017) 104:1153–8. doi: 10.1016/j.athoracsur.2017.02.074
14. Cha MJ, Lee HY, Lee KS, Jeong JY, Han J, Shim YM, et al. Micropapillary and solid subtypes of invasive lung adenocarcinoma: clinical predictors of histopathology and outcome. *J Thorac Cardiovasc Surg* (2014) 147:921–8.e2.5. doi: 10.1016/j.jtcvs.2013.09.045
15. Tsutani Y, Miyata Y, Nakayama H, Okumura S, Adachi S, Yoshimura M, et al. Prognostic significance of using solid versus whole tumor size on high-resolution computed tomography for predicting the pathological malignant grade of tumors in clinical stage IA lung adenocarcinoma: a multicenter study. *J Thorac Cardiovasc Surg* (2012) 143:607–12. doi: 10.1016/j.jtcvs.2011.10.037
16. Okada M, Nakayama H, Okumura S, Daisaki H, Adachi S, Yoshimura M, et al. Multicenter analysis of high-resolution computed tomography and positron emission tomography/computed tomography findings to choose therapeutic strategies for clinical stage IA lung adenocarcinoma. *J Thorac Cardiovasc Surg* (2011) 141:1384–91. doi: 10.1016/j.jtcvs.2011.02.007
17. Tsutani Y, Miyata Y, Nakayama H, Okumura S, Adachi S, Yoshimura M, et al. Prediction of pathologic node-negative clinical stage IA lung adenocarcinoma for optimal candidates undergoing sublobar resection. *J Thorac Cardiovasc Surg* (2012) 144(6):1365–71.18. doi: 10.1016/j.jtcvs.2012.07.012
18. Harada H, Okada M, Sakamoto T, Matsuoka H, Tsubota N. Functional advantage after radical segmentectomy versus lobectomy for lung cancer. *Ann Thorac Surg* (2005) 80:2041–5. doi: 10.1016/j.athoracsur.2005.06.010
19. Okada M, Koike T, Higashiyama M, Yamato Y, Kodama K, Tsubota N. Radical sublobar resection for small-sized non–small cell lung cancer: a multicenter study. *J Thorac Cardiovasc Surg* (2006) 132:769–75. doi: 10.1016/j.jtcvs.2006.02.063
20. Lardinois D, De Leyn P, Van Schil P, Porta RR, Waller D, Passlick B, et al. ESTS guidelines for intraoperative lymph node staging in non-small cell lung cancer. *Eur J Cardiothorac Surg* (2006) 30:787–92. doi: 10.1016/j.ejcts.2006.08.008
21. Ludwig MS, Goodman M, Miller DL, Johnstone PA. Postoperative survival and the number of lymph nodes sampled during resection of node-negative non-small cell lung cancer. *Chest* (2005) 128:1545–50. doi: 10.1378/chest.128.3.1545
22. Aokage K, Saji H, Suzuki K, Mizutani T, Katayama H, Shibata T, et al. Lung Cancer Surgical Study Group of the Japan Clinical Oncology Group A non-randomized confirmatory trial of segmentectomy for clinical T1N0 lung cancer with dominant ground glass opacity based on thin-section computed tomography (JCOG1211). *Gen Thorac Cardiovasc Surg* (2017) 65:267–72. doi: 10.1007/s11748-016-0741-1
23. Suda K, Mitsudomi T, Shintani Y, Okami J, Ito H, Ohtsuka T, et al. Clinical impacts of EGFR mutation status: analysis of 5780 surgically resected lung cancer cases. *Ann Thorac Surg* (2021) 111:269–76. doi: 10.1016/j.athoracsur.2020.05.041
24. Ito M, Miyata Y, Kushitani K, Yoshiya T, Kai Y, Tsutani Y, et al. Increased risk of recurrence in resected EGFR-positive pN0M0 invasive lung adenocarcinoma. *Thorac Cancer* (2018) 9:1594–602. doi: 10.1111/1759-7714.12866
25. Noguchi M, Morikawa A, Kawasaki M, Matsuno Y, Yamada T, Hirohashi S, et al. Small adenocarcinoma of the lung: histologic characteristics and prognosis. *Cancer* (1995) 75:2844–52. doi: 10.1002/1097-0142(19950615)75:12<2844::AID-CNCR2820751209>3.0.CO;2-#
26. Aoki T, Nakata H, Watanabe H, Nakamura K, Kasai T, Hashimoto H, et al. Evolution of peripheral lung adenocarcinomas: CT findings correlated with histology and tumor doubling time. *AJR Am J Roentgenol* (2000) 174:763–8. doi: 10.2214/ajr.174.3.1740763
27. Kakinuma R, Noguchi M, Ashizawa K, Kuriyama K, Maeshima AM, Koizumi N, et al. Natural history of pulmonary subsolid nodules: a prospective multicenter study. *J Thorac Oncol* (2016) 11:1012–28. doi: 10.1016/j.jtho.2016.04.006
28. Eriguchi T, Takeda A, Sanuki N, Tsurugai Y, Aoki Y, Y6 O, et al. Stereotactic body radiotherapy for operable early-stage non-small cell lung cancer. *Lung Cancer* (2017) 109:62–7. doi: 10.1016/j.lungcan.2017.04.022
29. Onishi H, Shioyama Y, Matsumoto Y, Shibamoto Y, Miyakawa A, Suzuki G, et al. Stereotactic body radiotherapy in patients with lung tumors composed of mainly ground-glass opacity. *J Radiat Res* (2020) 61(3):426–30. doi: 10.1093/jrr/rraa015
30. Kodama H, Yamakado K, Hasegawa T, Takao M, Taguchi O, Fukai I, et al. Radiofrequency ablation for ground-glass opacity-dominant lung adenocarcinoma. *J Vasc Interv Radiol* (2014) 25(3):333–9. doi: 10.1016/j.jvir.2013.11.035
31. Iguchi T, Hiraki T, Gobara H, Fujiwara H, Matsui Y, Soh J, et al. Percutaneous radiofrequency ablation of lung cancer presenting as ground-glass opacity. *Cardiovasc Interv Radiol* (2015) 38(2):409–15. doi: 10.1007/s00270-014-0926-x

Conflict of Interest: The authors declare that the research was conducted in the absence of any commercial or financial relationships that could be construed as a potential conflict of interest.

frontiers in Oncology

ORIGINAL RESEARCH
published: 27 April 2021
doi: 10.3389/fonc.2021.661821

Comparison of Perioperative Outcomes Between Precise and Routine Segmentectomy for Patients With Early-Stage Lung Cancer Presenting as Ground-Glass Opacities: A Propensity Score-Matched Study

Xianning Wu[1], *Tian Li*[1], *Chuankai Zhang*[1], *Gao Wu*[1], *Ran Xiong*[1], *Meiqing Xu*[1], *Dan Su*[2*] *and Mingran Xie*[1*]

[1] Department of Thoracic Surgery, The First Affiliated Hospital of USTC, Division of Life Sciences and Medicine, University of Science and Technology of China, Hefei, China, [2] School of Nursing, Anhui Medical University, Hefei, China

OPEN ACCESS

Edited by:
Chen Chen,
Central South University, China

Reviewed by:
Giulia Veronesi,
Humanitas Research Hospital, Italy
Xiao Li,
Peking University People's Hospital, China

***Correspondence:**
Dan Su
sudanwu1986@163.com
Mingran Xie
xmr1981@ustc.edu.cn

Specialty section:
This article was submitted to Thoracic Oncology, a section of the journal Frontiers in Oncology

Received: 31 January 2021
Accepted: 06 April 2021
Published: 27 April 2021

Citation:
Wu X, Li T, Zhang C, Wu G, Xiong R, Xu M, Su D and Xie M (2021) Comparison of Perioperative Outcomes Between Precise and Routine Segmentectomy for Patients With Early-Stage Lung Cancer Presenting as Ground-Glass Opacities: A Propensity Score-Matched Study. Front. Oncol. 11:661821. doi: 10.3389/fonc.2021.661821

Introduction: Segmentectomy is widely used for early-stage lung cancer presenting as single or multiple ground-glass opacities (GGOs). Precise segmentectomy is the recommended procedure in China. However, clinically, most routine segmentectomies are performed using only high-resolution computed tomography (CT). The aim of this study was to evaluate the effect of two segmentectomy approaches for GGOs in the lung.

Methods: From January 2020 to September 2020, 55 precise segmentectomies performed with real-time guidance using 3D reconstruction and 343 routine segmentectomies for patients with single or multiple GGOs were performed as uniportal procedures. To reduce bias related to outcomes, preoperative clinical factors were used for propensity score matching (1:1); 55 precision and 55 routine segmentectomies were selected and further analyzed. Perioperative outcomes, namely operation time, blood loss, resection margins, number of removed lymph nodes, postoperative pulmonary function (1 month after surgery), length of postoperative stay, and postoperative complications were compared between the two groups.

Results: Patients constituted 43 men and 67 women, with an age range of 25–68 years (median: 53 years). No significant differences were seen between the groups regarding blood loss, complications, histological type, and postoperative pulmonary function, and there were no 30-day postoperative deaths in either group. The median operation time for the Precision group (74 min) was longer than in the Routine group (55 min) (p <0.01), and the number of removed lymph nodes in the Precision group (5 ± 1.1) was higher than in the Routine group (3 ± 0.8) (p <0.01). Chest tube duration days and postoperative stay days were similar in both groups; however, the rate of air leakage on postoperative day 1 was higher in the Precision group (p = 0.020). All patients in the

Precision group had adequate resection margins. Four patients (7.3%) undergoing complex segmentectomy in the Routine group had inadequate resection margins and required resection of additional lung tissue.

Conclusion: Routine segmentectomy can significantly shorten the operation time and might prevent postoperative air leakage in uniportal segmentectomy for lung GGOs. However, precision segmentectomy may be more precise for complex cases, ensuring adequate resection margins and lymph node dissection.

Keywords: early-stage lung cancer, ground-glass opacities, segmentectomy, video-assisted thoracoscopy, propensity score

INTRODUCTION

Owing to widespread computed tomography (CT) screening, very early-stage primary lung cancer appearing as ground-glass opacities (GGOs) is increasingly detected (1). The current standard surgical procedure for early-stage lung cancer (T1) is lobectomy, in accordance with the randomized controlled trial results of the Lung Cancer Study Group in 1995 (2). As GGO-featured lung adenocarcinoma is generally indolent, the previous standard procedure of lobectomy remains controversial. However, the recent Japan Clinical Oncology Group study (JCOG0804) results provide timely and important evidence supporting sublobar resection for small GGO-dominant lung adenocarcinomas (3).

Segmentectomy, first described in 1939 (4), is an important mode of sublobar lung resection and is widely used in patients with GGO-featured lung adenocarcinoma. Regarding tumor treatment, achieving sufficient resection margins is critical to prevent local recurrence (5–7). To ensure adequate surgical margins and to overcome the challenges of identifying nodules, multiple localization techniques have been proposed, including video-assisted thoracoscopic (VATS) segmentectomy. However, this procedure is challenging because of the requirement to understand the complicated anatomical variations of the segmental bronchi and vessels.

Precise segmentectomy is a relative concept derived from 'precision surgery', which has not been well defined previously. Precise segmentectomy means more accurate identifying of small variations, transecting of small target segmental bronchi and vessels, as well as preserving of small intersegmental vessels. These 'small' anatomical structures are difficult to identify on CT and may not be essential for routine anatomical segmentectomy. Precise segmentectomy has been strongly promoted with the development of new techniques, such as three-dimensional (3D) reconstruction, 3D printing, and electromagnetic navigation bronchoscopy. Without precise techniques, incorrect bronchial transection and vessel ligation would be questioned and argued, especially for live surgery and meeting presentation in China. However, most routine anatomical segmentectomies are performed using only high-resolution CT, and higher complication rates have not been observed. We hypothesized that routine segmentectomy for GGOs could achieve the same safety and accuracy of precise segmentectomy. The aim of this study was to evaluate the effect of precise segmentectomy using real-time 3D reconstruction navigation vs routine segmentectomy, for lung GGOs. Actually, clinical selective tendency exist in the real world, 3D reconstruction techniques would be selected more frequently when surgery live teaching or communicating, during which complex segmentectomies are more popular owing to high difficulty and educational value. Propensity score matching was used to reduce the selective bias in this retrospective study.

METHODS

Patient Selection and Data Collection

We retrospectively analyzed 398 patients with single or multiple GGOs diagnosed as T1aN0M0 stage IA lung cancer at the First Affiliated Hospital of USTC from January 2020 to September 2020. Fifty-five precise segmentectomies guided by 3D reconstruction (Precision group) and 343 routine segmentectomies (Routine group) were performed as uniportal procedures. All protocols were reviewed and approved by the Ethics Committee of the First Affiliated Hospital of USTC. We retrospectively collected the following data from the medical databases: patients' demographics; perioperative outcomes, namely operation time, blood loss, resection margin distance, number of dissected lymph nodes, postoperative pulmonary function (1 month after surgery), and complications; and length of postoperative stay.

The indications for segmentectomy and preoperative evaluation were in accordance with the National Comprehensive Cancer Network (NCCN) guidelines, as follows: all enrolled patients with peripheral nodules <2 cm in size with at least one of the following were included: (1) pure adenocarcinoma in-situ, histologically; (2) nodules with 50% ground glass appearance on CT imaging; and (3) radiologic images confirming a long doubling time (>400 days) (8). Patients with insufficient cardiopulmonary function or other contraindications for segmentectomy were excluded. We limited the inclusion criteria to unilateral and single anatomical resection in each operation. Patients undergoing synchronous double anatomical resection, concurrent bilateral surgery, and repeated surgery in the same hemithorax were excluded (**Figure 1**).

Preoperative examinations constituted routine blood testing, pulmonary function testing, and high-resolution CT of the chest

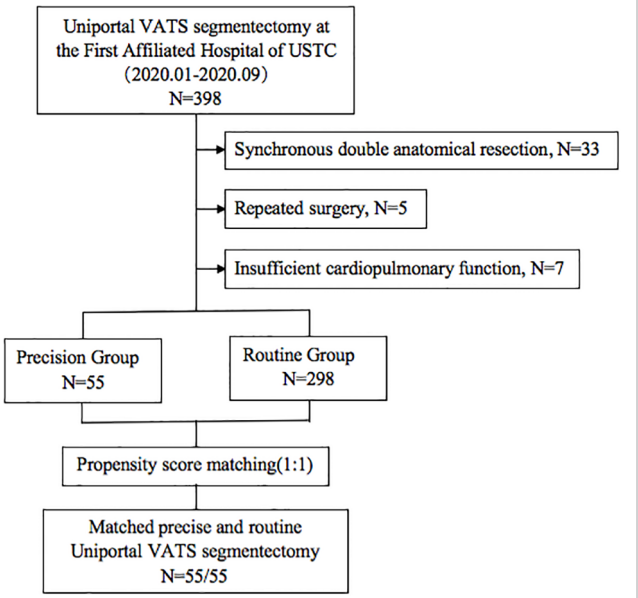

FIGURE 1 | The flow chart of patient selection.

with or without contrast. Brain magnetic resonance imaging (MRI), bone scintigraphy, or flexible bronchoscopy were selected if necessary (e.g. for patients with complaints of dizziness, non-traumatic bone pain and irritable cough). Positron emission tomography, mediastinoscopy and endobronchial ultrasound-guided transbronchial needle aspiration (EBUS-TBNA) were not routinely performed on the basis of no swelling of mediastinal or hilar lymph nodes were revealed according to CT results. The pathological staging was in accordance with the criteria of the American Joint Committee on Cancer (AJCC) pathological tumor/node/metastasis (pTNM) classification (eighth edition). The pathological results of the GGOs were classified according to the 2011 International Association for the Study of Lung Cancer (IASLC), American Thoracic Society (ATS), and European Respiratory Society (ERS) (IASLC/ATS/ERS) classification (9). Postoperative complications were defined as grade ≥2 according to the Clavien–Dindo classification system (10).

Preoperative Surgical Plan and 3D Reconstruction

The target segment and surgical plans were devised by surgeons with expert knowledge of the anatomic structures, and with correct and thorough interpretation of the CT images. All patients underwent preoperative CT with a slice thickness of 1.0 mm. Localization techniques were routinely used to mark the nodule, especially for GGOs located in basal segment or nearby intersegmental plane. For easily identified GGOs (e.g. subpleural nodule in relation to fissure) and simple segmentectomies with GGOs far from resection margin, localization techniques were waived (13/55 in Precision group, 14/55 in Routine group). The localization devices with small four-hook anchor and scaled suture were used as previously reported (11). The safe resection margin was defined as a sphere, extending 2 cm outside the primary tumor.

In the Routine group, the diagnostic and surgical plans were devised according to the serial CT images (**Figure 2**). Surgical margins were confirmed by intraoperative exploration and specimen frozen sections. Enlarged wedge resection was performed for insufficient margins. In the Precision group, contrast-enhanced CT was necessary, and digital imaging and communications in medicine (DICOM) data for each patient were recorded. 3D images were reconstructed using Inlook3D (INCOOL Tec., Wuhan, China). The validity of the reconstructions was confirmed, and images were preoperatively evaluated by the thoracic surgeons. All vessels and bronchi to the target segment were checked and marked on the 3D images, and safe resection margins and the relationships between the margins and the intersegmental veins were evaluated (12) (**Figure 3**).

VATS Segmentectomy Procedure

Patients underwent surgery with general anesthesia with selective one-lung ventilation. Segmentectomy was performed in all patients *via* a uniportal approach with an incision of approximately 3–4 cm in the fourth or fifth intercostal space between the anterior and posterior axillary lines (13). Segmentectomy is defined as resection of the target segment after dividing the segmental pulmonary bronchus and artery, and selectively, the inter- and intrasegmental pulmonary veins. The intersegmental plane was demarcated using an inflation-deflation method (14). Intersegmental fissures and the bronchus were transected using a stapler, and stapling was also used to perform the segmentectomy to minimize air leakage from the lung parenchyma. Sealant tissue glue was routinely used. Sampling or dissection of segmental, lobar, hilar and mediastinal lymph nodes was performed when frozen section diagnosis of malignancy was performed.

In the Precision group, 3D reconstructions were available inside the operating room, and the segmental vein, artery, and bronchus were individually dissected according to the real-time 3D reconstruction guidance. The actual anatomy was compared with the 3D reconstructions, when there was any doubt. In the Routine group, the bronchus and main vessels were identified according to the CT images and the relationships between the blood vessel direction and the target segment. When thin vessels could not be identified, we attempted to preserve the vein and selectively dissect the artery.

Propensity Score Matching (PSM)

The propensity scores were analyzed by logistic regression models to increase the sensitivity of the comparisons between the groups, and the matched factors were sex, body mass index (BMI), surgery type (complex vs simple), and the percentage of forced expiratory volume in 1 s (FEV1). Segmentectomy that created several, intricate intersegmental planes, with a more complicated procedure, was considered complex segmentectomy; that is, segmentectomy other than simple segmentectomy (15). Through the matching procedure for propensity scores, the Precision group and Routine group showed similar distributions of propensity scores, indicating that the differences in covariates

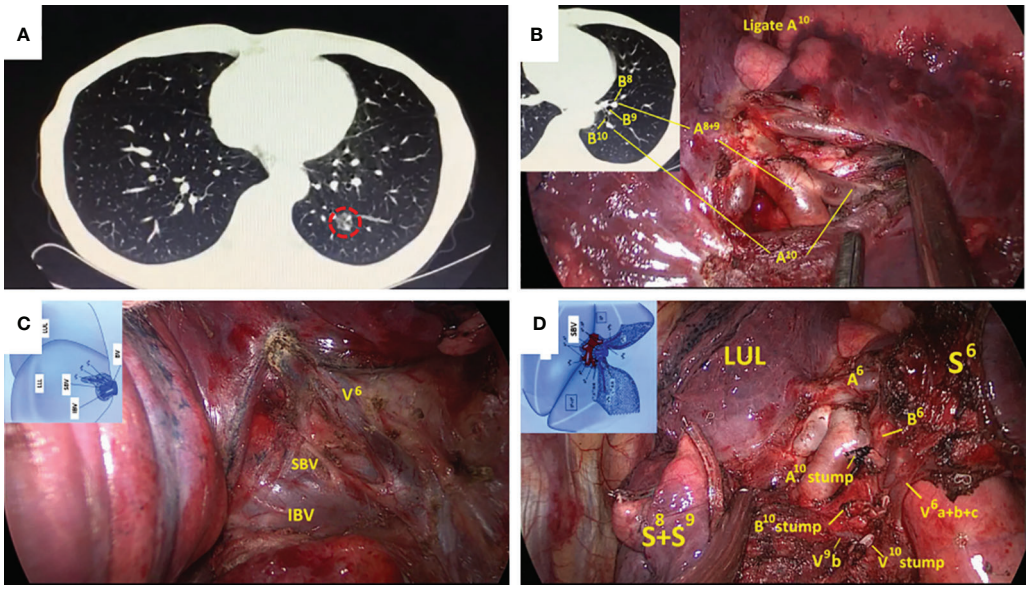

FIGURE 2 | Routine left S^{10} segmentectomy based on CT scan and normal anatomic characteristics. **(A)** CT scan showed a GGOs lesion in the left S^{10}; **(B)** The branches of the pulmonary artery exposed in the VATS were consistent with CT. **(C, D)** Surgical details were compared with segmental atlas written by Hiroaki Nomori and Morihito Okada. CT, computed tomography; VATS, video-assisted thoracoscopy; GGOs, ground-glass opacities.

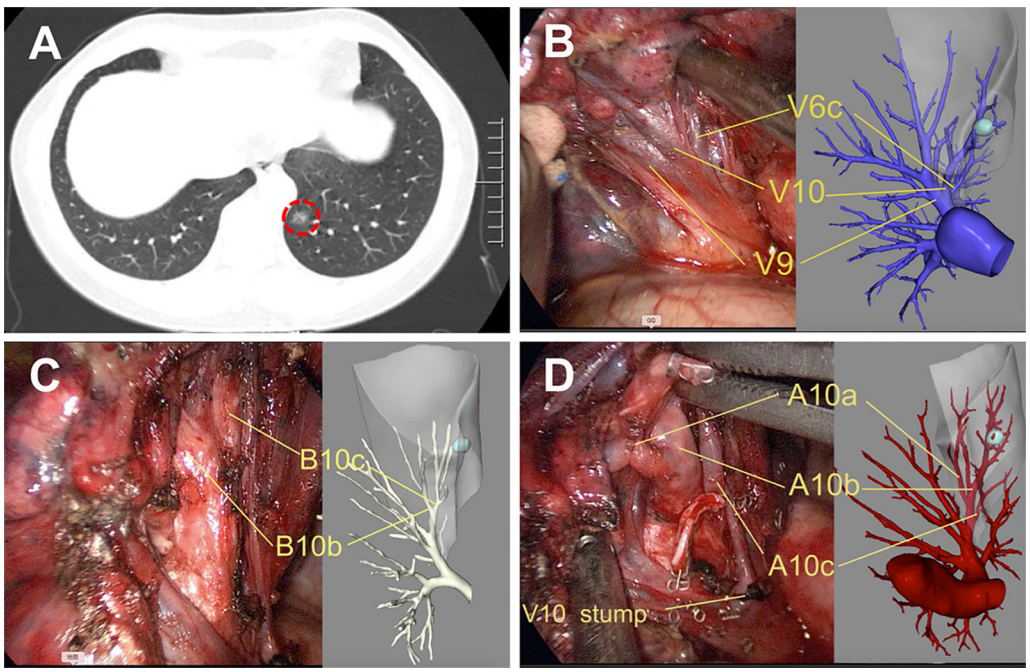

FIGURE 3 | Precise left S^{10} segmentectomy according to the real-time 3D reconstruction guidance. **(A)** CT scan showed a GGOs lesion in the left S^{10}; Branches pulmonary vein **(B)**, bronchus **(C)**, and pulmonary artery **(D)** of the target segment were confirmed by real-time guidance of 3D reconstruction. 3D, three-dimensional.

between the two groups were minimized. Propensity scores were matched one by one using nearest neighbor matching methods, no replacement, caliper 0.025, and match 1:1.

Statistical Analyses

Statistical analyses were performed using SPSS version 20.0 (IMB Corp., Armonk, NY). Normally distributed data are

shown as the mean ± standard deviation. Mean values were compared using Student's t-test, and frequency distributions were compared using the Chi-square test or Fischer's exact test. A p-value of <0.05 was considered significant.

RESULTS

A total of 353 patients who underwent VATS segmentectomies were included in this study. 55 (15.6%) patients constituted the Precision group, and 298 (84.4%) patients constituted the Routine group. Before matching, there was a tendency toward more complex segmentectomies in the Precision group (p = 0.057). After matching, there were 43 male and 67 female patients, aged 25–68 years (median: 53 years). The matched groups were comparable regarding the patients' baseline characteristics (**Table 1**), and the distribution of the complex segmentectomies is detailed in **Table 2**.

There was no 30-day postoperative mortality in either group. Perioperative outcomes are compared in **Table 3**; no significant differences were seen between the groups for blood loss, histological type, complications, and postoperative pulmonary function. In the Precision group, pathological results identified four patients with adenocarcinoma, 41 with microinvasive adenocarcinoma (MIA), and 10 with adenocarcinoma *in situ* (AIS). In the Routine group, three patients had adenocarcinoma, 46 had MIA, and six had AIS, pathologically.

The median operation time in the Precision group (74 min) was longer than that in the Routine group (55 min) (p <0.01). No lymph node metastasis was detected in any of the patients. Most of the examined lymph nodes were from stations 10 to 12, mediastinal lymph nodes were less and mainly from invasive adenocarcinoma cases. The number of dissected lymph nodes in the Precision group (5 ± 1.1) was higher than in the Routine group (3 ± 0.8) (p <0.01). Chest tube duration days and postoperative stay days were similar in both groups; however, the rate of air leakage on postoperative day 1 was higher in the Precision group (p = 0.020).

All cases in the Precision group had adequate resection margins (as defined in *Methods*). Four patients (7.3%) undergoing complex segmentectomy in the Routine group had inadequate resection margins (less than 2 cm) confirmed by intraoperative specimen evaluation, and additional wedge resection were performed. All resection margins were negative, identified by pathological analysis.

DISCUSSION

Excellent survival and low recurrence is associated with lung cancers involving GGOs (16). Therefore, it is reasonable to consider limited resection as an alternative to lobectomy for small, indolent lesions. Segmentectomy and wedge resection are the main sublobar resection procedures with the advantage of lung sparing. Results from JCOG0804 indicated that simpler procedure

TABLE 2 | Types of VATS segmentectomy in Precision group and Routine group.

Surgery types	Precision group	Routine group
Rright upper lobe	12 (21.8%)	13 (23.6%)
S^1	2	2
S^2	2	2
S^3	3	3
S^{2b+3a}	5	6
Right lower lobe	14 (25.5%)	13 (23.6%)
S^6	3	3
S^8	3	3
S^9	2	2
S^{10}	5	5
S^{9+10}	1	0
Left upper lobe	16 (29.1%)	16 (29.1%)
$S^{1+2(a+b)}$	7	6
$S^{1+2(c)}$	1	2
S^{1+2}	3	3
S^3	2	3
S^{1+2+3}	1	1
S^{4+5}	2	1
Left lower lobe	13 (23.6%)	13 (23.6%)
S^6	2	2
S^8	1	1
S^9	3	2
S^{10}	6	7
S^{9+10}	1	1

Complex segmentectomy: Right S^{2b+3a}, S^3; left $S^{1+2(a+b)}$, S^3; and all S^8, S^9, S^{10} and S^{9+10}.

TABLE 1 | Demographic data of precise and routine VATS uniportal segmentectomy.

Variables*	Before matching				After matching		
	All (N = 353)	Precision (N = 55)	Routine (N = 298)	p Value	Precision (N = 55)	Routine (N = 55)	p Value
Age(years)	50.5 ± 5.3	52.9 ± 10.4	47.6 ± 12.6	0.108	52.9 ± 10.4	53.1 ± 11.9	0.978
Gender							
Male	162 (45.9)	20 (36.4)	142 (47.7)	0.142	20 (36.4)	23 (41.8)	0.696
Female	191 (54.1)	35 (63.6)	156 (52.3)		35 (63.6)	32 (58.2)	
BMI	23.6 ± 3.2	23.9 ± 3.6	23.5 ± 2.7	0.342	23.9 ± 3.6	23.8 ± 3.0	0.898
Surgery Type							
Simple	164 (46.5)	19 (34.5)	145 (48.7)	0.057	19 (34.5)	19 (34.5)	1.000
Complex	189 (53.5)	36 (65.5)	153 (51.3)		36 (65.5)	36 (65.5)	
Pre-op FEV1(L)	2.36 ± 0.42	2.38 ± 0.61	2.30 ± 0.38	0.406	2.38 ± 0.61	2.37 ± 0.74	0.933

**Variables used for estimating propensity score. BMI, body mass index; FEV1, forced expiratory volume in 1 s; VATS, video-assisted thoracoscopic surgery.*

TABLE 3 | Intraoperative and postoperative characters of Precision group and Routine group.

Variables	Precision group (N = 55)	Routine group (N = 55)	*p* Value
Operation time (min)	74 ± 14.6	55 ± 17.8	<0.01
Intraoperative blood loss (ml)	33 ± 7.5	28 ± 9.0	0.215
Inadequate resection margins	0	4 (7.3%)	0.118
Number of removed lymph nodes	5 ± 1.1	3 ± 0.8	<0.01
Histological type			0.108
Adenocarcinoma *in situ*	10 (18.2%)	3 (5.5%)	
Microinvasive adenocarcinoma	41 (74.5%)	46 (83.6%)	
Invasive adenocarcinoma	4 (7.3%)	6 (10.9%)	
Chest tube duration days	3.9 ± 1.7	3.7 ± 1.9	0.687
Air leakage on POD1	31 (56.4%)	19 (16.4%)	0.020
Postoperative hospital stay (days)	4.4 ± 1.3	4.1 ± 2.2	0.619
Postoperative complications			
Air leakage (>7 days)	2 (3.6%)	3 (5.5%)	
Pneumonia	0	1 (1.8%)	
Atrial fibrillation	1 (1.8%)	0	
Hemoptysis (>10 ml)	0	0	
Total	3 (5.5%)	4 (7.3%)	1.000
Post-op FEV1 (L)*	2.00 ± 0.53	1.89 ± 0.71	0.741

**Postoperative pulmonary functions were evaluated 1 month after surgery. POD, Postoperative Day. All patients' air leakage on POD1 were under grade II.*

of wedge resection is suitable for GGOs with consolidation-to-tumor ratio ≤0.25. Whether segmentectomy could be the standard of care for other type GGOs, more randomized controlled trial results are needed. When choosing segmental lung resection, the oncologic curative effect should be verified first. Sufficient resection margins are critical to achieve a curative effect (5–7). If the expected oncologic outcomes are equivalent between procedures, the simpler procedure is preferred. In our study, routine segmentectomies were performed six times more often than precise segmentectomies during the same period. There are non-surgical reasons for this difference; precise segmentectomy takes more time because of the need to prepare the 3D reconstructions, and using 3D simulation services increases the medical costs. In comparison, for routine segmentectomy, non-enhanced CT is sufficient, and this method is more convenient and acceptable to patients. Additionally, clinical selective tendency existed in our clinical practice, 3D reconstruction techniques were selected more frequently for complex cases, because complex segmentectomies with high difficulty and educational value were more popular for surgery live teaching or communicating.

Segmentectomy is more complicated than lobectomy owing to the complex anatomy and variations in peripheral bronchi and vessels. In our study, the operation time in the Routine group was significantly shorter than that in the Precision group, which differs from findings in previous reports (17). The following reasons may explain this difference: For precise segmentectomy, 3D reconstruction can illustrate variations in anatomical details (18). To ensure accuracy and safety in precise segmentectomy, it is necessary to compare the actual anatomy with the 3D reconstructions repeatedly, especially for tiny vessels. Additional operation time may also be required for extended dissection of the lung tissue. In routine segmentectomy, which is based on normal patterns and individual CT data, the main anatomical characteristics are sufficient to achieve safe and quick segmentectomy, as confirmed by past clinical experience. With routine segmentectomy, thin vessels are not a concern, and unnecessary lung dissection is avoided. The incidence of complications in the two groups in this study was similar, and complications were rare. There was no thoracotomy-related or postoperative 30-day mortality in either group, which confirmed the safety of routine segmentectomy.

Despite extensive dissection in the Precision group, the chest tube duration days and postoperative stay days were similar in both groups. Moreover, we observed that the rate of air leakage on postoperative day 1 was higher in the Precision group. Air leakage is common with segmentectomy because of the dissection of the lung parenchyma (19). Most of the patients in this study had adequate lung function before surgery, indicating good lung compliance and elasticity. Additionally, using sealant tissue glue may be very helpful to prevent prolonged air leakage.

Ensuring adequate surgical margins is important with segmentectomy. In the Precision group in this study, all patients had adequate resection margins, which may have resulted from an accurate surgical plan; accurate vessel handling leads to clearer segmental boundaries showed by inflation–deflation method. Four patients undergoing complex segmentectomy in the Routine group had inadequate resection margins. In addition to unclear boundaries resulting from inappropriate transection of small vessels, the boundaries of simple segments are generally planar, whereas the boundaries of complex segments are often multiplanar (20). For planar unclear boundaries, intentional extended resection is easy, however, extended resection in angle area between unclear miltiplanar boundaries of complex segments is difficult to plan and perform, which may result in inadequate resection margins. Therefore, clear segmental boundaries obtained from precise segmentectomy are valuable for complex cases. Compared with inflation-deflation method, alternative techniques like indocyanine green injection may enhance the identification of the right intersegmental plane based on accurate vessel handling (21).

The guidance of 3D reconstructed images not only enables achieving safe surgical margins but also minimizes the anatomic resection of the lung tissues, which ensures oncological efficacy and retains more healthy tissue (18). However, no postoperative

pulmonary function benefits were observed in this study because the pulmonary function of most of the enrolled patients was normal.

Generally, intentional lymph nodes sampling or dissection would be done for MIA and invasive adenocarcinoma respectively. In real world, we often harvest lymph nodes during bronchus and vessel dissection process. In the Precision group, segmental hilar structures were freed very well, which maybe the reason for the higher numbers of examined lymph nodes. Whether lymph nodes sampling or dissection is necessary for MIA patients remains controversy. This procedure may increase surgical injury. And excessive dissection may take more difficulties for possible second surgery in young patients. Further studies should work on this.

All of the patients in this study underwent intensive radical segmentectomy according to the NCCN guidelines for non-small-cell lung cancer (NSCLC), including seven patients diagnosed with adenocarcinoma with >5-mm invasive range. It is not uncommon that GGO-dominant lesions turn out to be invasive adenocarcinoma, pathologically (22). Whether segmentectomy is sufficient for invasive adenocarcinoma requires validation in future studies.

One of the limitations of this study was the retrospective design. Furthermore, although we used PSM to minimize baseline differences between the two groups, there were additional limitations. First, the sample size was small. Second, no long term follow-up results were included. Moreover, our results revealed an advantage of precision segmentectomy regarding ensuring adequate surgical margins in complex segmentectomy; however, the subgroup sample was too small to confirm this advantage between the two groups. Prospective studies with larger patient numbers are warranted to identify which surgical pattern is feasible and efficient for real-world segmentectomy to treat GGOs.

CONCLUSION

Routine segmentectomy can significantly shorten the operation time and might prevent postoperative air leakage in uniportal segmentectomy for lung GGOs. However, precision segmentectomy may be more precise for complex cases, ensuring adequate resection margins and lymph node dissection.

DATA AVAILABILITY STATEMENT

The raw data supporting the conclusions of this article will be made available by the authors, without undue reservation.

ETHICS STATEMENT

This study involving human participants was reviewed and approved by the Ethics Committee of the First Affiliated Hospital of the University of Science and Technology of China. Written informed consent for participation was not required for this study in accordance with our national legislation and the institutional requirements.

AUTHOR CONTRIBUTIONS

All listed authors have made a substantial, direct, and intellectual contribution to the work, and approved the manuscript for publication. XW and MrX contributed to the study design. TL, CZ, GW, and MqX were responsible for interpreting the results. DS, RX, and XW contributed to the statistical analysis. DS and XW wrote the manuscript. All authors contributed to data collection and analysis. All authors contributed to the article and approved the submitted version.

FUNDING

This work was supported by the Anhui Provincial Natural Science Foundation (1808085QH270; 2008085QH428), Fundamental Research Funds for the Central Universities (WK9110000121), and Key Research and Development Projects in Anhui Province (202004j07020017).

ACKNOWLEDGMENTS

We thank Jane Charbonneau, DVM, from Liwen Bianji, Edanz Group China (http://www.liwenbianji.cn/ac), for editing the English text of a draft of this manuscript.

REFERENCES

1. Zhang Y, Jheon S, Li H, Zhang H, Xie Y, Qian B, et al. Results of Low-Dose Computed Tomography as a Regular Health Examination Among Chinese Hospital Employees. *J Thorac Cardiovasc Surg* (2020) 160(3):824–31. doi: 10.1016/j.jtcvs.2019.10.145
2. Ginsberg RJ, Rubinstein LV. Randomized Trial of Lobectomy Versus Limited Resection for T1 N0 Non-Small Cell Lung Cancer. Lung Cancer Study Group. *Ann Thorac Surg* (1995) 60(3):615–22, 622-3. doi: 10.1016/0003-4975(95)00537-u
3. Suzuki K, Watanabe SI, Wakabayashi M, Saji H, Aokage K, Moriya Y, et al. A Single-Arm Study of Sublobar Resection for Ground-Glass Opacity Dominant Peripheral Lung Cancer. *J Thorac Cardiovasc Surg* (2020). doi: 10.1016/j.jtcvs.2020.09.146
4. Churchill ED, Belsey R. Segmental Pneumonectomy in Bronchiectasis: The Lingula Segment of the Left Upper Lobe. *Ann Surg* (1939) 109(4):481–99. doi: 10.1097/00000658-193904000-00001
5. El-Sherif A, Fernando HC, Santos R, Pettiford B, Luketich JD, Close JM, et al. Margin and Local Recurrence After Sublobar Resection of non-Small Cell Lung Cancer. *Ann Surg Oncol* (2007) 14(8):2400–5. doi: 10.1245/s10434-007-9421-9
6. Sawabata N, Ohta M, Matsumura A, Nakagawa K, Hirano H, Maeda H, et al. Optimal Distance of Malignant Negative Margin in Excision of Nonsmall Cell Lung Cancer: A Multicenter Prospective Study. *Ann Thorac Surg* (2004) 77(2):415–20. doi: 10.1016/S0003-4975(03)01511-X
7. Koike T, Koike T, Yoshiya K, Tsuchida M, Toyabe S. Risk Factor Analysis of Locoregional Recurrence After Sublobar Resection in Patients With Clinical

Stage IA Non-Small Cell Lung Cancer. *J Thorac Cardiovasc Surg* (2013) 146 (2):372–8. doi: 10.1016/j.jtcvs.2013.02.057
8. Ettinger DS, Wood DE, Aggarwal C, Aisner DL, Akerley W, Bauman JR, et al. NCCN Guidelines Insights: Non-Small Cell Lung Cancer, Version 1.2020. *J Natl Compr Canc Netw* (2019) 17(12):1464–72. doi: 10.6004/jnccn.2019.0059
9. Travis WD, Brambilla E, Noguchi M, Nicholson AG, Geisinger KR, Yatabe Y, et al. International Association for the Study of Lung Cancer/American Thoracic Society/European Respiratory Society International Multidisciplinary Classification of Lung Adenocarcinoma. *J Thorac Oncol* (2011) 6(2):244–85. doi: 10.1097/JTO.0b013e318206a221
10. Dindo D, Demartines N, Clavien PA. Classification of Surgical Complications: A New Proposal With Evaluation in a Cohort of 6336 Patients and Results of a Survey. *Ann Surg* (2004) 240(2):205–13. doi: 10.1097/01.sla.0000133083.54934.ae
11. Fan L, Yang H, Yu L, Wang Z, Ye J, Zhao Y, et al. Multicenter, Prospective, Observational Study of a Novel Technique for Preoperative Pulmonary Nodule Localization. *J Thorac Cardiovasc Surg* (2020) 160(2):532–9. doi: 10.1016/j.jtcvs.2019.10.148
12. Iwano S, Yokoi K, Taniguchi T, Kawaguchi K, Fukui T, Naganawa S. Planning of Segmentectomy Using Three-Dimensional Computed Tomography Angiography With a Virtual Safety Margin: Technique and Initial Experience. *Lung Cancer* (2013) 81(3):410–5. doi: 10.1016/j.lungcan.2013.06.001
13. Hernandez-Arenas LA, Purmessur RD, Gonzalez-Rivas D. Uniportal Video-Assisted Thoracoscopic Segmentectomy. *J Thorac Dis* (2018) 10(Suppl 10): S1205–14. doi: 10.21037/jtd.2018.02.47
14. Wei H, Zhu Y, Wang Q, Chen L, Wu W. Assessment of the Accuracy of Modified Inflation-Deflation Methods for Distinguishing the Intersegmental Border. *Zhongguo Fei Ai Za Zhi* (2020) 23(6):526–31. doi: 10.3779/j.issn.1009-3419.2020.104.15
15. Handa Y, Tsutani Y, Mimae T, Miyata Y, Okada M. Complex Segmentectomy in the Treatment of Stage IA Non-Small-Cell Lung Cancer. *Eur J Cardiothorac Surg* (2020) 57(1):114–21. doi: 10.1093/ejcts/ezz185
16. Ito H, Suzuki K, Mizutani T, Aokage K, Wakabayashi M, Fukuda H, et al. Long-Term Survival Outcome After Lobectomy in Patients With Clinical T1 N0 Lung Cancer. *J Thorac Cardiovasc Surg* (2020). doi: 10.1016/j.jtcvs.2019.12.072
17. Xue L, Fan H, Shi W, Ge D, Zhang Y, Wang Q, et al. Preoperative 3-Dimensional Computed Tomography Lung Simulation Before Video-Assisted Thoracoscopic Anatomic Segmentectomy for Ground Glass Opacity in Lung. *J Thorac Dis* (2018) 10(12):6598–605. doi: 10.21037/jtd.2018.10.126
18. Wu WB, Xu XF, Wen W, Xu J, Zhu Q, Pan XL, et al. Three-Dimensional Computed Tomography Bronchography and Angiography in the Preoperative Evaluation of Thoracoscopic Segmentectomy and Subsegmentectomy. *J Thorac Dis* (2016) 8(Suppl 9):S710–5. doi: 10.21037/jtd.2016.09.43
19. Suzuki K, Saji H, Aokage K, Watanabe SI, Okada M, Mizusawa J, et al. Comparison of Pulmonary Segmentectomy and Lobectomy: Safety Results of a Randomized Trial. *J Thorac Cardiovasc Surg* (2019) 158(3):895–907. doi: 10.1016/j.jtcvs.2019.03.090
20. Handa Y, Tsutani Y, Mimae T, Tasaki T, Miyata Y, Okada M. Surgical Outcomes of Complex Versus Simple Segmentectomy for Stage I Non-Small Cell Lung Cancer. *Ann Thorac Surg* (2019) 107(4):1032–9. doi: 10.1016/j.athoracsur.2018.11.018
21. Pardolesi A, Veronesi G, Solli P, Spaggiari L. Use of Indocyanine Green to Facilitate Intersegmental Plane Identification During Robotic Anatomic Segmentectomy. *J Thorac Cardiovasc Surg* (2014) 148(2):737–8. doi: 10.1016/j.jtcvs.2014.03.001
22. Fu F, Zhang Y, Wen Z, Zheng D, Gao Z, Han H, et al. Distinct Prognostic Factors in Patients With Stage I Non-Small Cell Lung Cancer With Radiologic Part-Solid or Solid Lesions. *J Thorac Oncol* (2019) 14(12):2133–42. doi: 10.1016/j.jtho.2019.08.002

Conflict of Interest: The authors declare that the research was conducted in the absence of any commercial or financial relationships that could be construed as a potential conflict of interest.

frontiers in Oncology

ORIGINAL RESEARCH
published: 27 April 2021
doi: 10.3389/fonc.2021.661067

Characteristics of Ground-Glass Nodules Detected by Low-Dose Computed Tomography as a Regular Health Examination Among Chinese Hospital Employees and Their Parents

Bihan Ouyang[1], *Maoyuan Li*[2], *Li Li*[2], *Shaohui Liu*[1] *and Min Li*[2,3,4,5]*

[1] Health Management Center, Xiangya Hospital of Central South University, Changsha, China, [2] Department of Respiratory Medicine, National Key Clinical Specialty, Branch of National Clinical Research Center for Respiratory Disease, Xiangya Hospital, Central South University, Changsha, China, [3] Xiangya Lung Cancer Center, Xiangya Hospital, Central South University, Changsha, China, [4] Clinical Research Center for Respiratory Diseases in Hunan Province, Changsha, China, [5] National Clinical Research Center for Geriatric Disorders, Changsha, China

OPEN ACCESS

Edited by:
Chen Chen,
Central South University, China

Reviewed by:
Ziming Li,
Shanghai Jiaotong University, China
Yijiu Ren,
Shanghai Pulmonary Hospital, China

***Correspondence:**
Min Li
limin2050@csu.edu.cn

Specialty section:
This article was submitted to Thoracic Oncology, a section of the journal Frontiers in Oncology

Received: 30 January 2021
Accepted: 16 March 2021
Published: 27 April 2021

Citation:
Ouyang B, Li M, Li L, Liu S and Li M (2021) Characteristics of Ground-Glass Nodules Detected by Low-Dose Computed Tomography as a Regular Health Examination Among Chinese Hospital Employees and Their Parents. Front. Oncol. 11:661067. doi: 10.3389/fonc.2021.661067

Introduction: Annual LDCT has been offered as a regular examination among many unit staff in China. Along with the wide application of LDCT, more and more ground-glass nodules were found. We focused on characteristics and relationship of ground-glass nodules detected by LDCT as a regular health examination among Chinese hospital employees and their parents.

Methods: We recorded LDCT-detected ground-glass nodules (GGNs) in the hospital employees and parents between 2019 and 2020. Clinical information, including age, gender, smoking status was collected and analyzed.

Results: A total of 5,574 employees and 2,686 employs' parents ≥60 years in Xiangya hospital performed annual physical examination. In total, LDCT incidentally detected ground-glass nodules 392 (24.78%, 392/1,582) in hospital employees and 254 in parents (10.80%, 254/2,352). The GGN-detection rate was significantly greater in employee group than parent group and more non-smokers in former (P <0.001). The detection rate was significantly greater in female than male both in employees group and parents group, and the proportion of female was bigger in employees group (P <0.001). There were more pure-GGNs both in employees group and parents group. There were less participants with solitary GGN in employee group than parent group (P = 0.033). Besides, there were more large GGNs (≥10 mm) (P <0.001), LU-RADS 4 GGNs (P <0.001) and LU-RADS 4B GGNs (P = 0.003), LU-RADS 4C-5 GGNs (P = 0.001) in parent group than employee group. There were 36 employee–parent pairs (27.07%) both had GGNs among 133 pairs who both performed LDCT. GGNs in employees were smaller and lower-grade than their parents (P < 0.001, P = 0.001).

Conclusions: Among the employees and parents who had ground glass nodules, 1/4 of them both detected GGNs. Although the detection rate of GGNs in the parent group was lower than that in the employee group, the grade of nodules was significantly higher. All these suggest that the occurrence and development of ground glass nodules may be related to genetic factors.

Keywords: ground glass nodules, health examination, low-dose computed tomography, genetic, family history

INTRODUCTION

In recent years, annual LDCT has been applied for early lung cancer screening worldwide, especially in China. LDCT has been offered as a regular examination among many unit staff among which many are not eligible high-risk participants according to NLST. Along with the wide application of LDCT, more and more ground-glass nodules were found. The International Early Lung Cancer Action Program reported that nonsolid and part-solid nodules were found in 9.2% of 57,496 baseline screenings (1, 2). Zhang et al. (3) retrospectively analyzed LDCT screening among 15,686 Chinese hospital employees and found that 95.5% of patients with screening-detected lung cancer presented as GGO nodules on CT scans. As family history is the main risk factor for lung cancer, the present study focused on characteristics and relationship of ground-glass nodules detected by low-dose computed tomography as a regular health examination among Chinese hospital employees and their parents.

METHODS

Participants and CT Scans

LDCT was performed as a part of regular health examination in staff above 40-year-old of the Xiangya Hospital and staff's parents above 60-year-old between 2019 and 2020. The employees below 40-years-old were offered with X-ray but some of them changed for LDCT at their own expense. In general, all the participants were volunteered to take the test. Revolution CT (GE Medical Systems) was used in the examination with 1.3 mm slice thickness, 1mm slice spacing, 100 kV tube voltage, 40–100 mA tube current.

Clinical Data

LDCT-detected ground-glass nodules (GGNS) in hospital employees and parents were recorded. Clinical information, including age, gender, smoking status was collected and analyzed.

Nodule Measurements

Fleischner Society defined "a nodule appears as a rounded or irregular opacity, well or poorly defined, measuring up to 3 cm in diameter" and ground-glass nodule (GGN) manifests as hazy increased attenuation in the lung that does not obliterate the bronchial and vascular margins (4). GGNs include pure ground-glass and part-solid nodule. Pure ground-glass nodule has no solid components. A part-solid nodule consists of both ground-glass and solid soft-tissue attenuation components. ALL information of nodules were recorded mainly from CT reports by a radiologist, if there were any ambiguous issues about the nodules, the radiologist would check the CT images. Nodules were measured in long- and short-axi length or diameter. Nodules were classified by The Lung Reporting and Data System (LU-RADS) categories (5).

Statistical Analysis

We used the Pearson χ^2 test to compare the GGNs detection rate, and paired-t test to compare the characteristics of GGNs in employee–parent pairs. Statistical analysis was performed in SPSS 23.0.

RESULTS

Characteristics of Hospital Employees and CT-Detected GGN

There were a total of 5,574 employees in Xiangya hospital, among them female employees were 4,224 (75.78%), male employees were 1,350 (24.22%). The overall LDCT participation rate was 28.38% (1,582/5,574), among them female participation rate was 25.33% (1,070/4,224), male participation rate was 37.93% (512/1,350). The percentages of patients performed CT <40 years, 40 to 60 years, and >60 years were 3.49% (120/3,442), 66.32% (961/1,449), 73.35% (501/683), respectively (**Table 1**, **Figure 1**).

In total, LDCT incidentally detected ground-glass nodules 392 (24.78%, 392/1,582) in hospital employees. Among employees with GGN, 290 (27.10%, 290/1,070) were female and 102 (19.92%, 102/512) were male; the detection rate was significantly greater in female than male (27.10% vs 19.92%, P = 0.002). Among employees with GGNs, 349 (89.02%) participants were non-smokers. The GGN-detection rate in employees age <40 years, 41 to 60 years, and >60 years were 18.33% (22/120), 26.12% (251/961), and 23.75% (119/501), respectively. 68.62% (269/392) had solitary GGN and 31.38% (123/392) had multiple GGNs. There were more employees with pure-GGN than employees with mixed-GGN (331 vs 61). The percentage of GGN <5 mm, 5–9 mm, and ≥10 mm was 27.30% (107/392), 63.77% (250/392), and 8.93% (35/392), respectively. According to the LU-RADS classification, there were 113 (28.83%) employees had LU-RADS 2 GGNs, 246 (62.75%) had LU-RADS 3 GGNs, and 32 (8.42%) had LU-RADS 4 GGNs.

TABLE 1 | The proportion of employees performing LDCT and which with GGNs according to sex and age.

Characteristics	No. of employees	No. of employees performed LDCT	Rate of employees performed LDCT (%)	CT-detected GGNsN, Rate (%)	*P* value
Total detection rate	5,574	1,582	28.38	392 (24.78)	
Sex					0.002
female	4,224	1,070	25.33	290 (27.10)	
male	1,350	512	37.93	102 (19.92)	
Age					0.143
<40	3,442	120	3.49	22 (18.33)	
40–60	1,449	961	66.32	251 (26.12)	
>60	683	501	73.35	119 (23.75)	

Among them, there were 11 nodules were LU-RADS 4B and 14 were LU-RADS 4C or 5 (**Table 2**, **Figure 1**).

Characteristics of Hospital Employees' Parents and CT-Detected GGN

In total, there were 2,686 employees' parents ≥60 years participated the regular examination, the average age of parents was 67.85 ± 6.18, among them 1,338 were female and 1,348 were male. The overall participation rate of LDCT was 87.57% (2,352/2,686), female and male participation rate was 86.62% (1,159/1,338), 88.50% (1,193/1,348), respectively.

The overall GGN-detection rate was 10.80% (254/2,352), among them female was 12.68% (147/1,159), male was 8.97% (107/1,193), the detection rate was significantly greater in female than male (12.68% vs 8.97%, P = 0.004). Among parents with GGNs, 195 participants were non-smokers. There were more parents with pure-GGN than those with mixed-GGN (214 vs 40), and more with solitary GGN other than multiple GGNs (194 vs 60). The percentages of GGNs <5 mm, 5–9 mm, and ≥10 mm was 17.72% (45/254), 57.09% (145/254), and 25.19% (64/254), respectively. According to the LU-RADS classification, there were 52 (20.47%) parents had LU-RADS 2 GGNs, 150 (59.06%) had LU-RADS 3 GGNs, and 49 (19.29%) had LU-RADS 4 GGNs among them 20 were 4B, 25 were 4C or 5 (**Table 2**, **Figure 1**).

Comparation and Correlation Analysis of GGNs in Hospital Employees and Their Parents

In total, the GGN-detection rate was significantly greater in employee group than parent group (24.78% vs 10.80%, P <0.001). The detection rate was significantly greater in female than male both in employees group and parents group, and the proportion of female was bigger than that in parents' group (P < 0.001). There were more non-smokers in employees than in parents' group (P <0.001). There were more pure-GGNs both in employees group and parents group. There were less participants with solitary GGN in employee group than parent group (68.62% vs 76.38%, P = 0.033). Besides, there were more large GGNs (≥10 mm) (25.19% vs 8.93%, P <0.001), LU-RADS 4 GGNs

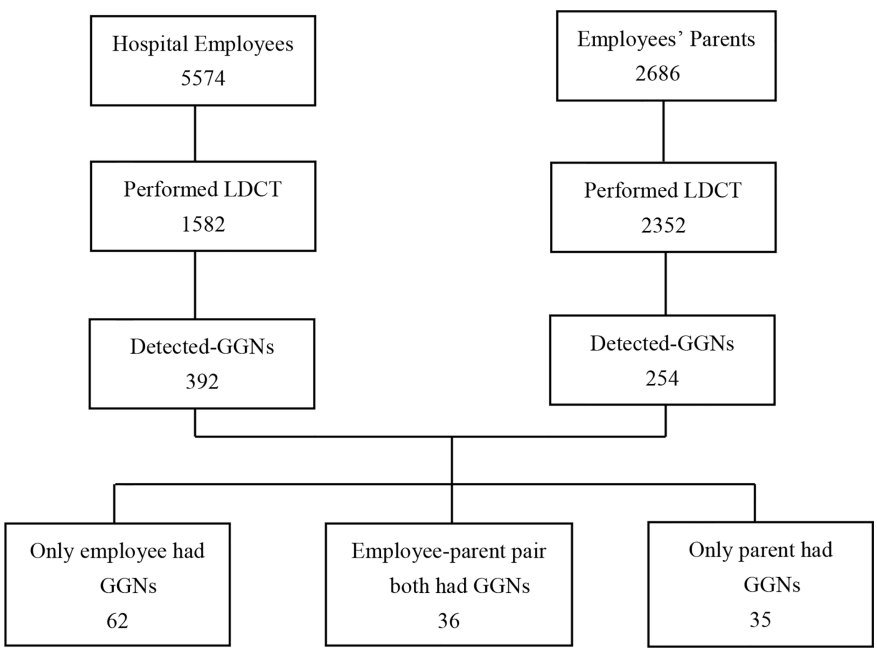

FIGURE 1 | Flowchart of the study analyzed the hospital employees and employee' parents performing LDCT as regular examination. LDCT, low-dose computed tomography; GGNs, ground-glass nodules.

TABLE 2 | Comparing characteristics of GGNs in employees with GGNs in parents.

Characteristics	GGNs of employees N, Rate (%)	GGNs of parents N, Rate (%)	*P* value
Total detection rate	392/1,582	254/2,352	<0.001
	(24.78)	(10.80)	
Gendar			<0.001
female	290 (73.98)	147 (57.87)	
male	102 (26.02)	107 (42.13)	
Smoking status			<0.001
non-smoker	349 (89.02)	195 (76.72)	
smoker	43 (10.98)	59 (23.28)	
Numbers			0.033
solitary	269(68.62)	194 (76.38)	
multiple	123(31.38)	60 (23.62)	
Density			0.949
pure GGNs	331 (84.44)	214 (84.25)	
part-solid nodules	61 (15.56)	40 (15.75)	
Size (mm)			
<5	107 (27.30)	45 (17.72)	
5–9	250 (63.77)	145 (57.09)	
≥10	35 (8.93)	64 (25.19)	<0.001
LU-RADS			
category 2	113(28.83)	52 (20.47)	
category 3	246(62.75)	150 (59.06)	
category 4	32 (8.16)	49 (19.29)	<0.001
category 4B	11 (2.81)	20 (7.87)	0.003
category 4C-5	14 (3.57)	25 (9.84)	0.001

(19.29% vs 8.16%, P <0.001) and LU-RADS 4B GGNs (7.87% vs 2.81%, P = 0.003), LU-RADS 4C-5 GGNs (9.84% vs 3.57%, P = 0.001) in parents' group than employees group (**Table 2**).

There were 36 pairs (27.07%) had GGNs, among 133 pairs of employees and their mother/father both performed LDCT. There were more female than male employees in those pairs (75%). GGNs in employees were smaller than their parents (6.11 ± 0.62 vs 11.42 ± 1.38, F = 35, P <0.001), and the LU-RADS categories were lower in employees than their parents (2.64 ± 0.11 vs 3.22 ± 0.14, F = 35, P = 0.001). The rate of multiple GGNs was 36.11% in employees and 33.33% in parents among the pairs. However, there was no significant difference in the density of nodules in employees and their parents, neither in gender (**Table 3**, **Figures 1**, **2**).

Sixty-two employees-only had GGNs but their parent did not. Among them, 80.65%(50/62)were female, 91.94% (57/62) had pure-GGN, and 72.58% (45/62) were solitary GGN. However, only 1 of 62 (1.6%) had GGN ≥10 mm and 2 of 62 (3.2%) were classified as LU-RADS 4. Compared these 62 employees with those employees in 36 employee–parent pairs group, there were no significant difference in the age, gender, and density, number, size, LU-RADS category of GGNs (*P* >0.05) (**Table 3**, **Figure 1**).

Thirty-five parents-only had GGNs but their son/daughter did not. Among them, 74.29% (26/35) were mothers, 85.71% (30/35) had pure-GGN and 62.86% (22/35) were solitary GGN. However, 6 of 35 (17.14%) had GGNS ≥10 mm, and 4 of 35 (11.43%) were classified as LU-RADS 4. Compared these 35

TABLE 3 | Comparing age, gender, and characteristics of GGNs among three groups in 133 pairs of employees and their parent both performed CT.

Characteristics	GGNs of employee-only group N (%)	Employee-parent pair group		GGNs of parent-only group N (%)
		GGNs of employees N (%)	GGNs of parents N (%)	
Age	46.37 ± 0.63	45.47 ± 0.74	73.22 ± 0.95	69.80 ± 0.94
P	0.372	/		0.012
Gender				
female	50 (80.65)	27 (75.00)	19 (52.78)	26 (74.29)
male	12 (19.35)	9 (25.00)	17 (47.22)	9 (25.71)
P	0.511	0.05		0.06
Numbers				
solitary	45 (72.58)	23 (63.89)	24 (66.67)	22 (62.86)
multiple	17 (27.42)	13 (36.11)	12 (33.33)	13 (37.14)
P	0.368	0.804		0.737
Density				
pure GGN	57 (91.94)	31 (86.11)	29 (80.56)	30 (85.71)
part-solid nodules	5 (8.06)	5 (13.89)	7 (19.44)	5 (14.29)
P	0.358	0.527		0.562
Size (mm)				
<5	22 (35.48)	10 (27.78)	5 (13.89)	6 (17.14)
5–9	39 (62.90)	24 (66.67)	17 (47.22)	23 (65.72)
≥10	1 (1.62)	2 (5.55)	14 (38.89)	6 (17.14)
P	0.109	<0.001		0.042
LU-RADS				
category 2	22 (35.48)	16 (44.45)	7 (19.44)	6 (17.14)
category 3	38 (61.29)	17 (47.22)	16 (44.44)	25 (71.43)
category 4	2 (3.23)	3 (8.33)	11 (30.56)	4 (11.43)
category 4B	1(1.61)	1(2.78)	3(8.33)	3(8.57)
category 4C-5	0	1(2.78)	8(22.22)	1(2.86)
P	0.75	0.001		0.015
Total	62 (100)	36 (100)	36 (100)	35 (100)

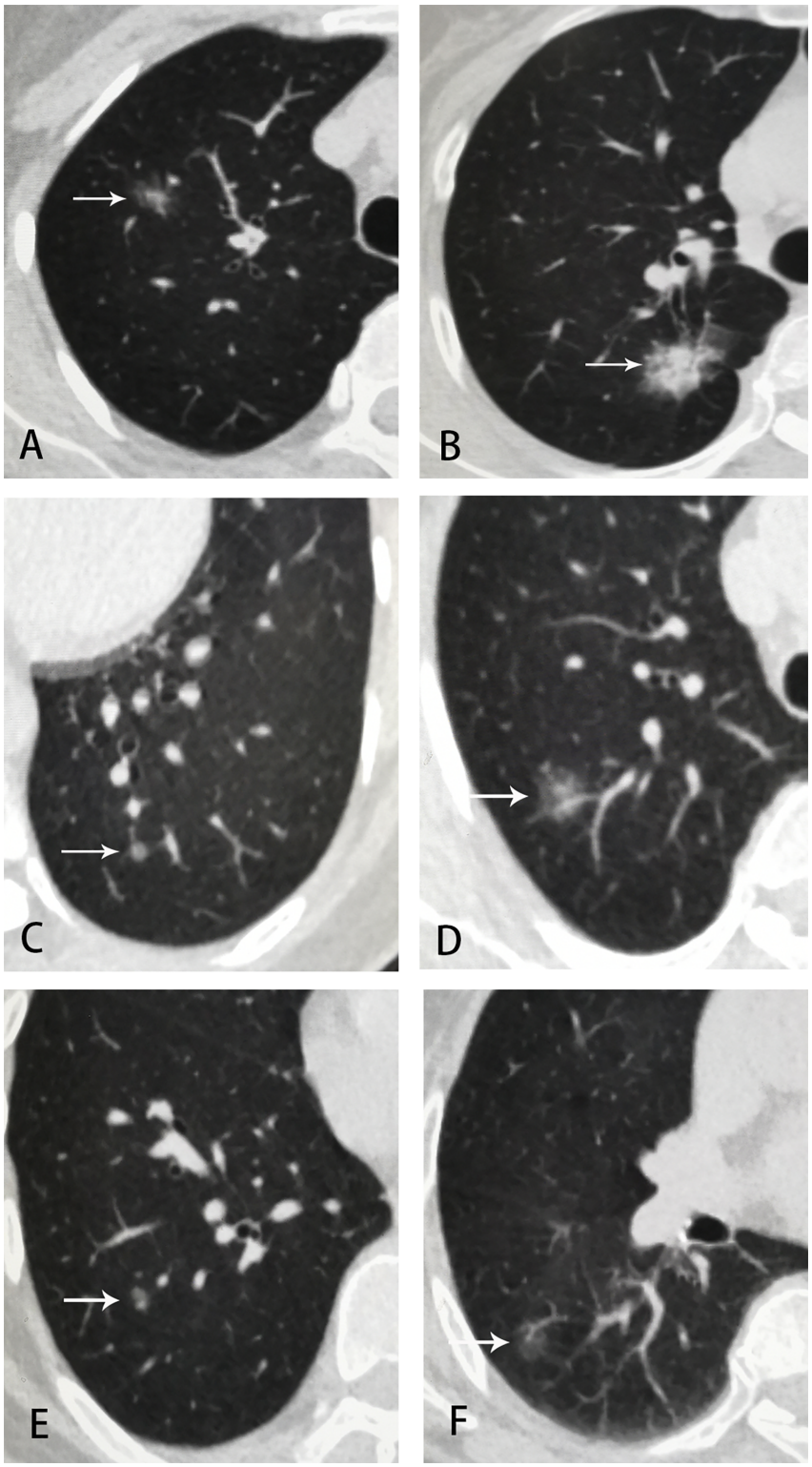

FIGURE 2 | Examples of GGNs in employee-parent pair groups. **(A)** employee 1, female, 42 y, part-solid nodule at right upper lobe, 15 × 10 mm, LU-RADS 4C; **(B)** employee 1's mother, 67 y, part-solid nodule at right upper lobe, 25 × 18 mm, LU-RADS 5; **(C)** employee 2, female, 51 y, pure-GGN at left lower lobe, 5 mm, LU-RADS 3; **(D)** employee 2's mother, 73 y, part-solid nodule at right upper lobe, 13mm, LU-RADS 4C; **(E)** employee 3, male, 51 y, pure-GGN at right lower lobe, 6 mm, LU-RADS 3; **(F)** employee 3's mother, 79 y, pure-GGN at right lower lobe, 14 × 9 mm, LU-RADS 4B.

parents with those parents in 36 employee–parent pairs group, parents were older (P = 0.012) in latter group and there were more large GGNs (P = 0.042) and LU-RADS 4-5 nodules (P = 0.015) (**Table 3**, **Figure 1**).

DISCUSSION

Due to the application of LDCT screening for early stage lung cancer, the number of lung cancer appeared as GGO or GGN is increasing. GGO/GGN is a non-specific radiologic finding, can caused by inflammation or neoplastic proliferation and so on. In Asia, GGO nodules were detected in 7.5% of 2,255 asymptomatic Korean adults (6), and 28.69% of 1,279 LDCT positive participants in a screening program in Taiwan China (7). In our study, the proportion of GGN detected using screening CT was 24.78% in employees group and 10.80% in parents' group. The different detection rates among studies are probably due to different calculation methods, population ages and performing methods. In the study in Korean, participants were above 45 years old and CT machines with 5-mm thickness with 4-mm intervals were used. However, in the study in Taiwan participants were 19–86 years old and nodule >4 mm in diameter was identified as positive, all CT scans were performed on thin-slice (0.625 mm) machines.

As the age of participants increasing, Zhang et al. showed the lung cancer detection rate were increasing gradually in the "age ≤40 years", "40 < age ≤ 55 years" and "age >55 years" group, respectively (2). However, we found no significantly increasing of GGN-detection rate as age increasing, the most significant rate was in group "41 to 60 years", but there were more large, high-grade nodules representing high risk of malignancy in the older-group. Our findings showed age was a key factor for risk of malignance consistent with Zhang's study. Besides, Li et al. found the average age at diagnosis had significantly decreased from 66.40 to 59.06 in the past two decades using a cumulative meta-analysis (8).

Many authoritative guidelines proposed heavy smoking history as the key factor for risk assessment of lung cancer, that meant most female would not be eligible for lung cancer screening. However, more and more studies showed the proportion of female non-smokers with lung cancer was increasing in recent years, especially in East Asia. She et al. found 587 (65%) of 898 cases with solitary pure GGNs pathologically confirmed as lung adenocarcinoma were female in Shanghai, China (9). Hattori et al. from Japan evaluated 616 surgically resected clinical N0M0 non-small cell lung cancers and found the rate of female was 62% (10). A study in Korea showed 162 (56%) female of 288 patients (non-smoker 68.1%) with lung adenocarcinoma proven by surgery and which appeared as GGNs (11). In our study, the detection rate was significantly greater in female than male either in employee group (non-smokers, 89.02%) or parent group (non-smokers, 76.72%), and in each age group as well. Our study was completely consistent with these researches, as for reasons of these findings are still ambiguous. It may be related to genetic susceptibility (such as EGFR high mutation rate) (12), estrogen and receptors (13), air pollution indoor (such as second-hand smoking or cooking) (14, 15), and history of lung diseases, however further investigation is need to be conducted. As for non-smokers, especially female in Asian, it's worthy to determine high-risk factors for lung cancer about them based on those possible causes above. Maybe there should be a new adjusted screening criterion for this population, so as to achieve early effective diagnosis and treatment of lung cancer.

In our study, there were 27% employee–parent pair had GGNs at the same time. This result reminded us GGNs may be related to genetic factors, family environment and living habits as well. In recent decades, many researches showed consistently that family history is important etiology for cancers especially lung cancer. Ooi et al. (16) found that the risk of lung cancer in patients with a family history of lung cancer was 2.4 times compared with those without family history. Guo et al. (17) showed the risk of lung cancer in the first-degree relatives of lung cancer patients was about seven times higher than that of healthy people. However, there are a few studies on genetics, family history and living habits about GGNs currently. Because most GGNs remain on follow and few participants have received resection, we have no more genetic information between them to date.

As for lung cancer, genetics had been proved to be a key etiology, but it remains uncertain about family history and living habits. Therefore, the potential relevance of employee-parent pairs is worthy for us to follow on.

Furthermore, former studies discovered first-degree female relatives was a stronger predictor than first-degree male relatives for lung cancer, and a first degree family member with cancer diagnosis before age 50 were associated with increased lung cancer risk, especially among never smokers (18–21). In our research, there were more female (75%) than male employees detected GGNs when their parents had GGNs too, and all of them were non-smokers. It may indicate that female non-smokers are more likely to obtain genetic susceptibility of GGNs from parents. In addition, we found GGNs in employees were less and lower-grade than nodules in their parents among the 36 employee–parent pairs. We speculated nodules in employees would be at earlier stage and grow into nodules like their parents' when they get old. We also found GGNs of parents in employee-parent pair group were larger and higher-grade than GGNs of parent-only. Whether it suggested that larger and more suspicious nodules were more likely to be passed on to offspring need further research.

CONCLUSION

Our study retrospectively analyzed LDCT-detected GGNs among employees and parents. Among the employees and parents who had ground glass nodules, 1/4 of them both detected GGNs. Although the detection rate of GGNs in the parent group was lower than that in the employee group, the grade of nodules was significantly higher. All these suggest that the occurrence and development of ground glass nodules may be related to genetic factors.

DATA AVAILABILITY STATEMENT

The original contributions presented in the study are included in the article/supplementary material. Further inquiries can be directed to the corresponding author.

ETHICS STATEMENT

The studies involving human participants were reviewed and approved by the Centre for Medical Ethics of Xiangya Medical College of Central South University. The patients/participants provided their written informed consent to participate in this study.

AUTHOR CONTRIBUTIONS

BO mainly finished the research data processing, chart production, and article writing. MaL, LL, and SL helped collect clinical information. MiL mainly designed the research, participated in the discussion about the results, and revised the draft. All authors contributed to the article and approved the submitted version.

ACKNOWLEDGMENTS

This investigation was supported by National Multidisciplinary Cooperative Diagnosis and Treatment Capacity Building Project for Major Diseases (Lung Cancer).

REFERENCES

1. Yankelevitz DF, Yip R, Smith JP, Liang M, Liu Y, Xu DM, et al. CT Screening for Lung Cancer: Nonsolid Nodules in Baseline and Annual Repeat Rounds. *Radiology* (2015) 277(2):555–64. doi: 10.1148/radiol.2015142554
2. Henschke CI, Yip R, Smith JP, Wolf AS, Flores RM, Liang M, et al. CT Screening for Lung Cancer: Part-Solid Nodules in Baseline and Annual Repeat Rounds. *AJR Am J Roentgenol* (2016) 207(6):1176–84. doi: 10.2214/AJR.16.16043
3. Zhang Y, Jheon S, Li H, Zhang H, Xie Y, Qian B, et al. Results of low-dose computed tomography as a regular health examination among chinese hospital employees. *J Thoracic Cardiovasc Surg* (2020) 16(3):824–31. doi: 10.1016/j.jtcvs.2019.10.145
4. Hansell DM, Bankier AA, MacMahon H, McLoud TC, Müller NL, Remy J. Fleischner Society: glossary of terms for thoracic imaging. *Radiology* (2008) 246(3):697–722. doi: 10.1148/radiol.2462070712
5. Manos D, Seely JM, Taylor J, Borgaonkar J, Roberts HC, Mayo JR. The Lung Reporting and Data System (LU-RADS): a proposal for computed tomography screening. *Can Assoc Radiol J* (2014) 65(2):121–34. doi: 10.1016/j.carj.2014.03.004
6. Chong S, Lee KS, Chung MJ, Kim TS, Kim H, Kwon OJ, et al. Lung cancer screening with low-dose helical ct in korea: Experiences at the samsung medical center. *J Korean Med Sci* (2005) 20(3):402–8. doi: 10.3346/jkms.2005.20.3.402
7. Chen CY, Chen CH, Shen TC, Cheng WC, Hsu CN, Liao CH, et al. Lung cancer screening with low-dose computed tomography: Experiences from a tertiary hospital in Taiwan. *J Formos Med Assoc* (2016) 115(3):163–70. doi: 10.1016/j.jfma.2015.11.007
8. Li X, Ren F, Wang S, He Z, Song Z, Chen J, et al. The Epidemiology of Ground Glass Opacity Lung Adenocarcinoma: A Network-Based Cumulative Meta-Analysis. *Front Oncol* (2020) 10:1059. doi: 10.3389/fonc.2020.01059
9. She Y, Zhao L, Dai C, Ren Y, Zha J, Xie H, et al. Preoperative nomogram for identifying invasive pulmonary adenocarcinoma in patients with pure ground-glass nodule: A multi-institutional study. *Oncotarget* (2017) 8 (10):17229–38. doi: 10.18632/oncotarget.11236
10. Hattori A, Matsunaga T, Takamochi K, Oh S, Suzuki K. Neither Maximum Tumor Size nor Solid Component Size Is Prognostic in Part-Solid Lung Cancer: Impact of Tumor Size Should Be Applied Exclusively to Solid Lung Cancer. *Ann Thorac Surg* (2016) 102(2):407–15. doi: 10.1016/j.athoracsur.2016.02.074
11. Choi SH, Chae EJ, Shin SY, Kim EY, Kim JE, Lee HJ, et al. Comparisons of clinical outcomes in patients with and without a preoperative tissue diagnosis in the persistent malignant-looking, ground-glass-opacity nodules. *Med (Baltimore)* (2016) 95(34):e4359. doi: 10.1097/MD.0000000000004359
12. Steuer CE, Behera M, Berry L, Kim S, Rossi M, Sica G, et al. Role of race in oncogenic driver prevalence and outcomes in lung adenocarcinoma: Results from the lung cancer mutation consortium[J]. *Cancer* (2016) 122(5):766–72. doi: 10.1002/cncr.29812
13. Sun S, Schiller JH, Gazdar AF. Lung cancer in never smokers-a different disease[J]. *Nat Rev Cancer* (2007) 7(10):778–90. doi: 10.1038/nrc2190
14. Li W, Tse LA, Au JSK, Wang F, Qiu H, Yu IT. Secondhand smoke enhances lung cancer risk in male smokers: An interaction[J]. *Nicotine Tob Res* (2016) 18(11):2057–64. doi: 10.1093/ntr/ntw115
15. Chen HC, Wu CE, Chong IW, Wu MT. Exposure to cooking oil fumes and chronic bronchitis in nonsmoking women aged 40 years and over: a health-care based study[J]. *BMC Public Health* (2018) 18(1):246. doi: 10.1186/s12889-018-5146-x
16. Ooi WL, Elston RC, Chen VW, Bailey-Wilson JE, Rothschild H. Increased familial risk for lung cancer. *J Natl Cancer Inst* (1986) 76(2):217–22.
17. Guo ZR, Lu QX. A exploration on aggregation factors of lung cancer[J]. *Hereditas* (1987) 1:32–5.
18. Wu PF, Lee CH, Wang MJ, Goggins WB, Chiang TA, Huang MS. Cancer aggregation and complex segregation analysis of families with female non-smoking lung cancer probands in Taiwan. *Eur J Cancer* (2004) 40(2):260–6. doi: 10.1016/j.ejca.2003.08.021
19. Gao Y, Goldstein AM, Consonni D, Pesatori AC, Wacholder S, Tucker MA, et al. Family history of cancer and nonmalignant lung diseases as risk factors for lung cancer. *Int J Cancer* (2009) 125(1):146–52. doi: 10.1002/ijc.24283
20. Brenner DR, Hung RJ, Tsao MS, Shepherd FA, Johnston MR, Narod S, et al. Lung cancer risk in never-smokers: a population-based case-control study of epidemiologic risk factors. *BMC Cancer* (2010) 10(14):285. doi: 10.1186/1471-2407-10-285
21. Lin H, Huang YS, Yan HH, Yang XN, Zhong WZ, Ye HW, et al. A family history of cancer and lung cancer risk in never-smokers: A clinic-based case-control study. *Lung Cancer* (2015) 89(2):94–8. doi: 10.1016/j.lungcan.2015.05.017

Conflict of Interest: The authors declare that the research was conducted in the absence of any commercial or financial relationships that could be construed as a potential conflict of interest.

The handling editor declared a shared affiliation with with several of the authors MaL, LL, SL, and MiL at time of review.

frontiers in Oncology

ORIGINAL RESEARCH
published: 24 May 2021
doi: 10.3389/fonc.2021.653988

Molecular Identification and Genetic Characterization of Early-Stage Multiple Primary Lung Cancer by Large-Panel Next-Generation Sequencing Analysis

*Guotian Pei[1], Mingwei Li[2], Xianjun Min[1], Qiang Liu[1], Dasheng Li[3], Yingshun Yang[1], Shuai Wang[1], Xiaoyu Wang[1], Huina Wang[2], Huanqing Cheng[2], Shanbo Cao[2] and Yuqing Huang[1]**

[1] Department of Thoracic Surgery, Beijing Haidian Hospital, Beijing, China, [2] Department of Medicine, Acornmed Biotechnology Co., Ltd, Beijing, China, [3] Department of Radiology, Beijing Haidian Hospital, Beijing, China

OPEN ACCESS

Edited by:
Kezhong Chen,
Peking University People's Hospital, China

Reviewed by:
Jianchun Duan,
Chinese Academy of Medical Sciences and Peking Union Medical College, China
Xiaochun Zhang,
The Affiliated Hospital of Qingdao University, China

***Correspondence:**
Yuqing Huang
huangyuqing555@gmail.com

Specialty section:
This article was submitted to Thoracic Oncology, a section of the journal Frontiers in Oncology

Received: 15 January 2021
Accepted: 23 April 2021
Published: 24 May 2021

Citation:
Pei G, Li M, Min X, Liu Q, Li D, Yang Y, Wang S, Wang X, Wang H, Cheng H, Cao S and Huang Y (2021) Molecular Identification and Genetic Characterization of Early-Stage Multiple Primary Lung Cancer by Large-Panel Next-Generation Sequencing Analysis. Front. Oncol. 11:653988. doi: 10.3389/fonc.2021.653988

Objective: The incidence of early stage multiple primary lung cancer (MPLC) has been increasing in recent years, while the ideal strategy for its diagnosis and treatment remains controversial. The present study conducted genomic analysis to identify a new molecular classification method for accurately predicting the diagnosis and therapy for patients with early stage MPLC.

Methods: A total of 240 tissue samples from 203 patients with multiple-non-small-cell lung cancers (NSCLCs) (n = 30), early stage single-NSCLC (Group A, n = 94), and advanced-stage NSCLC (Group B, n = 79) were subjected to targeted multigene panel sequencing.

Results: Thirty patients for whom next-generation sequencing was performed on >1 tumor were identified, yielding 45 tumor pairs. The frequencies of *EGFR, TP53, RBM10, ERBB2*, and *CDKN2A* mutations exhibited significant differences between early and advanced-stage NSCLCs. The prevalence of the *EGFR L858R* mutation in early stage NSCLC was remarkably higher than that in advanced-stage NSCLC (P = 0.047). The molecular method classified tumor pairs into 26 definite MPLC tumors and four intrapulmonary metastasis (IM) tumors. A high rate of discordance in driver genetic alterations was found in the different tumor lesions of MPLC patients. The prospective Martini histologic prediction of MPLC was discordant with the molecular method for three patients (16.7%), particularly in the prediction of IM (91.7% discordant).

Conclusions: Comprehensive molecular evaluation allows the unambiguous delineation of clonal relationships among tumors. In comparison, the Martini and Melamed criteria have notable limitations in the recognition of IM. Our results support the adoption of a large

panel to supplement histology for strongly discriminating NSCLC clonal relationships in clinical practice.

Keywords: early-stage multiple primary lung cancer, multigene sequencing, molecular classification, genetic characterization, epidermal growth factor receptor (EGFR), *L858R*, clonal relationships

INTRODUCTION

Multiple primary lung cancer (MPLC) refers to the synchronous or metachronous occurrence of two or more primary malignant tumors in the lungs of an individual patient and can be further divided into synchronous MPLC (sMPLC) and metachronous MPLC (mMPLC), the latter of which is defined by a diagnosis interval of 6 months between tumors (1). In 1924, Beyreuther first described cases of "double primary lung cancer" and introduced the concept of MPLC (2). MPLC is believed to be a rare disease. However, recent clinical evidence has shown that the incidence of MPLC has been increasing, which may be attributed to advances in chest computed tomography (CT) and increased awareness among clinicians regarding MPLC screening (3). Therefore, higher-accuracy diagnostic methods and better treatment options for MPLC are urgently needed. Multinodular lesions are usually observed in approximately 16% of patients with operable stage I, II, and III non-small-cell lung cancer (NSCLC) by preoperative imaging analysis (4). Overall, MPLC accounts for 1–8% of all multinodular lesions according to a recent report (5), and adenocarcinoma accounts for 86.5% of multinodular lesions, which may be related to the higher incidence of lung adenocarcinoma (6). Chang et al. reported that the upper lobes of both lungs are prone to MPLC, and multiple lesions have the same pathological type in 50–70% of patients (7).

In 1975, Martini and Melamed proposed some criteria for differentiating multiple primary lung tumors from pulmonary metastatic tumors (8). However, this empirical classification does not include molecular analysis and cannot fully identify the link between multiple tumors. The histological characteristics of multiple tumors often overlap in lung cancer, especially in adenocarcinoma (9). Therefore, it is challenging to distinguish multiple primary tumors and multiple intrapulmonary metastases in the absence of molecular characteristics. Currently, intratumor heterogeneity is often interpreted using the trunk-branch model (10). In this model, trunk gene mutations drive tumor growth in each subcloning and tumor region. As the disease progresses, branch gene mutations occur heterogeneously in primary lesions and/or metastases and may induce intratumor heterogeneity. Based on this theory, lesions with multiple identical mutations could originate from the same clone. Numerous studies have shown that mutations in certain proto-oncogenes and cancer suppressor genes, such as *EGFR*, *KRAS*, and *BRAF*, can be used as molecular markers in multiple lung cancers (11, 12). However, only a few hotspot cancer driver gene mutations have been analyzed, and these mutation hotspots are not sufficiently reliable to analyze the differentiation of MPLC and intrapulmonary metastasis (IM).

Recently, numerous studies thoroughly investigated the genomic changes and clonal structures of advanced lung tumors (13, 14). However, there are relatively few reports regarding the genomic characteristics of early stage NSCLC, especially the molecular clonal relationship among tumors in patients thus far. Therefore, we adopted next-generation sequencing (NGS) to detect multiple cancer-related genes in multiple lung cancer (MLC) using tumor samples obtained *via* surgical resection and compared the identification-based molecular mutation spectrum with the histopathological evaluation of the tumors. Importantly, the genomic characterizations of early stage MPLC were comprehensively defined by comparing early stage NSCLC and advanced-stage NSCLC.

MATERIALS AND METHODS

Patient Enrolment

The subjects were patients with multiple NSCLC who underwent surgical resection synchronously or metachronously at the Department of Thoracic Surgery of Beijing Haidian Hospital between September 2017 and December 2019. Patients who received neoadjuvant therapy and had extrathoracic metastases were excluded (**Figure 1**). A total of 67 surgical specimens sufficient for histological and molecular analyses were obtained from 30 patients who had more than one tumor and were eligible for selection in this study. Synchronous tumors, or metachronous tumors, were defined by a diagnosis interval of 6 months or less. All patients underwent a chest CT scan before the surgery. Meanwhile, 94 patients who underwent surgical resection with early stage (IA stage) disease were enrolled in Group A, and 79 specimens were obtained using ultrasound-guided transbronchial needle aspiration from 79 patients who had advanced lung cancer and were allocated to Group B. The study was approved by the Medical Ethics Committee of Beijing Haidian Hospital (No. 2020-041), and individual consent for this retrospective analysis was waived.

Criteria of Martini and Melamed

According to the Martini and Melamed criteria published in 1975 (8), multiple NSCLCs are classified into MPLC by histological type and clinical data. If they presented with similar histological types, different anatomical distributions,

Abbreviations: MPLC, multiple primary lung cancer; MLC, multiple lung cancer; sMPLC, synchronous MPLC; mMPLC, metachronous MPLC; CT, computed tomography; NSCLC, non-small-cell lung cancer; IM, intrapulmonary metastasis; NGS, next-generation sequencing; TMB, tumor mutational burden; IAC, invasive adenocarcinoma; AIS, adenocarcinoma *in situ*; MIA, minimally invasive adenocarcinoma; MA, Mucinous adenocarcinoma; GGO, ground-glass opacity; GGN, ground-glass nodule.

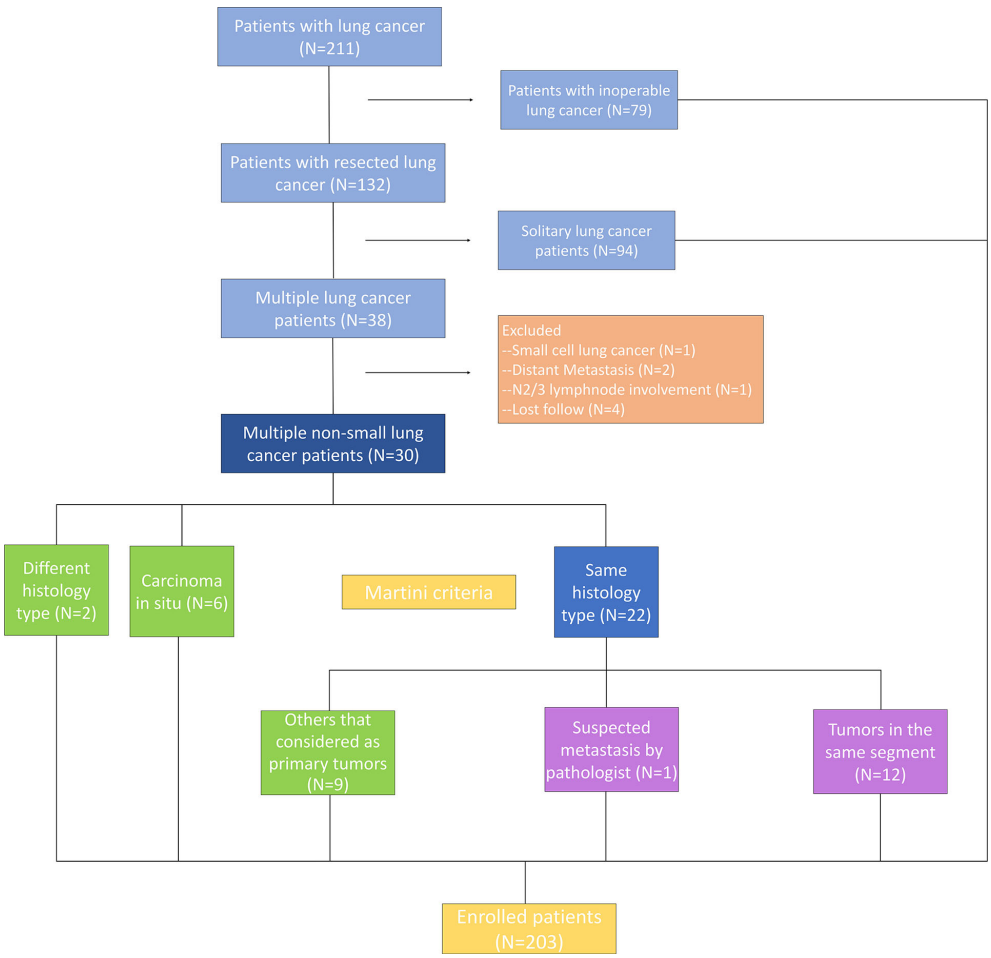

FIGURE 1 | The flowchart of the patients' inclusion criteria.

different origins of carcinoma *in situ*, long intervals, and no lymphatic or systemic metastasis in different segments, synchronous tumors are classified as MPLC. If the diagnosis interval was more than two years, metachronous tumors are classified as MPLC. Histologic assessment of tumor relatedness was performed by experienced thoracic pathologists.

Targeted Multigene Panel Sequencing

For each tumor, DNA was extracted from the formalin-fixed paraffin-embedded block containing the highest percentage of tumor cells. DNA extraction and NGS analysis were performed by using an Acornmed panel targeting 808 cancer-related hotspot genes that provided data on non-synonymous somatic mutations, copy number alterations, small insertions or deletions, copy number variants and rearrangements. This analysis focused on targetable genetic alterations annotated by categories of evidence Levels 1–3 and Level R1 in OncoKB (Memorial Sloan Kettering Cancer Center, New York, NY, http://oncokb.org/). Synonymous mutations are detected and maintained in the database but not clinically reported.

Tissue DNA was extracted using an QIAamp Genomic DNA Kit (Qiagen GmbH). Quality and quantification of the DNA were measured using an Agilent 2100 BioAnalyzer (Agilent Technologies, Inc.) and a Qubit ds DNA HS detection kit (Thermo Fisher Scientific, Inc.). Various libraries were hybridized with the 808-gene panel that contained coding regions and introns. The target-enriched libraries were pooled and sequenced on an Illumina HiSeq2500 NGS platform. The quality criteria used as endpoints were a detection threshold of 5% and an average coverage depth of 10,000×. The genome data were processed with the relevant bioinformatics platform to identify multiple types of gene mutations. By analysing somatic mutations, including coding base substitution and fragment insertion and deletion, the tumor mutational burden (TMB) was estimated as the number of mutations per million bases.

Statistical Analyses

GraphPad Prism and SPSS were used for statistical analysis. Differences in continuous variables were assessed using unpaired t-tests. Fisher's exact test or $\chi 2$ test was used to analyze the

association of clinical characteristics, genetic characteristics, and molecular markers of immunotherapy between different groups. A two-sided P <0.05 was considered to be statistically significant.

RESULTS

Clinical Characteristics of Patients With MLC

We identified a total of thirty patients with NGS performed on >1 resected NSCLC tumor. The proportions of females, non-smokers, and patients with adenocarcinomas were 71.3, 80.0, and 100%, respectively. The median age was 60 years (range, 46–82 years). For 22 patients (73.3%), all the tumors were located on the same side. Twenty-four patients had two tumors, five patients had three tumors, and one patient had four tumors, for a total of 67 individual tumors. Most of the tumors were detected at early stages, including 25 foci (37.3%) at stage IA1. The maximum diameter of 34 tumors was ≤10 millimetres (50.8%). Invasive adenocarcinoma (IAC) (n = 34) and minimally invasive adenocarcinoma (MIA) (n = 21) were the main pathological types. Imaging examination showed that there were 16 tumors with pure ground-glass opacity (GGO) and 30 tumors with mixed-density ground-glass nodules (GGNs) (**Table 1**). Clinically, either all patients were considered to have separate primary tumors or the relationship of the tumors was uncertain at the time of surgery; none of the patients was known to have IM prior to surgery.

TABLE 1 | Clinical and radiological characteristics of 30 patients with MLC.

Patient characteristics (N = 30)	Number (%)
Sex, n (%)	
Male	8 (28.7%)
Female	22 (71.3%)
Age (year), y (range)	
Median	60
Range	41–78
≤60	15 (50.0%)
>60	15 (50.0%)
Smoking history, n (%)	
Yes	6 (20.0%)
No	24 (80.0%)
Tumor chronology, n (%)	
Synchronous	25 (83.3%)
Metachronous	5 (16.7%)
Tumor distribution, n (%)	
Ipsilateral (same lobe)	11 (36.7%)
Ipsilateral (different lobe)	11 (36.7%)
Contralateral	8 (26.7%)
Tumor characteristics (n = 67)	
Stage*, n (%)	
AAH	1 (1.5%)
0	5 (7.46%)
IA1	25 (37.3%)
IA2	15 (22.4%)
IA3	6 (9.0%)
IB	1 (1.5%)
IIB	12 (17.9%)
IV	2 (3.0%)
Histology, n (%)	
AAH	1 (1.5%)
AIS	5 (7.5%)
MIA	21 (31.3%)
IAC	34 (50.7%)
SCC	3 (4.5%)
MA	3 (4.5%)
Side, n (%)	
Left	22 (32.8%)
Right	45 (67.2%)
Maximum diameter, mm (range)	
Median	9.4
Range	2.5–40
≤6	14 (20.9%)
6-10	20 (29.9%)
10-20	22 (32.8%)
>20	11 (16.4%)
Radiological feature	
Solid	20 (29.9%)
Subsolid	30 (44.8%)
pGGO	16 (23.9%)
Thin-walled cavity	1 (1.5%)

At primary surgery according to the International Union Against Cancer (UICC) eighth TNM staging.

MLC, multiple lung cancer; AAH, atypical adenomatous hyperplasia; AIS, adenocarcinoma in situ; MIA, minimally invasive adenocarcinoma; IAC, invasive adenocarcinoma; SCC, squamous-cell carcinoma; MA, Mucinous adenocarcinoma; pGGO, pure ground-glass opacity.

Tumor Molecular Characteristics

Overall, a total of 542 mutations were detected in these 67 tumors. Major oncogenic driver alterations were identified from 59 out of 67 (88.06%) tumors, and at least two mutations were detected in 80.6% (54/67) of specimens. The most commonly mutated genes were *EGFR* (63%, including 23 patients with *EGFR L858R*, 12 with exon 19 deletions, and seven with rare mutations), *TP53* (18%), *KRAS* (15%), *RBM10* (13%), *MDC1* (13%), *BRAF* (12%), and *KMT2D* (12%) (**Figure 2**). Moreover, *ALK* fusion was observed in two patients, and *ROS1* fusion was seen in one patient. Only one lesion had two concomitant driver mutations. Gene amplification (*e.g.*, *EGFR, TERT, MYC*, and *ERBB2*) was identified in tumor samples from 10 patients but was present only in paired tumors for one patient (**Figure 2**).

Comparison of Genomic Characterization Among Early Stage and Advanced-Stage NSCLC

Since most MPLCs are early stage, the molecular characteristics of early stage lung cancer help identify the clonal relationship between different primary tumors. To comprehensively investigate the genomic characterization of stage IA lung cancer, 94 patients (Group A) with early stage NSCLC and 79 patients with advanced-stage NSCLC (Group B) were included in the study. A comparative analysis of the two groups was further performed. The clinical characteristics of Groups A and B are shown in **Tables S1** and **S2**, respectively. Moreover, sex, smoking history, and pathological type were significantly different between Groups A and B (**Table S3**).

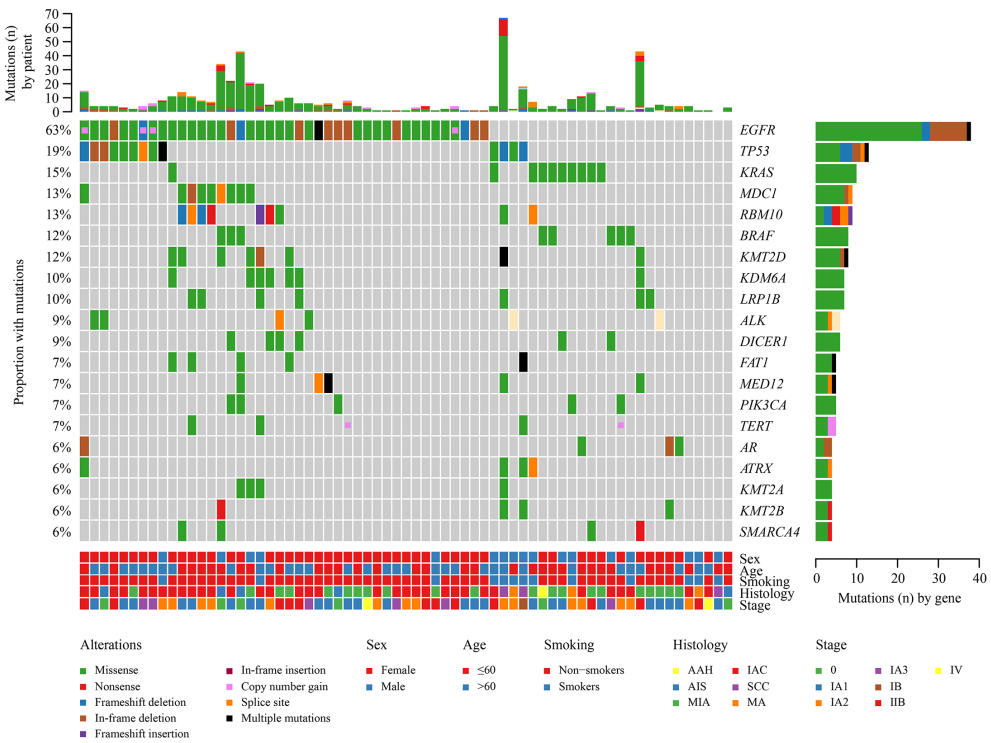

FIGURE 2 | Landscape of genomic alterations in 67 multiple lung cancer samples. Genetic mutations were identified by targeted next-generation sequencing in the tumor tissues of the patients. The upper panel shows the numbers of non-synonymous single-nucleotide variants, small insertions or deletions, and copy number variants in each tumor. The heat map below shows the genes with somatic mutations sorted according to the mutation frequency. Clinical features are annotated in the lower panel.

A total of 520 genomic mutations were identified in Group A. Frequently mutated genes included *EGFR* (56%), *TP53* (26%), *RBM10* (15%), *KRAS* (13%), and *KMT2C* (10%) (**Figure S1**). In Group B, a total of 873 genetic mutations were identified. *TP53* (62%) was the most commonly mutated gene, followed by *EGFR* (41%), *CDKN2A* (14%), *ERBB2* (14%), *KRAS* (13%), and *RB1* (11%). Among all the mutations, *ALK* fusion was observed in four patients, *ROS1* fusion in one patient, and *RET* fusion in two patients (**Figure S2**). Compared with those in advanced-stage NSCLC, significantly more genomic mutations in *EGFR* and *RBM10* ($P = 0.038$ and $P = 0.019$, respectively) and significantly fewer mutations in *TP53* and *CDKN2A* ($P < 0.0001$ and $P = 0.0001$, respectively) were identified in early stage MPLC (**Figure 3**). Furthermore, the TMB was evaluated among the patients based on the mutation data. Advanced-stage NSCLC showed a higher frequency of a high TMB than early stage NSCLC ($P = 0.001$) (**Figure 4**). According to the results, early stage NSCLC tended to exhibit a low TMB more often than advanced-stage NSCLC.

Comprehensive Analysis of *EGFR* Alterations

EGFR is the most commonly mutated gene in early lung cancer, and thus we further analyzed its subtypes. Among all *EGFR* mutations, the most common were *EGFR L858R* substitution and *exon 19 deletion* (*19Del*). The frequencies of different *EGFR* mutation types were compared between Groups A and B. For the *EGFR L858R* mutation, a remarkable difference between Groups A and B was identified ($P = 0.047$) (**Figure 5A**). However, for *EGFR 19Del*, no significant difference was observed between the two groups ($P = 0.2369$) (**Figure 5B**). Additionally, for other *EGFR* mutations (excluding *EGFR L858R* substitution and *19Del*), no striking difference between Groups A and B was observed (**Figure 5C**).

Clonality Assessment Based on Large Panel NGS Results

To determine the clonal relationship between two or more tumors, we compared somatic mutations and copy number alterations. **Table 2** summarizes the NGS-classified tumors among the patients as detailed below. Twenty-one patients (70%) exhibited inconsistent driver mutations and entirely unique mutation profiles in each tumor (**Figure S3**). These cases were classified as definite MPLC. Conversely, three patients (10%) shared driver mutations and additional multiple (≥2) non-synonymous somatic alterations (mean 5.3, up to 10). These cases were thus classified as definite IM. Compared with the number of shared mutations, the number of unique mutations in IM was substantially lower.

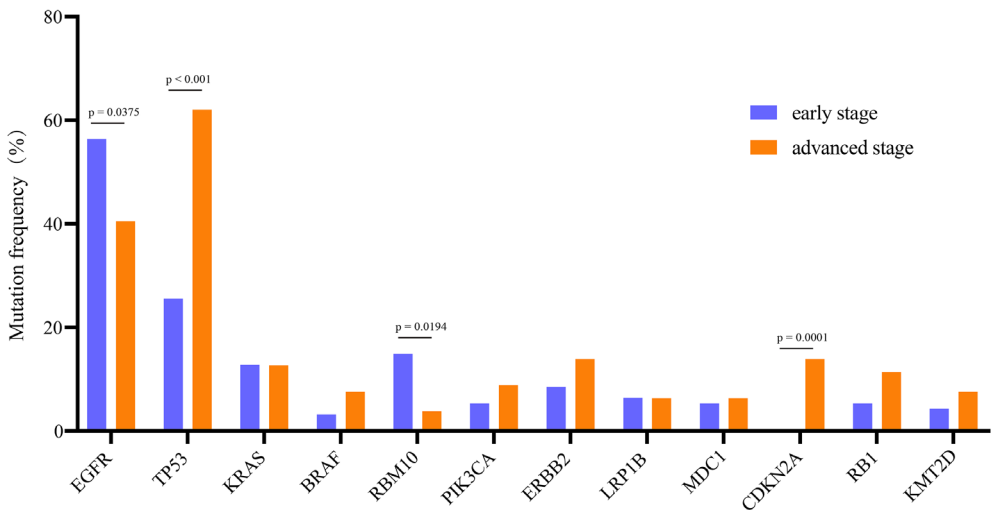

FIGURE 3 | Comparison of the prevalence of frequently mutated genes in early stage and advanced-stage NSCLCs. The commonly mutated genes are arranged in order on the horizontal axis. The vertical axis represents the mutation frequency obtained from a different cohort.

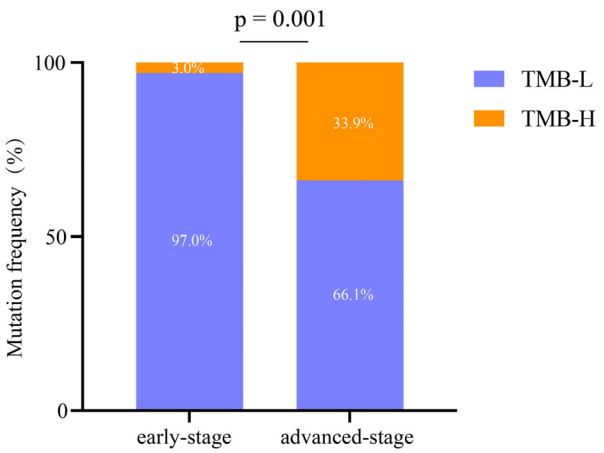

FIGURE 4 | Analysis of the characteristics of immunotherapy biomarkers in early stage and advanced-stage NSCLCs. TMB-H, high tumor mutation burden; TMB-L, low tumor mutation burden.

A total of seven patients (20%) shared single identical mutations (**Figures S4A, B**); their classification was adjudicated individually by extended molecular review. Six patients shared single *EGFR* hotspot mutations (*L858R* in five and *19Del* in one), and one patient shares an other/rare mutation (*TERT Amplification*); each tumor also harbored an abundance of unique mutations, ranging from four to 28 mutations per tumor, with no shared additional mutations.

Of those, five patients shared a single *EGFR L858R* driver mutation. Classification of those tumors as MPLC was supported by 1) the fair probability of coincidentally shared driver mutation; in particular, given the prevalence of *EGFR L858R* mutation in our population of 52%, the odds of coincidental occurrence of this mutation in two unrelated tumors was very high; and 2) the substantially higher unique/total mutation ratio (>75%) compared with definite IM in our series.

One other patient shared a single *TERT Amplification*. These tumors also harboured distinct *EGFR 19Del versus BRAF V601E* driver mutations plus multiple unique non-synonymous mutations in each tumor, resulting in a high-probability classification of MPLC with coincidental *TERT Amplification*.

Lastly, one patient shared a single *EGFR 19Del* mutation with one and five unique mutations per tumor. On manual review, all mutations had low VAF (<10%). Such findings indicated low tumor purity and the likelihood of the incomplete detection of mutations. Moreover, there was no significant difference in *EGFR 19Del* in early and advanced-stage NSCLC; thus, the tumor was classified as an unambiguous IM.

Therefore, we propose herein a molecular method for classifying patients as having MPLC or IM as *per* the analysis of multiple cancer-related gene somatic mutations and the molecular mutation characteristics of MPLC (**Figure 6**), which is described as follows: (1) MPLC can be identified when tumors have no mutation in common or when they had different driver-gene hotspot mutations (*EGFR*, *KRAS*, *BRAF*, *ERBB2*, *ALK*, *ROS1*, *MET*, or *RET*); (2) MPLC can be identified when an *EGFR L858R* mutation is the single consistent mutation between the lung cancer tumors in the patient; (3) IM can be identified when the same driver gene mutation (exclusive to *EGFR L858R*) is shared between tumors or when all alterations are common between the tumors in the patient; and (4) the tumor could not be classified if no mutation is detected in the tumor lesions. Then, the tumor should be classified separately based on the histopathological and clinical data.

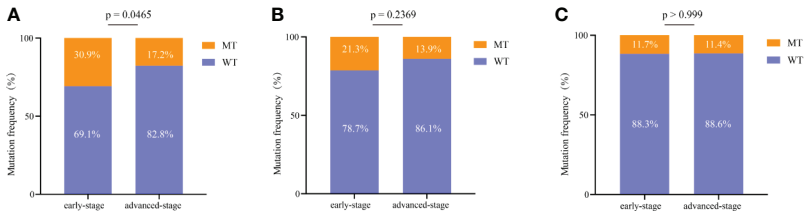

FIGURE 5 | Comprehensive analysis of *EGFR* mutations in early stage and advanced-stage NSCLC. **(A)** Comparison of the difference in the *EGFR L858R* mutation between the two groups. **(B)** Comparison of the difference in the *EGFR exon 19 deletion* between the two groups. **(C)** Comparison of the difference in the other *EGFR* mutations (excluding *EGFR L858R* substitution and *exon 19 deletion*) between the two groups. 19del, exon 19 deletion; WT, wild type; MT, mutation type.

TABLE 2 | Patients with MLC classified by the Martini and Melamed criteria and molecular methods.

Case No.	Martini & Melamed criteria	Mutational evaluation	Number of matching mutations	Matching genes
Martini and Melamed criteria-based MPLC cases (n = 18)				
1	MPLC	MPLC	0	–
2	MPLC	MPLC	0	–
3	MPLC	MPLC	0	–
6	MPLC	MPLC	0	–
7	MPLC	MPLC	0	–
10	MPLC	MPLC	0	–
12	MPLC	MPLC	1	*TERT Amplification*
13	MPLC	MPLC	0	–
15	MPLC	MPLC	0	–
20	MPLC	MPLC	1	*EGFR L858R*
21	MPLC	MPLC	0	–
24	MPLC	MPLC	0	–
25	MPLC	MPLC	0	–
26	MPLC	MPLC	0	–
27	MPLC	MPLC	0	–
9	MPLC	IM	4	*EGFR/ALK/ TP53/IKZF2*
29[a]	MPLC	IM	1	*EGFR L858R/ T790M*
30	MPLC	IM	1	*EGFR 19Del*
Martini & Melamed criteria-based IM cases (n = 12)				
4	IM	MPLC	0	–
5	IM	MPLC	0	–
11	IM	MPLC	0	–
14[a]	IM	MPLC	0	–
16	IM	MPLC	1	*EGFR L858R*
17[a]	IM	MPLC	1	*EGFR L858R*
18	IM	MPLC	0	–
19	IM	MPLC	0	–
22	IM	MPLC	0	–
23	IM	MPLC	1	*EGFR L858R*
28	IM	MPLC	0	–
8	IM	IM	10	*EGFR/KDM6A/ KMT2D*

[a]*Tumor 1 vs Tumor 2.*

IM, intrapulmonary metastasis; MPLC, multiple primary lung cancer.

Consistency Between Molecular Methods and Martini Criteria in Identifying MPLC

According to the Martini and Melamed criteria, 13 patients were classified as having MPLC, whereas the remaining patients were classified as having IM. Using the NGS molecular classification, we identified four patients with IM and 26 patients with MPLC (**Table 2**). According to the above results, our molecular method analysis showed 53.3% (16/30) consistency with the clinical and histopathological classification of MPLC. With respect to previous literature on the molecular identification of MPLC, our results showed consistency with the histopathological classification (15–19). However, of the patients histopathologically identified with MPLC (n = 18), fifteen (83.3%) were diagnosed with MPLC by NGS molecular classification as well, and the remaining patients showed matching mutations. Among these, the paired tumors of three patients harbored consistent driver mutations (excluding *EGFR L858R*) and ≥two matching mutations. Of the patients histopathologically identified with IM (n = 12), only one (8.3%) was diagnosed with IM by NGS molecular classification as well. Among these, the paired tumors from eight patients showed no matching mutations, and three patients shared single *EGFR L858R* mutations.

Notably, the classification results for P9 were inconsistent. According to the imaging results, the two tumors of the patient were 10–20 mm in diameter, and both showed early mixed GGNs with pre-infiltration lesions shown on pathological examination (**Figures 7A, B**). Molecular results showed that the mutations of the two tumors are exactly the same (**Figure 7C**). Although P9 was diagnosed with MPLC based on the histopathological classification, they more likely had intrapulmonary metastases based on the molecular characteristics.

In particular, it is challenging to clinically evaluate the relationship between the tumors of MPLC if they are pathologically classified as squamous cell carcinoma because of a lower frequency of driver mutations. Conventionally, metastasis is often considered by clinicians if the squamous cell carcinoma is pathologically identified in two tissues in one patient, especially with heterochrony. In our study of P13, the first primary tumor (squamous cell carcinoma) was observed in November 2018; the second tumor (adenocarcinoma) with an *EGFR L858R* mutation was observed in March 2019, and the patient was diagnosed with MPLC; the third tumor (squamous cell carcinoma) was observed in October 2019 and had the same pathology as the first tumor (**Figures 8A, B**). The three tumors had inconsistent genetic mutations and may have a primary clonal relationship, suggesting MPLC (**Figures 8C, D**). The third tumor was a metachronous multiple primary lung squamous cell

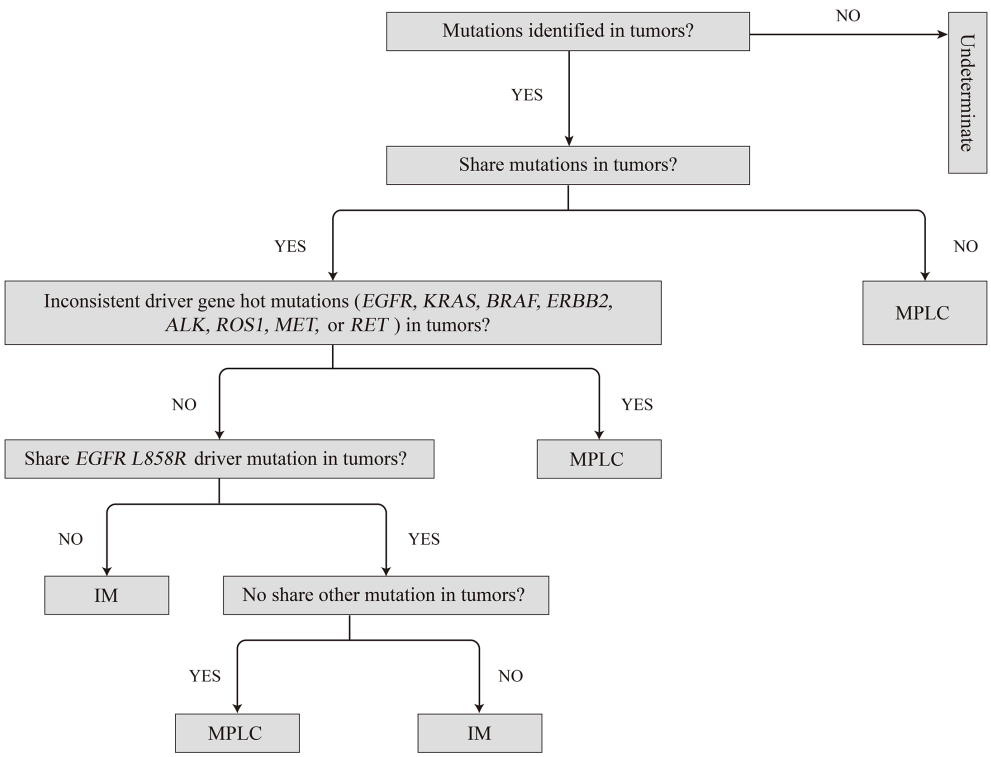

FIGURE 6 | Proposed algorithm for classifying multiple primary lung cancers based on molecular criteria. IM, intrapulmonary metastasis; MPLC, multiple primary lung cancer.

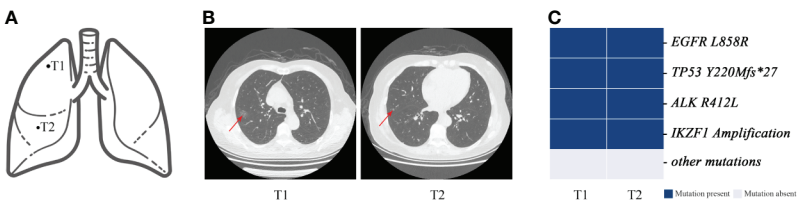

FIGURE 7 | Genomic mutations and computed tomography (CT) images of patient 9. Patient 9 was classified as having MPLC using the Martini and Melamed criteria. The lesions of the patient were found to have multiple consistent mutation sites and were diagnosed as IM by mutation evaluation. **(A)** Schematic diagrams of lung lesions. **(B)** and **(C)** Corresponding CT images and mutation distributions of patient 9.

carcinoma. Our study has suggested that molecular methods can assist in the diagnosis of metachronous multiple squamous cell carcinomas.

DISCUSSION

MPLC has historically been considered a rare phenomenon, but it has been reported with increasing frequency due to improvements in imaging technology and surveillance mechanisms. However, it remains difficult to distinguish the second primary lesion and metastases (20). For clinical management, it is important to classify the disease as intrapulmonary metastasis or multiple primary lung carcinoma to the define TNM classification and optimize the therapeutic options. With the development of high-throughput sequencing technology, molecular genetic analysis using cancer driver gene mutations as biomarkers can greatly assists in distinguishing multiple primary tumors and metastatic tumors in patients with lung cancer (21). Recent evidence has shown that the analysis of genetic mutations in MPLC patients is limited by the small number of cancer driver gene mutations (15, 16). Begg et al. believed that a single or a small number of gene loci are insufficient for identifying IM and MPLC (22). To improve the

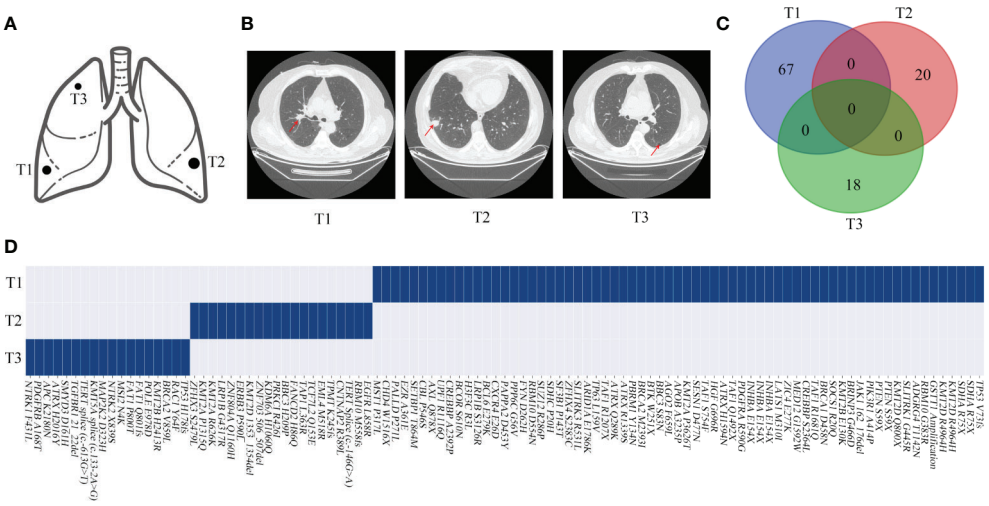

FIGURE 8 | Genomic mutations and computed tomography (CT) images of patient 13. **(A, B)** Schematic diagrams of lung lesions and corresponding CT images. **(C, D)** Relationship of the mutations between different lesions exhibited by a Venn diagram and the mutation distributions of patient 13. The arrow indicates the tumor lesions.

accuracy of diagnosis, at least 20 gene mutation sites are needed to distinguish IM from MPLC. Multi-gene assessment of MPLC is essential. Moreover, the current knowledge of the molecular characteristics of MPLC is insufficient to provide an accurate molecular diagnosis.

In our study, multigene panel sequencing was used to comprehensively analyze the genomic signature in early stage NSCLC. According to our results, a significant difference in genetic characteristics between early stage and advanced-stage NSCLC was observed. We found that early stage NSCLCs are characterized by a high frequency of driver gene mutations and a small number of mutations. Moreover, *EGFR*, *TP53*, *RBM10*, *LRP1B*, and *MDC1* mutations were observed in early stage NSCLC. These mutations are also found in the early lesions of AIS/MIA (23). Hence, these genes may be involved in early tumorigenesis.

Consistent with previous studies, *EGFR* was the most commonly mutated gene in early stage lung cancer (24). In this study, *EGFR* mutations were identified in 56% of patients with early stage NSCLC, which is higher than that in previous reports (30–40% in patients with early stage lung adenocarcinoma in Asia) (25). In this study, most patients were women without a smoking history. Additionally, previous studies have shown that GGO nodular lung adenocarcinoma had a higher frequency (up to 63%) of *EGFR* mutations than other types of adenocarcinoma (26). Consistently, our study also found that most patient samples had GGO features. Therefore, the specific clinical characteristics of the enrolled patients might correlate with the high prevalence of *EGFR* mutations. Further analysis showed that the prevalence of *EGFR L858R* mutations was significantly different between early and advanced-stage NSCLC, but the frequencies of *EGER 19Del* and other *EGFR* mutations (excluding *EGFR L858R* substitution and *19Del*) were not significantly different. All these results indicate that early stage NSCLC shows distinct *EGFR L858R* mutation characteristics, which may be associated with its carcinogenic properties.

Unlike previously used smaller gene panels (27, 28), large-panel NGS provides a way to examine multiple mutations simultaneously, yielding robust discrimination of tumor relatedness. In our research, an 808-gene panel NGS approach was used to analyze the surgically excised tumor of a patient with MLC. In this series, the tumors harbored a median of 4 (up to 67) non-synonymous somatic alterations per case. Thus, for tumors classified as IMs, multiple shared alterations (median 4, up to 10) and consistent driver mutations were present. We also found that the large-panel NGS robustly identified MPLC by demonstrating entirely unique mutational profiles comprising multiple alterations (median 4, up to 67 per tumor pair), representing an advantage over panels that examine only major drivers or non-comprehensive NGS. In particular, we found that comprehensive NGS allows the clear recognition of MPLC with coincidentally shared single hotspot mutations. Overall, our molecular classification was able to establish definitive tumor clonal relationships in virtually all tumor pairs during the study period.

Recent advances in tumor molecular biology have resulted in the identification of several candidate biomarkers, such as *EGFR*, that can be used in the diagnosis of MPLC (29). Molecular classification is based on the presence of a common driver gene as a biomarker of a similar tumor origin. This assumption may be controversial, particularly when a common driver alteration is used as a unique classifier. We found that MPLC based on mutational evaluation was enriched in *EGFR* mutations (59%), in line with the lack of smoking history, the female sex, and the Asian ethnicity of those patients. Multifocal early stage tumors are frequently present in such patients. Indeed, 5 patients

(P16, P17, P20, P23, and P30) consistently presented with the *EGFR L858R* mutation in this study, but previous studies have also reported that *EGFR* driver gene mutations between tumors are consistently judged as MPLC. Thus, mutations at the same hotspot site need to be interpreted more cautiously, especially the *EGFR L858R* mutation. Notably, in European and American populations, MPLC is dominated by *KRAS* mutations (19, 30), likely reflecting the overall known geographic differences in genomic profiles of NSCLC. The only other instance of coincidentally shared hotspot mutations in our series was a *TERT Amplification* in an otherwise unambiguous MPLC. In this study, we illustrated that a large NGS panel can readily identify MPLC despite the presence of shared single hotspot mutations by demonstrating numerous additional unique mutations in each of the tumors. A significant advantage of the comprehensive NGS panel of the type used here is its ability to discriminate MPLCs that share a single common hotspot mutation by chance.

n fact, in our series, shared *EGFR L858R* mutations were almost as likely to occur coincidentally in MPLC as in IM. Notably, there was an identical mutation (including *EGFR L858R* mutation) in the two separated tumor lesions from patient 9 (P9). Many studies have shown that the concordance rate of gene mutations in the primary tumor and metastasis is >90%, while that in multiple lung tumors, *e.g.*, MPLC, is 10.3–32.6% (31, 32). We believe that the tumor pairs of these two patients were metastatically assessed from a molecular perspective. However, CT showed that these two patients had partially solid and pre-invasive tumors without lymphatic metastasis. The results showed that IM might also be found according to the histopathology of MPLC, indicating that they may have aerosol metastasis. Therefore, the 2-year disease-free survival of the patient should be observed.

In our research, the molecular method based on an evaluation of driver gene mutations and the number of alterations for classifying MPLC were summarized, contributing to accurately defining the tumor stage and adjusting the treatment strategies. When comparing the performance of histologic assessment to the definitive NGS molecular classification, we found that histologic prediction was consistent in 53.3% of patients, and up to 47% of tumor stages were changed. Overall, this was similar to the discrepancy rates that ranged from 30 to 50% across different platforms in prior studies (17, 33). Among patients histopathologically diagnosed with MPLC, we found a good concordance rate (83.3%) with the diagnosis based on the mutational evaluation. In contrast, among patients histopathologically diagnosed with IM, the concordance rate with the diagnosis based on the mutational evaluation was only 8.3%. Difficulties with histologic prediction were substantially more frequent in the recognition of IM than MPLC. Thus, there is a limitation in the histopathological diagnosis of MLC, and clonality analysis by mutational evaluation may be helpful for distinguishing MPLC from IM.

This molecular method optimizes the previous methods based on genomic alterations, provides new criteria, and may improve the diagnostic accuracy for early stage MPLC, especially in cases where the lesions have the same pathological type and cannot be identified traditionally (36.7%). We note that the histology in this series was dominated by adenocarcinomas, and only two tumors in a patient were squamous cell carcinomas, precluding detailed analysis of this subset. Nevertheless, these cases illustrate the effectiveness of a large NGS panel in unambiguously establishing tumor relationships in such pairs due to their high tumor mutational burden even in the absence of driver alterations. Conversely, due to the relative homogeneity of cytologic features in squamous cell carcinoma (9), histologic features may not be sufficiently distinctive for the definitive classification of tumor relationships.

Although this molecular method performed well in the diagnosis of early stage MPLC, several limitations of the present study should be acknowledged. The size of our study cohort was relatively small, and further investigation and larger prospective studies are necessary to find more definitive molecular clonal relationships. Since some patients have not reached 2 years after surgery, and the follow-up time span is not long enough to appropriately assess long-term survival. Therefore, the present study has not yet analyzed these data. However, no incidents have occurred in the patients so far. Studies with a larger cohort of patients, long-term follow-up, and survival data would be helpful in substantiating our observations and validating our molecular method.

CONCLUSIONS

Comprehensive NGS evaluation highlights select scenarios in which histologic assessment has limitations and should allow for refinement of the Martini and Melamed criteria for evaluating tumor relatedness. In patients with histopathologically confirmed IM or patients with discordance between the histopathological and mutational evaluations, consideration of our molecular classification can be helpful for differentiation. Overall, our findings suggest that a comprehensive diagnostic approach incorporating histology and molecular analysis is essential to drawing this critical distinction in clinical practice. Molecular staging has the potential to revolutionize the current staging practice in patients with multiple tumors, providing robust confirmation of tumor clonality and information on actionable mutations at the same time.

DATA AVAILABILITY STATEMENT

The datasets presented in this study can be found in online repositories. The names of the repository/repositories and accession number(s) can be found in the article/**Supplementary Material**. Accession of the submission is: HRA000836 (https://bigd.big.ac.cn/gsa-human/browse/HRA000836).

ETHICS STATEMENT

The study was approved by the Medical Ethics Committee of Beijing Haidian Hospital (No.2020-041). The patients/

participants provided their written informed consent to participate in this study. Written informed consent was obtained from the individual(s) for the publication of any potentially identifiable images or data included in this article.

AUTHOR CONTRIBUTIONS

YH and GP contributed to the study design. ML, HW, HC and SC contributed to data bioinformatic analysis and interpretation. YH, GP, XM, QL, DL, YY, SW, and XW contributed to data collection. YH, GP, and ML contributed to the drafting of the article and to its revisions. All authors contributed to the article and approved the submitted version. We thank all the contributing authors for their great effort on this article.

ACKNOWLEDGMENTS

The authors wish to thank all the patients who participated in this study.

SUPPLEMENTARY MATERIAL

The Supplementary Material for this article can be found online at: https://www.frontiersin.org/articles/10.3389/fonc.2021.653988/full#supplementary-material

REFERENCES

1. Rahn DA, 3rd, Thakur S, Makani S, Sandhu A. Stereotactic Body Radiation Therapy (SBRT) for Multiple Primary Lung Cancers (MPLC): A Review and Case Series. *J Radiosurg SBRT* (2013) 2:135–40.
2. Beyreuther H. Multiplicität Von Carcinomen Bei Einem Fall Von Sog. "Schneeberger" Lungenkrebs Mit Tuberkulose. *Virchows Arc* (1924) 250:230–43. doi: 10.1007/BF01891568
3. Koubkova L, Hrstka R, Dobes P, Vojtesek B, Vyzulaet R. Second Primary Cancers—Causes, Incidence and the Future. *Klin Onkol* (2014) 27:11–7. doi: 10.14735/amko201411
4. Port JL, Korst RJ, Lee PC, Kansler AL, Kerem Y, Altorki NK. Surgical Resection for Multifocal (T4) non-Small Cell Lung Cancer: Is the T4 Designation Valid? *Ann Thorac Surg* (2007) 83:397–400. doi: 10.1016/j.athoracsur.2006.08.030
5. Ishikawa Y, Nakayama H, Ito H, Yokose T, Tsuboi M, Nishii T, et al. Surgical Treatment for Synchronous Primary Lung Adenocarcinomas. *Ann Thorac Surg* (2014) 98:1983–8. doi: 10.1016/j.athoracsur.2014.07.006
6. Wang H, Hou J, Zhang G, Zhang M, Li P, Yan X, et al. Clinical Characteristics and Prognostic Analysis of Multiple Primary Malignant Neoplasms in Patients With Lung Cancer. *Cancer Gene Ther* (2019) 26:419–26. doi: 10.1038/s41417-019-0084-z
7. Chang YL, Wu CT, Lin SC, Hsiao CF, Jou YS, Lee YC. Clonality and Prognostic Implications of p53 and Epidermal Growth Factor Receptor Somatic Aberrations in Multiple Primary Lung Cancers. *Clin Cancer Res* (2007) 13:52–8. doi: 10.1158/1078-0432.CCR-06-1743
8. Martini N, Melamed MR. Multiple Primary Lung Cancers. *J Thorac Cardiovasc Surg* (1975) 70:606–12. doi: 10.1016/S0022-5223(19)40289-4
9. Travis WD, Brambilla E, Burke A, Marx A, Nicholson AG. The 2015 World Health Organization Classification of Lung Tumors: Impact of Genetic, Clinical and Radiologic Advances Since the 2004 Classification. *J Thorac Oncol* (2015) 10:1243–60. doi: 10.1097/JTO.0000000000000630
10. Swanton C. Intratumor Heterogeneity: Evolution Through Space and Time. *Cancer Res* (2012) 72:4875–82. doi: 10.1158/0008-5472.CAN-12-2217
11. Asmar R, Sonett J, Singh G, Mansukhani M, Borczuk A. Use of Oncogenic Driver Mutations in Staging of Multiple Primary Lung Carcinomas: A Single-Center Experience. *J Thorac Oncol* (2017) 12:1524–35. doi: 10.1016/j.jtho.2017.06.012
12. Wu C, Zhao C, Yang Y, He Y, Hou L, Li X, et al. High Discrepancy of Driver Mutations in Patients With NSCLC and Synchronous Multiple Lung Ground-Glass Nodules. *J Thorac Oncol* (2015) 10:778–83. doi: 10.1097/JTO.0000000000000487
13. de Bruin EC, McGranahan N, Mitter R, Salm M, Wedge DC, Yates L, et al. Spatial and Temporal Diversity in Genomic Instability Processes Defines Lung Cancer Evolution. *Science* (2014) 346:251–6. doi: 10.1126/science.1253462
14. Wen S, Dai L, Wang L, Wang W, Wu D, Wang K, et al. Genomic Signature of Driver Genes Identified by Target Next-Generation Sequencing in Chinese non-Small Cell Lung Cancer. *Oncologist* (2019) 24:e1070–81. doi: 10.1634/theoncologist.2018-0572
15. Tanabe Y, Ichikawa H, Kohno T, Yoshida H, Kubo T, Kato M, et al. Comprehensive Screening of Target Molecules by Next-Generation Sequencing in Patients With Malignant Solid Tumors: Guiding Entry Into Phase I Clinical Trials. *Mol Cancer* (2016) 15(1):73. doi: 10.1186/s12943-016-0553-z
16. Lei L, Wang WX, Yu ZY, Liang XB, Pan WW, Chen HF, et al. A Real-World Study in Advanced non-Small Cell Lung Cancer With KRAS Mutations. *Transl Oncol* (2020) 13:329–35. doi: 10.1016/j.tranon.2019.12.004
17. Takahashi Y, Shien K, Tomida S, Oda S, Matsubara T, Sato H, et al. Comparative Mutational Evaluation of Multiple Lung Cancers by Multiplex Oncogene Mutation Analysis. *Cancer Sci* (2018) 109:3634–42. doi: 10.1111/cas.13797
18. Goto T, Hirotsu Y, Mochizuki H, Nakagomi T, Shikata D, Yokoyama Y, et al. Mutational Analysis of Multiple Lung Cancers: Discrimination Between Primary and Metastatic Lung Cancers by Genomic Profile. *Oncotarget* (2017) 8:31133–43. doi: 10.18632/oncotarget.16096
19. Mansuet-Lupo A, Barritault M, Alifano M, Janet-Vendroux A, Zarmaev M, Biton J, et al. Proposal for a Combined Histomolecular Algorithm to Distinguish Multiple Primary Adenocarcinomas From Intrapulmonary Metastasis in Patients With Multiple Lung Tumors. *J Thorac Oncol* (2019) 14:844–56. doi: 10.1016/j.jtho.2019.01.017
20. Detterbeck FC, Jones DR, Kernstine KH, Naunheim KS. American College of Physicians. Lung Cancer Special Treatment Issues. *Chest* (2003) 123(1 Suppl):244S–58S. doi: 10.1378/chest.123.1_suppl.244s
21. Romaszko AM, Doboszyńska A. Multiple Primary Lung Cancer: A Literature Review. *Adv Clin Exp Med* (2018) 27:725–30. doi: 10.17219/acem/68631
22. Begg CB, Eng KH, Hummer AJ. Statistical Tests for Clonality. *Biometrics* (2007) 63:522–30. doi: 10.1111/j.1541-0420.2006.00681.x
23. Chen H, Carrot-Zhang J, Zhao Y, Hu H, Freeman S, Yu S, et al. Genomic and Immune Profiling of Pre-Invasive Lung Adenocarcinoma. *Nat Commun* (2019) 10:5472. doi: 10.1038/s41467-019-13460-3
24. Li Y, Li X, Li H, Zhao Y, Liu Z, Sun K, et al. Genomic Characterisation of Pulmonary Subsolid Nodules: Mutational Landscape and Radiological Features. *Eur Respir J* (2020) 55:1901409. doi: 10.1183/13993003.01409-2019
25. Zhao M, Zhan C, Li M, Yang X, Yang X, Zhang Y, et al. Aberrant Status and Clinicopathologic Characteristic Associations of 11 Target Genes in 1,321 Chinese Patients With Lung Adenocarcinoma. *J Thorac Dis* (2018) 10:398–407. doi: 10.21037/jtd.2017.12.68
26. Sun F, Xi J, Zhan C, Yang X, Wang L, Shi Y, et al. Ground Glass Opacities: Imaging, Pathology, and Gene Mutations. *J Thorac Cardiovasc* (2018) 156:808–13. doi: 10.1016/j.jtcvs.2018.02.110
27. Patel SB, Kadi W, Walts AE, Marchevsky AM, Pao A, Aguiluz A, et al. Next-Generation Sequencing: A Novel Approach to Distinguish Multifocal Primary Lung Adenocarcinomas From Intrapulmonary Metastases. *J Mol Diagn* (2017) 19:870–80. doi: 10.1016/j.jmoldx.2017.07.006
28. Roepman P, Ten Heuvel A, Scheidel KC, Sprong T, Heideman DAM, Seldenrijk KA, et al. Added Value of 50-Gene Panel Sequencing to Distinguish Multiple Primary Lung Cancers From Pulmonary Metastases: A Systematic Investigation. *J Mol Diagn* (2018) 20:436–45. doi: 10.1016/j.jmoldx.2018.02.007

29. Han HS, Eom DW, Kim JH, Kim KH, Shin HM, An JY, et al. EGFR Mutation Status in Primary Lung Adenocarcinomas and Corresponding Metastatic Lesions: Discordance in Pleural Metastases. *Clin Lung Cancer* (2011) 12:380–6. doi: 10.1016/j.cllc.2011.02.006
30. Chang JC, Alex D, Bott M, Tan KS, Seshan V, Golden A, et al. Comprehensive Next-Generation Sequencing Unambiguously Distinguishes Separate Primary Lung Carcinomas From Intra-Pulmonary Metastases: Comparison With Standard Histopathologic Approach. *Clin Cancer Res* (2019) 25:7113–25. doi: 10.1158/1078-0432.CCR-19-1700
31. Vignot S, Frampton GM, Soria JC, Yelensky R, Commo F, Brambilla C, et al. Next-Generation Sequencing Reveals High Concordance of Recurrent Somatic Alterations Between Primary Tumor and Metastases From Patients With Non-Small-Cell Lung Cancer. *J Clin Oncol* (2013) 31:2167–72. doi: 10.1200/JCO.2012.47.7737
32. Chen K, Chen W, Cai J, Yang F, Lou F, Wang X, et al. Favorable Prognosis and High Discrepancy of Genetic Features in Surgical Patients With Multiple Primary Lung Cancers. *J Thorac Cardiovasc Surg* (2018) 155:371–9.e1. doi: 10.1016/j.jtcvs.2017.08.141
33. Schneider F, Derrick V, Davison JM, Strollo D, Incharoen P, Dacic S. Morphological and Molecular Approach to Synchronous Non-Small Cell Lung Carcinomas: Impact on Staging. *Mod Pathol* (2016) 29:735–42. doi: 10.1038/modpathol.2016.66

Conflict of Interest: ML, HC, HW, and SC are employees of Acornmed Biotechnology Co., Ltd.

The remaining authors declare that the research was conducted in the absence of any commercial or financial relationships that could be construed as a potential conflict of interest.

The handling editor declared a shared affiliation, though no other collaboration, with several of the authors GP, XM, QL, DL, YY, SW, XW, and YH.

frontiers in Oncology

ORIGINAL RESEARCH
published: 07 June 2021
doi: 10.3389/fonc.2021.622742

Identification of High-Risk of Recurrence in Clinical Stage I Non-Small Cell Lung Cancer

*Yasuhiro Tsutani[1], Yoshihisa Shimada[2], Hiroyuki Ito[3], Yoshihiro Miyata[1], Norihiko Ikeda[2], Haruhiko Nakayama[3] and Morihito Okada[1]**

[1] Department of Surgical Oncology, Hiroshima University, Hiroshima, Japan, [2] Department of Thoracic Surgery, Tokyo Medical University, Tokyo, Japan, [3] Department of Thoracic Surgery, Kanagawa Cancer Center, Yokohama, Japan

Objective: This study aimed to identify patients at a high risk of recurrence using preoperative high-resolution computed tomography (HRCT) in clinical stage I non-small cell lung cancer (NSCLC).

Methods: A total of 567 patients who underwent screening and 1,216 who underwent external validation for clinical stage I NSCLC underwent lobectomy or segmentectomy. Staging was used on the basis of the 8th edition of the tumor–node–metastasis classification. Recurrence-free survival (RFS) was estimated using the Kaplan–Meier method, and the multivariable Cox proportional hazards model was used to identify independent prognostic factors for RFS.

Results: A multivariable Cox analysis identified solid component size (hazard ratio [HR], 1.66; 95% confidence interval [CI] 1.30–2.12; P < 0.001) and pure solid type (HR, 1.82; 95% CI 1.11–2.96; P = 0.017) on HRCT findings as independent prognostic factors for RFS. When patients were divided into high-risk (n = 331; solid component size of >2 cm or pure solid type) and low-risk (n = 236; solid component size of ≤2 cm and part solid type) groups, there was a significant difference in RFS (HR, 5.33; 95% CI 3.09–9.19; 5-year RFS, 69.8% *vs.* 92.9%, respectively; P < 0.001). This was confirmed in the validation set (HR, 5.32; 95% CI 3.61–7.85; 5-year RFS, 72.0% *vs.* 94.8%, respectively; P < 0.001).

Conclusions: In clinical stage I NSCLC, patients with a solid component size of >2 cm or pure solid type on HRCT were at a high risk of recurrence.

Keywords: ground-glass opacity, high-resolution computed tomography, recurrence, non-small cell lung cancer, solid component size

OPEN ACCESS

Edited by:
Chen Chen,
Central South University, China

Reviewed by:
Diego Signorelli,
Niguarda Ca 'Granda Hospital, Italy
Rafael Lopez Castro,
Hospital Clínico Universitario de Valladolid, Spain

***Correspondence:**
Morihito Okada
morihito@hiroshima-u.ac.jp

Specialty section:
This article was submitted to Thoracic Oncology, a section of the journal Frontiers in Oncology

Received: *29 October 2020*
Accepted: *06 May 2021*
Published: *07 June 2021*

Citation:
Tsutani Y, Shimada Y, Ito H, Miyata Y, Ikeda N, Nakayama H and Okada M (2021) Identification of High-Risk of Recurrence in Clinical Stage I Non-Small Cell Lung Cancer. Front. Oncol. 11:622742. doi: 10.3389/fonc.2021.622742

INTRODUCTION

Early-stage non-small cell lung cancer (NSCLC) is frequently detected using more complex procedure, such as high-resolution computed tomography (HRCT) and widespread use of low-dose helical computed tomography (CT) for tumor screening (1, 2). The occasion to treat patients with early-stage NSCLC has increased, and pulmonary resection plays a main role in such treatment. Complete resection would be expected to lead a good prognosis for stage I NSCLC. However, complete resection does not always ensure the cure of disease and the 5-year disease-free survival rate for stage IA NSCLC is 84.3% and for stage IB NSCLC is 65.8% (3).

Although the tumor–node–metastasis (TNM) classification can stratify patients into different prognostic groups, stage I NSCLC is considered to be a heterogeneous group. Therefore, useful parameters are needed to predict postoperative recurrence when deciding on treatment strategies, such as the application of sublobar resection and additional perioperative systemic therapy. A high maximum standardized uptake value (SUVmax) with [18F]-fluoro-2-deoxy-D-glucose (FDG) positron emission tomography (PET)/CT reflects tumor invasiveness and has a negative impact on prognosis in patients with resected early-stage NSCLC (2, 4). However, because imaging protocols, equipment, and measurement methods vary between institutions, the optimal SUVmax cutoff value also differs by institution and between studies. Therefore, using FDG-PET/CT as a prognostic factor in a universal setting is challenging at present.

One of the important proposals in the 8th edition of the T classification of lung cancer is the size of the solid component excluding ground-glass opacity (GGO) to classify clinical T factors (5, 6). In the present study, we aimed to identify patients at a high risk of postoperative recurrence in clinical stage I NSCLC using preoperative HRCT, which is a globally applicable method. High-risk patients may be candidates for neoadjuvant therapy even in clinical stage I NSCLC. The primary endpoint of this study was recurrence-free survival (RFS).

MATERIALS AND METHODS

Patients

As the screening set, a total of 567 consecutive patients with clinical stage I NSCLC who underwent lobectomy or segmentectomy with systematic lymph node dissection at Hiroshima University between January 1st 2010 and December 31st 2016 were enrolled. All patients were staged according to the TNM Classification of Malignant Tumors, 8th edition (7). Endobronchial ultrasonography and mediastinoscopy were not routinely performed. Lymph node metastasis was determined as negative when swollen mediastinal or hilar lymph nodes measuring short axis of > 1 cm were not evident on HRCT, and FDG did not accumulate an SUXmax of >1.5 in these lymph nodes according to FDG-PET. The inclusion criteria included preoperative staging determined by HRCT and FDG-PET/CT and curative surgery with lobectomy or segmentectomy without induction therapy. The screening set of patients formed the high-risk group for recurrence. To externally validate the high-risk group, we used a combined cohort of two independent sets of 1,216 consecutive patients who underwent lobectomy or segmentectomy with systematic lymph node dissection (Tokyo Medical University and Kanagawa Cancer Center) between January 1st, 2010, and December 31st, 2016. The inclusion criteria were the same as those for the screening set (**Figure 1**).

The institutional review boards of the participating institutions approved this retrospective review, which was based on a prospective database, and waived the requirement for informed consent from individual patients (Kanagawa Cancer Center: February 28th, 2013; 24-KEN-54; Tokyo Medical University Hospital: February 25th, 2015; SH2969; Hiroshima University Hospital: June 13th, 2018; E-1216).

HRCT

Sixteen-row multidetector CT was used to obtain chest images independent of subsequent FDG-PET/CT examinations. For high-resolution tumor images, the following parameters were used: 120 kVp, 200 mA, 1–2-mm section thickness, 512 × 512-pixel resolution, 0.5–1.0-s scan time, a high spatial reconstruction algorithm with a 20-cm field of view, and mediastinal (level, 40 HU; width, 400 HU) and lung (level, −600 HU; width, 1600 HU)

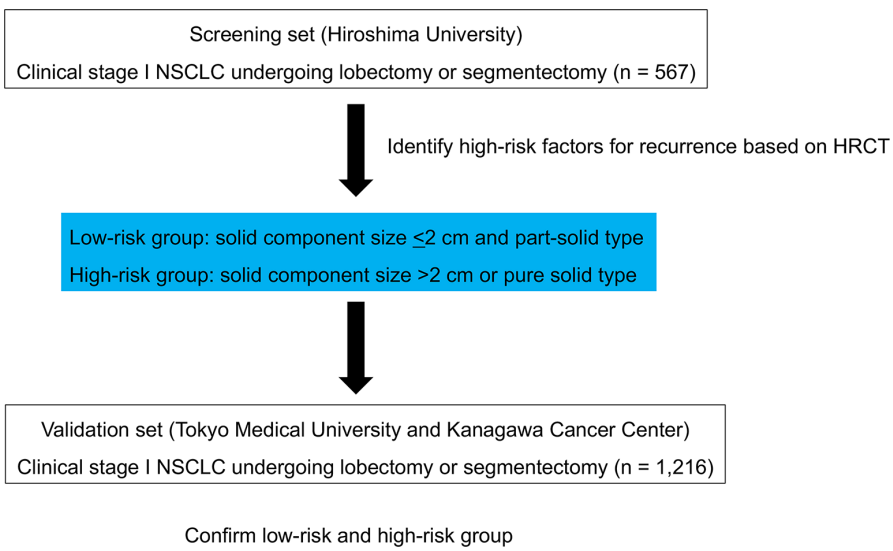

FIGURE 1 | Scheme of the study.

window settings. GGO was defined as a misty increase in lung attenuation without obscuring the underlying vascular markings. The size of the solid component of the tumor was defined as the maximum dimension of the solid component measured using lung window settings, excluding GGO (8). Pure solid tumor was defined as a tumor without GGO component. Part-solid tumor was defined as a tumor with GGO component. CT scans were reviewed and tumor sizes were determined by radiologists from each institution.

Pathological Examination

Tumor size was defined as the maximum dimension of the invasive tumor component, excluding the lepidic growth component described previously (9). Lymphatic and vascular invasion were assessed by immunohistochemistry with D2-40, which stains lymphatic ducts, and elastic Van Gieson staining of vessel elastic fibers. Lymphatic and vascular invasion were positive when penetration was detected as an extension of the malignant neoplasm. To evaluate pleural invasion, elastic tissue fibers were subject to elastic Van Gieson staining. Pleural invasion was defined as positive if cancer had invaded beyond the elastic layer, including invasion into the visceral pleural surface or neighboring organs. Histological examinations were determined by pathologists at each institution.

Follow-Up Evaluation

All patients who underwent lung resection were followed up from the day of surgery. Postoperative follow-up procedures, including a physical examination, chest roentgenogram every three months, and chest and abdominal CT examinations every six months, were performed for the first two years. Subsequently, a physical examination and chest roentgenogram were performed every six months, and a chest CT examination was performed every year.

Statistical Analysis

Data is presented as number (%) or median and interquartile range (IQR) unless otherwise stated. The χ (2) test was used to compare the frequencies of categorical variables. Receiver operating characteristic curve of the solid component size for the prediction of recurrence were generated to determine the cutoff value that yielded optimal sensitivity and specificity. An independent-samples t-test was used to compare continuous variables. RFS was defined as the interval from the day of surgery until the first event (relapse or death from any cause) or right censoring on the day of final follow up. Overall survival (OS) was defined as the time from the day of surgery until death from any cause or right censoring at the day of final follow up. The Kaplan–Meier method was used to analyze RFS and OS. The log-rank test was used to assess differences in RFS and OS between groups. The multivariable Cox proportional hazards model was used to identify independent prognostic factors for RFS. The multivariable logistic regression analysis was used to identify independent predictive factors for lymph node metastasis. A P value of <0.05 was considered statistically significant. JMP 14.0 (SAS Institute, Cary, NC, USA) was used to statistically analyze the data.

RESULTS

Screening Set

Patient characteristics from the screening set (n = 567) are shown in **Table 1**.

A multivariable analysis revealed that age (hazard ratio [HR], 1.03; P = 0.002), solid component size (HR, 1.66; P <0.001), and pure solid type (HR, 1.82; P = 0.017) were independent prognostic factors for RFS (**Table 2**). The optimal cutoff value of solid component size to predict recurrence was set as 2.0 cm from the receiver operating characteristic curve (**Supplementary Figure 1**).

A multivariable analysis revealed that age (odds ratio [OR], 1.03; P = 0.002), gender (male, OR, 1.67; P = 0.013), solid component size (OR, 1.75; P <0.001), pure solid type (OR, 2.85; P<0.001), and lobectomy (OR, 3.25; P = 0.001) were independent predictive factors for lymph node metastasis (**Table 3**).

There was a significant difference in RFS between patients with a solid component size of ≤2 cm (n = 363; 5-year RFS, 88.1%) and those with a solid component size of >2 cm (n = 204; 5-year RFS, 64.0%; P < 0.0001; **Figure 2A**). There was a significant difference in RFS between patients with part-solid tumors (n = 291; 5-year RFS, 89.5%) and those with pure solid tumors (n = 276; 5-year RFS, 68.8%; P < 0.0001; **Figure 2B**). When patients were divided into four groups based on the solid component size and pure or part-solid type, RFS of patients with a solid component size of ≤2 cm with a part-solid tumor (n = 129) were favorable with a 5-year RFS of 92.5%. RFS in the other three groups was similar; 5-year RFS was 79.6% for patients with a solid component size of ≤2 cm with a pure solid tumor (n = 126), 75.9% for those with a solid component size of >2 cm with a part solid tumor (n = 54), and 58.9% for those with a solid component size of >2 cm with a pure solid tumor (n = 150; **Figure 2C**). Based on these findings, we defined patients as at a low risk of recurrence with a solid component size of <2 cm and part-solid type, and at a high risk of recurrence with a solid component size of >2 cm or pure solid type. Pathological findings, such as histology; invasive component size; lymphatic, vascular and pleural invasion; and lymph node metastasis were significantly different between the low-risk and high-risk groups (**Table 4**). There was a significant difference in RFS between the low-risk (n = 236; 5-year RFS, 92.9%) and high-risk (n = 331; 5-year RFS, 69.8%; HR, 5.33; P < 0.0001; **Figure 2D**) groups. There was a significant difference in OS between the low-risk group (n = 236; 5-year OS, 94.0%) and the high-risk group (n = 331; 5-year OS, 80.4%; HR, 3.81; P < 0.0001; **Figure 2E**).

Validation Set

The characteristics of patients in the validation set (n = 1,216) are shown in **Table 1**.

When patients were divided into the low risk of recurrence group (n = 553) and the high risk of recurrence group (n = 663), there were significant differences in pathological findings, such as histology; invasive component size; lymphatic, vascular, and pleural invasion; and lymph node metastasis between the two groups (**Table 4**).

TABLE 1 | Patient characteristics in the screening set and validation set.

		Screening set (n = 567)	Validation set (n = 1,216)	P value
Age, median (IQR)		68 (62-74)	69 (63-75)	0.090
Gender	Male	334 (58.9%)	603 (49.6%)	<0.001
Smoking history		321 (56.6%)	657 (54.0%)	0.307
Solid component size (cm), median (IQR)		1.6 (1.1-2.5)	1.7 (1.1-2.4)	0.828
Pure solid type		276 (48.7%)	502 (41.3%)	0.003
Histology	Adenocarcinoma	452 (79.7%)	1,033 (85.0%)	0.049
	Squamous cell carcinoma	67 (11.8%)	109 (9.0%)	
	Others	48 (8.5%)	73 (6.0%)	
Procedure	Lobectomy	366 (64.6%)	1,060 (87.2%)	<0.001
	Segmentectomy	201 (35.4%)	156 (12.8%)	
Lymphatic invasion		111 (19.6%)	265 (21.8%)	0.283
Vascular invasion		140 (24.7%)	353 (29.0%)	0.055
Pleural invasion		87 (15.3%)	230 (18.9%)	0.064
Lymph node metastasis		47 (8.3%)	138 (11.3%)	0.045
Pathological stage	0	20 (3.5%)	43 (3.5%)	0.002
	IA1	118 (20.8%)	350 (28.8%)	
	IA2	171 (30.2%)	321 (26.4%)	
	IA3	83 (14.6%)	130 (10.7%)	
	IB	93 (16.4%)	179 (14.7%)	
	IIA	7 (1.2%)	16 (1.3%)	
	IIB	51 (9.0%)	110 (9.1%)	
	IIIA	24 (4.2%)	58 (4.8%)	
	IIIB	0 (0%)	9 (0.7%)	
Adjuvant chemotherapy	Yes	189 (33.3%)	240	<0.001

IQR, interquartile range.

TABLE 2 | Multivariable analysis of recurrence-free survival.

Screening set		Univariable analysis			Multivariable analysis		
Variable		**HR**	**95% CI**	**P value**	**HR**	**95% CI**	**P value**
Age		1.04	1.02-1.07	<0.001	1.03	1.01-1.05	0.002
Gender	Male (*vs.* female)	1.87	1.24-2.83	0.003	1.07	0.63-1.83	0.792
Smoking history		2.15	0.42-3.26	0.001	1.48	0.84-2.61	0.173
Solid component size (cm)		2.01	1.66-2.46	<0.001	1.66	1.30-2.12	<0.001
Pure solid type		3.31	2.17-5.04	<0.001	1.82	1.11-2.96	0.017
Histology	Adenocarcinoma (*vs.* non-adenocarcinoma)	0.39	0.26-0.58	<0.001	0.98	0.61-1.61	0.915
Procedure	Lobectomy (*vs.* segmentectomy)	1.46	0.95-2.24	0.081	1.02	0.64-1.55	0.944

TABLE 3 | Multivariable analysis of lymph node metastasis.

Screening set		Univariable analysis			Multivariable analysis		
Variable		**OR**	**95% CI**	**P value**	**OR**	**95% CI**	**P value**
Age		1.02	1.00-1.03	0.033	1.03	1.01-1.04	0.002
Gender	Male (*vs.* female)	1.67	1.22-2.30	0.001	1.67	1.11-2.50	0.013
Smoking history		1.26	0.93-1.72	0.136	0.67	0.44-1.02	0.064
Solid component size (cm)		2.21	1.97-2.61	<0.001	1.75	1.44-2.13	<0.001
Pure solid type		4.13	2.94-5.82	<0.001	2.85	1.94-4.20	<0.001
Histology	Adenocarcinoma (*vs.* non-adenocarcinoma)	0.61	0.42-0.87	0.009	1.28	0.84-1.95	0.257
Procedure	Lobectomy (*vs.* segmentectomy)	5.44	2.76-10.75	<0.001	3.25	1.61-6.56	0.001

There was a significant difference in RFS between the low-risk group (5-year RFS, 94.8%) and high-risk group (5-year RFS, 72.0%; HR, 5.32; P < 0.0001; **Figure 3A**). There was a significant difference in OS between the low-risk group (5-year OS, 95.7%) and high-risk group (5-year OS, 84.2; HR, 3.54; P < 0.0001; **Figure 3B**).

DISCUSSION

We identified patients at a high risk of recurrence using preoperative HRCT for clinical stage I NSCLC. Patients with a solid component size of >2 cm or a pure solid tumor were at a high risk of recurrence. The HR values of RFS and OS in the

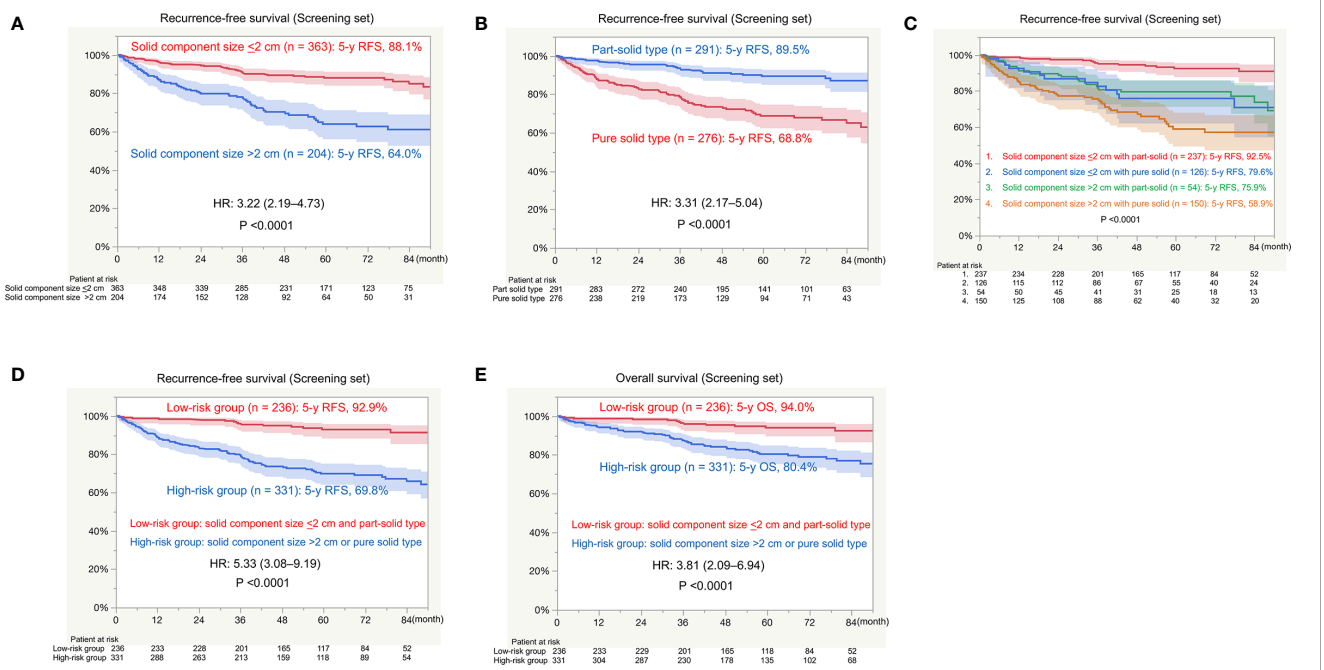

FIGURE 2 | Survival in the screening set. RFS, recurrence-free survival; HR, hazard ratio; OS, overall survival. **(A)** RFS between patients with a solid component size of ≤2 cm and those with a solid component size of >2 cm. **(B)** RFS between patients with part-solid tumors and those with pure solid tumors. **(C)** RFS among patients with a solid component size of ≤2 cm with part-solid tumors or pure solid tumors and those with a solid component size of >2 cm with part-solid tumors or pure solid tumors. **(D)** RFS between the low-risk group (solid component size of ≤2 cm and a part-solid tumor) and high-risk group (solid component size of >2 cm and a pure solid tumor). **(E)** OS between the low-risk group (solid component size of ≤2 cm and a part-solid tumor) and high-risk group (solid component size of >2 cm or a pure solid tumor).

low-risk group in the screening set were 5.33 and 3.81, respectively. These findings were confirmed in the external validation set with high concordance, with a HR of 5.32 for RFS and 3.54 for OS.

Several studies have reported the utility of solid component size to predict pathological tumor invasiveness and prognosis compared with whole tumor size (8, 10–12). As recommended in the 8th edition of the T classification (6), using solid component

TABLE 4 | Comparison of pathological findings between low-risk and high-risk groups.

		Screening set			Validation set		
		Low risk (n = 236)	High risk (n = 331)	P value	Low risk (n = 553)	High risk (n = 663)	P value
Histology	Adenocarcinoma	234 (99.2%)	218 (65.9%)	<0.001	539 (97.5%)	494 (74.5%)	<0.001
	Squamous cell carcinoma	1 (0.42%)	66 (19.9%)		11 (2.0%)	98 (14.8%)	
	Others	1 (0.42%)	47 (14.2%)		3 (0.5%)	71 (10.7%)	
Invasive component size (cm)		1.1 (0.6-1.8)	2.0 (1.5-2.9)	<0.001	0.8 (0.3-1.4)	2.0 (1.5-2.8)	<0.001
Lymphatic invasion		13 (5.5%)	98 (29.6%)	<0.001	45 (8.1%)	220 (33.2%)	<0.001
Vascular invasion		13 (5.5%)	127 (38.4%)	<0.001	34 (6.2%)	319 (48.1%)	<0.001
Pleural invasion		12 (5.1%)	75 (22.7%)	<0.001	26 (4.7%)	204 (30.8%)	<0.001
Lymph node metastasis		0 (0%)	47 (14.2%)	<0.001	18 (3.3%)	120 (18.1%)	<0.001
Pathological stage	0	20 (8.5%)	0 (0%)	<0.001	38 (6.9%)	5 (0.8%)	<0.001
	IA1	85 (36.0%)	33 (10.0%)		287 (51.9%)	63 (9.5%)	
	IA2	83 (35.2%)	88 (26.6%)		155 (28.0%)	166 (25.0%)	
	IA3	22 (9.3%)	61 (18.4%)		28 (5.1%)	102 (15.4%)	
	IB	14 (5.9%)	79 (23.9%)		22 (4.0%)	157 (23.7%)	
	IIA	3 (1.3%)	4 (1.2%)		1 (0.2%)	15 (2.3%)	
	IIB	9 (3.8%)	42 (12.7%)		14 (2.5%)	96 (14.5%)	
	IIIA	0 (0%)	24 (7.3%)		7 (1.3%)	51 (7.7%)	
	IIIB	0 (0%)	0 (0%)		1 (0.2%)	8 (1.2%)	
Adjuvant chemotherapy	Yes	57 (24.2%)	132 (39.9%)	<0.001	48 (8.7%)	192 (29.0%)	<0.001

IQR, interquartile range.

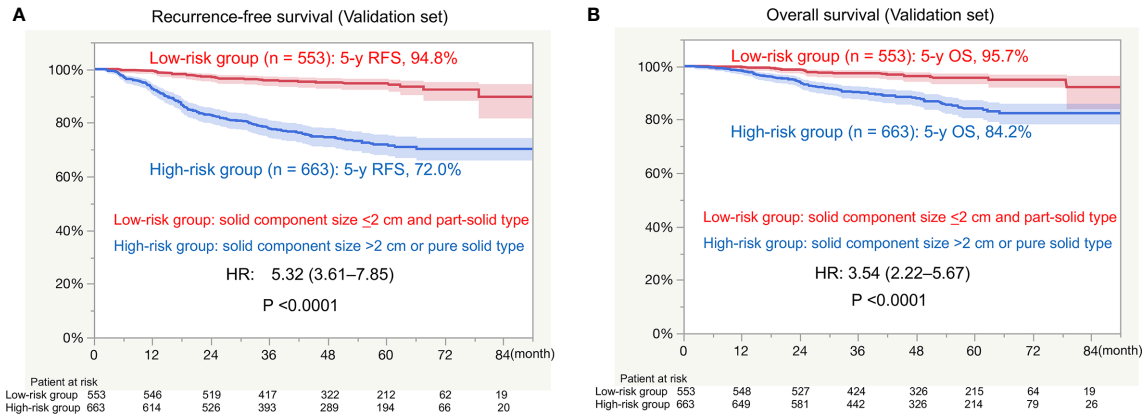

FIGURE 3 | Survival in the external validation set. RFS, recurrence-free survival; HR, hazard ratio; OS, overall survival. **(A)** RFS between the low-risk group (solid component size of ≤2 cm and a part-solid tumor) and high-risk group (solid component size of >2 cm and a pure solid tumor). **(B)** OS between the low-risk group (solid component size of ≤2 cm and a part-solid tumor) and high-risk group (solid component size of >2 cm and a pure solid tumor).

size as a prognostic factor seems to be reasonable from the results of the present study, which show that solid component size is an independent prognostic factor for RFS.

The presence of GGO was also reported as a prognostic factor in previous studies (13–15). The multivariable analysis of pure solid versus part-solid tumors showed this characteristic as an independent unfavorable prognostic factor for RFS, which is consistent with previous reports. Although survival after surgical resection for tumors with GGO was usually favorable (13–15), we need to pay attention to GGO tumors with a large solid component size. As shown in **Figure 2C**, RFS in patients with a part-solid tumor with a solid component size of >2 cm is similar to that of pure solid tumors in this study. This finding was also supported by a previous study (16).

The group at a high risk of recurrence reflected the pathological findings in the current study. The frequency of non-adenocarcinoma histology; a larger invasive component size; lymphatic, vascular, and pleural invasion; and lymph node metastasis were significantly higher in the high-risk group compared with the low-risk group in both the screening and validation sets. In the multivariable analysis, solid component size and the pure solid type were proven to be predictive factors for lymph node metastasis. Patients at a high-risk of recurrence were also at high-risk of lymph node metastasis.

Preoperative prediction of the risk of postoperative recurrence is useful to decide treatment strategies. The excellent prognosis would be expected after lobectomy or segmentectomy with lymph node dissection in patients at a low risk of recurrence that show minimal malignant pathological findings in our study. There seems to be no role of neoadjuvant therapy in low-risk patients. However, when nodal metastasis is proven, adjuvant chemotherapy should be considered. In contrast, patients at a high risk of recurrence should undergo standard therapy, such as lobectomy with systematic lymph node dissection, because they potentially have lymph node metastasis with a probability of approximately 20%. Although the use of perioperative adjuvant therapy for stage I NSCLC has not been established, additional systemic therapy, such as neoadjuvant chemotherapy or immunotherapy may be needed to improve outcomes in high-risk patients with stage I NSCLC. We are currently conducting a multicenter pilot study of neoadjuvant anti-programmed cell death-1 antibody for high-risk clinical stage I NSCLC with a solid component size of >2 cm or pure solid type on HRCT (17).

The current study has some limitations. Only HRCT was used to predict risk factors for postoperative recurrence while several previous studies suggested that SUVmax on FDG-PET/CT was a promising predictor of prognosis (2, 4, 10). Although no standardization of SUVmax on FDG-PET/CT in a global setting can be used at present, further studies should be done to elucidate the significance of FDG-PET using a novel standardization method, such as semiquantitative PET evaluation (18). Also, we did not routinely perform invasive mediastinal staging for node-negative tumors, although invasive staging is recommended for tumors >3 cm (mainly adenocarcinoma with high FDG uptake) in the guideline (19). High-risk patients may also be candidates of invasive staging. Although we identified high-risk patients using preoperative HRCT findings to decide the application of neoadjuvant therapy, postoperative adjuvant therapy should be considered on the basis of pathological findings such as nodal involvement and pleural invasion.

In conclusion, we established patients at a high risk of recurrence using preoperative HRCT for clinical stage I NSCLC with high concordance HR in the external validation set. Patients with a solid component size of >2 cm or pure solid tumors are potential candidates for perioperative systemic therapy to prevent postoperative recurrence.

DATA AVAILABILITY STATEMENT

The raw data supporting the conclusions of this article will be made available by the authors, without undue reservation.

ETHICS STATEMENT

The studies involving human participants were reviewed and approved by Hiroshima University IRB, Kanagawa Cancer Center IRB, and Tokyo Medical University Hospital IRB. Written informed consent for participation was not required for this study in accordance with the national legislation and the institutional requirements.

AUTHOR CONTRIBUTIONS

YT: conceptualization, data curation, methodology, data analysis, and writing-original draft. YS: data collections, writing-review, and editing. HI: data collections, writing-review, and editing. YM: writing-review and editing. NI: writing-review and editing. HN: writing-review and editing. MO: writing-review and editing, supervision. All authors contributed to the article and approved the submitted version.

ACKNOWLEDGMENTS

The authors would like to thank Atsushi Kagimoto, MD, Yoshinori Handa, MD, PhD, Takashi Kumada, MD, and Takahiro Mimae, MD, PhD, for the conception and interpretation of the article. The authors would like to thank Enago (www.enago.jp) for the English language review.

SUPPLEMENTARY MATERIAL

The Supplementary Material for this article can be found online at: https://www.frontiersin.org/articles/10.3389/fonc.2021.622742/full#supplementary-material

Supplementary Figure 1 | Receiver operating characteristic curve of solid component size to predict recurrence. AUC, area under the curve.

REFERENCES

1. Aberle DR, Adams AM, Berg CD, Black WC, Clapp JD, Fagerstrom RM, et al. Reduced Lung Cancer Mortality With Low-Dose Computed Tomographic Screening. *N Engl J Med* (2011) 365:395–409. doi: 10.1056/NEJMoa1102873
2. Uehara H, Tsutani Y, Okumura S, Nakayama H, Adachi S, Yoshimura M, et al. Prognostic Role of Positron Emission Tomography and High-Resolution Computed Tomography in Clinical Stage IA Lung Adenocarcinoma. *Ann Thorac Surg* (2013) 96:1958–65. doi: 10.1016/j.athoracsur.2013.06.086
3. Okami J, Shintani Y, Okumura M, Ito H, Ohtsuka T, Toyooka S, et al. Demographics, Safety and Quality, and Prognostic Information in Both the Seventh and Eighth Editions of the TNM Classification in 18,973 Surgical Cases of the Japanese Joint Committee of Lung Cancer Registry Database in 2010. *J Thorac Oncol* (2019) 14:212–22. doi: 10.1016/j.jtho.2018.10.002
4. Nair VS, Barnett PG, Ananth L, Gould MK. Veterans Affairs Solitary Nodule Accuracy Project Cooperative Studies Group. PET Scan 18f-Fluorodeoxyglucose Uptake and Prognosis in Patients With Resected Clinical Stage IA Non-Small Cell Lung Cancer. *Chest* (2010) 137:1150–6. doi: 10.1378/chest.09-2356
5. Rami-Porta R, Bolejack V, Crowley J, Ball D, Kim J, Lyons G, et al. The IASLC Lung Cancer Staging Project: Proposals for the Revisions of the T Descriptors in the Forthcoming Eighth Edition of the TNM Classification for Lung Cancer. *J Thorac Oncol* (2015) 10:990–1003. doi: 10.1097/JTO.0000000000000559
6. Travis WD, Asamura H, Bankier AA, Beasley MB, Detterbeck F, Flieder DB, et al. The IASLC Lung Cancer Staging Project: Proposals for Coding T Categories for Subsolid Nodules and Assessment of Tumor Size in Part-Solid Tumors in the Forthcoming Eighth Edition of the TNM Classification of Lung Cancer. *J Thorac Oncol* (2016) 11:1204–23. doi: 10.1016/j.jtho.2016.03.025
7. Goldstraw O, Chansky K, Crowley J, Rami-Porta R, Asamura H, Eberhardt WE, et al. The IASLC Lung Cancer Staging Project: Proposals for Revision of the TNM Stage Groupings in the Forthcoming (Eighth) Edition of the TNM Classification for Lung Cancer. *J Thorac Oncol* (2016) 11:39–51. doi: 10.1016/j.jtho.2015.09.009
8. Tsutani Y, Miyata Y, Nakayama H, Okumura S, Adachi S, Yoshimura M, et al. Prognostic Significance of Using Solid Versus Whole Tumor Size on High-Resolution Computed Tomography for Predicting Pathologic Malignant Grade of Tumors in Clinical Stage IA Lung Adenocarcionma: A Multicenter Study. *J Thorac Cardiovasc Surg* (2012) 143:607–12. doi: 10.1016/j.jtcvs.2011.10.037
9. Tsutani Y, Miyata Y, Mimae T, Kushitani K, Takeshima Y, Yoshimura M, et al. The Prognostic Role of Pathologic Invasive Component Size, Excluding Lepidic Growth, in Stage I Lung Adenocarcinoma. *J Thorac Cardiovasc Surg* (2013) 146:580–5. doi: 10.1016/j.jtcvs.2013.04.032
10. Tsutani Y, Miyata Y, Nakayama H, Okumura S, Adachi S, Yoshimura M, et al. Solid Tumor Size on High-Resolution Computed Tomography and Maximum Standardized Uptake on Positron Emission Tomography for New Clinical T Descriptors With T1 Lung Adenocarcinoma. *Ann Oncol* (2013) 24:2376–81. doi: 10.1093/annonc/mdt230
11. Maeyashiki T, Suzuki K, Hattori A, Matsunaga T, Takamochi K, Oh S. The Size of Consolidation on Thin-Section Computed Tomography Is a Better Predictor of Survival Than the Maximum Tumour Dimension in Resectable Lung Cancer. *Eur J Cardiothorac Surg* (2013) 43:915–8. doi: 10.1093/ejcts/ezs516
12. Murakawa T, Konoeda C, Ito T, Inoue Y, Sano A, Nagayama K, et al. The Ground Glass Opacity Component Can Be Eliminated From T-Factor Assessment of Lung Adenocarcinoma. *Eur J Cardiothorac Surg* (2013) 43:925–32. doi: 10.1093/ejcts/ezs467
13. Tsutani Y, Miyata Y, Yamanaka T, Nakayama H, Okumura S, Adachi S, et al. Solid Tumors Versus Mixed Tumors With a Ground-Glass Opacity Component in Patients With Clinical Stage IA Lung Adenocarcinoma: Prognostic Comparison Using High-Resolution Computed Tomography Findings. *J Thorac Cardiovasc Surg* (2013) 146:17–23. doi: 10.1016/j.*jtcvs*.2012.11.019
14. Hattori A, Hirayama S, Matsunaga T, Hayashi T, Takamochi K, Oh S, et al. Distinct Clinicopathologic Characteristics and Prognosis Based on the Presence of Ground Glass Opacity Component in Clinical Stage IA Lung Adenocarcinoma. *J Thorac Oncol* (2019) 14:265–75. doi: 10.1016/j.jtho.2018.09.026
15. Hattori A, Suzuki K, Takamochi K, Wakabayashi M, Aokage K, Saji H, et al. Prognostic Impact of a Ground-Glass Opacity Component in Clinical Stage IA non-Small Cell Lung Cancer. *J Thorac Cardiovasc Surg* (2020) 161:1469–80. doi: 10.1016/j.jtcvs.2020.01.107
16. Mimae T, Tsutani Y, Miyata Y, Imai K, Ito H, Nakayama H, et al. Solid Tumor Size of 2 Cm Divides Outcomes of Patients With Mixed Ground Glass Opacity Lung Tumors. *Ann Thorac Surg* (2020) 109:1530–6. doi: 10.1016/j.athoracsur.2019.12.008
17. Kagimoto A, Tsutani Y, Mimae T, Miyata Y, Ikeda N, Ito H, et al. Preoperative Nivolumab to Evaluate Pathological Response in Patients With Stage I Non-Small Cell Lung Cancer: A Study Protocol of Phase II Trial (POTENTIAL). *BMJ Open* (2021) 11:e043234. doi: 10.1136/bmjopen-2020-043234
18. Kagimoto A, Tsutani Y, Izaki Y, Handa Y, Mimae T, Miyata Y, et al. Prediction of Lymph Node Metastasis Using Semiquantitative Evaluation of PET for Lung Adenocarcinoma. *Ann Thorac Surg* (2020) 110:1036–42. doi: 10.1016/j.athoracsur.2020.03.032
19. Postmus PE, Kerr KM, Oudkerk M, Senan S, Waller DA, Vansteenkiste J, et al. Early and Locally Advanced Non-Small-Cell Lung Cancer

(NSCLC): ESMO Clinical Practice Guidelines for Diagnosis, Treatment and Follow-Up. *Ann Oncol* (2017) 28(suppl 4):iv1–iv21. doi: 10.1093/annonc/mdx222

Conflict of Interest: The authors declare that the research was conducted in the absence of any commercial or financial relationships that could be construed as a potential conflict of interest.

frontiers in Oncology

ORIGINAL RESEARCH
published: 05 August 2021
doi: 10.3389/fonc.2021.698053

Evaluation of the Radiomics Method for the Prediction of Atypical Adenomatous Hyperplasia in Patients With Subcentimeter Pulmonary Ground-Glass Nodules

Bin Wang[1], *Preeti Hamal*[2], *Xue Meng*[2], *Ke Sun*[1], *Yang Yang*[1], *Yangyang Sun*[2*] *and Xiwen Sun*[1*]

[1] Department of Radiology, Shanghai Pulmonary Hospital, Tongji University School of Medicine, Shanghai, China,
[2] Department of Radiology, Shanghai East Hospital, Tongji University School of Medicine, Shanghai, China

OPEN ACCESS

Edited by:
Chen Chen,
Central South University, China

Reviewed by:
Xianning Wu,
University of Science and Technology of China, China
Guangjian Zhang,
The First Affiliated Hospital of Xi'an Jiaotong University, China

***Correspondence:**
Yangyang Sun
syy940311@163.com
Xiwen Sun
sunxiwen5256@163.com

Specialty section:
This article was submitted to Cancer Imaging and Image-directed Interventions, a section of the journal Frontiers in Oncology

Received: 20 April 2021
Accepted: 16 July 2021
Published: 05 August 2021

Citation:
Wang B, Hamal P, Meng X, Sun K, Yang Y, Sun Y and Sun X (2021) Evaluation of the Radiomics Method for the Prediction of Atypical Adenomatous Hyperplasia in Patients With Subcentimeter Pulmonary Ground-Glass Nodules. Front. Oncol. 11:698053. doi: 10.3389/fonc.2021.698053

Objectives: We aimed to develop a prediction model to distinguish atypical adenomatous hyperplasia (AAH) from early lung adenocarcinomas in patients with subcentimeter pulmonary ground-glass nodules (GGNs), which may help avoid aggressive surgical resection for patients with AAH.

Methods: Surgically confirmed cases of AAH and lung adenocarcinomas manifesting as GGNs of less than 1 cm were retrospectively collected. A prediction model based on radiomics and clinical features identified from a training set of cases was built to differentiate AAH from lung adenocarcinomas and tested on a validation set.

Results: Four hundred and eighty-five eligible cases were included and randomly assigned to the training (n = 339) or the validation sets (n = 146). The developed radiomics prediction model showed good discrimination performance to distinguish AAH from adenocarcinomas in both the training and the validation sets, with, respectively, 84.1% and 82.2% of accuracy, and AUCs of 0.899 (95% CI: 0.867–0.931) and 0.881 (95% CI: 0.827–0.936).

Conclusion: The prediction model based on radiomics and clinical features can help differentiate AAH from adenocarcinomas manifesting as subcentimeter GGNs and may prevent aggressive resection for AAH patients, while reserving this treatment for adenocarcinomas.

Keywords: lung neoplasms, radiomics, tomography; spiral computed, forecasting, thoracic surgery

INTRODUCTION

The detection rate of lung ground-grass nodules (GGNs) is increasing rapidly, many of which are identified as atypical adenomatous hyperplasia (AAH), whereas others are early lung adenocarcinomas (1, 2). Determining appropriate timing of surgical intervention for treatment of neoplastic GGNs represents a big challenge in clinics. Lung AAH consists of proliferating type II alveolar pneumocytes and/or Clara cells, which display different cellular and molecular manifestations compared to lung adenocarcinomas (3, 4), and is usually considered as a precancerous lesion (5, 6). Yet, in clinical practice, AAH nodules are also considered benign. Therefore, the patients with AAH may need different treatment strategies than those with adenocarcinomas and require a follow-up approach rather than surgery. Nevertheless, a large part of the patients with AAH have undergo surgical treatment because of the difficulty to discriminate between AAH and adenocarcinomas based solely on preoperative CT images. Thus, accurate diagnosis of AAH *versus* neoplastic GGNs is essential to decision-making on the treatment to provide to the patients and would help surgeons determine which patients with GGNs should receive surgical treatment and avoid unnecessary or premature surgeries.

Radiomics is a new method that can transform medical images into large numbers of detailed quantitative tumors features, at histologic, cytologic, molecular, and even genetic levels (7–10). The use of radiomics allows doctors to get not only conventional measurements and eye observations, but also abundant microscale quantitative features of the tumor lesions that can help provide precision diagnosis for the patients (11–14). In addition, much research already used radiomics to assist the pathological classification of lung adenocarcinomas. Many of these studies demonstrated that the radiomics method had a better diagnostic performance than radiologists using traditional medical imaging methods (15–17).

Although many studies developed tools for the prediction of lung adenocarcinomas based on radiomics, there has been no research aiming at distinguishing AAH from lung adenocarcinomas. However, accurate discrimination between AAH and early lung adenocarcinomas is of utmost significance to help doctors determine whether a patient is suitable for follow-up or surgical treatment. In this study, we attempted to differentiate AAH from adenocarcinomas manifesting as subcentimeter GGNs. To our knowledge, this is the first study aiming to predict AAH using radiomics method, and we hope that the introduction of our precise predictive approach will help personalized management for patients with malignant GGNs.

MATERIALS AND METHODS

Patients

This study was approved by the institutional review board of our hospital. Owing to the retrospective nature of this research, the provision of informed consent form signed by the patients was waived.

The hospital electronic medical records and radiology working system were searched for cases of lung GGNs, identified as AAH and early lung adenocarcinomas by surgeries between January 2018 and October 2019, and complying with the inclusion criteria. Since AAH is generally considered benign and follow-up treatment is usually recommended, the AAH cases identified by surgeries were a lot fewer than the cases of early-stage lung adenocarcinomas, including adenocarcinoma *in situ*, minimally invasive adenocarcinoma, and invasive adenocarcinoma. To get similar numbers of AAH and adenocarcinomas cases, all AAH cases and 30% of the adenocarcinoma cases, selected by stratified sampling according to the pathological types, were included in the preliminary data of our study. These preliminary data were further selected against the exclusion criteria. The inclusion and exclusion criteria are as follows.

The inclusion criteria were (i) preoperative CT examination performed within 1 month before the surgery; (ii) GGNs' maximum diameter ≤1 cm; (iii) CT image layer thickness <2 mm; (iv) peripheral GGNs; and (v) confirmed as adenocarcinomas or AAH by surgery. The exclusion criteria were (i) obvious artifacts around the nodules on CT images; (ii) injected with contrast medium for CT; and (iii) tightly connected with the pleura.

The demographics and clinical data of the patients (e.g., age and gender) were also collected. Finally, the included nodules were assigned to a training or a validation set at a 7:3 ratio. The study flowchart is shown in **Supplementary Figure S1**.

CT Image Acquisition

The preoperative CT examinations were conducted at deep inspiration to avoid the influence of respiratory artifacts. The scanned images were acquired on a Brilliance 40 scanner (Philips Medical Systems, Netherlands) and a Somatom Definition AS scanner (Siemens Medical Systems, Germany). The CT scan parameters and conditions were as follows: 120 kV, 180–220 mAs, 64 × 0.625 mm or 40 × 0.625 mm detector, 0.4 or 1.0 pitch, 512 × 512 matrix, reconstructed at 1.0 mm thickness with 0.7 mm increment, and a standard soft tissue kernel.

Pathologic Diagnosis

The final pathologic classification was based on histological diagnosis from postoperative paraffin sections. Most diagnoses were made by two pathologists. In case of disagreement, a third senior pathologist was invited to participate to the diagnosis of the disputed case. The results were reported according to the classification of lung adenocarcinomas made by the International Association for the Study of Lung Cancer/American Thoracic Society/European Respiratory Society in 2011.

Segmentation of Lung Nodules

To extract the region of interest (ROI) from the CT images, a segmentation was performed using the 3D-slicer software (version of 4. 11). Additional manual corrections were conducted by a radiologist with 6 years of experience in the diagnosis of chest imaging and reviewed by another radiologist with 20 years of experience in diagnosis based on chest imaging.

Extraction of Radiomics Features

The radiomic features were extracted from the segmented ROI area and classified into three categories: intensity, shape, and texture features. Except for the shape features, all features could be obtained from one or several filters, including wavelet, square root, square, gradient, logarithm, gaussian Laplace (LoG) filters, and exponential filters (18).

Radiomics Features Selection

In the training set, the selection of radiomics features was conducted before the model construction. A Kruskal–Wallis test was used to investigate the relationship between the features and the pathological diagnosis of the selected nodules. A correlation matrix was used to remove redundant features. The absolute columnar mean correlation (CWAAC) was calculated for each feature. When the correlation coefficient of each pair exceeded the 0.8 threshold, the feature was considered with high CWAAC value and was removed.

Finally, intra- and interclass correlation coefficients (ICCs) were used to estimate the intra- and interobserver reproducibility of the radiomics feature extraction. We randomly chose 50 cases for segmentation and feature extraction. The ROI segmentation of these 50 cases was conducted by two radiologists. Then, the first radiologists repeated the same process after 1 week. ICC > 0.75 indicated good agreement of the feature extractions (12).

Construction of the Radiomics Prediction Model

After selection of the radiomics features, the prediction model was constructed by a random forest method using the training set and tested with the validation set. The ROC curves, AUC value, accuracy, specificity, positive predictive value (PPV), and negative predictive value (NPV) were used to evaluate the predictive performance of the established radiomics model.

Statistical Analysis

The quantitative clinical and radiomics characteristics are shown as mean ± standard deviation or median [25th–75th]; qualitative characteristics are shown as *n* (%). Comparisons of qualitative features were achieved by the Chi-square test or Fisher exact test, whereas comparisons of quantitative features were performed using a *t*-test or Wilcoxon test. Differences reaching a P value < 0.05 by two-tailed tests were considered statistically significant. The statistical analysis was performed with R statistical software (version 3.3.1) and SPSS software (version 20.0).

RESULTS

Clinical Information

The initial search retrieved 1,417 nodules matching the inclusion criteria, of which 190 were AAH cases and 1,227 were adenocarcinoma cases. We randomly selected 30% of the adenocarcinoma cases and all AAH cases for our primary study. Then, according to the exclusion criteria, 17 AAH and 56 adenocarcinomas cases were excluded. Six AAH and 21 adenocarcinomas cases had obvious respiration artifacts around the nodules, 4 AAH and 16 adenocarcinomas cases had been injected with contrast medium for CT, and 7 AAH and 19 adenocarcinomas cases were tightly connected with the pleura. In total, 485 nodules, including 173 AAH cases, 193 AIS cases, 99 MIA cases, and 20 IAC cases from 443 patients were included in our final study. Examples of selected nodules are shown in **Figure 1**. For every 10 modules, 7 were randomly assigned to the training set, and the remaining 3 were assigned to the validation set (7:3 ratio). The process of random selection was performed according to the stratified sampling method based on pathological results. Eventually, 121 AAH and 218 adenocarcinoma cases constituted the training set, and 52 AAH and 94 adenocarcinoma cases constituted the validation set. Detailed information related to the selected nodules is shown in **Table 1**. The study flowchart is shown in **Supplementary Figure S1**.

Selection of the Radiomics Features

Initially, the number of extracted radiomics features was 386. After Kruskal–Wallis tests, correlation tests, and ICC assessment, 46 radiomics features were retained. Then, the random forest method was used for further selection of 57 features, including 46 radiomics features and 11 traditional features (listed in **Table 1**). The 57 features were classified by order of importance using the random forest method (**Figure 2**). Seventeen features (including 11 radiomics and 6 traditional features), the importance level of which surpassed 0.02, were selected to establish a prediction model. The 11 selected radiomics features are shown in **Supplementary Table S1**, and 6 traditional features (long diameter, maximum CT value, variance of CT value, mean CT value, minimum CT value, and volume) are shown in **Table 1**.

Establishment of a Radiomics Prediction Model

We aimed to construct a prediction model to distinguish AAH and adenocarcinomas manifesting as subcentimeter GGNs. The selected 11 radiomics and 6 clinical features were used to construct a prediction model based on the training set, according to the random forest classifier. The performance of the established model was further tested on the validation set. The diagram of the prediction model is shown in **Figure 3**.

Performance of the Radiomics Prediction Model

The detailed prediction results obtained with the radiomics model are shown in **Table 2**. The predictive accuracy was 84.1% and 82.2% in the training and the validation set, respectively. The specificity, positive predictive value, and negative predictive values were all over 70% (**Table 3**). The AUC of the prediction model was 0.899 (95% CI: 0.867–0.931) and 0.881 (95% CI: 0.827–0.936) for, respectively, the training and the validation set (**Figure 4**). Compared with the training set, the predictive performance of the radiomics model on the validation set was not significantly lower. These indicators demonstrated that our newly established prediction model

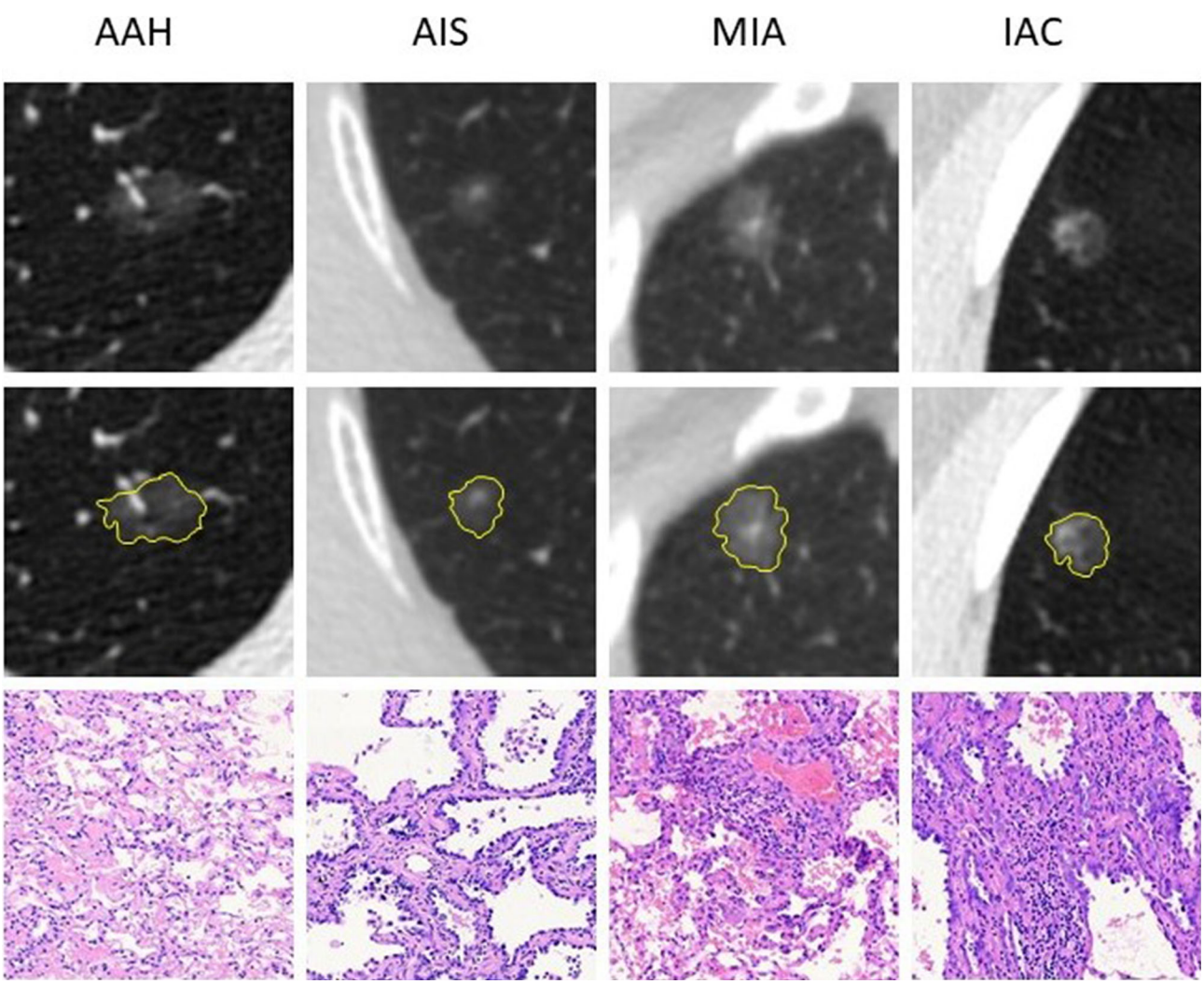

FIGURE 1 | Examples of the included nodules. The yellow shadow represents the shape of the lesions. The pathological pictures are from paraffin sections [hematoxylin and eosin (H&E), ×100 for AAH, AIS, and MIA; H&E, ×40 for IAC]. AAH, atypical adenomatous hyperplasia; AIS, adenocarcinoma *in situ*; MIA, minimally invasive adenocarcinoma; IAC, invasive adenocarcinoma.

performs well to discriminate between AAH and early lung adenocarcinomas with subcentimeter GGNs.

DISCUSSION

Lung cancer is the most common cancer and the primary cause of cancer-related death (19) and adenocarcinomas have been the main histological subtype of lung cancer (20). The widening utilization of chest CT in clinics has reduced the mortality of lung cancer (21, 22), while increasing the detection of many subcentimeter GGNs. Proper management strategy for these detected GGNs is very important for the overall control of lung cancer because of the high prognosis variability linked to different stages of lung adenocarcinomas (23, 24). AAH is considered a precancerous adenocarcinoma lesion. Therefore, accurate discrimination between AAH and adenocarcinomas would be beneficial to the personalized treatment of these two different GGNs. At present, preoperative CT images are the most useful tools to identify the pathologic stage of GGNs. However, a large part of AAH and subcentimeter adenocarcinomas may have only little morphological differences on CT images and are difficult to distinguish for the radiologists. This difficulty may lead to many AAH nodules being treated by aggressive surgical treatment as if they were adenocarcinomas.

Some studies investigated the performance of the radiomics method to predict the pathologic classification of GGNs (16, 17). However, these studies did not try to differentiate AAH nodules from adenocarcinomas. In addition, the diameter of the nodules included in these studies was less than 3 cm, but few AAH nodules had a diameter greater than 1 cm. Consequently, the pathological classification of subcentimeter nodules remained a

TABLE 1 | Clinical information of the cases in the training and the validation sets.

Clinical features	Training set			Validation set		
	AAH (*n* = 121)	Adenocarcinomas (*n* = 218)	*p*	AAH (*n* = 52)	Adenocarcinomas (*n* = 94)	*p*
Age (years)	50.2 ± 10.1	48.6 ± 11.5	0.193	51.8 ± 11.3	49.5 ± 10.3	0.208
Gender			0.296			0.410
Male	41 (33.9)	62 (28.4)		16 (30.8)	23 (24.5)	
Female	80 (66.1)	156 (71.6)		36 (69.2)	71 (75.5)	
Nodule type			<0.01			<0.05
Pure GGNs	36 (29.8)	33 (15.1)		19 (36.5)	20 (21.3)	
Part solid GGNs	85 (70.2)	185 (84.9)		33 (63.5)	74 (78.7)	
Location (lobe)			0.253			0.246
Upper right	42 (34.7)	71 (32.6)		14 (26.9)	22 (23.4)	
Middle right	13 (10.7)	32 (14.7)		6 (11.5)	13 (13.8)	
Lower right	41 (33.9)	57 (26.1)		18 (34.6)	23 (24.5)	
Upper left	18 (14.9)	49 (22.5)		9 (17.3)	31 (33.0)	
Lower left	7 (5.8)	9 (4.1)		5 (9.6)	3 (5.3)	
Long diameter	9.0 [7.5, 10.2]	9.8 [-8.7, 11.0]	<0.001	8.2 [7.1, 9.2]	9.9 [9.0, 11.2]	<0.001
Short diameter	6.1 [5.5, 7.1]	6.7 [5.9, 7.6]	<0.001	5.9 [4.9, 6.5]	6.7 [5.8, 7.5]	<0.001
Mean CT value	−666.5 [−698.7, −629.8]	−591.8 [−651.5, −540.7]	<0.001	−670.3 [−697.6, −642.1]	−595.7 [−643.1, −533.3]	<0.001
Maximum CT value	−574.0 [−655.0, −494.5]	412.0 [−548.5, −289.8]	<0.001	−580.0 [−649.8, −507.8]	−404 [−504.7, −284.8]	<0.001
Minimum CT value	−800 [−800, −786]	−800 [−800, −768.0]	<0.001	−800 [−800, −789.0]	−800 [−800, −764.3]	<0.001
Variance of CT value	60.8 [39.2, 85.9]	105.5 [71.6, 135.8]	<0.001	59.9 [43.8, 77.5]	109.2 [79.7, 141.7]	<0.001
Volume	219.9 [143.8, 302.0]	281.8 [215.8, 399.5]	<0.001	176.4 [120.7, 246.4]	300.5 [207.6, 404.9]	<0.001

Mean CT value, maximum CT value, minimum CT value, and variance of CT value were measured in the largest circle within the lesion at the maximum cross-section.
AAH, atypical adenomatous hyperplasia.

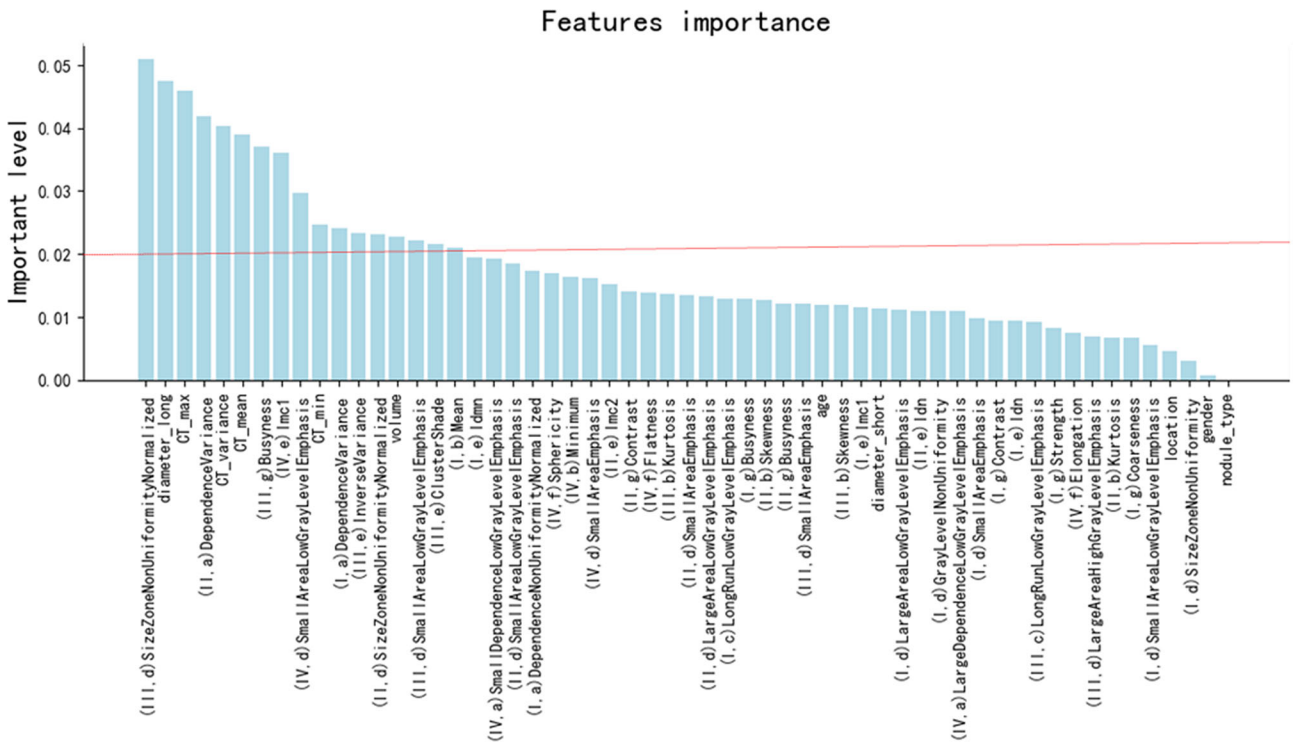

FIGURE 2 | The order of the importance level of the radiomics features and clinical features. I: the filter of log_sigma_5_0_mm, II: the filter of log_sigma_4_0_mm, III: the filter of log_sigma_3_0_mm, IV: from original pictures. a: Gray Level Dependence Matrix features, b: First-Order features, c: Gray Level Run Length Matrix features, d: Gray Level Size Zone Matrix features, e: Gray Level Co-occurrence Matrix feature, f: Shape features, g: Neighboring Gray Tone Difference Matrix features. CT_max, CT_variance, CT_mean, and CT_min indicate maximum CT value, variance of CT value, mean CT value, and minimum CT value, respectively.

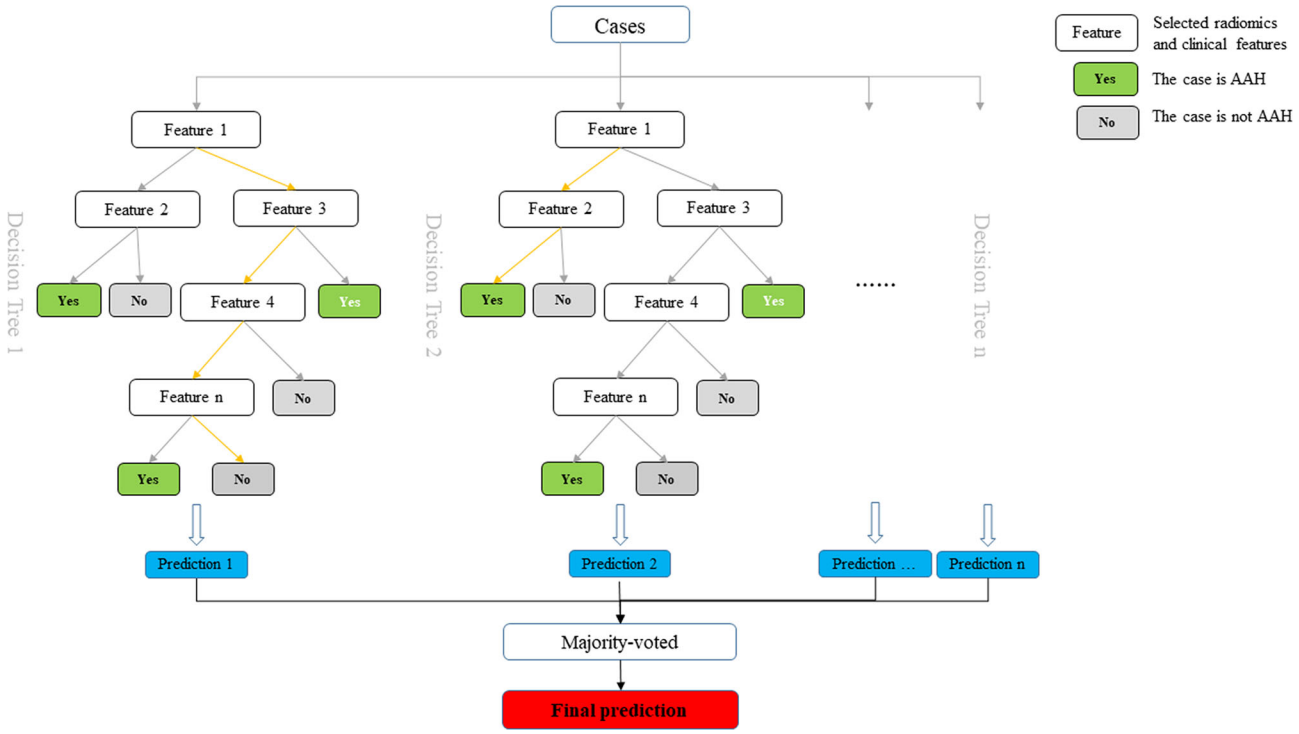

FIGURE 3 | The diagram of established prediction model based on random forest classifier.

TABLE 2 | Confusion matrix of the prediction results obtained from the validation set by the prediction model.

Predictions	Final pathological classification		
	AAH (*n* = 52)	Adenocarcinomas (*n* = 94)	Total (*n* = 146)
AAH	44 (84.6%)	18 (19.1%)	62
Adenocarcinomas	8 (15.4%)	76 (80.9%)	84

Adenocarcinomas include adenocarcinoma in situ, minimally invasive adenocarcinoma, and invasive adenocarcinoma.
AAH, atypical adenomatous hyperplasia.

problem to be solved in clinics. Therefore, we sought to investigate whether a prediction model based on radiomics and clinical features could be used as an effective method to discriminate between these two pathologic types of GGNs.

The accuracy of our newly developed radiomics prediction model was 84.1% and 82.2% in the training and the validation set, respectively (**Table 3**). This accuracy was satisfactory for both sets, and the performance for the validation set displayed no significant reduction compared to that obtained for the training set. These results demonstrated the stability of the prediction model, although further validation is needed. In addition, the sensitivity, specificity, PPV, and NPV were all above 70%, which indicated a good comprehensive performance for the prediction model. Similarly, the analysis by ROC curves revealed AUCs of the prediction model of 0.899 (95% CI: 0.867–0.931) and 0.881 (95% CI: 0.827–0.936) for the training and validation set, respectively (**Figure 4**), indicative of good performance. These indicators proved that our prediction model, based on radiomics

TABLE 3 | Performance of the radiomics model on the training and the validation sets.

Group	Accuracy	Sensitivity	Specificity	PPV	NPV
Training set	84.1%	78.5%	87.2%	77.2%	88.0%
Validation set	82.2%	84.6%	80.9%	71.0%	90.5%

PPV, positive predictive value; NPV, negative predictive value.

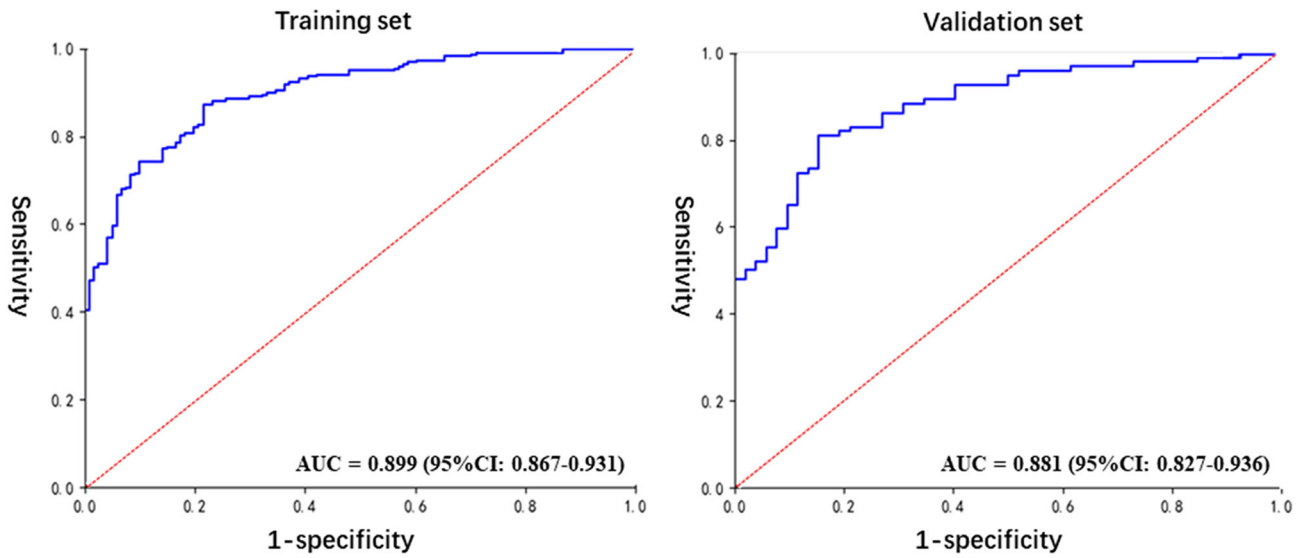

FIGURE 4 | The ROC curves for the diagnosis of the radiomics model in the training and validation sets.

and traditional features, is an effective method to distinguish AAH and adenocarcinomas manifesting as subcentimeter GGNs on CT images.

Ranking of the features' importance level (**Figure 2**) revealed that the radiomics features were as important as the main clinical features. One radiomics feature was in the top three most important features, and four radiomics features were found in the top 10 most important features. These results demonstrate the necessity and meaningfulness of introducing the radiomics method to clinical practice to improve tumor diagnosis.

In this study, one of the most important inclusion criteria was that the diameter of the nodules was less than 1 cm, rather than 3 cm in other studies, to better fit the clinical needs. Preoperative pathological prediction on subcentimeter GGNs is a big challenge for clinicians, because the pathological classification of these lesions, based on different morphological features, is usually difficult to achieved with the naked eye. In this study, our prediction model reached a satisfactory prediction performance, although the included nodules had stricter requirement on the diameter criteria than other studies.

The main limitation of our research was the lack of multicenter data and prospective validation. Therefore, our newly established radiomics classifier will need further stability and applicability validation. Our future research will expand the size of the data set and conduct multicenter clinical trials to verify and improve the effectiveness of the model.

CONCLUSION

This study showed that our newly established prediction model performed well in discriminating between AAH and early adenocarcinomas manifesting as subcentimeter lung GGNs on CT images. This model has the potential to improve preoperative prediction accuracy for AAH nodules and may help avoid aggressive surgical treatment for AAH patients. In the future, larger multicenter data and prospective validations will be needed to improve and test the clinical values of this new radiomics classifier.

DATA AVAILABILITY STATEMENT

The raw data supporting the conclusions of this article will be made available by the authors, without undue reservation.

ETHICS STATEMENT

The studies involving human participants were reviewed and approved by Shanghai Pulmonary Hospital, Tongji University School of Medicine. Written informed consent for participation was not required for this study in accordance with the national legislation and the institutional requirements. Written informed consent was not obtained from the individual(s) for the publication of any potentially identifiable images or data included in this article.

AUTHOR CONTRIBUTIONS

The XS and YS proposed the study. BW and PH conducted the research and wrote the manuscript. XM, YY auxiliarily analyzed the data. KS collected and classified the data. All authors contributed to the article and approved the submitted version.

FUNDING

This work was supported by the Natural Science Foundation of Shanghai [Grant Number 19ZR1443100] and clinical research project of Shanghai pulmonary hospital [Grant Number fk18007].

SUPPLEMENTARY MATERIAL

The Supplementary Material for this article can be found online at: https://www.frontiersin.org/articles/10.3389/fonc.2021.698053/full#supplementary-material

REFERENCES

1. Sawada S, Komori E, Nogami N, Segawa Y, Shinkai T, Yamashita M. Evaluation of Lesions Corresponding to Ground-Glass Opacities That Were Resected After Computed Tomography Follow-Up Examination. *Lung Cancer* (2009) 65(2):176–9. doi: 10.1016/j.lungcan.2008.11.013
2. Liu YN, Sun H, Zhou F, Su CX, Gao GH, Ren SX, et al. Imaging Features of TSCT Predict the Classification of Pulmonary Preinvasive Lesion, Minimally and Invasive Adenocarcinoma Presented as Ground Glass Nodules. *Lung Cancer* (2017) 108:192–7. doi: 10.1016/j.lungcan.2017.03.011
3. Ogata S, Kameda K, Kono T, Ozeki Y, Hashimoto H, Tominaga S, et al. Expressions of ATF6, XBP1, and GRP78 in Normal Tissue, Atypical Adenomatous Hyperplasia, and Adenocarcinoma of the Lung. *Hum Pathol* (2019) 83:22–8. doi: 10.1016/j.humpath.2018.08.009
4. Sivakumar S, Lucas FAS, McDowell TL, Lang WH, Xu L, Fujimoto J, et al. Genomic Landscape of Atypical Adenomatous Hyperplasia Reveals Divergent Modes to Lung Adenocarcinoma. *Cancer Res* (2017) 77(22):6119–30. doi: 10.1158/0008-5472.CAN-17-1605
5. Kadara H, Scheet P, Wistuba II, Spira AE. Early Events in the Molecular Pathogenesis of Lung Cancer. *Cancer Prev Res (Phila)* (2016) 9(7):518–27. doi: 10.1158/1940-6207.CAPR-15-0400
6. Mori M, Rao SK, Popper HH, Cagle PT, Fraire AE. Atypical Adenomatous Hyperplasia of the Lung: A Probable Forerunner in the Development of Adenocarcinoma of the Lung. *Mod Pathol* (2001) 14(2):72–84. doi: 10.1038/modpathol.3880259
7. Tu WT, Sun GY, Fan L, Wang Y, Xia Y, Guan Y, et al. Radiomics Signature: A Potential and Incremental Predictor for EGFR Mutation Status in NSCLC Patients, Comparison With CT Morphology. *Lung Cancer* (2019) 132:28–35. doi: 10.1016/j.lungcan.2019.03.025
8. Chang C, Sun X, Wang G, Yu H, Zhao W, Ge Y, et al. A Machine Learning Model Based on PET/CT Radiomics and Clinical Characteristics Predicts ALK Rearrangement Status in Lung Adenocarcinoma. *Front Oncol* (2021) 11:603882. doi: 10.3389/fonc.2021.603882
9. Zhu XZ, Dong D, Chen ZD, Fang MJ, Zhang LW, Song JD, et al. Radiomic Signature as a Diagnostic Factor for Histologic Subtype Classification of Non-Small Cell Lung Cancer. *Eur Radiol* (2018) 28(7):2772–8. doi: 10.1007/s00330-017-5221-1
10. Zhang B, Qi S, Pan X, Li C, Yao Y, Qian W, et al. Deep CNN Model Using CT Radiomics Feature Mapping Recognizes EGFR Gene Mutation Status of Lung Adenocarcinoma. *Front Oncol* (2021) 10:598721. doi: 10.3389/fonc.2020.598721
11. Park HJ, Park B, Lee SS. Radiomics and Deep Learning: Hepatic Applications. *Korean J Radiol* (2020) 21(4):387–401. doi: 10.3348/kjr.2019.0752
12. Wu SX, Zheng JJ, Li Y, Yu H, Shi SY, Xie WB, et al. A Radiomics Nomogram for the Preoperative Prediction of Lymph Node Metastasis in Bladder Cancer. *Clin Cancer Res* (2017) 23(22):6904–11. doi: 10.1158/1078-0432.CCR-17-1510
13. Kniep HC, Madesta F, Schneider T, Hanning U, Schönfeld MH, Schön G, et al. Radiomics of Brain MRI: Utility in Prediction of Metastatic Tumor Type. *Radiology* (2019) 290(2):479–87. doi: 10.1148/radiol.2018180946
14. Lee SH, Park H, Ko ES. Radiomics in Breast Imaging From Techniques to Clinical Applications: A Review. *Korean J Radiol* (2020) 21(7):779–92. doi: 10.3348/kjr.2019.0855
15. Fan L, Fang MJ, Li ZB, Tu WT, Wang SP, Chen WF, et al. Radiomics Signature: A Biomarker for the Preoperative Discrimination of Lung Invasive Adenocarcinoma Manifesting as a Ground-Glass Nodule. *Eur Radiol* (2019) 29(2):889–97. doi: 10.1007/s00330-018-5530-z
16. She YL, Zhang L, Zhu HY, Dai CY, Xie D, Xie HK, et al. The Predictive Value of CT-Based Radiomics in Differentiating Indolent From Invasive Lung Adenocarcinoma in Patients With Pulmonary Nodules. *Eur Radiol* (2018) 28(12):5121–8. doi: 10.1007/s00330-018-5509-9
17. Xue X, Yang Y, Huang Q, Cui F, Lian YQ, Zhang SY, et al. Use of a Radiomics Model to Predict Tumor Invasiveness of Pulmonary Adenocarcinomas Appearing as Pulmonary Ground-Glass Nodules. *BioMed Res Int* (2018) 2018:6803971. doi: 10.1155/2018/6803971
18. van Griethuysen JJM, Fedorov A, Parmar C, Hosny A, Aucoin N, Narayan V, et al. Computational Radiomics System to Decode the Radiographic Phenotype. *Cancer Res* (2017) 77(21):e104–7. doi: 10.1158/0008-5472.CAN-17-0339
19. Siegel RL, Miller KD, Jemal A. Cancer Statistics, 2020. *CA Cancer J Clin* (2020) 70(1):7–30. doi: 10.3322/caac.21590
20. Ito H, Matsuo K, Tanaka H, Koestler DC, Ombao H, Fulton J, et al. Nonfilter and Filter Cigarette Consumption and the Incidence of Lung Cancer by Histological Type in Japan and the United States: Analysis of 30-Year Data From Population-Based Cancer Registries. *Int J Cancer* (2011) 28:1918–28. doi: 10.1002/ijc.25531
21. de Koning HJ, van der Aalst CM, de Jong PA, Scholten ET, Nackaerts K, Heuvelmans MA, et al. Reduced Lung-Cancer Mortality With Volume CT Screening in a Randomized Trial. *N Engl J Med* (2020) 382(6):503–13. doi: 10.1056/NEJMoa1911793
22. National Lung Screening Trial Research Team, Aberle DR, Adams AM, Berg CD, Black WC, Clapp JD, et al. Reduced Lung-Cancer Mortality With Low-Dose Computed Tomographic Screening. *N Engl J Med* (2011) 365(5):395–409. doi: 10.1056/NEJMoa1102873
23. Fan XH, Zhang XY, Wang HM, Jin B. Reevaluation of Survival and Prognostic Factors in Pathologic Stage I Lung Adenocarcinoma by the New 2009 TNM Classification. *Tumour Biol* (2014) 35(6):5905–10. doi: 10.1007/s13277-014-1781-8
24. Travis WD, Brambilla E, Noguchi M, Nicholson AG, Geisinger KR, Yatabe Y, et al. International Association for the Study of Lung Cancer/American Thoracic Society/European Respiratory Society International Multidisciplinary Classification of Lung Adenocarcinoma. *J Thorac Oncol* (2011) 6(2):244–85. doi: 10.1097/JTO.0b013e318206a221

Conflict of Interest: The authors declare that the research was conducted in the absence of any commercial or financial relationships that could be construed as a potential conflict of interest.

Publisher's Note: All claims expressed in this article are solely those of the authors and do not necessarily represent those of their affiliated organizations, or those of the publisher, the editors and the reviewers. Any product that may be evaluated in this article, or claim that may be made by its manufacturer, is not guaranteed or endorsed by the publisher.

frontiers in Oncology

ORIGINAL RESEARCH
published: 08 September 2021
doi: 10.3389/fonc.2021.705888

Decreased IL-6 and NK Cells in Early-Stage Lung Adenocarcinoma Presenting as Ground-Glass Opacity

Pengfei Zhang[1,2†], Boxue He[1,2†], Qidong Cai[1,2], Guangxu Tu[1,2], Xiong Peng[1,2], Zhenyu Zhao[1,2], Weilin Peng[1,2], Fenglei Yu[1,2], Min Wang[3], Yongguang Tao[1,2,4,5] and Xiang Wang[1,2*]*

[1] Department of Thoracic Surgery, Second Xiangya Hospital, Central South University, Changsha, China, [2] Hunan Key Laboratory of Early Diagnosis and Precision Therapy, Second Xiangya Hospital, Central South University, Changsha, China, [3] Department of Laboratory Medicine, Second Xiangya Hospital, Central South University, Changsha, China, [4] Key Laboratory of Carcinogenesis and Cancer Invasion, Ministry of Education, Department of Pathology, Xiangya Hospital, Central South University, Changsha, China, [5] National Health Commission of the People's Republic of China (NHC), Key Laboratory of Carcinogenesis (Central South University), Cancer Research Institute and School of Basic Medicine, Central South University, Changsha, China

OPEN ACCESS

Edited by:
Kezhong Chen, Peking University People's Hospital, China

Reviewed by:
Edouard Auclin, Hôpital Européen Georges-Pompidou (HEGP), France
Jianxiang Li, Soochow University Medical College, China

***Correspondence:**
Yongguang Tao
taoyong@csu.edu.cn
Xiang Wang
wangxiang@csu.edu.cn

[†]These authors have contributed equally to this work

Specialty section:
This article was submitted to Thoracic Oncology, a section of the journal Frontiers in Oncology

Received: *06 May 2021*
Accepted: *13 August 2021*
Published: *08 September 2021*

Citation:
Zhang P, He B, Cai Q, Tu G, Peng X, Zhao Z, Peng W, Yu F, Wang M, Tao Y and Wang X (2021) Decreased IL-6 and NK Cells in Early-Stage Lung Adenocarcinoma Presenting as Ground-Glass Opacity. Front. Oncol. 11:705888. doi: 10.3389/fonc.2021.705888

Background: Lung ground-glass opacities (GGOs) are an early manifestation of lung adenocarcinoma. It is of great value to study the changes in the immune microenvironment of GGO to elucidate the occurrence and evolution of early lung adenocarcinoma. Although the changes of IL-6 and NK cells in lung adenocarcinoma have caught global attention, we have little appreciation for how IL-6 and NK cells in the lung GGO affect the progression of early lung adenocarcinoma.

Methods: We analyzed the RNA sequencing data of surgical specimens from 21 patients with GGO-featured primary lung adenocarcinoma and verified the changes in the expression of IL-6 and other important immune molecules in the TCGA and GEO databases. Next, we used flow cytometry to detect the protein expression levels of important Th1/Th2 cytokines in GGO and normal lung tissues and the changes in the composition ratio of tumor infiltrating lymphocytes (TILs). Then, we analyzed the effect of IL-6 on NK cells through organoid culture and immunofluorescence. Finally, we explored the changes of related molecules and pathway might be involved.

Results: IL-6 may play an important role in the tumor microenvironment of early lung adenocarcinoma. Further research confirmed that the decrease of IL-6 in GGO tissue is consistent with the changes in NK cells, and there seems to be a correlation between these two phenomena.

Conclusion: The IL-6 expression status and NK cell levels of early lung adenocarcinoma as GGO are significantly reduced, and the stimulation of IL-6 can up-regulate or activate NK cells in GGO, providing new insights into the diagnosis and pathogenesis of early lung cancer.

Keywords: early lung adenocarcinoma, IL-6, NK cells, tumor microenvironment, ground-glass opacities

INTRODUCTION

Lung cancer is the leading cause of cancer-related mortality worldwide, killing an estimated 1.6 million people each year, with 5-year overall survival rates ranging from 85% in stage IA to 6% in stage IV (1). Thanks to high-resolution computed tomography (HRCT), the diagnosis of ground-glass opacity or ground-glass nodules (GGO or GGN) found in the surrounding lung field is increasing (2, 3). GGO is defined radiologically as a focal lesion that visually preserves lung parenchyma, airways, and blood vessels in it (4). GGO can be regarded as the symbol of both benign or malignant lesions, and its occurrence and growth are involved in various molecular changes (5). Many of these GGOs are associated with early lung adenocarcinoma (LUAD) which is the dominant histologic subtype in lung cancer (2). A consensus on the importance of preoperative characterization of lesions has been reached. The molecular and cellular changes in GGO may provide new insights into the pathogenesis of early lung adenocarcinoma.

Abnormality in the immune microenvironment is one of the most important characteristics of cancer initiation and progression. For example, the expression of the Programmed Death-Ligand 1 (PD-L1) stimulated by the PD-1/PD-L1 axis is a major immunosuppressive mechanism in non-small cell lung cancer (NSCLC) (6, 7). Some tumor-infiltrating lymphocytes (TILs) also are closely tied with cytokines in the tumor microenvironment (8). Many preclinical and clinical studies have shown that tumor-infiltrating lymphocytes (TILs) such as CD3+ cells, CD8+ cells, or CD45RO+ cells have the potential to be used as prognostic markers (9). Besides, in addition to immune cells, cytokines such as interleukins (IL)-4 and IL-6 also play a prominent role in the process of tumor immunity (8, 10). According to the theory of the cancer-immunity cycle, multistep processes along with various molecules and immune cells are involved in lung cancer such as the release of inflammatory cytokines, the recruitment of immune cells, the recognition of immune cells with tumor cells, and so on (11, 12). It will be more accurate and reliable to consider more steps in this cycle, that is, find more valuable biomarkers and further analyze their impact on pathological types and disease prognosis.

MATERIALS AND METHODS

Acquisition of Clinical Samples

All specimens were collected from the specimen bank of our center (Department of Thoracic Surgery, Second Xiangya Hospital, Central South University) by members of this project.

The specimens collected met the following conditions: (1) The GGO tissue and paired normal lung tissue were surgically resected and got reserved in liquid nitrogen or got intervention immediately. The GGO tissue was collected from the middle of the primary lesion, and each pair of normal lung tissue and lung cancer tissue were from the same patient; (2) The diameter of each sample was more than 5 mm and less than 2 cm. The volume of each sample was less than 1/2 of the volume of the primary lesion; (3) All the collected specimens were confirmed as lung adenocarcinoma (LUAD) by the Department of Pathology; (4) The patients had not received any form of radiotherapy, chemotherapy, targeted drug therapy, immune drug therapy, and other tumor therapies before the operation; (5) The patients had no special systemic diseases or other diseases that affected the experimental results; (6) Specimens were obtained with the informed consent of the patients and the approval of the ethics committee.

At the same time, we collected some clinical characteristics of the GGO patients in the cohort, including age, gender, smoking history, differentiation, TNM stage, the expression of PD-L1.

Study Cohort and RNA-seq

Totally, 73 primary lung GGO patients intended for surgical removal at the Thoracic Surgery Department of the Second Xiangya Hospital were involved in our study between February 2020 and August 2021. Because that the GGO size limited repeated usage of a lot of specimens, we finally utilized 21 pairs of tissues for RNA-seq, 26 for flow cytometry (in which a representational one for immunohistochemical staining), 1 for organoid culture, and 25 for qPCR. All the GGO samples were demonstrated to be early lung adenocarcinoma (mostly IA stage) pathologically. A panel of RNA sequencing (RNA-seq) was performed by BGI Gene Biological Company (Wuhan, China, http://www.genomics.cn/) with 21 pairs of surgical GGO specimens and normal lung tissues. All patients allowed specimen collection, clinical data provision, and biomarker analysis by written informed consent prior to enrolling in the study. We completed the study according to the Declaration of Helsinki with a protocol approved by the Ethics Committee of the Second Xiangya Hospital, Central South University, Changsha (Project identification code: 2020S609).

Flow Cytometry

Flow cytometry was performed as per manufacturer's protocol asked. BD Multitest CD3/CD8/CD45/CD4 reagent and BD Multitest CD3/CD16+CD56/CD45/CD19 reagent (BD Bioscience, CA, USA) were used to measure the lymphocyte percentage. Human Th1/Th2/Th17 Phenotyping Kit (Cell-Genebio, China) was used for the determination of IL-2, IL-4, IL-6, IL-10, TNF-α, IFN-γ, and IL-17a. All tests were performed on FACSCalibur (BD Biosciences, USA) instruments. The software FlowJo (LLC, version 10.6.0) was used for the data analysis.

Data From TCGA, GEO, and Other Literature

To verify the flow cytometry results of IL-6 in lung adenocarcinoma, common shared RNA-seq data of LUAD were selected from the TCGA (The Cancer Genome Atlas) database (https://portal.gdc.cancer.gov/). The data were gotten from 59 normal cases and 535 tumors. GSE40419 RNA-seq dataset was selected from GEO (Gene Expression Omnibus) database, among which 77 normal samples and 87 LUAD tumor samples were selected, and FPKM (Fragments Per Kilobase per Million) was used to demonstrate the expression. To reinforce the generality of the results in GGO, we cited shared data in a study of lung GGO from Lee H et al. (13). In this study,

researchers did a RNA-seq between 9 pairs of normal lung tissue and GGO tissue, and the pathological results of all the 9 GGO tissues are lung adenocarcinoma.

Multiple Staining Immunohistochemical

Immunohistochemical staining was performed on 10% formalin-fixed and paraffin-embedded tissues. Antibodies of CD16 (Anti-CD16: Abcam, ab246222, at a dilution of 1:100), CD56 (Anti-NCAM1: Abcam, ab75813, at a dilution of 1:100), IL-6 (Anti-IL6: Bioworld, MB9296, at a dilution of 1:50), and PD-1 (Anti-PD-1: Abcam, ab137132, at a dilution of 1:250) were used. By the way, in the stained sections PD-1 was negative, we predicted that there is not any PD-1 expression in the selected samples, so it was not reflected in the text. The mean gray value method was used for the quantification of immunohistochemistry and immunofluorescence by ImageJ (NIH 64-bit Java 1.8.0).

Organoid Culture and Immunofluorescence

After surgical removal of fresh GGO tissue and normal lung tissue, each tissue block is clipped into about 200mg. The specific steps of organoid culture were shown in **Figure S1**, where IL-6 was applied by PEPROTECH (Recombinant Human IL-6, Catalog:200-06, USA, at the concentration of 2ng/ml). The culture scaffolds (Millipore, PIHP01250, USA) were used as containers. Small molecules added in culture: EGF, FGF-10, FGF-basic and HGF (PEPROTECH, USA), N2, B27 (ThemerFisher, USA). Tissues were collected for immunofluorescence followed by the standard protocol. Two antibodies CD16 (Proteintech, 16559-1-AP, China, at the dilution of 1:100), and CD56 (Proteintech, 14255-1-AP, China, at the dilution of 1:3000) were used. The administration of IL-6 and controlled PBS for three groups is with 0h/24h/48h duration.

RNA Isolation and Quantitative Real-Time PCR

Total cellular RNA was isolated from tissue samples by Trizol reagent (Invitrogen) and reversely transcribed into cDNA using the SuperScript First Strand cDNA system (Invitrogen) according to the manufacturer's protocol. The qPCR amplifications were performed in an Applied Biosystems Stepone Plus System (Applied Biosystems, Foster, CA) using an SYBR Green PCR Master Mix (Roche, Indianapolis, IN). Primer sequences used for performing qRT-PCR are as follows:

IL-6 forward, 5′-CACTGGTCTTTTGGAGTTTGAG-3′;
IL-6 reverse, 5′-GGACTTTTGTACTCATCTGCAC-3′;
CD16 forward, 5′-GGTGACTTGTCCACTCCAGTGT-3′;
CD16 reverse, 5′-ACCATTGAGGCTCCAGGAACAC-3′;
CD56 forward, 5′-CATCACCTGGAGGACTTCTACC-3′;
CD56 reverse, 5′-CAGTGTACTGGATGCTCTTCAGG-3′;
PD-1 forward, 5′-AAGGCGCAGATCAAAGAGAGCC-3′;
PD-1 reverse, 5′-CAACCACCAGGGTTTGGAACTG-3′;
PD-L1 forward, 5′-CGTTGTGCTTGAACCCTTGA-3′;
PD-L1 reverse, 5′-ACACAAGGAGCTCTGTTGGA-3′;
JAK1 forward, 5′-GAGACAGGTCTCCCACAAACAC-3′;
JAK1 reverse, 5′-GTGGTAAGGACATCGCTTTTCCG-3′;
STAT3 forward, 5′-CTTTGAGACCGAGGTGTATCACC-3′;
STAT3 reverse, 5′-GGTCAGCATGTTGTACCACAGG-3′;
β-actin forward, 5′-AAAGACCTGTACGCCAACAC-3′;
β-actin reverse, 5′-GTCATACTCCTGCTTGCTGAT-3′.

Results are expressed as mean ± SD of three independent experiments.

Statistical Analysis

All data were analyzed by SPSS 22.0 software (SPSS, Chicago, IL) and plotted by GraphPad Prism 8.0 software (GraphPad Software, La Jolla, CA). Paired T-test was performed to obtain p values between two groups when complete one-to-one correspondence, otherwise the unpaired t-test was used. A $p > 0.05$ was considered statistically nonsignificant (ns), while the statistical difference levels were set at $^*P < 0.05$; $^{**}P < 0.01$; $^{***}P < 0.001$; $^{****}P < 0.0001$.

RESULTS

Genes in Immune Regulation Behaved Abnormally in Lung GGO Tissues

After screening the results of RNA-seq, 1654 differentially expressed genes between normal and GGO tissues were obtained ($|FC| \geq 2$, $p < 0.05$), of which 572 were up-regulated in GGO and other 1082 were down-regulated (**Figure 1A, B**). It was illustrated that most of the down-regulated genes involved in immune regulation varied greatly, whereas the interleukin 6 (IL-6), CXCL13, MMP9, and some other genes seem to take crucial roles in related gene pathway models (**Figure 1C, D**). However, previous studies have shown that blocked IL-6 can inhibit the progression of some lung cancers (14), which is obviously inconsistent with our conclusion. Thus, we tried to take further study to explore this contradiction.

The Lower Expression of IL-6 In Lung GGO Tissues

We selected 21 pairs of fresh normal lung tissue and lung GGO tissue samples, extracted their proteins *in vitro*, and detected the content of IL-2, IL-4, IL-6, IL-10, TNF-α, IFN-γ, and IL-17a by cytometric bead array (CBA) microsphere method of flow cytometry (**Figure 2A** and **Supplementary Table S1**). The results showed that the expression of IL-6 in normal tissues was significantly higher than that in GGO tissues (P = 1.2e-2). Then we tried to discuss whether several important clinical characteristics affect the decrease of IL-6 in GGO patients. The result shows that age (P=0.897), gender (P=0.609), smoking history (P=0.993), differentiation (P=0.476), T stage (P=0.691) and PD-L1 (P=428) do not influence the downregulation of IL-6 (**Table 1**). To explore whether the changing trend of IL-6 level in lung adenocarcinoma from public databases is the same as our experimental result, we queried the mRNA expression of IL-6 in The Cancer Genome Atlas (TCGA) database and Gene Expression Omnibus (GEO, GSE40419)dataset—whose samples are also tissues rather than serum—and found a consistent result that the IL-6 is down-expressed in lung

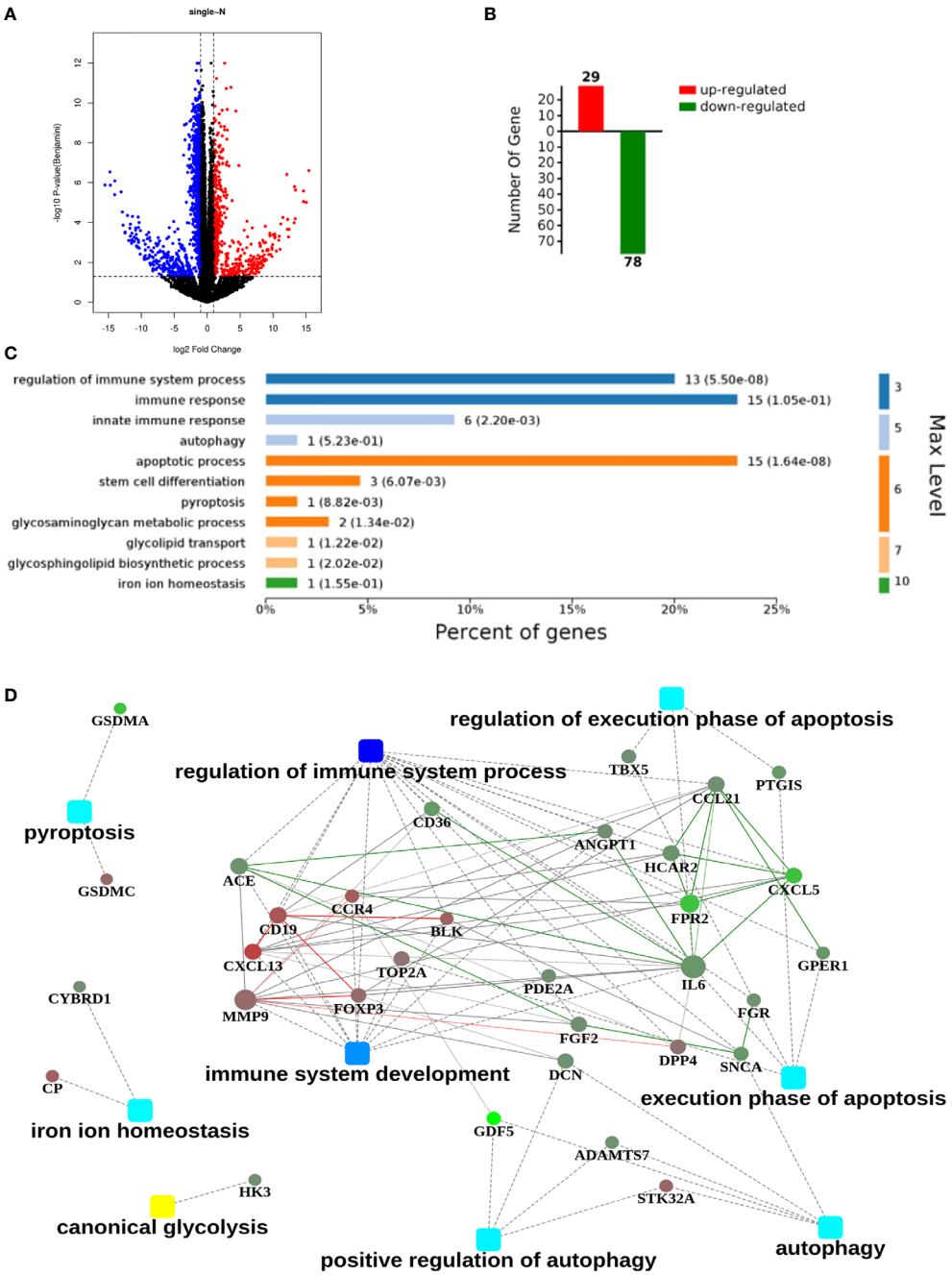

FIGURE 1 | An RNA sequencing (RNA-seq) analysis with 21 pairs of surgical GGO specimens and normal lung tissues from primary lung GGO patients. **(A, B).** Process of obtaining the up-regulated and down-regulated genes after RNA-seq in GGO (|Fold Change|≥2, p<0.05). **(C, D).** Clustering of differentially expressed genes and the related hub genes in different pathways. Square nodes represent different pathways and round nodes represent hub genes; the size of the circle represents the number of nodes involved in hub genes.

adenocarcinoma, where P value equals to 7.21e-26 and 4.29e-07, respectively (**Figure 2B** and **Supplementary Table S2**). Then we explored the shared transcriptome sequencing results from Lee H et al. In this cohort which included 9 normal tissues and 9 GGO tissues, the expression of IL-6 seems decreased in GGO as we predicted (**Supplementary Figure S2**).

The Amount of NK Cells Is Down-Regulated in Lung GGO Tissues

To simultaneously explore the changes of immune cells in the GGO tumor microenvironment, we got single-cell suspensions from 23 GGO tissues and the paired normal tissues, then applied cell differentiation by flow cytometry (**Figure 3A, B** and

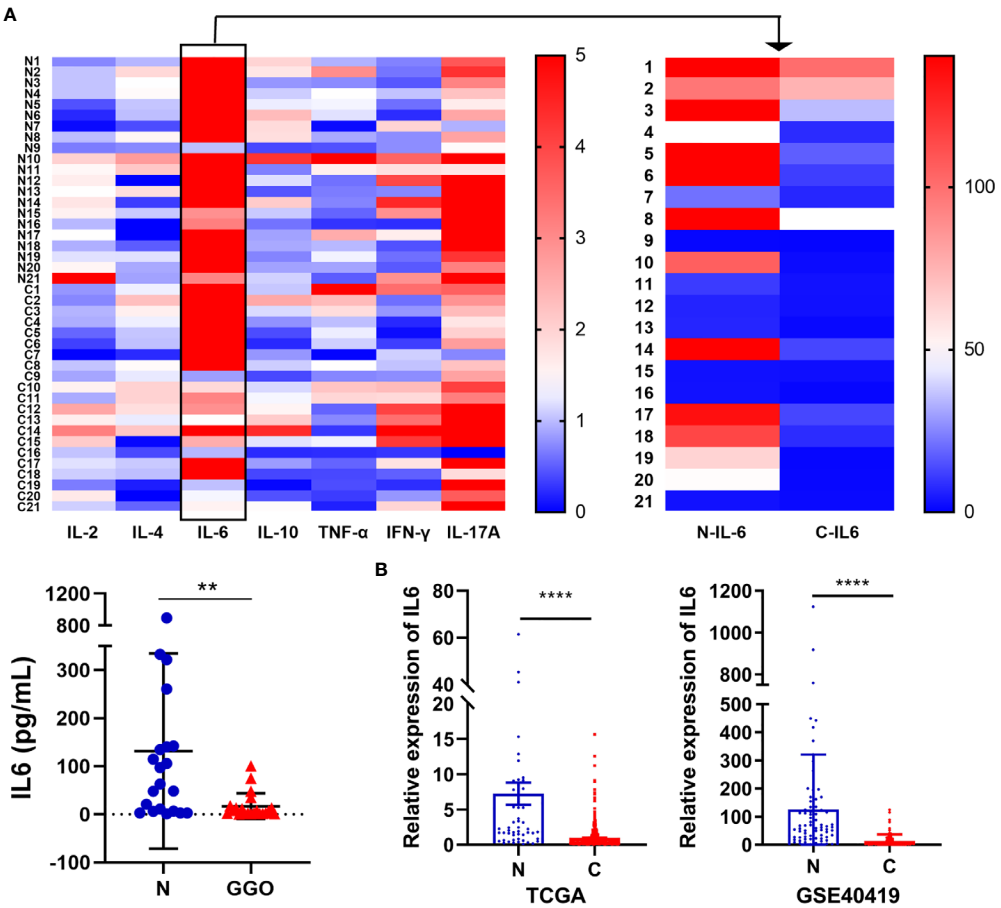

FIGURE 2 | The decrease of IL-6 in lung adenocarcinoma with GGO. **(A)** The flow cytometry result of several cytokines. The heatmap shows the expression status of 7 cytokines in 21 GGO patients (upper), while the scatter plot shows the expression of IL-6 (lower). **(B)** The mRNA level of IL-6 in TCGA (left, 59 normal and 535 cancer) and GEO (GSE40419) database (right, 77 normal and 87 cancer). Each dot represents an individual patient. Results are expressed as mean ± SEM. **P < 0.01; ****P < 0.0001. N, normal; C, cancer. .

TABLE 1 | The fold change (FC) of IL-6 expression level with main characteristic of the patients in the flow cytometry.

Characteristics	n	Average FC of IL-6	P value
Age			0.897
<60	11	0.299	
≥60	10	0.230	
Gender			0.609
Female	15	0.299	
Male	6	0.230	
Smoking history			0.993
No	17	0.279	
Yes	4	0.280	
Differentiation			0.476
Well	8	0.224	
Else	13	0.313	
T stage			0.691
T1a	8	0.436	
T1b	13	0.517	
PD-L1			0.428
Negative	6	0.207	
Positive	12	0.307	

Supplementary Table S3). The 6th patient had 3 GGO tissues, and 16 of the other patients got overlapped in the cytokines test. We examined the percentages of T cell ($CD45^+CD3^+$), $CD4^+$ T cell ($CD45^+CD3^+CD4^+$), $CD8^+$ T cell ($CD45^+CD3^+CD8^+$), B cell ($CD45^+CD3^-CD19^+$ $CD16/CD56^-$), and natural killer (NK) cell ($CD45^+CD3^-CD19^-CD16/CD56^+$) in the total cell count, where the proportion of NK cells in normal lung tissues was statistically higher than that of GGO tissues (P = 9.2e-6), whereas the proportion of T cells (P = 7.4e-4), CD4 cells (P = 2.3e-4), and B cells (P = 6.5e-3) were all increased in GGO tissues. We also explore whether some clinical characteristics could affect the decrease of NK cells in GGO patients. The result shows that age (P=0.347), gender (P=0.263), smoking history (P=0.689), differentiation (P=0.528), T stage (P=0.636) and PD-L1 (P=267) do not influence the change of NK cells in GGO tissues (**Table 2**).The multiple staining immunohistochemical experiment and its quantified results also verified the differential expressions of IL-6, CD16, and CD56 between normal and GGO tissues (**Figure 3C** and **Supplementary Figure S3**), These results

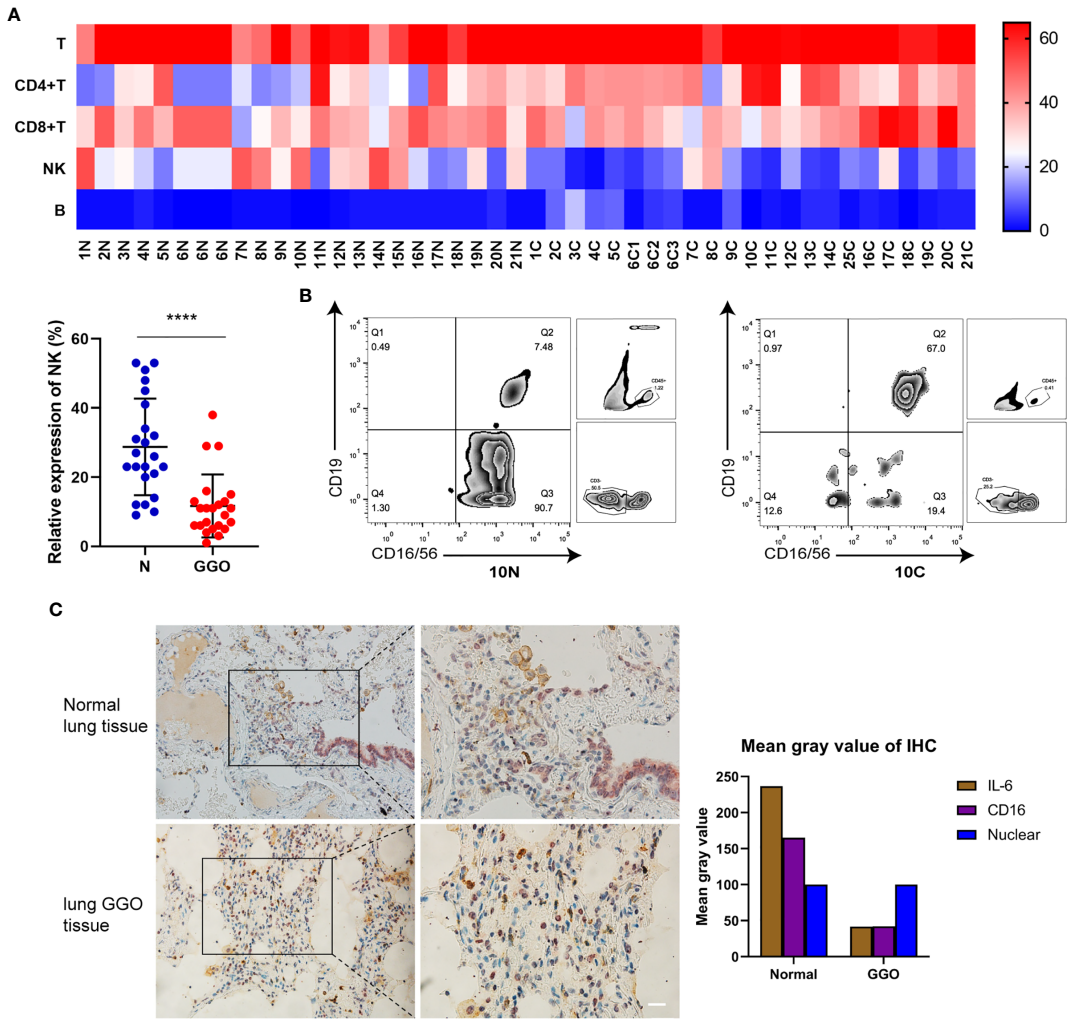

FIGURE 3 | The decrease of NK cells in lung adenocarcinoma with GGO. **(A)** The flow cytometry result of immune cells. The heatmap shows the expression status of 5 kinds of cells in 21 GGO patients (upper), and the scatter plot shows the expression of NK cells (lower). **(B)** The expression of NK cells (CD16/CD56+) on total CD45+CD3- cells within the lymphocyte gate from one representative patient with paired normal (left, 10N) and GGO (right, 10C) tissues. In the paired samples selected, NK cells in normal lung tissues made up about 90.7% of all non-T lymphocytes, while the content in GGO tissues was 19.4% around. **(C)** The multiple staining immunohistochemical results of IL-6 (in brown) and CD16 (in purple) in normal lung tissue or GGO lung tissue. Each dot represents an individual patient. Results are expressed as mean ± SEM. ****P<0.0001. N, normal; C, cancer. Scale bar, 50 μm.

further indicated the decreases in IL-6 and some important NK cell markers at the protein level in GGO.

The Effect of IL-6 on NK Cells

It has been preliminary elucidated that IL-6 secreted by tumor cells could restrict the activity and function of NK cells through the JAK1 pathway (15). However, the inconsistent changes in PD-1 and STAT3 are intriguing and seem to be incompatible with the classical IL-6 pathway, which requires further research. The dysfunction of NK cells favors tumor immune-evasion, so a comprehensive understanding and restoration of their functions mechanically will aid the treatment of lung cancer (16). Consequently, we analyzed the effect of IL-6 on NK cells preliminary by organoid tissue culture with normal lung tissue and lung GGO tissue from the same characteristic patient *in vitro*. Compared to the control group (treated with PBS), the markers of NK cells—CD16 and CD56—were up-regulated in the IL-6-treated group (**Figures 5A, B**). By quantifying the results of immunofluorescence (calculated by the mean gray values of different fluorescence channels), we found that there were consistent changes in normal lung organoid tissue, but the effect of IL-6 in increasing NK cells was more obvious in GGO organoid tissue (**Figures 4A, B**). Besides, considering the importance of NK cells for checkpoint immunotherapy (17), we analyzed gene expression data and overall survival information from TCGA, finding that the lower expression of NCAM1 (CD56), NKG2D, and NCR3 (three important markers of NK cells) indicated a poor prognosis of the lung

TABLE 2 | The fold change (FC) of NK cell expression level with main characteristic of the GGOs in the flow cytometry.

Characteristics	n	Average FC of NK cells	P value
Age			0.347
<60	12	0.391	
≥60	11	0.581	
Gender			0.263
Female	13	0.580	
Male	10	0.354	
Smoking history			0.689
No	18	0.503	
Yes	5	0.405	
Differentiation			0.528
Well	9	0.402	
Else	14	0.533	
T stage			0.636
T1a	10	0.416	
T1b	13	0.517	
PD-L1			0.267
Negative	8	0.333	
Positive	12	0.588	

Patient No.6 had 3 GGO nodules, which were included and calculated three times.

adenocarcinoma ($P < 0.05$, **Figure S4**). This laterally reflects the effect of decreased NK cells on tumor progression.

IL-6/JAK/STAT3 Pathways Function in Lung GGO Tissues

To further reveal whether these involved mechanisms mentioned before also are related to IL-6 and NK cells in early lung adenocarcinoma with GGO or not, we then compared the expression of seven genes (IL-6, CD16, CD56, PD-1, PD-L1, JAK1, and STAT3) with 25 pairs of early lung adenocarcinoma samples by quantitative real-time PCR (qPCR) (**Figure 5A** and **Supplementary Table S4**) and analyzed their expression data in RNA-seq (**Figure 5B** and **Supplementary Table S5**). Even though the relative expression of CD56 by qPCR did not have significant difference (P=2.73e-1 in qPCR, and P=1.66e-1 in RNA-seq), the expression of CD16 (P=1.74e-3 in qPCR, and P=1.42e-3 in RNA-seq) and IL-6 (P=1.37e-02 in RNA-seq, although P=5.28e-2 in qPCR) showed the consistent results by qPCR and RNA-seq both. We also found that PD-L1 (P=7.20e-4 in qPCR, although P=1.66e-1 in RNA-seq) and JAK1 (P=4.74e-2 in RNA-seq, although P=4.73e-1

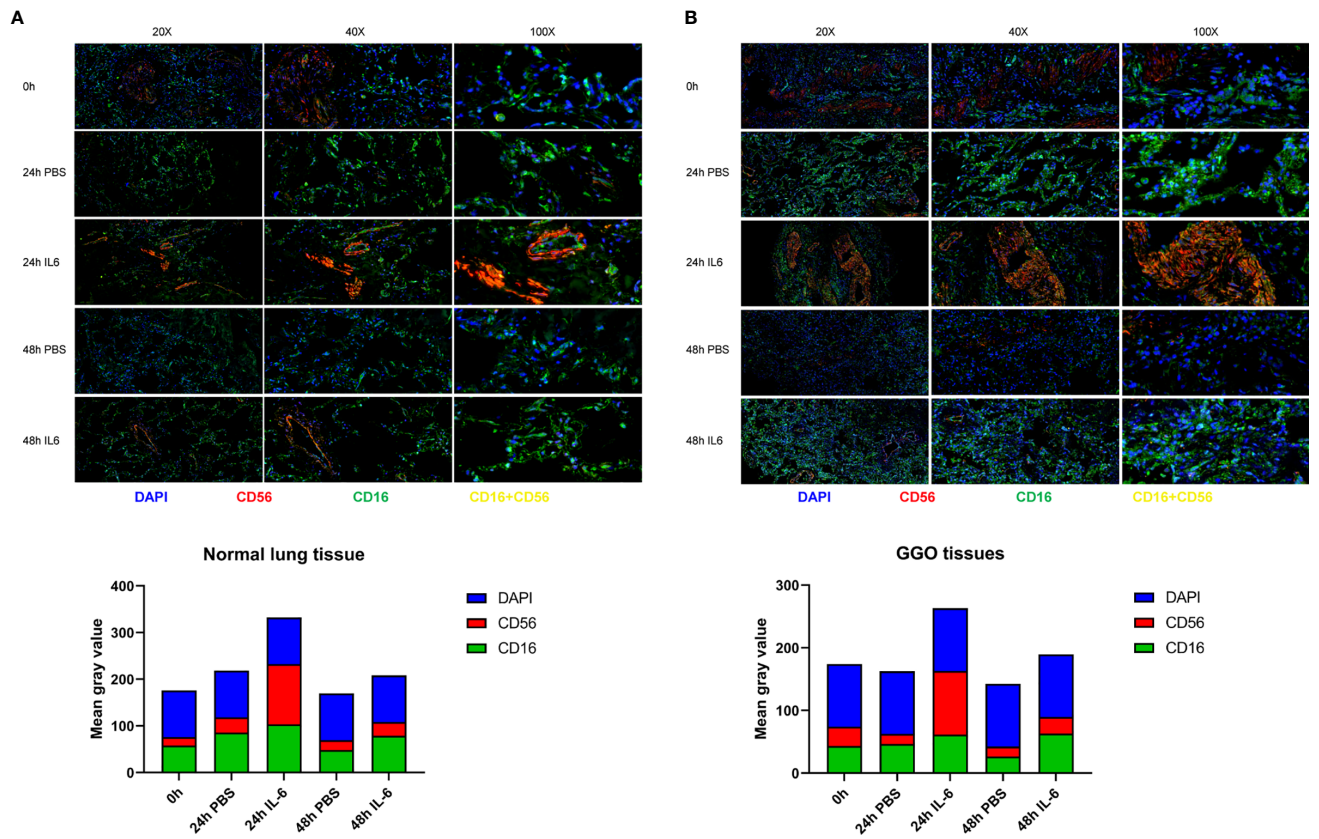

FIGURE 4 | The correlation between the expression of IL-6 and NK cells in lung adenocarcinoma with GGO. Images (upper) and the mean gray value (lower) show the immunofluorescence results in GGO tissues **(A)** and their paired normal tissues **(B)** after IL-6/PBS treatment.

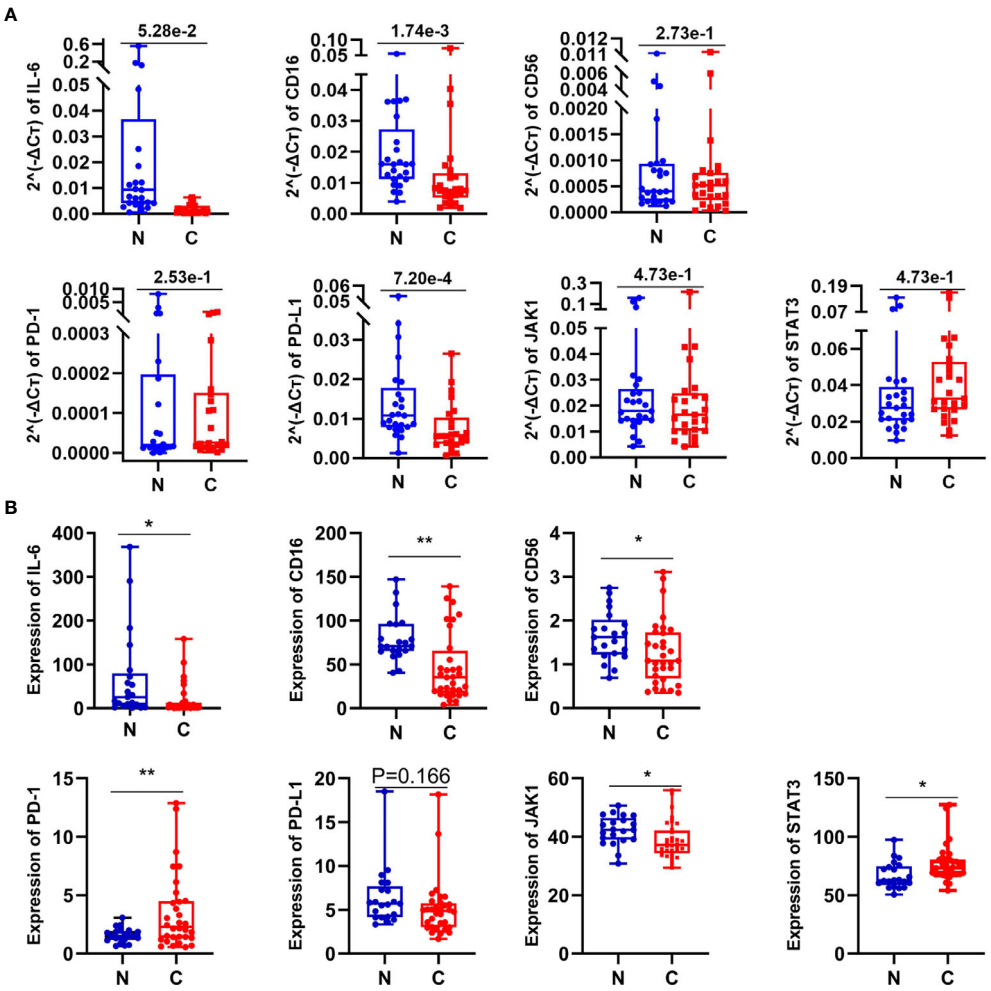

FIGURE 5 | The expression of some related molecules in lung GGO tissues. **(A)** Relative expression of seven genes in 25 paired normal and cancer tissues by qPCR. **(B)** The expression of seven genes reflected by RNA-seq data come from 21 GGO patients. Each dot represents an individual patient. Results are expressed as mean ± SEM. *P < 0.05; **P < 0.01. N, normal; C, cancer.

in qPCR) seems to be down-regulated in GGO, while PD-1 (P=8.70e-3 in RNA-seq, although P=2.53e-1 in qPCR) and STAT3 (P=1.76e-2 in RNA-seq, although P=4.73e-1 in qPCR) seems to be over-regulated in GGO.

DISCUSSION

Through the whole research process, we mainly drew two main conclusions: First, in the microenvironment of lung adenocarcinoma tissue with early lesions of GGO, IL-6 and NK cells showed a consistent decrease; Second, the decrease of NK cells is correlated with IL-6, and the proliferation or activation of NK cells can be stimulated by increasing IL-6 in the GGO tumor microenvironment. However, the specific mechanism of the increase of NK cells caused by IL-6 still needs to be further studied.

Interleukin-6 (IL-6) has been shown its significant characteristics in the pathological processes of inflammation, autoimmunity, and a series of cancers since its identification in the 1980s (18, 19). As a typical cytokine member of the IL-6 family, it was originally taken as B-cell stimulating factor-2 (BSF-2) which functions in immunoglobulin production (20). IL-6 binds to responding cells and takes various biological roles on them by working with transmembrane IL-6 receptors, as well as some soluble IL-6 receptors. It was widely accepted that IL-6 mainly exerted its effect through activating Janus kinase (JAK) family tyrosine kinases with the help of gp130, further causing the activation of regulatory factors such as signal transducer and activator of transcription (STAT) family transcription factors (mainly STAT3) and Src homology region 2 domain-containing phosphatase 2 (SHP-2) (21, 22). In previous studies, IL6 was generally considered as an important cancer-promoting molecule. To be more specific, IL-6 has been demonstrated to be responsible for

VEGF-dependent angiogenesis in cervical cancer (23); IL-6–activated STAT3 helps cell survival and promotes cell proliferation during colitis-induced tumorigenesis of gastrointestinal cancer (24); IL-6-induced epithelial-mesenchymal transition (EMT) is critical for the metastasis of breast cancer (25) and head and neck cancers (26). As for lung cancer, IL-6 was thought to promote cancer malignancy with the functions in migratory, chemotactic, and angiogenetic properties of cancer cells by USP24 (27); microRNA-218, a down-regulated miRNA that targets the IL-6/STAT3 pathway, was illustrated to suppress lung cancer (28); meanwhile, IL-6 blockade could reduce tumorigenesis in a kind of LUAD mouse model (29). A prospective study conducted by Barrera et al. demonstrated that there are higher levels of IL-6 in the plasma of patients with non-small-cell lung cancer (NSCLC) comparing to controls ($p = 0.001$) (30), while a retrospective analysis by Ryan et al. also showed IL-6 has a significant association with worse survival (hazard ratio, 1.33; 95% confidence interval, 1.08-1.64; $p = 0.007$) with hundreds of European American lung cancer patients (31). The information above all emphasized the positive relationship between IL-6 expression and cancer development. However, as we confirmed repeatedly, IL-6 was decreased in lung adenocarcinoma with GGO. So, there seems to be a contradiction in the early tumor microenvironment regarding the change of IL-6 level. We speculate that there is a different immune response in early lung GGO tissues than in solid tumors. It was reported that in the early stages of tumor growth, immune suppression decreases immune surveillance (32). It has also been shown that some tumor suppressor cells appear in the tumor microenvironment in the early stage of tumor development (33). Obeid E et al. found that a kind of important TILs—TAMs—initially infiltrated at the tumorigenesis site as a tumor-inhibitory phenotype (M1), and then transformed into tumor-promoting macrophages (M2) in the tumor microenvironment (34). These results indicated that the content of some immune components differed in different stages of the tumor.

Natural killer (NK) cells belong to the innate lymphoid cell (ILC) family that was initially described in 1973 (35, 36). They are of lymphoid origin and recognize MHC Class I (MHC-I) molecules by their cell surface inhibitory receptors (37). According to the expression of two markers (CD56 and CD16), NK cells are classified into two main subsets: $CD56^{dim}$ $CD16^{+}$ NK cells and $CD56^{bright}$ $CD16^{-}$ NK cells. The former subset is a mature cytotoxic group that accounts for the majority of circulating NK cells, while the latter subset is less mature, less cytotoxic, primarily immunomodulatory, and mostly be found in secondary lymphoid organs (38). It was well demonstrated that NK cells function in tumor immunosurveillance as they can kill cancer cells without prior sensitization (39–41). As a kind of important tumor-infiltrating lymphocytes (TILs), low-expressed NK cells are discovered on multiple cancers, which are linked with a poor prognosis of patients, too (42, 43). A single cell sequencing study of lung GGO and solid nodules concluded that NK cell cytotoxicity was lower in solid nodules, which showed that the function of the NK cell decreased during the progression of lung adenocarcinoma (44). Mechanism researches also indicate the functional improvement of NK cells may induce tumor regression (36, 45). A study on NSCLC showed there are fewer NK cells in cancer tissues than in normal lung tissues followed by obviously reduced cytolytic potential, which mostly be caused by the decrease of $CD56^{dim}$ $CD16^{+}$ NK cells (46). Another study also reported that NK cells principally infiltrate the tumor stroma of lung cancer, and low levels of NK cells are associated with a bigger primary cancer size, history of tobacco smoking, and poorer prognosis (47). Specifically, we noticed that natural killer (NK) cells have the potential to be key lymphocytes involved in the early stage of lung adenocarcinoma with GGO. The expression level of CD16 and CD56 tested by qPCR and RNA-seq also suggested that the number of NK cells mostly changed in the $CD56^{dim}$ $CD16^{+}$ subset. By the way, the decrease of NK cells could indicate a poorer overall survival status of LUAD patients, which further highlights its clinical significance.

By searching the literature, we found that IL-6 can affect the binding of PD-L1 and PD-1 on immune cells through the IL-6/JAK1/STAT3 pathway and mediate the immune escape of tumor cells, where IL-6 up-regulates PD-L1 by the glycosylation of PD-L1 (48). And in castration-resistant prostate cancer cells (CRPC), IL-6 knockdown would lead to the low expression of related proteins in the JAK/STAT3 pathway, which could down-regulate PD-L1 in CRPC cells and reduce its binding to PD-1 on the surface of NK cells, thus affecting the content of NK cells in the tumor microenvironment (49). It was also reported that JAK1 induces glycosylation of PD-L1 by phosphorylating PD-L1 protein-related sites (Y112), thereby promoting the stability of PD-L1, while IL-6 up-regulates PD-L1 by regulating the glycosylation of PD-L1. Therefore, IL-6 can affect the stability of PD-L1 and its binding to PD-1 on immune cells through the IL-6/JAK1/STAT3 pathway, thereby mediating the immune escape of tumor cells (48).

Through organoid culture, we concluded that exogenous addition of IL-6 to lung GGO tissues could stimulate the high expression of markers (CD16 and CD56) on the surface of NK cells. However, we have not determined whether IL-6 affects the content of NK cells or just activates the cytotoxic NK cells. IL-6 has been proved to directly improve the proliferation, cytotoxicity, and other important functions of NK cells (50). Research has shown that IL-6, which is abundant in the serum of patients got some infectious diseases, may downregulate NKG2D on NK cells, leading to impaired NK activity (51–53). However, it has also been demonstrated that down-regulation of IL-6 may also block IL-6-mediated NK cell activation through the effect of IL-2 or KIR2DL1 (54–56). The combined action of cytokine IL-6 and PGL-2 can reduce the immune factor IL-2 produced by Th1 cells and affect the activation of NK cells (57). These studies indicate that IL-6 may affect the content and function of NK cells through a variety of pathways, but its role in GGO still needs further experimental verification.

In this study, we briefly explored a possibly related pathway as well as several molecules we were interested in. Results illustrated that STAT3 may be influenced during the tumorigenesis process of lung GGO as it is expressed higher in the tumor tissues than in normal lung tissues, while the trend of JAK1 seems to be consistent with that of IL-6. Therefore, the hyperactivation of STAT3 maybe not according to the well-known IL-6/JAK/

STAT3 pathway (45). The STAT3 activation and signaling work through a variety of mechanisms not only related to IL-6, as SRC and some autocrine stimulation of growth factor receptors like EGFR can also lead to its induction (45). Besides, increased PD-1 and decreased PD-L1 seem to occur in the GGO tissues of lung adenocarcinoma, suggesting a probable molecular link with other changes in the immune microenvironment. The effect of IL-6 on NK cells also illustrated that there should be some underlying signaling pathway about IL-6 and NK cells in GGOs.

In summary, our study finds a significant decrease in IL-6 expression of early lung adenocarcinoma with GGO, along with the level of NK cells. It is a novel perspective that the stimulation of IL-6 can up-regulate NK cells in GGO. However, there are still some important points in the study that need to be further explored experimentally. First, why does IL-6 decrease occur in early lung adenocarcinoma manifested as GGO? We assume that it may be related to the overall low inflammatory response changes in the exceedingly early tumor microenvironment. Second, whether IL-6 affects NK cells by changing the number of NK cells in TME or by modulating the function of their surface receptors? Which may be verified by regulating the function of surface receptors.

The roles of IL-6 and NK cells in the production and development of GGO provide new insights into the early diagnosis and pathogenesis of lung adenocarcinoma. We believe further research could provide potential diagnostic biomarkers or available therapy targets for lung GGO and even take advanced benefits for studies about specific immune mechanisms in early lung adenocarcinoma.

DATA AVAILABILITY STATEMENT

The original contributions presented in the study are publicly available. This data can be found here: https://github.com/xxeyywx/RNA-seq-GGO.git. Publicly available datasets were analyzed in this study. This data can be found in **Supplementary Material**.

ETHICS STATEMENT

The studies involving human participants were reviewed and approved by the Ethics Committee of the Second Xiangya Hospital, Central South University, Changsha. The patients/participants provided their written informed consent to participate in this study. Written informed consent was obtained from the individual(s) for the publication of any potentially identifiable images or data included in this article.

AUTHOR CONTRIBUTIONS

All authors contributed to the article and approved the submitted version. YT and XW conceived and designed the work. MW helped to conduct the flow cytometry. Material preparation, experiment, data collection, and analysis were performed by PZ and BH. PZ and BH contributed equally. The first draft of the manuscript was written by PZ and BH. QC, XP, ZZ, and WP provide important support for the modification and polishing of the article. Tissue sample acquisition was performed by GT, BH, and PZ. The RNA-seq data results were aided by FY. All authors commented on previous versions of the manuscript and all authors read and approved the final manuscript.

FUNDING

This work was supported by the National Undergraduate Innovation Training Program of China (20190034020003 and 20200034020026, BH), the Fundamental Research Funds for the Central Universities of Central South University (2021zzts0383, BH), Hunan Provincial Science and Technology Innovation Plan Project (2020SK53424, XW) and Natural Science Foundation of Hunan Province (2021JJ30957, XW).

ACKNOWLEDGMENTS

Thanks to Dr. Xiaoling Zhu in the Department of Clinical Laboratory and Dr. Qingchun Liang in the Department of Pathology of the Second Xiangya Hospital of Central South University for their guidance on flow cytometry and immunohistochemistry. Thanks to Dr. Wenliang Liu, Mingjiu Chen, Jingqun Tang, and Chen Chen in the Department of Thoracic Surgery of the Second Xiangya Hospital of Central South University for their help in the specimen collection process. It is with regret that not all relevant researchers could be listed as co-authors.

SUPPLEMENTARY MATERIAL

The Supplementary Material for this article can be found online at: https://www.frontiersin.org/articles/10.3389/fonc.2021.705888/full#supplementary-material

Supplementary Figure 1 | Flow chart of organoid tissue culture and treatment of dosing before immunofluorescence operation.

Supplementary Figure 2 | Differences in IL-6 expression between 9 normal lung samples and 9 GGO samples were detected in the validation cohort (Lee H et al.). $^{**}P < 0.01$

Supplementary Figure 3 | The multiple staining immunohistochemical results of CD56 (in yellow) and PD-1(in purple, negative) in normal lung tissue (upper) or GGO lung tissue (lower). Scale bar, 50 μm.

Supplementary Figure 4 | High expression of NK cell markers suggests a better prognosis for lung adenocarcinoma (The data are from the TCGA-LUAD database).

REFERENCES

1. Rusch V, Chansky K, Kindler H, Nowak A, Pass H, Rice D, et al. The IASLC Mesothelioma Staging Project: Proposals for the M Descriptors and for Revision of the TNM Stage Groupings in the Forthcoming (Eighth) Edition of the TNM Classification for Mesothelioma. *J Thorac Oncol* (2016) 11 (12):2112–9. doi: 10.1016/j.jtho.2016.09.124
2. Ye T, Deng L, Wang S, Xiang J, Zhang Y, Hu H, et al. Lung Adenocarcinomas Manifesting as Radiological Part-Solid Nodules Define a Special Clinical Subtype. *J Thorac Oncol* (2019) 14(4):617–27. doi: 10.1016/j.jtho.2018.12.030
3. Infante M, Lutman RF, Imparato S, Di Rocco M, Ceresoli GL, Torri V, et al. Differential Diagnosis and Management of Focal Ground-Glass Opacities. *Eur Respir J* (2009) 33(4):821–7. doi: 10.1183/09031936.00047908
4. Hansell DM, Bankier AA, MacMahon H, McLoud TC, Müller NL, Remy J. Fleischner Society: Glossary of Terms for Thoracic Imaging. *Radiology* (2008) 246(3):697–722. doi: 10.1148/radiol.2462070712
5. Kobayashi Y, Mitsudomi T, Sakao Y, Yatabe Y, et al. Genetic Features of Pulmonary Adenocarcinoma Presenting With Ground-Glass Nodules: The Differences Between Nodules With and Without Growth. *Ann Oncol* (2015) 26(1):156–61. doi: 10.1093/annonc/mdu505
6. Horvath L, Thienpont B, Zhao L, Wolf D, Pircher A. Overcoming Immunotherapy Resistance in non-Small Cell Lung Cancer (NSCLC) - Novel Approaches and Future Outlook. *Mol Cancer* (2020) 19(1):141. doi: 10.1186/s12943-020-01260-z
7. Somasundaram A, Burns TF. The Next Generation of Immunotherapy: Keeping Lung Cancer in Check. *J Hematol Oncol* (2017) 10(1):87. doi: 10.1186/s13045-017-0456-5
8. Soyama T, Sakuragi A, Oishi D, Kimura Y, Aoki H, Nomoto A, et al. Photodynamic Therapy Exploiting the Anti-Tumor Activity of Mannose-Conjugated Chlorin E6 Reduced M2-Like Tumor-Associated Macrophages. *Transl Oncol* (2021) 14(2):101005. doi: 10.1016/j.tranon.2020.101005
9. Tada K, Kitano S, Shoji H, Nishimura T, Shimada Y, Nagashima K, et al. Immune Status at Pre-Treatment Impacts on Progression-Free Survival of Metastatic Colorectal Cancer Patients Treated With First-Line Chemotherapy. *J Immunother Cancer* (2015) 3(Suppl 2):P108. doi: 10.1186/2051-1426-3-S2-P108
10. Bednarz-Misa I, Diakowska D, Szczuka I, Fortuna P, Kubiak A, Rosińczuk J, et al. Interleukins 4 and 13 and Their Receptors Are Differently Expressed in Gastrointestinal Tract Cancers, Depending on the Anatomical Site and Disease Advancement, and Improve Colon Cancer Cell Viability and Motility. *Cancers (Basel)* (2020) 12(6):1463. doi: 10.3390/cancers12061463
11. Karasaki T, Nagayama K, Kuwano H, Nitadori JI, Sato M, Anraku M, et al. An Immunogram for the Cancer-Immunity Cycle: Towards Personalized Immunotherapy of Lung Cancer. *J Thorac Oncol* (2017) 12(5):791–803. doi: 10.1016/j.jtho.2017.01.005
12. Chen DS, Mellman I. Oncology Meets Immunology: The Cancer-Immunity Cycle. *Immunity* (2013) 39(1):1–10. doi: 10.1016/j.immuni.2013.07.012
13. Lee H, Joung JG, Shin HT, Kim DH, Kim Y, Kim H, et al. Genomic Alterations of Ground-Glass Nodular Lung Adenocarcinoma. *Sci Rep* (2018) 8(1):7691. doi: 10.1038/s41598-018-25800-2
14. Caetano MS, Zhang H, Cumpian AM, Gong L, Unver N, Ostrin EJ, et al. IL6 Blockade Reprograms the Lung Tumor Microenvironment to Limit the Development and Progression of K-Ras-Mutant Lung Cancer. *Cancer Res* (2016) 76(11):3189–99. doi: 10.1158/0008-5472.CAN-15-2840
15. Bhat AA, Nisar S, Maacha S, Carneiro-Lobo TC, Akhtar S, Siveen KS, et al. Cytokine-Chemokine Network Driven Metastasis in Esophageal Cancer; Promising Avenue for Targeted Therapy. *Mol Cancer* (2021) 20(1):2. doi: 10.1186/s12943-020-01294-3
16. Vivier E, Ugolini S, Blaise D, Chabannon C, Brossay L. Targeting Natural Killer Cells and Natural Killer T Cells in Cancer. *Nat Rev Immunol* (2012) 12 (4):239–52. doi: 10.1038/nri3174
17. Gauthier L, Morel A, Anceriz N, Rossi B, Blanchard-Alvarez A, Grondin G, et al. Multifunctional Natural Killer Cell Engagers Targeting NKp46 Trigger Protective Tumor Immunity. *Cell* (2019) 177(7):1701–1713.e16. doi: 10.1016/j.cell.2019.04.041
18. Hirano T. IL-6 in Inflammation, Autoimmunity and Cancer. *Int Immunol* (2021) 33(3):127–48. doi: 10.1093/intimm/dxaa078
19. Kishimoto T. The Biology of Interleukin-6. *Blood* (1989) 74(1):1–10.
20. Hirano T, Yasukawa K, Harada H, Taga T, Watanabe Y, Matsuda T, et al. Complementary DNA for a Novel Human Interleukin (BSF-2) That Induces B Lymphocytes to Produce Immunoglobulin. *Nature* (1986) 324(6092):73–6. doi: 10.1038/324073a0
21. Mihara M, Hashizume M, Yoshida H, Suzuki M, Shiina M. IL-6/IL-6 Receptor System and its Role in Physiological and Pathological Conditions. *Clin Sci (Lond)* (2012) 122(4):143–59. doi: 10.1042/CS20110340
22. Stark GR, Darnell JEJr. The JAK-STAT Pathway at Twenty. *Immunity* (2012) 36(4):503–14. doi: 10.1016/j.immuni.2012.03.013
23. Wei LH, Kuo ML, Chen CA, Chou CH, Lai KB, Lee CN, et al. Interleukin-6 Promotes Cervical Tumor Growth by VEGF-Dependent Angiogenesis *via* a STAT3 Pathway. *Oncogene* (2003) 22(10):1517–27. doi: 10.1038/sj.onc.1206226
24. Bollrath J, Phesse TJ, von Burstin VA, Putoczki T, Bennecke M, Bateman T, et al. Gp130-Mediated Stat3 Activation in Enterocytes Regulates Cell Survival and Cell-Cycle Progression During Colitis-Associated Tumorigenesis. *Cancer Cell* (2009) 15(2):91–102. doi: 10.1016/j.ccr.2009.01.002
25. Gao X, Liu X, Lu Y, Wang Y, Cao W, Liu X, et al. PIM1 is Responsible for IL-6-Induced Breast Cancer Cell EMT and Stemness *via* C-Myc Activation. *Breast Cancer* (2019) 26(5):663–71. doi: 10.1007/s12282-019-00966-3
26. Yadav A, Kumar B, Datta J, Teknos TN, Kumar P. IL-6 Promotes Head and Neck Tumor Metastasis by Inducing Epithelial-Mesenchymal Transition *via* the JAK-STAT3-SNAIL Signaling Pathway. *Mol Cancer Res* (2011) 9 (12):1658–67. doi: 10.1158/1541-7786.MCR-11-0271
27. Wang YC, Wu YS, Hung CY, Wang SA, Young MJ, Hsu TI, et al. USP24 Induces IL-6 in Tumor-Associated Microenvironment by Stabilizing P300 and β-TrCP and Promotes Cancer Malignancy. *Nat Commun* (2018) 9 (1):3996. doi: 10.1038/s41467-018-06178-1
28. Yang Y, Ding L, Hu Q, Xia J, Sun J, Wang X, et al. MicroRNA-218 Functions as a Tumor Suppressor in Lung Cancer by Targeting IL-6/STAT3 and Negatively Correlates With Poor Prognosis. *Mol Cancer* (2017) 16(1):141. doi: 10.1186/s12943-017-0710-z
29. Caetano MS, Hassane M, Van HT, Bugarin E, Cumpian AM, McDowell CL, et al. Sex Specific Function of Epithelial STAT3 Signaling in Pathogenesis of K-Ras Mutant Lung Cancer. *Nat Commun* (2018) 9(1):4589. doi: 10.1038/s41467-018-07042-y
30. Barrera L, Montes-Servín E, Barrera A, Ramírez-Tirado LA, Salinas-Parra F, Bañales-Méndez JL, et al. Cytokine Profile Determined by Data-Mining Analysis Set Into Clusters of non-Small-Cell Lung Cancer Patients According to Prognosis. *Ann Oncol* (2015) 26(2):428–35. doi: 10.1093/annonc/mdu549
31. Ryan BM, Pine SR, Chaturvedi AK, Caporaso N, Harris CC. A Combined Prognostic Serum Interleukin-8 and Interleukin-6 Classifier for Stage 1 Lung Cancer in the Prostate, Lung, Colorectal, and Ovarian Cancer Screening Trial. *J Thorac Oncol* (2014) 9(10):1494–503. doi: 10.1097/JTO.0000000000000278
32. Owusu Sekyere S, Schlevogt B, Mettke F, Kabbani M, Deterding K, Wirth TC, et al. HCC Immune Surveillance and Antiviral Therapy of Hepatitis C Virus Infection. *Liver Cancer* (2019) 8(1):41–65. doi: 10.1159/000490360
33. Makela AV, Gaudet JM, Foster PJ. Quantifying Tumor Associated Macrophages in Breast Cancer: A Comparison of Iron and Fluorine-Based MRI Cell Tracking. *Sci Rep* (2017) 7:42109. doi: 10.1038/srep42109
34. Obeid E, Nanda R, Fu YX, Olopade OI. The Role of Tumor-Associated Macrophages in Breast Cancer Progression (Review). *Int J Oncol* (2013) 43 (1):5–12. doi: 10.3892/ijo.2013.1938
35. Greenberg AH, Hudson L, Shen L, Roitt IM. Antibody-Dependent Cell-Mediated Cytotoxicity Due to a "Null" Lymphoid Cell. *Nat New Biol* (1973) 242(117):111–3. doi: 10.1038/newbio242111a0
36. Cózar B, Greppi M, Carpentier S, Narni-Mancinelli E, Chiossone L, Vivier E. Tumor-Infiltrating Natural Killer Cells. *Cancer Discov* (2020) 11 (1):34–44. doi: 10.1158/2159-8290.Cd-20-0655
37. Garrido F. MHC/HLA Class I Loss in Cancer Cells. *Adv Exp Med Biol* (2019) 1151:15–78. doi: 10.1007/978-3-030-17864-2_2
38. Freud AG, Mundy-Bosse BL, Yu J, Caligiuri MA. The Broad Spectrum of Human Natural Killer Cell Diversity. *Immunity* (2017) 47(5):820–33. doi: 10.1016/j.immuni.2017.10.008
39. Cadoux M, Caruso S, Pham S, Gougelet A, Pophillat C, Riou R, et al. Expression of NKG2D Ligands is Downregulated by β-Catenin Signalling and Associates With HCC Aggressiveness. *J Hepatol* (2021) 74 (6):1386–97. doi: 10.1016/j.jhep.2021.01.017
40. Zheng Y, Chen Z, Han Y, Han L, Zou X, Zhou B, et al. Immune Suppressive Landscape in the Human Esophageal Squamous Cell Carcinoma Microenvironment. *Nat Commun* (2020) 11(1):6268. doi: 10.1038/s41467-020-20019-0

41. Swaminathan S, Hansen AS, Heftdal LD, Dhanasekaran R, Deutzmann A, Fernandez WDM, et al. MYC Functions as a Switch for Natural Killer Cell-Mediated Immune Surveillance of Lymphoid Malignancies. *Nat Commun* (2020) 11(1):2860. doi: 10.1038/s41467-020-16447-7
42. Weil S, Memmer S, Lechner A, Huppert V, Giannattasio A, Becker T, et al. Natural Killer Group 2d Ligand Depletion Reconstitutes Natural Killer Cell Immunosurveillance of Head and Neck Squamous Cell Carcinoma. *Front Immunol* (2017) 8:387. doi: 10.3389/fimmu.2017.00387
43. Dai YJ, He SY, Hu F, Li XP, Zhang JM, Chen SL, et al. Bone Marrow Infiltrated Natural Killer Cells Predicted the Anti-Leukemia Activity of MCL1 or BCL2 Inhibitors in Acute Myeloid Leukemia. *Mol Cancer* (2021) 20(1):8. doi: 10.1186/s12943-020-01302-6
44. Lu T, Yang X, Shi Y, Zhao M, Bi G, Liang J, et al. Single-Cell Transcriptome Atlas of Lung Adenocarcinoma Featured With Ground Glass Nodules. *Cell Discovery* (2020) 6:69. doi: 10.1038/s41421-020-00200-x
45. Aktaş ON, Öztürk AB, Erman B, Erus S, Tanju S, Dilege Ş, et al. Role of Natural Killer Cells in Lung Cancer. *J Cancer Res Clin Oncol* (2018) 144 (6):997–1003. doi: 10.1007/s00432-018-2635-3
46. Stankovic B, Bjørhovde HAK, Skarshaug R, Aamodt H, Frafjord A, Müller E, et al. Immune Cell Composition in Human Non-Small Cell Lung Cancer. *Front Immunol* (2018) 9:3101. doi: 10.3389/fimmu.2018.03101
47. Jin S, Deng Y, Hao JW, Li Y, Liu B, Yu Y, et al. NK Cell Phenotypic Modulation in Lung Cancer Environment. *PloS One* (2014) 9(10):e109976. doi: 10.1371/journal.pone.0109976
48. Chan L, Li C, Xia W, Hsu J, Lee H, Cha J, et al. IL-6/JAK1 Pathway Drives PD-L1 Y112 Phosphorylation to Promote Cancer Immune Evasion. *J Clin Invest* (2019) 129(8):3324–38. doi: 10.1172/JCI126022
49. Xu L, Chen X, Shen M, Yang D-R, Fang L, Weng G, et al. Inhibition of IL-6-JAK/Stat3 Signaling in Castration-Resistant Prostate Cancer Cells Enhances the NK Cell-Mediated Cytotoxicity *via* Alteration of PD-L1/NKG2D Ligand Levels. *Mol Oncol* (2018) 12(3):269–86. doi: 10.1002/1878-0261.12135
50. Rabinowich H, Sedlmayr P, Herberman RB, Whiteside TL. Response of Human NK Cells to IL-6 Alterations of the Cell Surface Phenotype, Adhesion to Fibronectin and Laminin, and Tumor Necrosis Factor-Alpha/Beta Secretion. *J Immunol* (1993) 150(11):4844–55. doi: 10.1172/jci126022
51. Osman MS, van Eeden C, Cohen Tervaert JW. Fatal COVID-19 Infections: Is NK Cell Dysfunction a Link With Autoimmune HLH? *Autoimmun Rev* (2020) 19(7):102561. doi: 10.1016/j.autrev.2020.102561
52. Ge X, Li CR, Yang J, Wang GB. Aberrantly Decreased Levels of NKG2D Expression in Children With Kawasaki Disease. *Scand J Immunol* (2013) 77 (5):389–97. doi: 10.1111/sji.12022
53. Varchetta S, Mele D, Oliviero B, Mantovani S, Ludovisi S, Cerino A, et al. Unique Immunological Profile in Patients With COVID-19. *Cell Mol Immunol* (2021) 18(3):604–12. doi: 10.1038/s41423-020-00557-9
54. Luger TA, Krutmann J, Kirnbauer R, Urbanski A, Schwarz T, Klappacher G, et al. IFN-Beta 2/IL-6 Augments the Activity of Human Natural Killer Cells. *J Immunol* (1989) 143(4):1206–9.
55. Gazit R, Garty BZ, Monselise Y, Hoffer V, Finkelstein Y, Markel G, et al. Expression of KIR2DL1 on the Entire NK Cell Population: A Possible Novel Immunodeficiency Syndrome. *Blood* (2004) 103(5):1965–6. doi: 10.1182/blood-2003-11-3796
56. Lau B, Poole E, Krishna B, Montanuy I, Wills MR, Murphy E, et al. The Expression of Human Cytomegalovirus MicroRNA MiR-UL148D During Latent Infection in Primary Myeloid Cells Inhibits Activin A-Triggered Secretion of IL-6. *Sci Rep* (2016) 6:31205. doi: 10.1038/srep31205
57. Goldfarb Y, Ben-Eliyahu S. Surgery as a Risk Factor for Breast Cancer Recurrence and Metastasis: Mediating Mechanisms and Clinical Prophylactic Approaches. *Breast Dis* (2006) 26:99–114. doi: 10.3233/BD-2007-26109

Conflict of Interest: The authors declare that the research was conducted in the absence of any commercial or financial relationships that could be construed as a potential conflict of interest.

Publisher's Note: All claims expressed in this article are solely those of the authors and do not necessarily represent those of their affiliated organizations, or those of the publisher, the editors and the reviewers. Any product that may be evaluated in this article, or claim that may be made by its manufacturer, is not guaranteed or endorsed by the publisher.

frontiers in Oncology

SYSTEMATIC REVIEW
published: 13 September 2021
doi: 10.3389/fonc.2021.724692

Molecular Alterations in Lung Adenocarcinoma With Ground-Glass Nodules: A Systematic Review and Meta-Analysis

Zihan Wei[1,2†], Ziyang Wang[1,2†], Yuntao Nie[1], Kai Zhang[1], Haifeng Shen[1], Xin Wang[1,2], Manqi Wu[1,2], Fan Yang[1] and Kezhong Chen[1]*

[1] Department of Thoracic Surgery, Peking University People's Hospital, Beijing, China, [2] Health Science Center, Peking University, Beijing, China

OPEN ACCESS

Edited by:
Cheng Zhan,
Fudan University, China

Reviewed by:
Song Xu,
Tianjin Medical University General Hospital, China
Xiaoliang Shao,
First People's Hospital of Changzhou, China

****Correspondence:***
Kezhong Chen
chenkezhong@pkuph.edu.cn

[†]These authors have contributed equally to this work and share first authorship

Specialty section:
This article was submitted to Thoracic Oncology, a section of the journal Frontiers in Oncology

Received: *14 June 2021*
Accepted: *18 August 2021*
Published: *13 September 2021*

Citation:
Wei Z, Wang Z, Nie Y, Zhang K, Shen H, Wang X, Wu M, Yang F and Chen K (2021) Molecular Alterations in Lung Adenocarcinoma With Ground-Glass Nodules: A Systematic Review and Meta-Analysis. Front. Oncol. 11:724692. doi: 10.3389/fonc.2021.724692

Background and Aims: Nodular ground-glass lesions have become increasingly common with the increased use of computed tomography (CT), while the genomic features of ground-glass opacities (GGOs) remain unclear. This study aims to comprehensively investigate the molecular alterations of GGOs and their correlation with radiological progression.

Methods: Studies from PubMed, Embase, Cochrane Library, and Web of Science, using PCR, targeted panel sequencing, whole exosome sequencing, and immunohistochemistry, and reporting genomic alterations or PD-L1 expressions in lung nodules presenting as GGOs until January 21, 2021 were included in this study. Chi-square test, random-effects model, and Z-test analysis were adopted to analyze the data.

Results: A total of 22 studies describing mutations in lung adenocarcinoma (LUAD) with GGOs were analyzed. EGFR was the most frequently mutative gene (51%, 95%CI 47%–56%), followed by TP53 (18%, 95%CI 6%–31%), HER2 (10%, 95%CI 0%–21%), ROS1 (6%, 95%CI 0%–18%), and KRAS (6%, 95%CI 3%–9%). The correlation between the frequency of EGFR mutation and radiological was observed and the differences were found to be not statistically significant in the subgroups, which are listed as below: radiological: gGGO 47.40%, 95%CI [38.48%; 56.40%]; sGGO 51.94%, 95%CI [45.15%; 58.69%]. The differences of the frequency of KRAS mutation in the different subgroups were also consistent with this conclusion, which are listed as: radiological gGGO 3.42, 95%CI [1.35%; 6.13%]; sGGO 12.27%, 95%CI [3.89%; 23.96%]. The pooled estimated rate of PD-L1 was 8.82%, 95%CI [5.20%–13.23%]. A total of 11.54% (3/26) of the SMGGNs were confirmed to be intrapulmonary spread by WES.

Conclusions: Somatic genetic alterations are considered in early-stage GGO patients without distinct changes of the frequency following the progress of the tumor. This review sheds insight on molecular alterations in LUAD with GGOs.

Keywords: ground-glass-opacity, lung cancer, systematic review, molecular alteration, EGFR, PD-L1

INTRODUCTION

Ground-glass opacities (GGOs), defined as hazy increased density of the lungs with bronchial and vascular margins on computed tomography (CT) (1, 2), often associate with lung cancers, especially lung adenocarcinomas (LUADs), and are commonly detected in East-Asia patients. GGOs, being radiologically distinct clinical entities, which were known to have an indolent clinical course, present a superior survival after resection, especially pure GGOs with a nearly 100% long-term disease-free survival (DFS), shown in many previous studies (3, 4), indicating the unique biology of GGOs. However, the molecular characteristics of GGO-associated lung cancers have not been systematically reviewed due to the limitation of sample size and different criteria used while reporting, and, therefore, the tumor evolutionary mechanism behind the slow-growing appearance in GGOs is not clear. In addition, there are many patients with synchronous multiple ground-glass nodules (SMGGNs) on their initial CT. And some of them are found to have an intrapulmonary spread, even if the initial lesions seem to be in a fairly early-stage.

Therefore, we meta-analyzed the extracted data under certain criteria to demonstrate the dynamic genomic alterations in the diversity of GGO patients. This review can provide a novel insight into the molecular alterations in LUAD patients with GGOs and new views for the biology behavior of GGOs.

METHODS

Search Strategy

Three distinctive keywords were identified as follows: "ground-glass opacity", "gene alterations", and "PD-L1". MeSH term database from the National Center for Biotechnology Information (NCBI) was searched to find all the possible expressions for these keywords which were defined as free words. The final search strategy was combined with both the MeSH terms and free words, which is listed as follows: #1: "GGO" OR "GGN" OR "ground glass opacity" OR "ground glass nodule" OR "ground glass nodules" OR "ground-glass opacity" OR "ground-glass nodule" OR "ground-glass nodules" OR "subsolid nodule" OR "subsolid nodules" OR "subsolid pulmonary nodules", #2: "Gene" OR "Cistron" OR "Cistrons" OR "Genetic Materials" OR "Genetic Material" OR "genetic feature" OR "genetic characteristics" OR "genetic characteristic" OR "genetic features" OR "Genomic alteration" OR "Genomic alterations" OR "EGFR" OR "epidermal growth factor receptor" OR "TTF-1" OR "thyroid transcription factor 1" OR "ALK" OR "anaplastic lymphoma kinase" OR "KRAS" OR "Kirsten rat sarcoma" OR "HER2" OR "human epidermal growth factor receptor type 2" OR "oncogenic driver", and #3: "PD-L1" OR "programmed cell death 1 ligand 1 protein" OR "PDL1" OR "CD274" OR "B7-H1" OR "B7H1". "#1 AND #2" and "#1 AND #3" were searched in the four databases up to January 21, 2021, without language limitations, respectively.

Selection Criteria

Firstly, all the papers retrieved from the search were screened by reviewing the titles and abstracts, during which period, reviews, case studies, editorials, meeting abstracts, and papers not meeting any of our search criteria were excluded. Then, the full contents of the rest papers were evaluated carefully to distinguish the ones that perfectly fit our inclusion criteria, analyzing the molecular alterations in a consecutive cohort of patients with GGOs, during which period, some papers were excluded for the following reasons (1): the cohort was developed to analyze the characters of the nodules with specific molecular alterations (2); insufficient data for analyses; and (3) papers not written in English. Two authors (ZWe and ZWa) conducted the procedure independently to evaluate the study eligibility for our review. This analysis was performed according to the Preferred Reporting Items for Systematic Reviews and Meta-Analyses (PRISMA) statement (5).

Data Extraction

The following basic data were extracted from the selected papers: author(s), year of publication, size and region of the cohort, characteristics of the patients in the study, radiological and pathological details of the nodules, the methodological details, and relevant statistical findings for the entire cohort and/or by population subgroups. Two authors (ZWe and ZWa) collected these data independently, and any discrepancies between the two authors were resolved by discussions with a third author (KC).

Statistical Analysis

We firstly performed a descriptive analysis summarizing all the rates of gene alterations reported in the eligible works. Then, the rates of the gene alterations which had been reported in more than three studies were pooled using random-effects meta-analysis models allowing for the inherent heterogeneity of observational studies (6), after a data-transformation and normality-check using the variance-stabilizing double-arcsine transformation method (7). Q and I^2 statistics were calculated to assess the heterogeneity between study-specific estimates (8). Forest plots were adopted to show a graphical presentation of the meta-analysis results, whereas Z-test was applied to check the level of significance of the differences of the pooled estimated rates from different groups, where the values of p less than 0.05 were considered to be significant. The publication biases were assessed by Egger test, which is based on a weighted linear regression of the effect on its standard error. All the analyses were implemented with R (version 4.0.3).

Quality of Evidence

In this systematic review, the 25 included studies were all cross-sectional studies. All the patients had been diagnosed with lung cancer before or during their treatment. The authors finalized the list of included articles through discussion and agreement. Data from the articles were independently extracted by two authors (ZWe and ZWa) who were not involved in any of the reviewed studies. As recommended by the Agency for Healthcare Research and Quality, the assessment of the methodological quality of the

included studies was made from 11 perspectives with the Cross-Sectional/Prevalence Study Quality, a scoring system specific for a cross-sectional study (**Supplementary Table 1**).

RESULTS

Study Selection

After removing the duplicated records, 680 records related to gene alterations and 25 records related to PD-L1 expression were selected for further assessment with the titles and abstracts. From the remaining records, 27 records related to gene alterations and 6 records related to PD-L1 expression were carefully selected through the evaluation of the full contents as the second round of selection. Finally, 22 gene-alteration-reported articles and 4 PD-L1-expression-reported articles were included in the following analysis, as shown in a PRISMA diagram (**Figure 1**).

Study Characteristics

All the cohorts from the 25 studies included were composed of Asians (**Table 1**), except that one cohort (29) also included Caucasians. In the 22 cohorts reporting gene alterations, the median cohort size was 135 [interquartile range (IQR): 25–210], of which, 16 cohorts included patients with solitary pulmonary nodules, while 6 cohorts put their attention on multiple pulmonary nodules, and the pathological subtypes of all these nodules were adenocarcinoma. While nearly half of the studies (11/22) focused on early-stage LUAD, 8 of the 22 studies included some stage III/IV cases (3 articles did not mention the clinical stage of the nodules). No subgroup analysis was performed due to the lack of data. Only two studies used whole exosome sequencing in their analysis, other than PCR or targeted gene sequencing. Among the four articles reporting PD-L1 expression included (**Table 1**) in our review, only one article reported gene alterations at the same time. All four cohorts were formed with Asians, two with Chinese, and two with Japanese. No significant publication bias were seen in the analysis (EGFR, p = 0.9419; KRAS, p = 0.7106; ALK, p = 0.0918; PD-L1, p = 0.89).

Meta-Analysis

Being the most validated genetic mutation, EGFR was the most prominent variation as well [51%, 95%CI (47%, 56%)], followed by TP53 [18%, 95%CI (6%, 31%)], HER2 [10%, 95%CI (0%, 21%)], ROS1 [6%, 95%CI (0%, 18%)], KRAS [6%, 95%CI (3%, 9%)] (**Figure 2**). Meanwhile, we summarized the rates of the top two validated gene alterations, EGFR mutation and KRAS mutation, to conduct a subgroup analysis.

EGFR Mutation

All the 25 articles that were included reported the rates of EGFR mutations in their cohorts (**Table 1**), in which 2,536/4,944 cases (51.29%) were found to harbor EGFR mutations. After performing a meta-analysis with the random-effects model (**Figure 2A**), the pooled estimated rate of EGFR mutations was found to be 51.51% [95%CI (46.74%, 56.26%)].

Further analyses were conducted according to the radiological subgroups with the random-effects model (**Figure 3**). A G/T ratio, defined as the ratio of the ground-glass opacity (GGO) component to the tumor size at CT, ≥50% is suggested to be a sign of pathologically noninvasiveness. Additionally, the rates of lymph node metastasis range from 21% to 26% in lesions ≤3 cm with a G/T ratio ≤ 50% (34–36). Therefore, G/T ratio was used to divide the nodules into two groups in our review: gGGO (ground-glass dominant GGO) 50%<G/T ratio ≤ 100%; sGGO (solid dominant GGO) 0<G/T ratio ≤ 50%. The data of each subgroup were extracted from 10 articles that reported the necessary details according to the division criteria, and the EGFR mutation rate of each subgroup after analyzing with the random-effects model was listed in **Table 2**. It was found that the EGFR mutation rate has a marginal increment with the radiological progression of GGOs, but the difference was not statistically significant (p = 0.4828). Our results showed that with

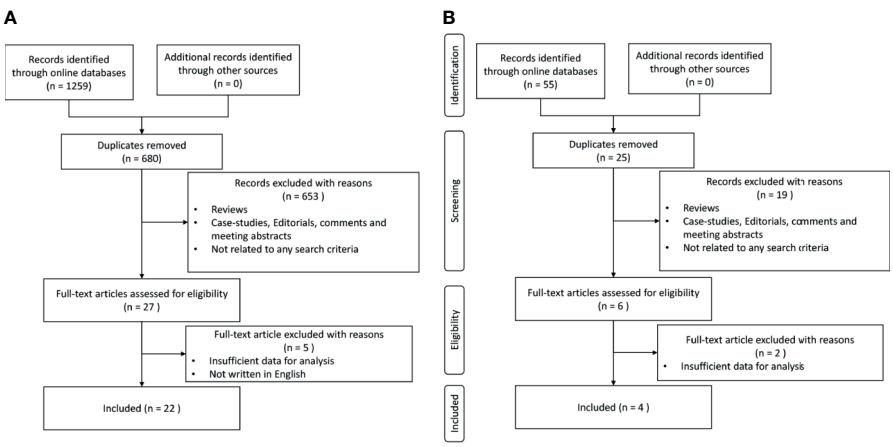

FIGURE 1 | Process of study selection. **(A)** Study selection with genetic alterations. **(B)** Study selection with PD-L1 expressions.

TABLE 1 | Characters of the studies included in the meta-analysis.

Study ID	Region	Cohort size	Method_gene	Genes tested	EGFR mutation rate
Zhao et al. (9)	Chinese	529	qPCR & Immunohistochemical	EGFR、KRAS、HER2、ALK、BRAF、RET、ROS1、PIK3CA、NRAS	54.82%
Aoki et al. (10)	Japanese	25	PCR	EGFR、KRAS	40.00%
Dai et al. (11)	Chinese	204	qPCR	EGFR	53.43%
Suda et al. (12)	Japanese	1871	unclear	EGFR	50.61%
Min et al. (13)	Chinese	338	direct dideoxynucleotide sequencing	EGFR	64.79%
Zou et al. (14)	Chinese	209	PCR	EGFR	73.68%
Sugano et al. (15)	Japanese	59	non-radioactive single-strand conformation polymorphism	EGFR、KRAS	49.15%
Liu et al. (16)	Chinese	78	qPCR	EGFR	33.33%
Yang et al. (17)	Chinese	158	qPCR	EGFR、KRAS、ALK	62.66%
Lu et al. (18)	Chinese	156	qPCR	EGFR	48.08%
Chung et al. (19)	Korean	24	nested PCR	EGFR	41.07%
Hsu et al. (20)	Chinese	67	PCR	EGFR	55.22%
Ko et al. (21)	Korean	215	PCR	EGFR、ALK	54.63%
Tomita et al. (22)	Japanese	68	PCR	EGFR	72.06%
Chen et al. (23)	Chinese	39	DNA sequencing	EGFR、KRAS、BRAF、PIK3CA、TP53、ALK、ROS1、RET	56.52%
Kobayashi et al. (24)	Japanese	96	reverse transcriptase-PCR	EGFR、KRAS、ALK、HER2	64.42%
Li et al. (25)	Chinese	120	WES*		50.00%
Ren et al. (26)	Chinese	31	PCR & WES*		17.39%
Wang et al. (27)	Chinese	212	PCR	EGFR、KRAS	36.79%
Usuda et al. (28)	Japanese	56	Cycleave PCR	EGFR	67.86%
Lui et al. (29)	Asian & Caucasian	224	unclear	EGFR、KRAS	32.59%
Hong et al. (30)	Korean	116	PCR	EGFR	56.03%

Study ID	Region	Cohort size	Antibody	Cut-off value	PD-L1 expression
Wu et al. (31)	Chinese	233	E1L3N	5%	14.16%
Suda et al. (32)	Japanese	45	E1L3N	1%	4.44%
Toyokawa et al. (33)	Japanese	189	SP142	5%	9.52%
Zhao et al., 2018 (9)	Chinese	328	28-8, SP142, E1L3N, BP6001	5%	6.40%

**Whole exosome sequencing or next generation sequencing was used in the research lots of alterations reported, so the genes tested were omitted.*
PCR, polymerase chain reaction; qPCR, quantitative polymerase chain reaction; NGS, next generation sequencing; WES, whole-exosome sequencing.

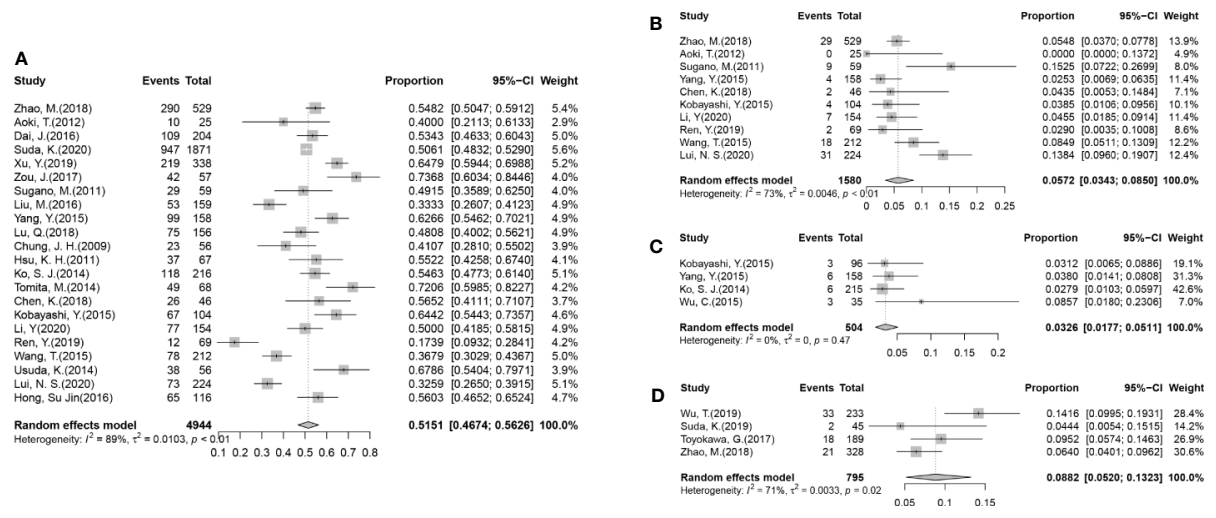

FIGURE 2 | Forest plots from the meta-analysis of published gene alterations in GGOs. **(A)** The pooled estimated rate of the EGFR mutation in 22 articles. **(B)** The pooled estimated rate of the KRAS mutation in 10 articles. **(C)** The pooled estimated rate of the ALK rearrangement in four articles. **(D)** The pooled estimated rate of the PD-L1 expression in four articles.

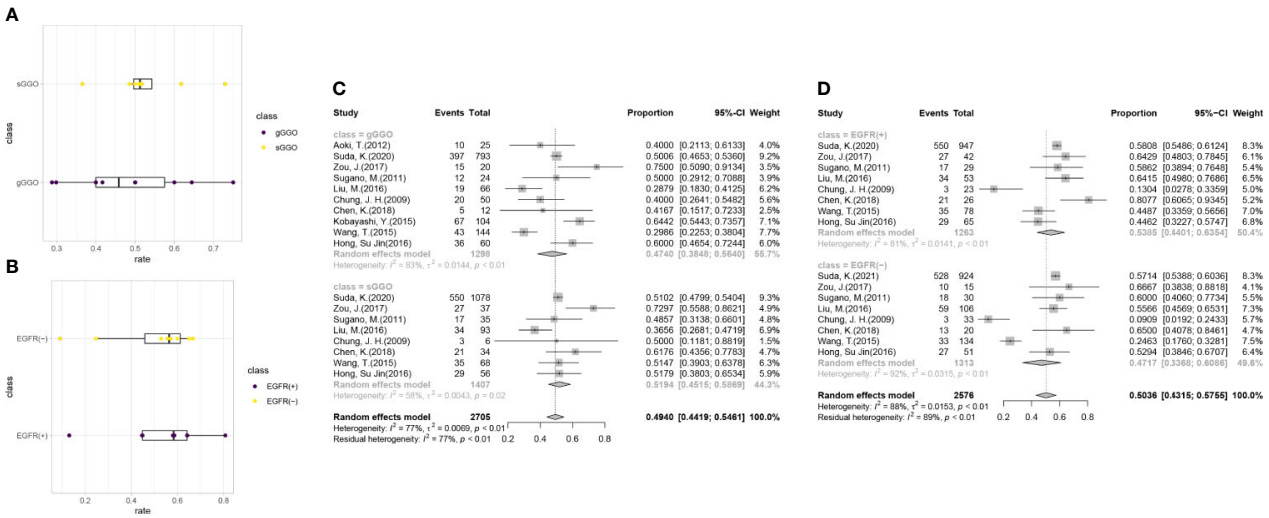

FIGURE 3 | Subgroup analysis for the EGFR mutations. **(A)** The distribution of the EGFR gene mutation rates in the subgroups with a different radiological density. **(B)** The distribution of sGGOs in the subgroups with a different status of EGFR mutation. **(C)** Forest plots from the subgroup meta-analysis of EGFR alterations in GGOs with different radiological subtypes. **(D)** Forest plots from the subgroup meta-analysis of the percentage of sGGOs in GGOs with a different status of EGFR mutation. gGGO, ground-glass dominant GGO; 50%<G/T ratio ≤ 100%; sGGO, solid dominant GGO; 0<G/T ratio ≤ 50%.

TABLE 2 | Details of the radiological subgroup analysis for the EGFR mutation and KRAS mutation by the random effect model.

EGFR	G/T ratio*	mut/total (n = 10)	Pooled estimated	95%CI	Heterogeneity		*Z-value*#	P-value#
					I^2	P-value		
	gGGO	624/1,298 (n = 10)	47.40%	38.48%–56.40%	83%	<0.01	0.7018	0.4828
	sGGO	716/1,407 (n = 8)	51.94%	45.15%–58.69%	58%	0.02		
	EGFR mut	sGGO/gGGO (n = 8)	pooled estimated	95%CI	Heterogeneity		*Z-value*#	P-value#
					I^2	P-value		
	EGFR (+)	716/1,263 (n = 8)	53.85%	44.01%–63.54%	81%	<0.01	0.6554	0.5122
	EGFR (–)	691/1,313 (n = 8)	47.17%	33.68%–60.86%	92%	<0.01		
KRAS	G/T ratio*	mut/total (n = 5)	pooled estimated	95%CI	Heterogeneity		*Z-value*#	P-value#
					I^2	P-value		
	gGGO	14/309 (n = 5)	3.42%	1.35%–6.13%	0%	0.50	1.8075	0.0707
	sGGO	19/137 (n = 3)	12.27%	3.89%–23.96%	66%	0.05		

**G/T ratio: gGGO, ground-glass dominant GGO; 0<G/T ratio ≤ 0.5; sGGO, solid dominant GGO; 0.5<G/T ratio ≤ 1.*
#Z-value was calculated by Z-test, p < 0.05 is considered statistically significant.

the radiological progression of GGOs, the frequency of EGFR mutation was stable.

Moreover, the mutation rates of EGFR subtypes were collected and analyzed (**Supplementary Figure 2**), and we found that the rate of L858R mutation was approximately equal to that of 19del mutation, composed over half of all EGFR mutations together. Though the rate of T790M mutation was relatively low (0.58%), there were still early-stage GGOs harboring T790M mutations.

In order to uncover whether EGFR mutation would have an influence on tumor progression, we divided the researches collected in our analysis into two groups by the mutation status of EGFR, among which, two studies included only cases with gGGOs and were excluded in the following analysis. The result shows that the proportion of the sGGOs was fairly the same in the groups with a different EGFR-mutation status, which is 53.85% [95%CI (44.01%, 63.54%)] in the EGFR(+) group and 47.17% [95%CI (33.68%, 60.86%)] in the EGFR (–) group, with a p-value at 0.5122 (**Table 2**). Though the heterogeneity between studies was still high, the result in each study can still confirm our results—sGGOs compose about 50% in whether EGFR(+) or EGFR (–) groups in each study.

KRAS Mutation

A total of 10 articles had reported the rates of KRAS mutation (**Figure 2B** and **Supplementary Figure 1**), in which 106/1,580 (6.71%) cases were reported to harbor the KRAS mutation, which was far less than the EGFR mutation. The pooled

estimated rate of the KRAS mutation was 5.72% [95%CI (3.43%, 8.50%)]. Subgroups were also divided according to the criteria mentioned before. In the radiological subgroups, it was clear to demonstrate that the rate of the KRAS mutation increased with the decrease of G/T ratio numerically (gGGO 3.42%, sGGO 12.27%), but the difference was not statistically significant ($p = 0.07$), due to the large 95% confidence intervals and high heterogeneities (**Table 2**).

ALK Rearrangement

The rate of ALK rearrangement in GGOs, reported in 4 of the 22 studies, was 18/504 (3.57%) after enumeration (**Figure 2C**), and the pooled estimated rate was 3.26% [95%CI (1.17%, 5.11%)]. The heterogeneity of the studies reporting an ALK arrangement was fairly low ($I^2 = 0\%$, $p = 0.47$).

PD-L1 Expression

Among all 795 cases, 74 (9.31%) were found with the PD-L1 expression (**Figure 2D**). Though with a significant heterogeneity in the method and cut-off values assessing the PD-L1 expression, it can be confirmed that the rate of the PD-L1 expression in GGOs is fairly low, as the pooled estimated rate of the PD-L1 expression of the nodules was 8.82% (95% CI 5.20%–13.23%). There was only one article (33) that provided details in the subgroups, so a meta-analysis could not be performed on the subgroups. Still, it was shown in the articles that the rate of PD-L1 expression was significantly lower in GGOs (4.44%–14.16%) than solid nodules (18.36%–35.04%) in the same cohorts (9, 31–33).

Molecular Alterations in Synchronous Multiple Ground-Glass Nodules

A total of 6/22 articles included synchronous multiple ground-glass nodules (SMGGNs) in their cohorts, while only the data from 4 articles could be extracted for analysis. In the 123 cases with SMGGNs included, 8 cases (6.50%) possessed identical mutations in their resected nodules which were doubted to be an intrapulmonary spread. Only one article used whole-exosome sequencing (WES) and confirmed 3/26 (11.54%) cases to have an intrapulmonary spread. The genetic alterations of the cases are listed below (**Table 3**). The distribution of genetic alterations appeared to have no significant differences between genetic alteration rates in whether multicentric origin nodules (**Table 3A**) or intrapulmonary spread nodules (**Table 3B**).

DISCUSSION

This systematic review investigated the molecular alterations in lung nodules presenting as ground-glass opacities and analyzed the trend of tumor genetic alterations along with the radiological progress.

As it is known to us that EGFR mutation was first reported in 2004 (37), and associate with non-smokers, female, LUAD tightly (38, 39). EGFR mutations were present in 10% of cases in Caucasians, while 30% in East Asians (40, 41), which may explain why the cohorts included in this review were mostly Asian. Among all the reported genetic alterations analyzed in this review, EGFR mutation was clearly the most validated and highest incidence genetic alteration, which is similar to previous studies (41). Some researchers had mentioned in their study (42) that EGFR functioned in tumor genesis, and also played an important role in tumor processing (41, 43). To the best of our best knowledge, this review is the first meta-analysis for the EGFR mutation rate especially in GGOs, which shows that with the progression in radiological, there is no significant difference in the rate of EGFR mutation ($p \geq 0.05$), suggesting that EGFR mutation, as a driver mutation for lung cancer, count for tumorigenesis in a relatively early stage, and maintain consistency in the progression of tumors. In addition, though relatively low, there were still early-stage GGOs harboring T790M mutations, indicating that T790M might play a role in tumorigenesis, which is known to associate with chemotherapy resistance.

Transforming from gGGOs to sGGOs have always been considered as a sign of tumor progression and is widely used in daily clinical work. So, we defined such transformation as tumor progression in our meta-analysis. Researchers have a heated discussion about the factors distinguishing between the easy-to-progress GGOs and indolent GGOs for a long time with no consensus, which mainly lie in a large size, the presence of a solid portion, old age, gene alterations, and so on (44–46). Unfortunately, our findings indicated that EGFR mutation has a little impact on tumor progression. Statistically, there is no difference between the distribution of gGGOs and sGGOs whether in the EGFR mutation group or in the wild type group. Whether some other signaling pathways can and under what conditions they will regulate the progression of GGOs, and whether there were any signs besides genetic alterations such as genetic heterogeneity or chromosome instability require more studies to confirm, which may help us get a deeper understanding of the biological behavior of GGOs.

When taking KRAS mutation as one of the earliest discoveries of genetic alterations in lung cancers (41, 47) and reported as very important for tumor progression (48) into account, there seemed to bear discrepancy at different stages of tumor progression. Though not statistically different, the frequency of KRAS mutation seems to increase with the increasing G/T ratio, suggesting a relationship between KRAS mutation and tumor progression, resulting in a higher frequency in more progressed lung nodules presenting with GGOs.

Using antibodies targeting the PD-1 pathway is a promising and effective option of immunotherapy, a newly developed treatment of NSCLC (49, 50), where PD-L1 is used as a biomarker to predict the immunotherapy response (51). We clearly showed that the incidence of PD-L1 expression was much lower in GGOs than pure-solid tumors in several articles, which was verified by Suda et al. in a clinical experiment including 124 qualified patients (4% vs. 25%, $p < 0.01$) (32). Wu et al. also found in a small-size cohort that even for the same patient, the volume of synchronous GGOs showed no significant change before and after treatment (4,160.2 vs 4,185.5 mm^3, $p = 0.6050$)

TABLE 3 | Gene mutations in synchronous multiple ground-glass nodules (SMGGNs).**TABLE 3A** Data extracted from four articles which showed the gene alterations among multicentric SMGGNs.

Author (year)	Gene_targeted	Amount	Leision_1	Leision_2	Leision_3	Leision_4	Leision_5
Liu, M (16).	EGFR	10	EGFR 19del	wild[#]			
		10	EGFR L858R	wild			
		8	EGFR L858R	EGFR 19del			
		1	EGFR 19del	wild			
		1	EGFR 19del	EGFR L858R			
		1	EGFR 19del	EGFR G719S			
		1	EGFR S768I	wild			
		1	EGFR L858R	EGFR 19del			
		1	EGFR L861Q	wild			
		1	EGFR L858R	EGFR L858R/19del			
Chung, J. H (19).	EGFR、KRAS	9	EGFR 19del	wild			
		6	wild	wild			
		4	EGFR 19del	EGFR L858R			
		1	EGFR 19del/ KRAS	wild			
		1	EGFR 19del/ F712L	wild			
		1	EGFR L858R	wild			
		1	EGFR L858R	G724S/L861Q			
		1	KRAS	wild			
Chen, K (23).	EGFR、KRAS、BRAF、TP53、ALK、ROS1、RET	1	EGFR others/TP53	wild			
		1	EGFR L858R	BRAF			
		1	EGFR L858R	wild			
		1	EGFR L858R/19del	wild			
		1	KRAS	wild			
		1	ROS1	wild			
Li, Y (25).	EGFR、KRAS、BRAF、TP53、ALK*	4	others	others			
		3	KRAS	others			
		3	others	others	others		
		2	EGFR	others			
		2	EGFR	EGFR			
		2	EGFR/TP53	EGFR			
		1	EGFR/TP53	others			
		1	EGFR/TP53	ALK			
		1	EGFR	ROS1			
		1	others	others	others	others	others
		1	EGFR	EGFR	others		
		1	EGFR	EGFR	EGFR		
		1	EGFR/TP53	others	others		

**whole exosome sequencing was used and the data showed only some specific gene alterations.*
[#]wild means no target gene alteration was found in the research.

TABLE 3B | Three cases confirmed by Li, Y (25). which applied WES to analyze gene alterations in their research.

Author(year)	Method	Gene	Gene_alterations
Li, Y (25).	WES	patient_1	EGFR/others
		patient_2	EGFR/TP53/others
		patient_3	EGFR/TP53/others

than solid nodules (52). Therefore, it is predictable that PD-1 treatment is less effective for patients with GGOs.

When compared to lung cancer presenting as solid nodule(s), Zhao et al (9) reported that the EGFR mutation rate was higher in solid nodules than in GGOs, especially the subtype mutation of 19 del, agreeing with previous studies (14). They also reported that in patients with GGOs, there are significantly more frequent HER2 mutations ($p = 0.033$), while less frequent ALK translocations ($p = 0.014$) and PIK3CA mutations ($p = 0.012$), compared to patients with solid nodules (GGOs/Solid nodules = 529/718). However, contrary to other studies in our analysis, Hong et al. (30) find that EGFR mutations were significantly more frequent in tumors with GGOs than in solid tumors, which may be caused by the different cohort sizes, regions of the cohorts, and the methods used to detect the mutations, suggesting that more researches are needed to elucidate the difference in the rates of mutations between GGOs and solid nodules.

Despite PCR, WES, and WGS which are used in the studies included in our study, with the development of molecular

diagnostic technology, the field of liquid biopsy has gradually developed a lot. Analyzing circulating tumor DNA (ctDNA) at the genomic level, a newly-emerged non-invasive approach, is proposed to have the ability to distinguish between malignant and benign disease (53, 54) and at the same time detect the molecular alterations carried by the nodules, and then guide targeted therapy and immunotherapy. However, it has been shown that indolent GGO-predominant lung cancers shed lower-level ctDNA, which is less detectable to help identify cancer in patients (55). Therefore, for very early lesions, such as GGOs, it is difficult to achieve an early diagnosis by ctDNA SNV testing under the current technology limitations with a low sensitivity.

Two studies reported independently that different pathological lesions could share identical mutations even in pre-invasive LUADs, such as AAH and AIS lesions (56, 57). This review also points out that different GGOs could share the same mutation in patients with SMGGNs, shows that SMGGNs might have an intrapulmonary spread, despite the multicentric regions. Detecting the mutation status of a specific gene by PCR is only a small fragment of the whole genome and does not represent the expression status of the whole genome, so using whole exon sequencing (WES) or whole-genome sequencing (WGS) to determine an intrapulmonary metastasis of GGO sounds more convincing. In the 26 cases with SMGGNs reported by Li et al. (25) using WES, 3 cases (11.54%) were confirmed to have an intrapulmonary spread. Despite the articles analyzed in our review, we noted that Li et al. (58) reported another two cases to be an intrapulmonary spread by WES in a case report. Though EGFR mutations were found in four of the five confirmed cases, it is still too early to come to a conclusion that specific molecular alterations are associated with the intrapulmonary spreading of GGOs. We need to be concerned that though GGO is usually considered an early-stage lesion, it has a certain probability of metastasis. However, the exact mechanism of metastasis in GGOs, non-invasive cancer, is still unclear. We noted that these GGOs were all in a close proximity which might result in dissemination along the airway. Furthermore, whether these multiple GGOs sharing the same mutation affects the prognosis needs to be explored by an in-depth longer follow-up clinical and mechanistic analysis.

With the development of an immune checkpoint inhibitor treatment, especially the inspiring results of neoadjuvant immune therapy, a series of studies have focused on the immune-environment of early-stage lung cancer patients. The TRACEx cohort reported that sparsely infiltrated tumors exhibited a waning of neoantigen editing during tumor evolution, compared with immune-infiltrated tumor regions exhibiting an ongoing immunoediting, with either loss of heterozygosity in human leukocyte antigens or depletion of expressed neoantigens (59).Recently, some researchers have used single-cell tumor sequencing to map the tumor microenvironment and have found that GGO has less endothelial cell angiogenesis, downregulated EGR1 expression, upregulated KLF6 expression, a significantly higher proportion of NK cells, and showing a marked metabolic disorder and immune response stress, compared to an advanced lung cancer (60, 61). These studies, although with a limited sample size, initially revealed distinct immune mechanisms in GGOs from non-GGO lung adenocarcinomas, helping us to further understand the essence of the inert progression of GGO and to identify the nodules with a poorer prognosis at an early stage.

CONCLUSION

Our research revealed that EGFR mutation is not associated with the radiological progression of GGOs, which means EGFR mutation was a driver mutation for lung cancer in a fairly early stage, and maintains consistency in the progression of tumors. On the contrary, the frequency of KRAS mutation was higher in progressed lung nodules, indicating a position for KRAS mutation in tumor progression. Immunotherapy, as one of the recently discovered effective therapies for advanced lung cancer, is less effective against GGOs, which may be due to the low expression level of PD-L1 in early-stage lung cancer, found by our research. Though GGOs are usually considered early-stage lesions, there does have a possibility for SMGGNs to have an intrapulmonary spread, the mechanism behind which is still unclear. The limitation of our meta-analysis lies in its retrospective design; postsurgical follow-up or treatment plans at recurrence would differ among attending surgeons. Also, the high heterogeneity between the methodologies and results of researches is another limitation of our research. Overall, this review summarizes the published estimates of the rates of molecular alterations in lung nodules presenting as GGOs, which may help clinical treatment decisions for GGOs and provide a novel insight in revealing the molecular alterations behind GGOs.

DATA AVAILABILITY STATEMENT

The original contributions presented in the study are included in the article/**Supplementary Material**. Further inquiries can be directed to the corresponding author.

AUTHOR CONTRIBUTIONS

ZWe and ZWa conceived and planned the experiments. ZWe and ZWa carried out the experiments. ZWe, ZWa, HS, XW, and MW contributed to the data preparation. ZWe, ZWa, YN, and KZ verified the analytical methods. ZWe, ZWa, YN, KZ, HS, XW, and MW contributed to the interpretation of the results. ZWe and ZWa took the lead in writing the manuscript. All authors contributed to the article and approved the submitted version.

FUNDING

This study was supported by the National Natural Science Funds (grant No. 82072566) and Peking University People's Hospital Research and Development Funds (grant No. RS2019-01).

ACKNOWLEDGMENTS

We thank our colleagues from the Department of Thoracic Surgery, Peking University People's Hospital, Beijing, China who provided their insight and expertise that greatly assisted the research, although they may not be informed of all the interpretations/conclusions of this paper.

SUPPLEMENTARY MATERIAL

The Supplementary Material for this article can be found online at: https://www.frontiersin.org/articles/10.3389/fonc.2021.724692/full#supplementary-material

REFERENCES

1. Austin JH, Müller NL, Friedman PJ, Hansell DM, Naidich DP, Remy-Jardin M, et al. Glossary of Terms for CT of the Lungs: Recommendations of the Nomenclature Committee of the Fleischner Society. *Radiology* (1996) 200 (2):327–31. doi: 10.1148/radiology.200.2.8685321
2. Henschke CI, Yankelevitz DF, Mirtcheva R, McGuinness G, McCauley D, Miettinen OS. CT Screening for Lung Cancer: Frequency and Significance of Part-Solid and Nonsolid Nodules. *AJR Am J Roentgenol* (2002) 178(5):1053–7. doi: 10.2214/ajr.178.5.1781053
3. Fu F, Zhang Y, Wen Z, Zheng D, Gao Z, Han H, et al. Distinct Prognostic Factors in Patients With Stage I Non-Small Cell Lung Cancer With Radiologic Part-Solid or Solid Lesions. *J Thorac Oncol* (2019) 14(12):2133–42. doi: 10.1016/j.jtho.2019.08.002
4. Hattori A, Hirayama S, Matsunaga T, Hayashi T, Takamochi K, Oh S, et al. Distinct Clinicopathologic Characteristics and Prognosis Based on the Presence of Ground Glass Opacity Component in Clinical Stage IA Lung Adenocarcinoma. *J Thorac Oncol* (2019) 14(2):265–75. doi: 10.1016/j.jtho.2018.09.026
5. Moher D, Liberati A, Tetzlaff J, Altman DG. Preferred Reporting Items for Systematic Reviews and Meta-Analyses: The PRISMA Statement. *Ann Intern Med* (2009) 151(4):264–9. doi: 10.7326/0003-4819-151-4-200908180-00136
6. DerSimonian R, Laird N. Meta-Analysis in Clinical Trials Revisited. *Contemp Clin Trials* (2015) 45(Pt A):139–45. doi: 10.1016/j.cct.2015.09.002
7. Freeman MF, Tukey JW. Transformations Related to the Angular and the Square Root. *Ann Math Stat* (1950) 21(4):607–11. doi: 10.1214/aoms/1177729756
8. Higgins JPT, Thompson SG, Deeks JJ, Altman DG. Measuring Inconsistency in Meta-Analyses. *BMJ* (2003) 327(7414):557–60. doi: 10.1136/bmj.327.7414.557
9. Zhao M, Zhan C, Li M, Yang X, Yang X, Zhang Y, et al. Aberrant Status and Clinicopathologic Characteristic Associations of 11 Target Genes in 1,321 Chinese Patients With Lung Adenocarcinoma. *J Thorac Dis* (2018) 10(1):398–407. doi: 10.21037/jtd.2017.12.68
10. Aoki T, Hanamiya M, Uramoto H, Hisaoka M, Yamashita Y, Korogi Y. Adenocarcinomas With Predominant Ground-Glass Opacity: Correlation of Morphology and Molecular Biomarkers. *Radiology* (2012) 264(2):590–6. doi: 10.1148/radiol.12111337
11. Dai J, Shi J, Soodeen-Lalloo AK, Zhang P, Yang Y, Wu C, et al. Air Bronchogram: A Potential Indicator of Epidermal Growth Factor Receptor Mutation in Pulmonary Subsolid Nodules. *Lung Cancer* (2016) 98:22–8. doi: 10.1016/j.lungcan.2016.05.009
12. Suda K, Mitsudomi T, Shintani Y, Okami J, Ito H, Ohtsuka T, et al. Clinical Impacts of EGFR Mutation Status: Analysis of 5780 Surgically Resected Lung Cancer Cases. *Ann Thorac Surg* (2021) 111(1):269–76. doi: 10.1016/j.athoracsur.2020.05.041
13. Zheng M, Wang N, Wang R. Comprehensive Study of Surgical Treated Lung Adenocarcinoma With Ground Glass Nodule Component. *Med Sci monitor Int Med J Exp Clin Res* (2019) 25:8492–8. doi: 10.12659/msm.919532
14. Zou J, Lv T, Zhu S, Lu Z, Shen Q, Xia L, et al. Computed Tomography and Clinical Features Associated With Epidermal Growth Factor Receptor Mutation Status in Stage I/II Lung Adenocarcinoma. *Thorac Cancer* (2017) 8(3):260–70. doi: 10.1111/1759-7714.12436
15. Sugano M, Shimizu K, Nakano T, Kakegawa S, Miyamae Y, Kaira K, et al. Correlation Between Computed Tomography Findings and Epidermal Growth Factor Receptor and KRAS Gene Mutations in Patients With Pulmonary Adenocarcinoma. *Oncol Rep* (2011) 26(5):1205–11. doi: 10.3892/or.2011.1412
16. Liu M, He W-X, Song N, Yang Y, Zhang P, Jiang G-N. Discrepancy of Epidermal Growth Factor Receptor Mutation in Lung Adenocarcinoma Presenting as Multiple Ground-Glass Opacities. *Eur J Cardiothorac Surg* (2016) 50(5):909–13. doi: 10.1093/ejcts/ezw113
17. Yang Y, Yang Y, Zhou X, Song X, Liu M, He W, et al. EGFR L858R Mutation is Associated With Lung Adenocarcinoma Patients With Dominant Ground-Glass Opacity. *Lung Cancer* (2015) 87(3):272–7. doi: 10.1016/j.lungcan.2014.12.016
18. Lu Q, Ma Y, An Z, Zhao T, Xu Z, Chen H. Epidermal Growth Factor Receptor Mutation Accelerates Radiographic Progression in Lung Adenocarcinoma Presented as a Solitary Ground-Glass Opacity. *J Thorac Dis* (2018) 10 (11):6030–9. doi: 10.21037/jtd.2018.10.19
19. Chung J-H, Choe G, Jheon S, Sung S-W, Kim TJ, Lee KW, et al. Epidermal Growth Factor Receptor Mutation and Pathologic-Radiologic Correlation Between Multiple Lung Nodules With Ground-Glass Opacity Differentiates Multicentric Origin From Intrapulmonary Spread. *J Thorac Oncol* (2009) 4 (12):1490–5. doi: 10.1097/JTO.0b013e3181bc9731
20. Hsu K-H, Chen K-C, Yang T-Y, Yeh Y-C, Chou T-Y, Chen H-Y, et al. Epidermal Growth Factor Receptor Mutation Status in Stage I Lung Adenocarcinoma With Different Image Patterns. *J Thorac Oncol* (2011) 6 (6):1066–72. doi: 10.1097/JTO.0b013e31821667b0
21. Ko S-J, Lee YJ, Park JS, Cho Y-J, Yoon HI, Chung J-H, et al. Epidermal Growth Factor Receptor Mutations and Anaplastic Lymphoma Kinase Rearrangements in Lung Cancer With Nodular Ground-Glass Opacity. *BMC Cancer* (2014) 14:312. doi: 10.1186/1471-2407-14-312
22. Tomita M, Ayabe T, Chosa E, Kawagoe K, Nakamura K. Epidermal Growth Factor Receptor Mutations in Japanese Men With Lung Adenocarcinomas. *Asian Pac J Cancer Prev* (2014) 15(24):10627–30. doi: dx.doi.org/10.7314//APJCP.2014.15.24.10627
23. Chen K, Chen W, Cai J, Yang F, Lou F, Wang X, et al. Favorable Prognosis and High Discrepancy of Genetic Features in Surgical Patients With Multiple Primary Lung Cancers. *J Thorac Cardiovasc Surg* (2018) 155(1):371–9.e1. doi: 10.1016/j.jtcvs.2017.08.141
24. Kobayashi Y, Mitsudomi T, Sakao Y, Yatabe Y. Genetic Features of Pulmonary Adenocarcinoma Presenting With Ground-Glass Nodules: The Differences Between Nodules With and Without Growth. *Ann Oncol* (2015) 26(1):156–61. doi: 10.1093/annonc/mdu505
25. Li Y, Li X, Li H, Zhao Y, Liu Z, Sun K, et al. Genomic Characterisation of Pulmonary Subsolid Nodules: Mutational Landscape and Radiological Features. *Eur Respir J* (2020) 55(2):1901409. doi: 10.1183/13993003.01409-2019
26. Ren Y, Huang S, Dai C, Xie D, Zheng L, Xie H, et al. Germline Predisposition and Copy Number Alteration in Pre-Stage Lung Adenocarcinomas Presenting as Ground-Glass Nodules. *Front Oncol* (2019) 9:288. doi: 10.3389/fonc.2019.00288
27. Wang T, Zhang T, Han X, Liu XI, Zhou N, Liu Y. Impact of the International Association for the Study of Lung Cancer/American Thoracic Society/European Respiratory Society Classification of Stage IA Adenocarcinoma of

the Lung: Correlation Between Computed Tomography Images and EGFR and KRAS Gene Mutations. *Exp Ther Med* (2015) 9(6):2095–103. doi: 10.3892/etm.2015.2422
28. Usuda K, Sagawa M, Motono N, Ueno M, Tanaka M, Machida Y, et al. Relationships Between EGFR Mutation Status of Lung Cancer and Preoperative Factors - are They Predictive? *Asian Pac J Cancer Prev* (2014) 15(2):657–62. doi: 10.7314/APJCP.2014.15.2.657
29. Lui NS, Benson J, He H, Imielski BR, Kunder CA, Liou DZ, et al. Sub-Solid Lung Adenocarcinoma in Asian Versus Caucasian Patients: Different Biology But Similar Outcomes. *J Thorac Dis* (2020) 12(5):2161–71. doi: 10.21037/jtd.2020.04.37
30. Hong SJ, Kim TJ, Choi YW, Park J-S, Chung J-H, Lee KW. Radiogenomic Correlation in Lung Adenocarcinoma With Epidermal Growth Factor Receptor Mutations: Imaging Features and Histological Subtypes. *Eur Radiol* (2016) 26(10):3660–8. doi: 10.1007/s00330-015-4196-z
31. Wu T, Zhou F, Soodeen-Lalloo AK, Yang X, Shen Y, Ding X, et al. The Association Between Imaging Features of TSCT and the Expression of PD-L1 in Patients With Surgical Resection of Lung Adenocarcinoma. *Clin Lung Cancer* (2019) 20(2):e195–207. doi: 10.1016/j.cllc.2018.10.012
32. Suda K, Shimoji M, Shimizu S, Sato K, Chiba M, Tomizawa K, et al. Comparison of PD-L1 Expression Status Between Pure-Solid Versus Part-Solid Lung Adenocarcinomas. *Biomolecules* (2019) 9(9):456. doi: 10.3390/biom9090456
33. Toyokawa G, Takada K, Okamoto T, Shimokawa M, Kozuma Y, Matsubara T, et al. Computed Tomography Features of Lung Adenocarcinomas With Programmed Death Ligand 1 Expression. *Clin Lung Cancer* (2017) 18(6):e375–e83. doi: 10.1016/j.cllc.2017.03.008
34. Aoki T, Tomoda Y, Watanabe H, Nakata H, Kasai T, Hashimoto H, et al. Peripheral Lung Adenocarcinoma: Correlation of Thin-Section CT Findings With Histologic Prognostic Factors and Survival. *Radiology* (2001) 220(3):803–9. doi: 10.1148/radiol.2203001701
35. Matsuguma H, Yokoi K, Anraku M, Kondo T, Kamiyama Y, Mori K, et al. Proportion of Ground-Glass Opacity on High-Resolution Computed Tomography in Clinical T1 N0 M0 Adenocarcinoma of the Lung: A Predictor of Lymph Node Metastasis. *J Thorac Cardiovasc Surg* (2002) 124(2):278–84. doi: 10.1067/mtc.2002.122298
36. Nakata M, Sawada S, Yamashita M, Saeki H, Kurita A, Takashima S, et al. Objective Radiologic Analysis of Ground-Glass Opacity Aimed at Curative Limited Resection for Small Peripheral Non-Small Cell Lung Cancer. *J Thorac Cardiovasc Surg* (2005) 129(6):1226–31. doi: 10.1016/j.jtcvs.2004.10.032
37. Lynch TJ, Bell DW, Sordella R, Gurubhagavatula S, Okimoto RA, Brannigan BW, et al. Activating Mutations in the Epidermal Growth Factor Receptor Underlying Responsiveness of non-Small-Cell Lung Cancer to Gefitinib. *N Engl J Med* (2004) 350(21):2129–39. doi: 10.1056/NEJMoa040938
38. Pao W, Miller V, Zakowski M, Doherty J, Politi K, Sarkaria I, et al. EGF Receptor Gene Mutations are Common in Lung Cancers From "Never Smokers" and are Associated With Sensitivity of Tumors to Gefitinib and Erlotinib. *Proc Natl Acad Sci USA* (2004) 101(36):13306–11. doi: 10.1073/pnas.0405220101
39. Tsao M-S, Sakurada A, Cutz J-C, Zhu C-Q, Kamel-Reid S, Squire J, et al. Erlotinib in Lung Cancer - Molecular and Clinical Predictors of Outcome. *N Engl J Med* (2005) 353(2):133–44. doi: 10.1056/NEJMoa050736
40. Shigematsu H, Takahashi T, Nomura M, Majmudar K, Suzuki M, Lee H, et al. Somatic Mutations of the HER2 Kinase Domain in Lung Adenocarcinomas. *Cancer Res* (2005) 65(5):1642–6. doi: 10.1158/0008-5472.CAN-04-4235
41. Kosaka T, Yatabe Y, Onozato R, Kuwano H, Mitsudomi T. Prognostic Implication of EGFR, KRAS, and TP53 Gene Mutations in a Large Cohort of Japanese Patients With Surgically Treated Lung Adenocarcinoma. *J Thorac Oncol* (2009) 4(1):22–9. doi: 10.1097/JTO.0b013e3181914111
42. Chou Y-T, Lin H-H, Lien Y-C, Wang Y-H, Hong C-F, Kao Y-R, et al. EGFR Promotes Lung Tumorigenesis by Activating miR-7 Through a Ras/ERK/Myc Pathway That Targets the Ets2 Transcriptional Repressor ERF. *Cancer Res* (2010) 70(21):8822–31. doi: 10.1158/0008-5472.CAN-10-0638
43. Sun F, Xi J, Zhan C, Yang X, Wang L, Shi Y, et al. Ground Glass Opacities: Imaging, Pathology, and Gene Mutations. *J Thorac Cardiovasc Surg* (2018) 156(2):808–13. doi: 10.1016/j.jtcvs.2018.02.110
44. Kobayashi Y, Mitsudomi T. Management of Ground-Glass Opacities: Should All Pulmonary Lesions With Ground-Glass Opacity be Surgically Resected? *Trans Lung Cancer Res* (2013) 2(5):354–63. doi: 10.3978/j.issn.2218-6751.2013.09.03
45. Lee SW, Leem C-S, Kim TJ, Lee KW, Chung J-H, Jheon S, et al. The Long-Term Course of Ground-Glass Opacities Detected on Thin-Section Computed Tomography. *Respir Med* (2013) 107(6):904–10. doi: 10.1016/j.rmed.2013.02.014
46. Huang C, Wang C, Wang Y, Liu J, Bie F, Wang Y, et al. The Prognostic Significance of Pure Ground Glass Opacities in Lung Cancer Computed Tomographic Images. *J Cancer* (2019) 10(27):6888–95. doi: 10.7150/jca.33132
47. Slebos RJ, Kibbelaar RE, Dalesio O, Kooistra A, Stam J, Meijer CJ, et al. K-Ras Oncogene Activation as a Prognostic Marker in Adenocarcinoma of the Lung. *N Engl J Med* (1990) 323(9):561–5. doi: 10.1056/NEJM199008303230902
48. Uras IZ, Moll HP, Casanova E. Targeting KRAS Mutant Non-Small-Cell Lung Cancer: Past, Present and Future. *Int J Mol Sci* (2020) 21(12):4325. doi: 10.3390/ijms21124325
49. Herbst RS, Baas P, Kim D-W, Felip E, Pérez-Gracia JL, Han J-Y, et al. Pembrolizumab Versus Docetaxel for Previously Treated, PD-L1-Positive, Advanced Non-Small-Cell Lung Cancer (KEYNOTE-010): A Randomised Controlled Trial. *Lancet* (2016) 387(10027):1540–50. doi: 10.1016/S0140-6736(15)01281-7
50. Qu J, Mei Q, Liu L, Cheng T, Wang P, Chen L, et al. The Progress and Challenge of Anti-PD-1/PD-L1 Immunotherapy in Treating non-Small Cell Lung Cancer. *Ther Adv Med Oncol* (2021) 13:1758835921992968–. doi: 10.1177/1758835921992968
51. Emancipator K. Keytruda and PD-L1: A Real-World Example of Co-Development of a Drug With a Predictive Biomarker. *AAPS J* (2020) 23(1):5. doi: 10.1208/s12248-020-00525-1
52. Wu F, Li W, Zhao W, Zhou F, Xie H, Shi J, et al. Synchronous Ground-Glass Nodules Showed Limited Response to Anti-PD-1/PD-L1 Therapy in Patients With Advanced Lung Adenocarcinoma. *Clin Trans Med* (2020) 10(3):e149. doi: 10.1002/ctm2.149
53. Jiang N, Zhou J, Zhang W, Li P, Liu Y, Shi H, et al. RNF213 Gene Mutation in Circulating Tumor DNA Detected by Targeted Next-Generation Sequencing in the Assisted Discrimination of Early-Stage Lung Cancer From Pulmonary Nodules. *Thorac Cancer* (2021) 12(2):181–93. doi: 10.1111/1759-7714.13741
54. Abbosh C, Birkbak NJ, Wilson GA, Jamal-Hanjani M, Constantin T, Salari R, et al. Phylogenetic ctDNA Analysis Depicts Early-Stage Lung Cancer Evolution. *Nature* (2017) 545(7655):446–51. doi: 10.1038/nature22364
55. Chabon JJ, Hamilton EG, Kurtz DM, Esfahani MS, Moding EJ, Stehr H, et al. Integrating Genomic Features for Non-Invasive Early Lung Cancer Detection. *Nature* (2020) 580(7802):245–51. doi: 10.1038/s41586-020-2140-0
56. Hu X, Fujimoto J, Ying L, Fukuoka J, Ashizawa K, Sun W, et al. Multi-Region Exome Sequencing Reveals Genomic Evolution From Preneoplasia to Lung Adenocarcinoma. *Nat Commun* (2019) 10(1):2978. doi: 10.1038/s41467-019-10877-8
57. Krysan K, Tran LM, Grimes BS, Fishbein GA, Seki A, Gardner BK, et al. The Immune Contexture Associates With the Genomic Landscape in Lung Adenomatous Premalignancy. *Cancer Res* (2019) 79(19):5022. doi: 10.1158/0008-5472.CAN-19-0153
58. Li R, Li X, Xue R, Yang F, Wang S, Li Y, et al. Early Metastasis Detected in Patients With Multifocal Pulmonary Ground-Glass Opacities (GGOs). *Thorax* (2018) 73(3):290–2. doi: 10.1136/thoraxjnl-2017-210169
59. Rosenthal R, Cadieux EL, Salgado R, Bakir MA, Moore DA, Hiley CT, et al. Neoantigen-Directed Immune Escape in Lung Cancer Evolution. *Nature* (2019) 567(7749):479–85. doi: 10.1038/s41586-019-1032-7
60. Xing X, Yang F, Huang Q, Guo H, Wang JJSA. Decoding the Multicellular Ecosystem of Lung Adenocarcinoma Manifested as Pulmonary Subsolid Nodules by Single-Cell RNA Sequencing. (2021) 7(5):eabd9738. doi: 10.1126/sciadv.abd9738
61. Lu T, Yang X, Shi Y, Zhao M, Tan LJCD. Single-Cell Transcriptome Atlas of Lung Adenocarcinoma Featured With Ground Glass Nodules. (2020) 6(1):69. doi: 10.1038/s41421-020-00200-x

Conflict of Interest: The authors declare that the research was conducted in the absence of any commercial or financial relationships that could be construed as a potential conflict of interest.

this article, or claim that may be made by its manufacturer, is not guaranteed or endorsed by the publisher.

frontiers in Oncology

ORIGINAL RESEARCH
published: 21 September 2021
doi: 10.3389/fonc.2021.725475

Comparison of Clinical and Pathological Characteristics Between Extremely Multiple GGNs and Single GGNs

*Xin Wang†, Manqi Wu†, Haifeng Shen, Yuntao Nie, Kai Zhang, Zihan Wei, Ziyang Wang, Fan Yang and Kezhong Chen**

Department of Thoracic Surgery, Peking University People's Hospital, Peking University, Beijing, China

Objective: This study aims to compare the clinical and pathological characteristics between patients undergoing surgery for extremely multiple ground-glass nodules (GGNs) and those for single GGN.

Methods: We defined extremely multiple GGNs as follows: (i) number of GGNs ≥3, (ii) GGN diameter between 3 and 30 mm, and (iii) no less than three nodules that were surgically removed and pathologically diagnosed. Patients with extremely multiple GGNs and single GGNs who underwent surgery at the same time were retrospectively analyzed. The patients were divided into three groups according to the number of nodules: exceedingly multiple nodules (EMN) group (>10), highly multiple nodules (HMN) group (three to 10), and single nodule (SN) group. The clinical and pathological characteristics, surgical methods and prognosis were analyzed.

Results: Ninety-nine patients with single nodules and 102 patients with extremely multiple nodules were enrolled. Among the patients with extremely multiple nodules, 43 (42.2%) had >10 nodules. There were no significant differences in demographic characteristics, such as age, sex, and smoking history, between the groups, but there were differences in tumor characteristics. All patients with >10 nodules showed bilateral pulmonary nodules and presented with both pure and mixed GGNs. The single GGNs were smaller in diameter, and the proportion of mixed GGNs and pathologically invasive adenocarcinoma was lower than that of the primary nodules in the exceedingly multiple GGNs group ($p < 0.05$). However, the proportion of both mixed GGNs and malignant nodules decreased significantly with the increasing number of total lesions. During postoperative follow-up, one patient in the highly multiple nodules group had a local recurrence, and 16 (15.7%) patients in the extremely multiple GGNs group and 10 (9.8%) patients in the single GGN group had enlarged unresected GGNs or additional GGNs.

Conclusions: Our study revealed the clinical and pathologic characteristics, surgical methods, and prognosis of patients with extremely multiple GGNs and compared them with those of patients with a single GGN. Although the primary nodules in extremely multiple GGNs may have higher malignancy than those in the single nodule group, the

OPEN ACCESS

Edited by:
Yijiu Ren,
Tongji University, China

Reviewed by:
Xiaonan Shao,
The Third Affiliated Hospital of Soochow University, China
Ming Li,
Fudan University, China

****Correspondence:***
Kezhong Chen
chenkezhong@pkuph.edu.cn

†These authors have contributed equally to this work and share first authorship

Specialty section:
This article was submitted to Thoracic Oncology, a section of the journal Frontiers in Oncology

Received: *15 June 2021*
Accepted: *24 August 2021*
Published: *21 September 2021*

Citation:
Wang X, Wu M, Shen H, Nie Y, Zhang K, Wei Z, Wang Z, Yang F and Chen K (2021) Comparison of Clinical and Pathological Characteristics Between Extremely Multiple GGNs and Single GGNs. Front. Oncol. 11:725475. doi: 10.3389/fonc.2021.725475

proportion of both mGGNs and malignant nodules decreased significantly with the increasing number of lesions, and the prognosis of patients with extremely multiple GGNs was satisfied.

Keywords: ground-glass nodule, clinical characteristics, prognosis, lung cancer, multiple

INTRODUCTION

Ground-glass nodules (GGNs) are nonspecific radiologic findings showing hazy opacity, without blocking the underlying pulmonary vessels or bronchial structures, on high-resolution computed tomography (HRCT) (1) and are classified as either pure ground-glass nodules (pGGNs) or mixed ground-glass nodules (mGGNs) according to the absence or presence of solid components. The pathology of GGNs can be malignant or benign and be associated with conditions such as inflammation, focal interstitial fibrosis, and hemorrhage (2).

The detection rate of GGN has steadily increased in recent years due to the widespread use of low-dose computed tomography, ranging from 2.7 to 95.5% in some lung cancer screening trials (3–7). In addition, GGNs frequently appear as extremely multiple nodules (≥3), which has made the diagnosis and treatment of extremely multiple GGNs a research hot spot (8, 9). Previous research has confirmed that GGNs are more likely to be detected in young female non-smokers (8) and more likely to be malignant (10). However, no scholars have reported the characteristics of extremely multiple nodules and compared these nodules with single GGNs. Furthermore, there exists some controversy about how to treat patients with GGNs.

We collected the clinical and pathology data of 201 patients who were diagnosed with extremely multiple GGNs (≥3) or single GGNs who underwent surgery in recent years for retrospective analysis. The objective of this study was to understand the characteristics, surgical method, and prognosis of patients undergoing surgery for extremely multiple GGNs.

METHODS

Patients

From September 2010 to March 2020, 1,556 patients with single GGNs and 149 patients with extremely multiple GGNs underwent surgery in our center. A total of 156 of the 1,556 (one out of 10) patients with single GGNs were randomly selected as the sample to match the number of patients with extremely multiple nodules in a ratio of 1:1. The data of the 156 patients with single GGNs and all the patients with extremely multiple GGNs was collected. The inclusion criteria for the single nodule (SN) group were as follows: (i) only one GGN was found on preoperative imaging and (ii) the GGN diameter was between 3 and 30 mm. The inclusion criteria for the extremely multiple nodules group were as follows: (i) number of GGNs ≥3, (ii) GGN diameter between 3 and 30 mm, and (iii) no less than three nodules were surgically removed and pathologically diagnosed. The patients in the extremely multiple nodules group were divided into two subgroups according to the number of nodules: the exceedingly multiple nodules (EMN) group (>10) and the highly multiple nodules (HMN) group (three to 10) (**Figure 1**). The primary nodule in the group with extremely multiple GGNs was defined as the main tumor to be surgically resected as decided upon by the surgeons, which primarily depended upon its radiologic invasiveness, the percentage of solid components, and the tumor size. All patients were regularly evaluated by HRCT scans from the day of surgery; the intervals were at the discretion of the attending physician. Generally, the patients were reviewed every 3 months within 2 years after surgery, every 6 months starting in the third year, and annually starting in the fifth year. The components of the follow-up review included chest CT, abdominal ultrasound and tumor markers, and brain magnetic resonance imaging. Whole-body bone scan imaging was considered according to the condition of the patient.

This study was reviewed and approved by the Institutional Review Board of Peking University People's Hospital.

Radiologic Evaluation

All CT scans were performed on 16-detector CT scanners and obtained at 120 kVp and 40–60 mA, with rotation times of up to 1 s. Images were reconstructed at 1.0-mm slice width with the use of the standard mediastinal (width, 350 HU; level, 40 HU) and lung (width, 1,500 HU; level, 600 HU) window width and window level settings. The diameter of the tumor was defined as the largest axial diameter of the nodule in the lung window setting. All image data were extracted independently by two thoracic radiologists.

Surgical Approach

With reference to corresponding guidelines and literature, different treatment strategies (follow-up or resection) were performed according to the characteristics of the pulmonary nodules (11–13). Our basic surgical strategies for multiple pulmonary nodules were as follows: (1) preliminary assessment of the location and the size of the nodules, imaging features, and estimation of postoperative respiratory function; (2) when the nodules were all pure GGNs, sublobar resection (wedge and segmental resection) was preferred, while in cases of subsolid nodules, lobectomy of the main solid nodules and sublobar resection of other scattered nodules were performed as per the usual practice. All palpable ipsilateral nodules were resected simultaneously. Unless GGNs were deeply embedded, they could not be resected by wedge resection; and (3) for contralateral tumors, two-stage surgery was generally recommended. If all contralateral lesions were small pure GGNs, a wait-and-see approach was adopted, and growth and

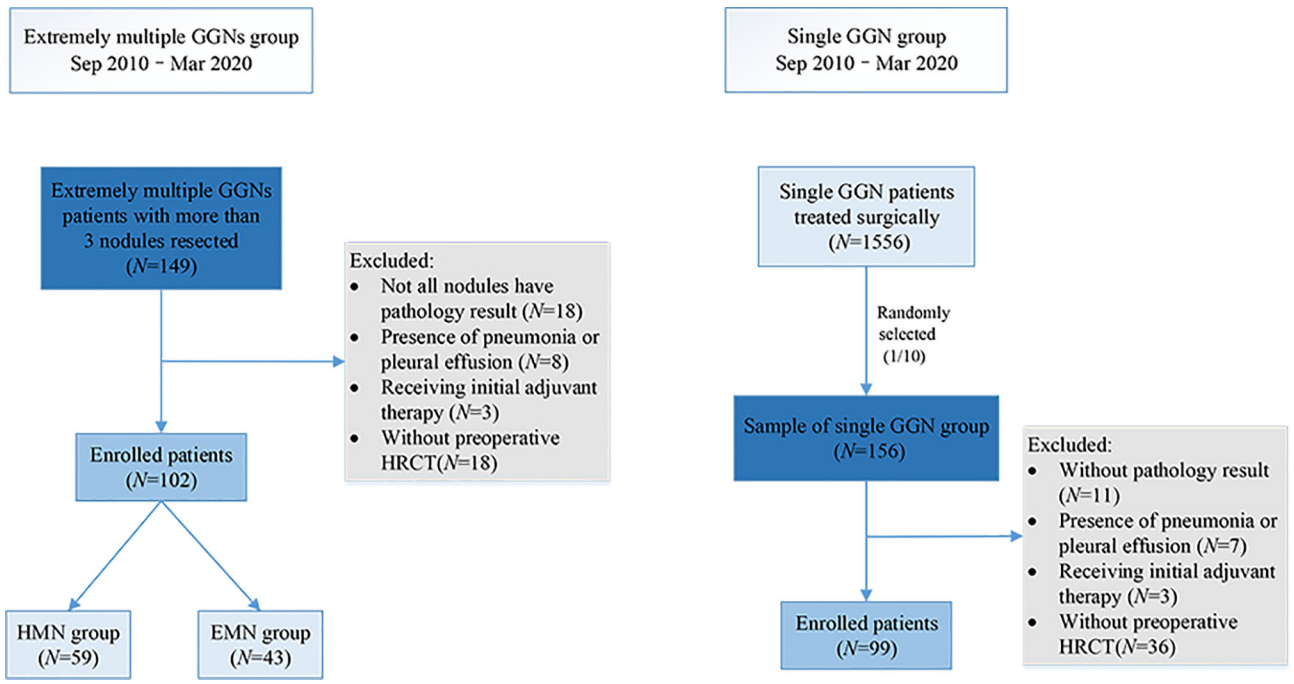

FIGURE 1 | Enrollment flow chart of the study.

invasion were monitored. Similarly, for single GGNs, sublobar resection was preferred when a sufficient margin could be assured, especially for peripheral ground glass opacity-dominant nodules smaller than 2 cm (14, 15).

Histologic Evaluation

All clinical specimens were examined and recorded by two pathology specialists. Lung adenocarcinoma was analyzed according to the World Health Organization classification (16), and each nodule was reviewed for size, location, pleural invasion, and lymphatic invasion according to the International Association for the Study of Lung Cancer (IASLC) (17).

Statistical Analysis

For most variables, we calculated descriptive statistics, such as medians with interquartile ranges (for data with skewed distribution) and proportions (percentages). Statistical comparisons between groups were evaluated by *t*-test, analysis of variance, Mann–Whitney *U*-tests, and Kruskal–Wallis tests when appropriate. To explore the variation of the variable with the increasing number of nodules, the Loess method was used for smoothing curve fitting. Data for the interval between surgical resection and the last follow-up visit were analyzed *via* the Kaplan–Meier method using confirmed recurrence deaths to calculate the recurrence-free survival and the overall survival. *P*-values less than 0.05 were considered to be statistically significant. The statistical analyses were performed using R, version 3.5.3.

RESULTS

Clinical Characteristics

Ninety-nine patients with single nodules and 102 patients with extremely multiple nodules were enrolled in the study (**Figure 1**), and the median number of nodules in the group with extremely multiple nodules was 10 (range, 3–82). Fifty-nine (55.6%) patients were in the HMN group, and 43 (44.4%) were in the EMN group. The characteristics and a comparison among the three groups are summarized in **Table 1**. There was a greater proportion of female patients in the HMN and EMN groups than in the SN group, although the difference between the two groups was not yet significant ($p = 0.06$). The mean age of the HMN group patients was 55.2 ± 8.9 years, while that of the EMN group patients was 57.1 ± 9.8 years ($p = 0.29$). Most patients had no complaints, no positive tumor markers, and no family history or smoking history, and these characteristics did not differ significantly among the three groups.

A total of 1,344 GGNs were detected in the HMN and EMN groups, including 1,078 pure GGNs and 266 mixed GGNs. Most of the nodules were located in the upper lobe of the right lung and the upper lobe of the left lung (32.7 and 29.1%, respectively), among which 68.6% were in the apical and posterior segments (**Table 2**). The median diameters of the primary nodules in the SN group, HMN group, and EMN group were 11.0 mm (range, 4.0–29.0 mm), 12.8 mm (range, 6.6–30.0 mm), and 17.2 mm (range, 10.2–30.0 mm), respectively. The proportions of mGGNs in the primary nodules were 56.6, 62.7, and 83.7% for the SN, HMN, and EMN groups, respectively. There were significant differences in the size

TABLE 1 | Clinical characteristics of the patients.

Variable	Extremely multiple ground-glass nodules (GGNs)				SN group (*N* = 99)	P^b
	HMN group (*N* = 59)	EMN group (*N* = 43)	P^a	Overall (*N* = 102)		
Sex (%)			0.64			0.06
Female	44 (74.6)	34 (79.1)		78 (76.5)	63 (63.6)	
Complaint (%)			0.47			0.73
Yes	11 (18.6)	11 (25.6)		22 (21.6)	19 (19.2)	
Age			0.29			0.83
Mean (SD)	55.2 (8.9)	57.1 (9.8)		56.0 (9.1)	55.7 (9.5)	
Family history (%)			0.72			0.35
Yes	4 (6.8)	4 (9.3)		8 (7.8)	12 (12.1)	
Smoking history (%)			1.00			0.31
Yes	10 (16.9)	7 (16.3)		17 (16.7)	11 (11.2)	
Emphysema (%)			0.70			0.79
Yes	5 (8.5)	2 (4.7)		7 (6.9)	8 (8.1)	
Positive tumor markers (%)			0.03			0.61
Yes	9 (15.3)	15 (34.9)		24 (23.5)	20 (20.2)	
Nodule distribution (%)			0.02			NA
Bilateral	51 (86.4)	43 (100.0)		66 (91.7)	NA	
Nodule type (%)			<0.01			NA
pGGN only	13 (22.0)	0 (0.0)		13 (12.7)	43 (43.4)	
mGGN only	4 (6.8)	0 (0.0)		4 (3.9)	56 (56.6)	
Both pGGN and mGGN	42 (71.2)	43 (100.0)		85 (83.3)	NA	
Bilateral surgery (%)			0.06			NA
Yes	26 (44.1)	11 (25.6)		23 (34.8)	NA	
Operation method (%)			0.77			NA
Sublobar resection	36 (61.0)	24 (55.8)		60 (58.8)	77 (77.8)	
Lobectomy	8 (13.6)	5 (11.6)		13 (12.7)	22 (22.2)	
Both	15 (25.4)	14 (32.6)		29 (28.4)	NA	
Lymph node (%)			0.27			0.87
No intervention	4 (6.8)	3 (7.0)		7 (6.9)	9 (9.1)	
Dissection	21 (35.6)	22 (51.2)		43 (42.2)	40 (40.4)	
Sampling	34 (57.6)	18 (41.9)		52 (51.0)	50 (50.5)	
Operation interval			0.27			NA
Median (IQR)	5.0 (4.0, 7.0)	4.0 (4.0, 4.5)		4.0 (4.0, 6.0)	NA	
Resection rate			<0.01			NA
Median (IQR)	75.0% (57.1%, 100.0%)	33.3% (25.8%, 46.3%)		50.0% (33.3%, 77.7%)	NA	

HMN, highly multiple nodules; EMN, exceedingly multiple nodules; SN, single nodule; SD, standard deviation; IQR, interquartile range.

[a]*Comparison between the HMN group and the EMN group.*

[b]*Comparison between patients with extremely multiple GGNs and those with a single GGN.*

NA, not available.

and the type of the primary nodules between the SN group and the EMN group ($p < 0.01$), while the differences in the other pairwise comparisons (the SN group *vs.* the HMN group and the HMN group *vs.* the EMN group) were not significant after Bonferroni correction (Bonferroni-adjusted significance threshold, $p < 0.017$) (**Table 3**). However, the proportion of mGGNs decreased significantly as the number of total lesions increased (correlation coefficient, r = -0.28, **Figure 2**). In the EMN group, all patients presented with bilateral nodules, with both pGGNs and mGGNs showing a wider distribution (100 *vs.* 85%, $p = 0.03$) and higher imaging heterogeneity (100 *vs.* 75%, $p = 0.004$) than the HMN group. Interestingly, in four patients, the nodules were clustered, and no less than 10 GGNs were concentrated in a single segment (**Figure 3**). The other characteristics did not differ significantly between the two groups.

Surgical Approach

All patients had the primary nodule excised, while only eight patients with three to five GGNs had all the lesions excised in the extremely multiple nodules group. The nodule resection rate in the EMN group was significantly lower than that in the HMN group (median, 33.3 *vs.* 75.0%, $p < 0.01$). More sublobar resection for primary nodules was performed in the SN group than in the HMN ($p = 0.02$) and EMN ($p < 0.01$) groups, and the difference between the SN group and the EMN group was significant after Bonferroni correction (**Table 3**). As shown in **Table 1**, in the extremely multiple GGNs group, 60 (58.8%) patients underwent sublobar resection (segmentectomy and wedge resection) only, 13 (12.7%) patients underwent lobectomy only, and 29 (28.4%) patients underwent lobectomy combined with sublobar resection. There was no significant difference in the choice of surgical method between the HMN and EMN groups ($p = 0.77$). In 51 patients who presented with bilateral pulmonary nodules, 26 (44.1%) underwent a two-stage bilateral surgery, with a median interval of 4 months (interquartile range, 4–6 months). Only 25.6% of patients in the EMN group had bilateral surgery, which was less than that in the HMN group (44.1%), although the difference between the two groups was not yet significant ($p = 0.06$).

TABLE 2 | Percentage distribution of the pulmonary nodules.

		Right superior lobe	Right middle lobe	Right inferior lobe	Left superior lobe	Left inferior lobe	*P*
Total nodules	EMN	31.96%	8.68%	16.67%	30.44%	12.26%	0.147
	HMN	32.94%	7.45%	18.04%	26.67%	14.90%	
	SN	39.39%	4.04%	23.23%	19.19%	14.14%	
Malignant nodules	EMN	29.27%	9.76%	30.49%	13.41%	17.07%	0.233
	HMN	29.81%	8.65%	18.27%	26.92%	16.35%	
	SN	37.80%	4.88%	21.95%	23.17%	12.20%	

TABLE 3 | Analysis of the characteristics of primary nodules.

	Single nodule group (*n* = 99) *n* (%)	Highly multiple nodules group (*n* = 59) *n* (%)	Exceedingly multiple nodules group (*n* = 43) *n* (%)	*P*	*P*[a]
Distribution				0.45	NA
Superior lobes	58 (58.6)	37 (62.7)	30 (69.8)		
Type				<0.01	<0.01
mGGN	56 (56.6)[a]	37 (62.7)	36 (83.7)[a]		
Size				<0.01	<0.01
Median (IQR)	11.0 (8.0, 17.5)[a]	12.8 (12.8, 18.5)	17.2 (17.2, 23.3)[a]		
Operation method				0.01	0.01
Sublobar resection	77 (77.8)[a]	36 (61.0)	24 (55.8)[a]		
Pathological pattern				0.01	0.01
IA	44 (44.4)[a]	36 (61.0)	30 (69.8)[a]		

IA, invasive adenocarcinoma.

[a]*The two groups were considered significantly different, with a P-value below 0.017 after Bonferroni correction for multiple pairwise comparisons (α = 0.05, n = 3), whereas in the other pairwise comparisons, there was no significant difference.*

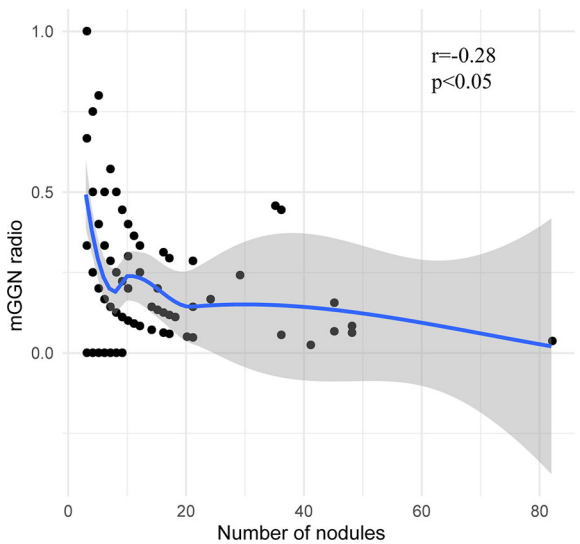

FIGURE 2 | The correlation between the proportion of mixed ground-glass nodules and the total number of nodules.

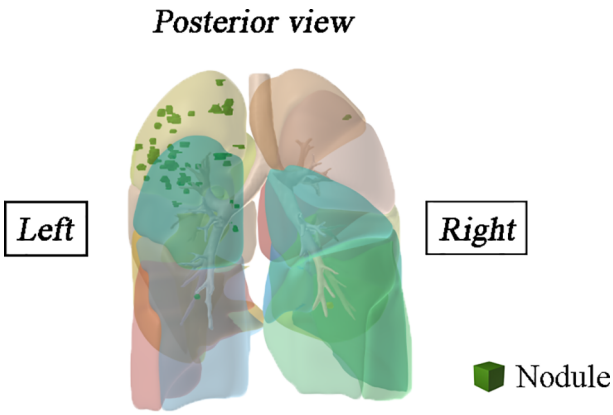

FIGURE 3 | Spatial location information of the multifocal samples of a patient was reconstructed in three-dimensional.

Pathological Characteristics

The proportion of invasive adenocarcinoma in the primary nodules of the SN group (44.4%) was less than those in the HMN (61.0%, $p = 0.04$) and EMN groups (69.8%, $p < 0.01$), and the difference between the SN group and the EMN group was significant after Bonferroni correction (**Table 3**). Among the resected nodules of the EMN and HMN groups, the malignant proportion was 73.7%, and the proportions of atypical adenomatoid hyperplasia, adenocarcinoma *in situ* (AIS), micro-invasive adenocarcinoma (MIA), and invasive adenocarcinoma were 7.0, 13.2, 27.8, and 33.7%, respectively. There was no significant difference in the incidence of invasive adenocarcinoma between the two groups (**Table 4**). The proportion of malignant nodules had no significant relationship with the age, sex, or smoking history of the patients but decreased with the increase in the number of nodules (**Figure 4**). Systematic lymph node dissection or lymph node sampling was performed in 94.4% of the patients, and no lymph node invasion was observed, neither in the patients with pure

TABLE 4 | Pathological analysis of ground-glass nodules.

	Highly mult iple nodules group (*n* = 220) *n* (%)	Exceedingly multiple nodules group (*n* = 278) *n* (%)	*P*
Benign (except AAH)	44 (20.0)	47 (16.9)	0.375[a]
AAH/AIS/MIA	108 (49.1)	132 (47.5)	0.391[b]
IA	68 (30.9)	99 (35.6)	

AAH, atypical adenomatous hyperplasia; AIS, adenocarcinoma in situ; MIA, minimally invasive adenocarcinoma.
[a]*Comparison between benign lesions and malignant lesions.*
[b]*Comparison between IA and AAH/AIS/MIA.*

ground-glass nodules nor in those with mixed ground-glass nodules.

Prognosis

A total of 4/201 patients were lost at the end of the follow-up period. The median follow-up period was 37 months (range, 13–120 months). No serious postoperative complications or perioperative deaths were observed in any group. Ten patients in the SN group had additional GGNs during postoperative follow-up, and none of them underwent intervention. Nine patients in the HMN group and seven patients in the EMN group had enlarged unresected GGNs or additional GGNs during postoperative follow-up, nine of whom had a second operation on the contralateral side, and the others had no intervention. There was no significant difference in the rate of nodule progression between the HMN group and the EMN group (15.3 *vs.* 16.3%, $p = 0.88$). Three nodules from the three patients who underwent the second surgery were pathologically confirmed to be invasive adenocarcinoma, with no lymph node invasion. One patient in the HMN group who presented preoperatively with a mixed ground-glass nodule with a solid component ratio greater than 50% was found to have a local recurrence 34 months after wedge resection. The pathology of the recurrent nodules was papillary adenocarcinoma. None of the other 200 patients experienced a recurrence and no death was recorded either during the follow-up period.

DISCUSSION

In this study, 76.5% of the patients in the HMN and EMN groups were female, a slightly higher percentage than that in the SN group (63.6%) and other studies (63.8–71.8%) on single nodules (18, 19).

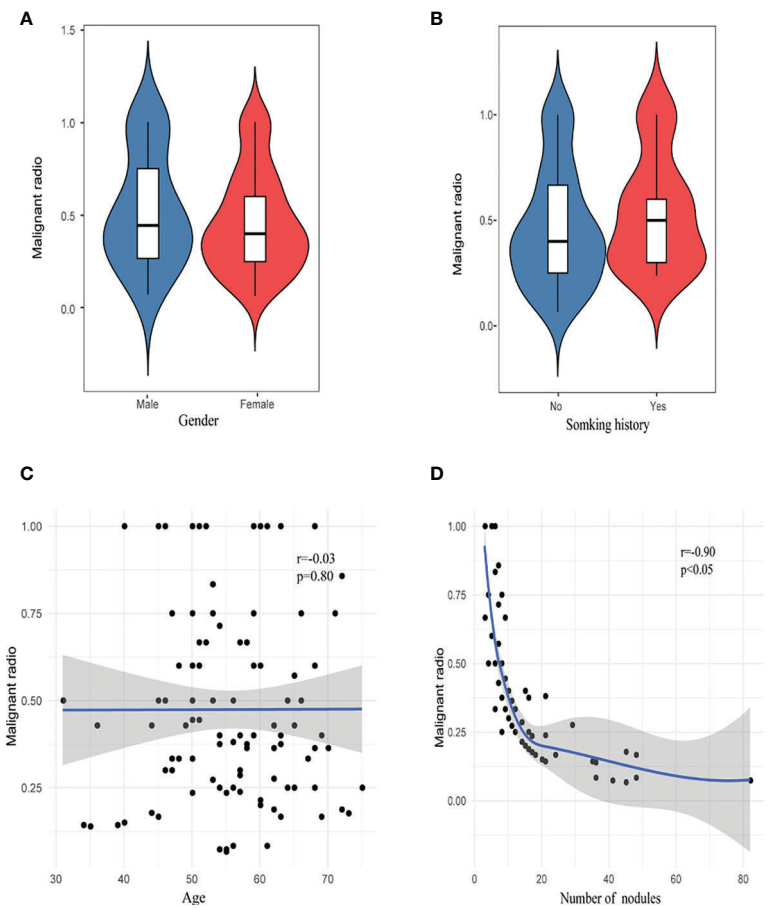

FIGURE 4 | Risk factor analysis of malignant rate. **(A)** Gender, **(B)** smoking history, **(C)** age, and **(D)** number of nodules.

Most patients had no chief complaint, no family history of lung cancer, and no positive tumor markers, which did not differ significantly among the SN group, the EMN group, and the HMN group and was consistent with studies on single GGNs (18, 19). Since our study participants were from the surgical population, a higher proportion of patients had mixed ground-glass nodules. In our study, the proportion of both mGGNs and malignant nodules decreased significantly with the increasing number of nodules, which indicated that patients with extremely multiple GGNs may not have higher malignancy or stronger invasiveness due to the increasing number of GGNs. However, among the primary nodules, compared with the SN group, the proportion of both mGGNs and invasive adenocarcinoma was higher in the HMN and EMN groups, especially in the EMN group. Furthermore, the size of the primary nodules in the EMN group was larger than that in the SN group. Therefore, the primary nodules in the extremely multiple nodules group may have higher malignancy than those in the single nodule group, and patients with extremely multiple GGNs should be assessed mainly for the primary nodules rather than the number of nodules.

Multiple GGNs are considered multiple primary lung cancers and at the early stage of tumorigenesis rather than metastatic tumors, according to the statements from the Fleischner Society and IASLC Staging and Prognostic Factors Committee (20). However, in some patients, most nodules are concentrated in a single segment. Previous studies have shown that four patients had two lesions that shared the same rare mutation (21, 22) identified by whole-exome sequencing. The exact metastatic routes remain unexplored, but metastasis possibly occurred *via* the airway. Therefore, in patients with clustered GGNs, attention should be given to the possibility of metastasis.

The scope of surgery for patients with multiple ground-glass nodules has always been controversial, and it is generally considered that sublobar resection is more appropriate than lobectomy for smaller GGNs and pGGNs. Miller and colleagues compared the outcomes of lobectomy and sublobar resection for tumors ≤10 mm, and they found that there was no significant difference in survival rate or local recurrence rate (23). Lee and colleagues suggested that the surgical approach of pGGN with pathological types of AIS and MIA is recommended to be sublobar resection rather than lobectomy (24). There are also reports in the literature that, for multiple GGN patients with surgical resection, the prognosis is satisfactory; even sublobectomy does not affect the prognosis (25, 26). Compared with the abovementioned studies that only focused on one or two GGNs, our study indicates that sublobar resection for pure GGNs and nonmain lesions also does not affect the prognosis for patients with extremely multiple GGNs, while the study of Nakao found that marginal or primary recurrence occurred in four of 26 GGN patients 5 years after local resection (27). Notably, in our study, a patient with mixed ground-glass nodules relapsed 34 months after sublobar resection. The main lesion in this patient had a few high-risk characteristics, such as a larger size (2.3 cm), worse pathological subtype (papillary adenocarcinoma), and a higher proportion of solid components (>50%). The other four patients with papillary adenocarcinoma underwent lobectomy. In summary, for pure GGNs and nonmain lesions in extremely multiple GGNs, sublobar resection may be a priority, while the clinical imaging characteristics and rapid freezing pathology during the operation are important factors in determining the surgical approach of the main lesions, especially for larger-sized and subsolid nodules.

Regarding whether to remove all nodules at the same time, according to IASLC guidelines, the nodules resected in patients with multiple ground-glass nodules should be considered as having a high probability of malignancy (20), which was confirmed by our study, showing an overall malignant rate of resected nodules at 73.7% and an even higher malignant rate of 89% for mixed ground-glass nodules, consistent with those studies of single GGNs (28). For multiple GGNs, some studies suggest that the main lesion be removed first and that the prognosis will not be affected whether other lesions are removed (25, 29). However, for extremely multiple GGNs, it remains uncertain whether excision of the main lesion alone is sufficient. In our study, the majority of patients (84.3%) did not experience an enlargement of the unresected nodules during postoperative follow-up, consistent with studies on multiple GGNs (84%) (30). The patients with nodule enlargement were treated with continued observation or secondary surgery, while their survival was not affected. Therefore, the survival rate of patients with extremely multiple GGNs may not be affected when the number of resected nodules is appropriately reduced to improve the quality of life. For the remaining GGN lesions, regular follow-up can be recommended; once the solid component of the lesion increases or the volume increases, repeat surgery can be considered.

Previous studies showed that the incidence of lymph node metastasis in GGNs with solid components greater than 50% was 10–26% (31–36). However, Suzuki *et al.* analyzed the data of 545 patients and proposed that, for adenocarcinoma with a diameter ≤3 cm and solid component ratio ≤50%, the specificity for the diagnosis of pathologically non-invasive adenocarcinoma reached 98.7% (37). Hattori *et al.* also reported that systemic lymph node dissection in patients with GGNs did not improve the survival rate (38). In our study, for extremely multiple GGNs, none of the patients had a lymph node invasion, which indicates that the risk of lymph node invasion does not increase with the increasing number of GGNs. Therefore, systematic lymph node dissection may not be necessary for extremely multiple GGNs, especially if with a solid component of less than 50%.

Our study has some limitations and shortcomings. First, the surgical intervention indications and intervention methods of multiple GGNs are still controversial and inconsistent, and the treatment strategy of our center may be different from that of other centers in the world. Second, the median follow-up time was short, and longer follow-ups are needed to further determine whether multiple unresected GGNs will progress in the future.

To the best of our knowledge, this study is the first to reveal the clinical and pathologic features, surgical methods, and prognosis of patients with extremely multiple GGNs and compare them with those of patients with single GGNs. The result shows that, although the primary nodules in extremely multiple GGNs may have higher malignancy than those in the single nodule group, which should be of concern to clinicians, the

proportion of both mGGNs and malignant nodules decreased significantly with the increasing number of lesions, and the prognosis of patients with extremely multiple GGNs was satisfactory. Systematic lymph node dissection may not be necessary for extremely multiple GGNs, which will provide insights for the treatment strategy of such patients.

DATA AVAILABILITY STATEMENT

The original contributions presented in the study are included in the article/supplementary material. Further inquiries can be directed to the corresponding author.

ETHICS STATEMENT

The studies involving human participants were reviewed and approved by Institutional Review Board of Peking University People's Hospital. The patients/participants provided their written informed consent to participate in this study.

AUTHOR CONTRIBUTIONS

XW, MW, HS, YN, ZYW, ZHW, and KZ participated in data collection. XW, MW, ZYW, KC, and FY participated in data analysis. XW, MW, ZYW, YN, and KC wrote the manuscript. XW, MW, KC, and FY revised the manuscript. All authors contributed to the article and approved the submitted version.

FUNDING

This study was supported by the National Natural Science Funds (grant number 82072566) and the Peking University People's Hospital Research and Development Funds (grant number RS2019-01).

ACKNOWLEDGMENTS

The authors sincerely thank all the patients who participated in this study.

REFERENCES

1. Hansell DM, Bankier AA, MacMahon H, McLoud TC, Müller NL, Remy J. Fleischner Society: Glossary of Terms for Thoracic Imaging. *Radiology* (2008) 246(3):697–722. doi: 10.1148/radiol.2462070712
2. Miura A, Akagi S, Nakamura K, Ohta-Ogo K, Hashimoto K, Nagase S, et al. Different Sizes of Centrilobular Ground-Glass Opacities in Chest High-Resolution Computed Tomography of Patients With Pulmonary Veno-Occlusive Disease and Patients With Pulmonary Capillary Hemangiomatosis. *Cardiovasc Pathol* (2013) 22(4):287–93. doi: 10.1016/j.carpath.2012.12.002
3. Scholten ET, de Jong PA, de Hoop B, van Klaveren R, van Amelsvoort-van de Vorst S, Oudkerk M, et al. Towards a Close Computed Tomography Monitoring Approach for Screen Detected Subsolid Pulmonary Nodules? *Eur Respir J* (2015) 45(3):765–73. doi: 10.1183/09031936.00005914
4. Henschke CI, Yankelevitz DF, Mirtcheva R, McGuinness G, McCauley D, Miettinen OS. CT Screening for Lung Cancer: Frequency and Significance of Part-Solid and Nonsolid Nodules. *AJR Am J Roentgenol* (2002) 178(5):1053–7. doi: 10.2214/ajr.178.5.1781053
5. Henschke CI. Early Lung Cancer Action Project: Overall Design and Findings From Baseline Screening. *Cancer* (2000) 89(11 Suppl):2474–82. doi: 10.1002/1097-0142(20001201)89:11+<2474::AID-CNCR26>3.0.CO;2-2
6. Chong S, Lee KS, Chung MJ, Kim TS, Kim H, Kwon OJ, et al. Lung Cancer Screening With Low-Dose Helical CT in Korea: Experiences at the Samsung Medical Center. *J Korean Med Sci* (2005) 20(3):402–8. doi: 10.3346/jkms.2005.20.3.402
7. Zhang Y, Jheon S, Li H, Zhang H, Xie Y, Qian B, et al. Results of Low-Dose Computed Tomography as a Regular Health Examination Among Chinese Hospital Employees. *J Thorac Cardiovasc Surg* (2020) 160(3):824–31.e4. doi: 10.1016/j.jtcvs.2019.10.145
8. Zhang Y, Fu F, Chen H. Management of Ground-Glass Opacities in the Lung Cancer Spectrum. *Ann Thorac Surg* (2020) 110(6):1796–804. doi: 10.1016/j.athoracsur.2020.04.094
9. Sihoe ADL, Petersen RH, Cardillo G. Multiple Pulmonary Ground Glass Opacities: Is it Time for New Guidelines? *J Thorac Dis* (2018) 10(11):5970–3. doi: 10.21037/jtd.2018.10.67
10. Wang J, Ma H, Ni CJ, He JK, Ma HT, Ge JF. Clinical Characteristics and Prognosis of Ground-Glass Opacity Nodules in Young Patients. *J Thorac Dis* (2019) 11(2):557–63. doi: 10.21037/jtd.2019.01.32
11. MacMahon H, Naidich DP, Goo JM, Lee KS, Leung ANC, Mayo JR, et al. Guidelines for Management of Incidental Pulmonary Nodules Detected on CT Images: From the Fleischner Society 2017. *Radiology* (2017) 284(1):228–43. doi: 10.1148/radiol.2017161659
12. Suzuki K. Whack-A-Mole Strategy for Multifocal Ground Glass Opacities of the Lung. *J Thorac Dis* (2017) 9(Suppl 3):S201–S7. doi: 10.21037/jtd.2017.04.03
13. Niu R, Shao X, Shao X, Wang J, Jiang Z, Wang Y. Lung Adenocarcinoma Manifesting as Ground-Glass Opacity Nodules 3 Cm or Smaller: Evaluation With Combined High-Resolution CT and PET/CT Modality. *AJR Am J Roentgenol* (2019) 213(5):W236–w45. doi: 10.2214/AJR.19.21382
14. Suzuki K, Watanabe SI, Wakabayashi M, Saji H, Aokage K, Moriya Y, et al. A Single-Arm Study of Sublobar Resection for Ground-Glass Opacity Dominant Peripheral Lung Cancer. *J Thorac Cardiovasc Surg* (2020). doi: 10.1016/j.jtcvs.2020.09.146
15. Handa Y, Tsutani Y, Okada M. Transition of Treatment for Ground Glass Opacity-Dominant Non-Small Cell Lung Cancer. *Front Oncol* (2021) 11:655651. doi: 10.3389/fonc.2021.655651
16. WHO. *Classification of Tumours Editorial Board. Thoracic Tumours*. Lyon (France: International Agency for Research on Cancer (2021).
17. Detterbeck FC, Franklin WA, Nicholson AG, Girard N, Arenberg DA, Travis WD, et al. The IASLC Lung Cancer Staging Project: Background Data and Proposed Criteria to Distinguish Separate Primary Lung Cancers From Metastatic Foci in Patients With Two Lung Tumors in the Forthcoming Eighth Edition of the TNM Classification for Lung Cancer. *J Thorac Oncol* (2016) 11(5):651–65. doi: 10.1016/j.jtho.2016.01.025
18. Ye T, Deng L, Wang S, Xiang J, Zhang Y, Hu H, et al. Lung Adenocarcinomas Manifesting as Radiological Part-Solid Nodules Define a Special Clinical Subtype. *J Thorac Oncol* (2019) 14(4):617–27. doi: 10.1016/j.jtho.2018.12.030
19. Fu F, Zhang Y, Wen Z, Zheng D, Gao Z, Han H, et al. Distinct Prognostic Factors in Patients With Stage I Non-Small Cell Lung Cancer With Radiologic Part-Solid or Solid Lesions. *J Thorac Oncol* (2019) 14(12):2133–42. doi: 10.1016/j.jtho.2019.08.002
20. Naidich DP, Bankier AA, MacMahon H, Schaefer-Prokop CM, Pistolesi M, Goo JM, et al. Recommendations for the Management of Subsolid Pulmonary Nodules Detected at CT: A Statement From the Fleischner Society. *Radiology* (2013) 266(1):304–17. doi: 10.1148/radiol.12120628
21. Li R, Li X, Xue R, Yang F, Wang S, Li Y, et al. Early Metastasis Detected in Patients With Multifocal Pulmonary Ground-Glass Opacities (GGOs). *Thorax* (2018) 73(3):290–2. doi: 10.1136/thoraxjnl-2017-210169

22. Li Y, Li X, Li H, Zhao Y, Liu Z, Sun K, et al. Genomic Characterisation of Pulmonary Subsolid Nodules: Mutational Landscape and Radiological Features. *Eur Respir J* (2020) 55(2):1901409. doi: 10.1183/13993003.01409-2019
23. Miller DL, Rowland CM, Deschamps C, Allen MS, Trastek VF, Pairolero PC. Surgical Treatment of non-Small Cell Lung Cancer 1 Cm or Less in Diameter. *Ann Thorac Surg* (2002) 73(5):1545–50; discussion 50-1. doi: 10.1016/S0003-4975(02)03525-7
24. Lee HY, Lee KS. Ground-Glass Opacity Nodules: Histopathology, Imaging Evaluation, and Clinical Implications. *J Thorac Imaging* (2011) 26(2):106–18. doi: 10.1097/RTI.0b013e3181fbaa64
25. Shimada Y, Saji H, Otani K, Maehara S, Maeda J, Yoshida K, et al. Survival of a Surgical Series of Lung Cancer Patients With Synchronous Multiple Ground-Glass Opacities, and the Management of Their Residual Lesions. *Lung Cancer (Amsterdam Netherlands)* (2015) 88(2):174–80. doi: 10.1016/j.lungcan.2015.02.016
26. Nakata M, Sawada S, Yamashita M, Saeki H, Kurita A, Takashima S, et al. Surgical Treatments for Multiple Primary Adenocarcinoma of the Lung. *Ann Thorac Surg* (2004) 78(4):1194–9. doi: 10.1016/j.athoracsur.2004.03.102
27. Nakao M, Yoshida J, Goto K, Ishii G, Kawase A, Aokage K, et al. Long-Term Outcomes of 50 Cases of Limited-Resection Trial for Pulmonary Ground-Glass Opacity Nodules. *J Thorac Oncol* (2012) 7(10):1563–6. doi: 10.1097/JTO.0b013e3182641b5c
28. Qu R, Hao Z, Zhang Y, Bie L, Fu X, Zhang N. Single-Center Experience of Simultaneous Bilateral Uni-Portal Video-Assisted Thoracoscopic Surgery for Multiple Ground-Glass Opacities. *J Cardiothoracic Surg* (2020) 15(1):69. doi: 10.1186/s13019-020-01107-0
29. Gao RW, Berry MF, Kunder CA, Khuong AA, Wakelee H, Neal JW, et al. Survival and Risk Factors for Progression After Resection of the Dominant Tumor in Multifocal, Lepidic-Type Pulmonary Adenocarcinoma. *J Thorac Cardiovasc Surg* (2017) 154(6):2092–9.e2. doi: 10.1016/j.jtcvs.2017.07.034
30. Chen K, Chen W, Cai J, Yang F, Lou F, Wang X, et al. Favorable Prognosis and High Discrepancy of Genetic Features in Surgical Patients With Multiple Primary Lung Cancers. *J Thorac Cardiovasc Surg* (2018) 155(1):371–9.e1. doi: 10.1016/j.jtcvs.2017.08.141
31. Asamura H, Suzuki K, Watanabe S, Matsuno Y, Maeshima A, Tsuchiya R. A Clinicopathological Study of Resected Subcentimeter Lung Cancers: A Favorable Prognosis for Ground Glass Opacity Lesions. *Ann Thorac Surg* (2003) 76(4):1016–22. doi: 10.1016/S0003-4975(03)00835-X
32. Ikeda N, Maeda J, Yashima K, Tsuboi M, Kato H, Akada S, et al. A Clinicopathological Study of Resected Adenocarcinoma 2 Cm or Less in Diameter. *Ann Thorac Surg* (2004) 78(3):1011–6. doi: 10.1016/j.athoracsur.2004.03.048
33. Suzuki K, Kusumoto M, Watanabe S, Tsuchiya R, Asamura H. Radiologic Classification of Small Adenocarcinoma of the Lung: Radiologic-Pathologic Correlation and its Prognostic Impact. *Ann Thorac Surg* (2006) 81(2):413–9. doi: 10.1016/j.athoracsur.2005.07.058
34. Aoki T, Tomoda Y, Watanabe H, Nakata H, Kasai T, Hashimoto H, et al. Peripheral Lung Adenocarcinoma: Correlation of Thin-Section CT Findings With Histologic Prognostic Factors and Survival. *Radiology* (2001) 220 (3):803–9. doi: 10.1148/radiol.2203001701
35. Matsuguma H, Yokoi K, Anraku M, Kondo T, Kamiyama Y, Mori K, et al. Proportion of Ground-Glass Opacity on High-Resolution Computed Tomography in Clinical T1 N0 M0 Adenocarcinoma of the Lung: A Predictor of Lymph Node Metastasis. *J Thorac Cardiovasc Surg* (2002) 124 (2):278–84. doi: 10.1067/mtc.2002.122298
36. Nakata M, Sawada S, Yamashita M, Saeki H, Kurita A, Takashima S, et al. Objective Radiologic Analysis of Ground-Glass Opacity Aimed at Curative Limited Resection for Small Peripheral non-Small Cell Lung Cancer. *J Thorac Cardiovasc Surg* (2005) 129(6):1226–31. doi: 10.1016/j.jtcvs.2004.10.032
37. Suzuki K, Koike T, Asakawa T, Kusumoto M, Asamura H, Nagai K, et al. A Prospective Radiological Study of Thin-Section Computed Tomography to Predict Pathological Noninvasiveness in Peripheral Clinical IA Lung Cancer (Japan Clinical Oncology Group 0201). *J Thorac Oncol* (2011) 6(4):751–6. doi: 10.1097/JTO.0b013e31821038ab
38. Hattori A, Matsunaga T, Takamochi K, Oh S, Suzuki K. Significance of Lymphadenectomy in Part-Solid Lung Adenocarcinoma: Propensity Score Matched Analysis. *Ann Thorac Surg* (2018) 106(4):989–97. doi: 10.1016/j.athoracsur.2018.04.069

Conflict of Interest: The authors declare that the research was conducted in the absence of any commercial or financial relationships that could be construed as a potential conflict of interest.

Publisher's Note: All claims expressed in this article are solely those of the authors and do not necessarily represent those of their affiliated organizations, or those of the publisher, the editors and the reviewers. Any product that may be evaluated in this article, or claim that may be made by its manufacturer, is not guaranteed or endorsed by the publisher.

Advantages of publishing in Frontiers

OPEN ACCESS
Articles are free to read for greatest visibility and readership

FAST PUBLICATION
Around 90 days from submission to decision

HIGH QUALITY PEER-REVIEW
Rigorous, collaborative, and constructive peer-review

TRANSPARENT PEER-REVIEW
Editors and reviewers acknowledged by name on published articles

Frontiers
Avenue du Tribunal-Fédéral 34
1005 Lausanne | Switzerland

Visit us: www.frontiersin.org
Contact us: frontiersin.org/about/contact

REPRODUCIBILITY OF RESEARCH
Support open data and methods to enhance research reproducibility

DIGITAL PUBLISHING
Articles designed for optimal readership across devices

FOLLOW US
@frontiersin

IMPACT METRICS
Advanced article metrics track visibility across digital media

EXTENSIVE PROMOTION
Marketing and promotion of impactful research

LOOP RESEARCH NETWORK
Our network increases your article's readership